c.1

FLUOROSULFATES OF THE NOBLE METALS, AND THEIR USE IN NOVEL SUPERACID SYSTEMS

by

KEITH CHEUK-LAP LEE

B.Sc., Honours, The University of British Columbia, 1976

A THESIS SUBMITTED IN PARTIAL FULFILMENT OF

THE REQUIREMENTS FOR THE DEGREE OF

DOCTOR OF PHILOSOPHY

in

THE FACULTY OF GRADUATE STUDIES

Department of Chemistry

We accept this thesis as conforming

to the required standard

THE UNIVERSITY OF BRITISH COLUMBIA

September 1980

Authorization

In presenting this thesis in partial fulfilment of the requirements for an advanced degree at the University of British Columbia, I agree that the Library shall make it freely available for reference and study. I further agree that permission for extensive copying of this thesis for scholarly purposes may be granted by the Head of my department or by his or her representatives. It is understood that copying or publication of this thesis for financial gain shall not be allowed without my written permission.

3rd Oct. 1980

Date

Keith Cheuk-Lap Lee

Abstract

This study was initiated by the search for novel superacid systems based on HSO_3F, the strongest simple protonic acid. Therefore, the synthesis of binary metal fluorosulfates, $M(SO_3F)_n$, was investigated, with special emphasis on compounds where M is in a medium or high oxidation state and formally coordinatively unsaturated, i.e., n = 3,4 or 5. Preferably, the resulting fluorosulfate would also display a sufficiently high thermal stability with respect to dissociations giving rise to SO_3 or $S_2O_5F_2$, and reasonable solubility in HSO_3F.

In order to obtain suitable binary fluorosulfates, a new, generally applicable synthetic method was developed, involving the oxidation of a metal with $S_2O_6F_2$ in the presence of HSO_3F:

$$M + n/2\ S_2O_6F_2 \xrightarrow{HSO_3F} M(SO_3F)_n ,$$

where M is primarily a 4d or 5d transition metal, in particular, palladium, platinum, gold and iridium. This fluorosulfonation mixture combines the strong oxidizing ability of $S_2O_6F_2$ with the good solvating property of HSO_3F towards ionic solutes. The ability of these binary fluorosulfates to act as fluorosulfate ion acceptors was established by the synthesis of anionic complexes of the type $[M(SO_3F)_{n+m}]^{m-}$, where m = 1,2.

Both $Au(SO_3F)_3$ and $Pt(SO_3F)_4$ were found to act as ansolvoacids in HSO_3F by the removal of fluorosulfate ions from the solvent ionization equilibrium:

$$2HSO_3F \rightleftharpoons H_2SO_3F^+ + SO_3F^-,$$

to form $[Au(SO_3F)_4]^-$ or $[Pt(SO_3F)_6]^{2-}$. Results from conductivity measurements indicate the resulting superacids have acid strengths comparable to that of the HSO_3F-SbF_5-SO_3 system and definitely superior to the HSO_3F-SbF_5 system. In both cases, the variety of ternary fluorosulfates synthesized included unusual cations such as Br_3^+ and Br_5^+. In the case of platinum, evidence for polynuclear oligomeric anions of the type of $[Pt(SO_3F)_5]_n^{n-}$ were obtained; similar observations were also made in the tin system.

The oxidation of palladium yielded $Pd(SO_3F)_2$ and a mixed valency compound, $Pd(II)[Pd(IV)(SO_3F)_6]$, both containing Pd(II) in a rather uncommon octahedral coordination sphere and a $^3A_{2g}$ electronic ground state. These magnetically dilute compounds allowed meaningful magnetic results and ligand field parameters to be interpreted.

Both $Ir(SO_3F)_3$ and $Ir(SO_3F)_4$ could be synthesized, along with some tenary fluorosulfate complexes. Some preliminary results were also obtained on the fluorosulfates of germanium, molybdenum, niobium and tantalum.

TABLE OF CONTENTS

LIST OF TABLES

LIST OF FIGURES

ACKNOWLEDGEMENT

I would like to express my sincere appreciation to Professor F. Aubke, my research supervisor, for his inspirations and guidance during my years of graduate study.

Thanks are also extended to other members of the faculty and staff of this department for their assistance in various aspects of this research, in particular, Professor R.C. Thompson and Dr. P.C. Leung for stimulating discussions, Dr. S.O. Chan for taking some of the n.m.r. spectra, and the glass-blowing and mechanical shops for the construction of most of the apparatus used. Professors J. Trotter and N.L. Paddock are thanked for reading parts of the manuscripts. Mrs. B. Krizsan is thanked for some of the illustrations. I would also like to thank my typists for doing such a fine job: Mr. Derek Lee and Miss Roselyn Lee, who did most of the typing, and Ms. Dorathea Baker and Mrs. Bev Gray.

The receipts of a National Science and Engineering Research Council Post Graduate Scholarship and a Dr. F.J. Nicholson Fellowship are gratefully acknowledged.

TO

MY PARENTS

CHAPTER 1 INTRODUCTION

1.A GENERAL INTRODUCTION

Fluorosulfuric acid, HSO_3F, was first prepared by Thorpe and Kirman by the reaction between sulfur trioxide and anhydrous hydrogen fluoride [1]:

$$HF + SO_3 \longrightarrow HSO_3F \ . \qquad (1.1)$$

Although completely ionic salts of the acid, such as KSO_3F, can be recrystallized from their neutral aqueous solutions [2], HSO_3F itself is nevertheless unstable in water, in which it is hydrolyzed almost spontaneously according to:

$$HSO_3F + H_2O \longrightarrow HF + H_2SO_4 \ . \qquad (1.2)$$

The instability of the S-F bond towards hydrolysis is also illustrated by the fact that most fluorosulfates are extremely sensitive to moisture. While there have been questionable reports on the existence of pure aqueous solutions [3,4] and hydrates [5] of the acid, HSO_3F is incompatible with the aqueous system for all practical purposes [6-9]. On the other hand, the acid has been studied extensively as an ionizing and protonic non-aqueous solvent. This can be reflected in a number of reviews on HSO_3F and its derivatives, in particular those by Lange [10], Gillespie et al [11,12], Thompson [13], Jache et al [14,15] and Olah et al [16]. The subject has also been described in related articles by Cady [17], Williamson [18], and, De Marco and Shreeve [19]. In addition, the versatility of HSO_3F can be illustrated by its

use as a fluorinating agent in reactions with oxides and oxyacid salts, summarized in an article by Englbrecht [20].

HSO_3F is the strongest simple protonic acid, more so than HSO_3CF_3, $H_2S_2O_7$, H_2SO_4, HSO_3Cl and $HClO_4$. Its high dielectric constant makes it a very suitable medium for the formation and generation of ionic solutes [21].

Since the neat solvent displays such a high acidity, it is not surprising that HSO_3F is widely used as a basis for superacid systems (sometimes called 'magic acids' by some workers in the field of carbonium ion chemistry [22,23]). The definition of a superacid is by no means universal; some refer to it as any protonic acid with an acidity greater than that of 100% H_2SO_4 [12]. According to this classification, HSO_3F itself would be a superacid. Another definition, preferred and subsequently used in this thesis, views a superacid as a multicomponent system with an acidity unattainable by simple protonic acids.

In terms of solvo-system terminology, an acid in HSO_3F increases the acidium ion concentration, $[H_2SO_3F^+]$. It can accomplish this either by the protonation of the solvent according to:

$$HA + HSO_3F \rightleftharpoons H_2SO_3F^+ + A^- \quad , \qquad (1.3)$$

or by the removal of the fluorosulfate ion, SO_3F^-, from the self ionization equilibrium by:

$$A + 2HSO_3F \rightleftharpoons H_2SO_3F^+ + A{\cdot}SO_3F^- \quad . \qquad (1.4)$$

Due to the extremely high acidity of HSO_3F, the direct protonation of HSO_3F by a simple protonic acid is not possible.

While most solutes are bases in HSO_3F, only a few strong Lewis acids have been found to act as ansolvo-acids according to equation (1.4).

The most thoroughly studied superacid system in HSO_3F contains the fluoride or fluoride-fluorosulfates of antimony (V) as the ansolvo-acids. The fluoride-fluorosulfates are usually formed in situ in these mixtures by the addition of SO_3 in a reaction such as [24]:

$$SbF_5 + SO_3 \longrightarrow SbF_4(SO_3F) \ . \qquad (1.5)$$

These compounds have been found to be stronger acids than the pentafluorides in HSO_3F; $SbF_2(SO_3F)_3$, identified only in HSO_3F solutions, gives rise to the strongest acid of the group. It is apparent that the successive substitution of fluorine atoms by fluorosulfate groups increases the acidity of the superacid system [11]. This leads to the expectation that the pentakis-(fluorosulfate) should yield a solution of even greater acidity than the fluoride-fluorosulfates. Unfortunately, a higher degree of substitution is not possible in this system, and only $SbF_4(SO_3F)$ [25] and $SbF_3(SO_3F)_2$ [26] have hitherto been isolated; attempts to prepare $Sb(SO_3F)_5$ have failed [27].

Although there is no implied correlation between the acidity and basicity of a solvent, the existence of the highly electrophilic acidium ion, $H_2SO_3F^+$, in a superacid system indicates that other unusual cations may be stabilized in the medium. The complexation of the strongest base in the fluorosulfuric acid system — SO_3F^-, to give larger, less

nucleophilic anions such as $[SbF_2(SO_3F)_4]^-$, is expected to decrease the basicity of the resulting solution. Therefore, in order for an ansolvo-acid to give rise to a strongly acidic and weakly basic solution in HSO_3F, it must possess strong Lewis acidity towards SO_3F^- with the resulting complex anion, $A{\cdot}SO_3F^-$, showing minimal reverse dissociation according to:

$$A{\cdot}SO_3F^- \rightleftharpoons A + SO_3F^- \quad . \qquad (1.6)$$

In the antimony (V) fluoride-fluorosulfate superacid system, additional modes of dissociation of the compounds in solution by [22,24]:

$$[SbF_2(SO_3F)_4]^- \rightleftharpoons [SbF_3(SO_3F)_3]^- + SO_3 \quad , \qquad (1.7)$$

and the decomposition of the ansolvo-acids themselves by [26]:

$$SbF_3(SO_3F)_2 \rightleftharpoons SbF_4(SO_3F) + SO_3 \quad , \qquad (1.8)$$

can lead to the formation of SO_3, a reasonably powerful oxidizing agent. The presence of SO_3 may give rise to oxidative side reactions in these media, in particular with species such as carbonium ions [22] and polyhalogen cations [28-30].

Hence, it becomes necessary to look for other fluorosulfates that may be better ansolvo-acids in the HSO_3F solvent system than those presently known. A good fluorosulfate acceptor should have the following properties:

a) a reasonable thermal stability, especially towards SO_3 elimination and ligand redistribution reactions,

b) an incompletely filled coordination sphere in order to facilitate the addition of SO_3F group(s),

c) a high solubility in HSO_3F to give reasonable

concentrations, and

d) a low oxidative power, to reduce side reactions and to allow the study of a wide range of species.

A review of the previously reported fluorosulfates reveals that only a few form anionic complexes, and of these, none are really suitable as ansolvo-acids. For example, although salts containing the anion - $[Sn(SO_3F)_6]^{2-}$ can be prepared [31,32], $Sn(SO_3F)_4$ is virtually insoluble in HSO_3F [33]. Both $Br(SO_3F)_3$ and $I(SO_3F)_3$ form anionic complexes of the type of $[Hal(SO_3F)_4]^-$ [31,34,35], but they can also exist in cationic species of the type - $[Hal(SO_3F)_2]^+$ [28,31]. This indicates that the $Hal(SO_3F)_3$ can act as both an acceptor and a donor towards a SO_3F group. Not surprisingly, $I(SO_3F)_3$ has been found to be amphoteric in HSO_3F, capable of both acidic and basic reactions in the solvent [36]. Furthermore, both these compounds are oxidizing [37,38], and thus are unsuitable as ansolvo-acids in the HSO_3F acid system.

It appeared that other fluorosulfates would have to be synthesized, and possibly by new methods. Fluorosulfates of the 4d and 5d elements have not been studied extensively, but are likely suitable for the following reasons:

a) The halides of these metals are capable of the formation of halocomplexes, indicating Lewis acidity in the halides system which most likely should extend to the fluorosulfate system.

b) The Lewis acidity of this type of fluorosulfates is

expected to increase with the metal's oxidation number, and high oxidation states of these metals are relatively easily attainable.

In order to establish that the metal fluorosulfate will accept fluorosulfate ions, the successful synthesis of anionic fluorosulfato-complexes will provide the first test. The characterization of these ternary fluorosulfates by various spectroscopic means, including Raman, i.r., n.m.r. and u.v.-visible, should facilitate their subsequent detection in superacid systems. Their acidic behavior in HSO_3F can then be assessed by the use of electrical conductivity measurements.

In HSO_3F, as in H_2SO_4 and H_2O, the ions produced by autoprotolysis display much higher mobilities than any other ions in the solvent. This has been explained by the concept that they conduct by the proton-transfer mechanism in these strongly hydrogen bonded solvents [39]. Consequently, strong acids and strong bases give rise to highly conductive solutions in HSO_3F, and titrations with KSO_3F (a strong base in HSO_3F) can then be used to distinguish between acidic and basic conductivities.

In the following sections in this chapter, a few important topics will be reviewed in more detail.

1.B PROPERTIES OF HSO_3F

The properties of HSO_3F are compared with those of the more familiar protonic solvents, H_2SO_4 and H_2O, in Table 1.1.

As can be seen, HSO_3F has a long liquid range; and a low

TABLE 1.1 Properties of HSO_3F, H_2SO_4 and H_2O (at 25°C)

	HSO_3F [13]	H_2SO_4 [39]	H_2O [40]
Freezing point, °C	-88.98	10.371	0.00
Boiling point, °C	162.7	290	100.00
Density ($g \cdot cc^{-1}$)	1.7264	1.8269	0.9971
Viscosity (cp)	1.56	24.54	0.8904
Dielectric constant	~120	100	78.33
κ ($\Omega^{-1}cm^{-1}$)	1.085×10^{-4}	1.044×10^{-2}	4.3×10^{-8}
Λ^+	185	250	350
Λ^-	135	166	200
K_{ap} (mol^2kg^{-2})	3.8×10^{-8}	2.7×10^{-4}	1.0×10^{-14}
$-H_o$	15.07	11.93	-7.00

viscosity. These two factors have made HSO_3F a very useful medium for n.m.r. studies at low temperatures [22,24,41-45]. In such conditions, individual components of an exchange reaction can be identified.

In contrast to H_2SO_4, in which a series of dissociative reactions, represented by equations (1.9) to (1.12), have been observed [39],

$$2H_2SO_4 \rightleftharpoons H_3SO_4^+ + HSO_4^- \qquad K=2.7\times10^{-4} \qquad (1.9)$$

$$2H_2SO_4 \rightleftharpoons H_3O^+ + HS_2O_7^- \qquad K=5.1\times10^{-5} \qquad (1.10)$$

$$H_2S_2O_7 + H_2SO_4 \rightleftharpoons H_3SO_4^+ + HS_2O_7^- \qquad K=1.4\times10^{-2} \qquad (1.11)$$

$$H_2O + H_2SO_4 \rightleftharpoons H_3O^+ + HSO_4^- \qquad K=1\ , \qquad (1.12)$$

HSO_3F undergoes only two minor autodissociative reactions in the pure state [46]:

$$2HSO_3F \rightleftharpoons H_2SO_3F^+ + SO_3F^- \qquad K=3.8\times10^{-8} \qquad (1.13)$$

$$HSO_3F \rightleftharpoons HF + SO_3 \qquad K<3\times10^{-7}\ . \qquad (1.14)$$

For all practical purposes, these dissociations do not interfere with the interpretation of conductivity and cryoscopic data in

HSO_3F [13].

A decrease in intermolecular association in HSO_3F, due to the presence of one less hydrogen per molecule than in H_2SO_4, can be reflected in its lower viscosity and the lower molar conductivities for $H_2SO_3F^+$ and SO_3F^-. Nevertheless, the ion mobilities of the autoprotolysis ions are still much higher than those of the other ions in HSO_3F. For example, K^+ has a Λ^+ value of only 17 in HSO_3F (the data for $H_2SO_3F^+$ and SO_3F^- are listed in Table 1.1). The high acidity of HSO_3F as compared to other strong acids in terms of H_o of the pure acids is illustrated below [12,47-49]:

$HF(-11) < H_2SO_4(-11.93) < HSO_3Cl(-13.80) < HSO_3CF_3(-14.00) < HSO_3F(-15.07)$.

1.C SUPERACID SYSTEMS BASED ON HSO_3F

As mentioned previously, the SbF_5-$3SO_3$ superacid has been found to be the strongest acid in HSO_3F. Solutions of SbF_5 in HSO_3F, although slightly less acidic, have been used extensively in organic chemistry for the stabilization of carbonium ions, because they contain less SO_3. The SbF_5-HSO_3F system is very complex, and can be represented by the following equilibria [22,24]:

$$HSO_3F + SbF_5 \rightleftharpoons H[SbF_5(SO_3F)] \quad (1.15)$$

$$H[SbF_5(SO_3F)] + HSO_3F \rightleftharpoons H_2SO_3F^+ + [SbF_5(SO_3F)]^- \quad (1.16)$$

$$2H[SbF_5(SO_3F)] \rightleftharpoons H_2SO_3F^+ + [Sb_2F_{10}(SO_3F)]^- \quad (1.17)$$

$$HSO_3F \rightleftharpoons HF + SO_3 \quad (1.18)$$

$$2HF + 3SbF_5 \rightleftharpoons HSbF_6 + HSb_2F_{11} \quad (1.19)$$

$$3SO_3 + 2HSO_3F \rightleftharpoons HS_2O_6F + HS_3O_9F \quad (1.20)$$

This interactive series of reactions gives rise to different dominant species in solutions, depending on the concentration of SbF_5. This can lead to side reactions and may present difficulties when attempts are made to isolate a particular product from the mixture. Also, because the mixture is so complex, the use of spectroscopic techniques such as F-19 n.m.r. and Raman are difficult.

Since SbF_5 is an ansolvo-acid of the HSO_3F system, other pentafluorides of Group V elements, such as AsF_5 and TaF_5, should also be expected to behave as acids in the solvent. While they do give rise to conducting solutions in HSO_3F, these solutions are only very weakly acidic (when either PF_5 or NbF_5 is dissolved in HSO_3F, the resulting solutions are hardly conducting). Titrations of these solutions with KSO_3F also indicate only weakly acidic behaviors. Broad and ill-defined conductivity minima at the base/acid ratios of 0.06, 0.01, and 0.31 are found for solutions of BiF_5, AsF_5 and $AsF_5 \cdot SO_3$, respectively [50]. In the HSO_3F-AsF_5 system, SO_3 presumably behaves as it does in the HSO_3F-SbF_5 system.

While the conductometric titration with KSO_3F can provide a semi-quantitative assessment of a solute's acidity in HSO_3F, a ranking of its acidity can be made by two other methods discussed below:

a) The Bronsted acidity of a solution governs the degree of protonation of bases in it. By using a series of weakly basic nitro-aromatic compounds, the Hammett Acidity Function,-H_o, has been determined for a number of strong acids and superacids [48,49].

The results parallel those obtained from conductometry, namely, that the effectiveness of a solute in increasing the acidity of HSO_3F increases in the order of $SO_3<AsF_5<SbF_5<SbF_5\text{-}3SO_3$. The behavior of SO_3 as an extremely weak acid in HSO_3F, forming polyfluorosulfuric acids of the type $H(SO_3)_nF$, has also been demonstrated by the spectroscopic methods of Raman and F-19 n.m.r. [41,43]. A 7% molar solution of $SbF_5 \cdot 3SO_3$ in HSO_3F gave an H_o value of -19.35, the highest one measured thus far. The lack of suitable bases prevented the extension of the work to more concentrated, and presumably more acidic solutions. By an extrapolation of the results obtained at lower concentrations in the HSO_3F-SbF_5 system, the 1:1 molar mixture - sometimes called 'magic acid' - has an H_o value of -19.5, making that solution an extremely acidic medium. Figure 1.1 shows the H_o function plot for a number of solutes in HSO_3F [49].

While the original H_o measurements, as defined by Hammett, were obtained by the spectrophotometric monitoring of the concentrations of the base and its protonated species, an alternative method has been proposed recently by Sommer [51,52]. This method is based on determining the increase in the barrier of rotation around the phenyl-carbonyl bond, in compounds such as p-methoxybenzaldhyde, upon protonation as measured by n.m.r. shifts. A value equivalent to H_o of -21.4 was obtained for a 25 mol% of SbF_5 in HSO_3, suggesting an extremely high proton donating ability in the medium [51]. However, the increase in the rotation barrier for the C-C bond in the indicator could conceivably be dependent

FIG 1.1

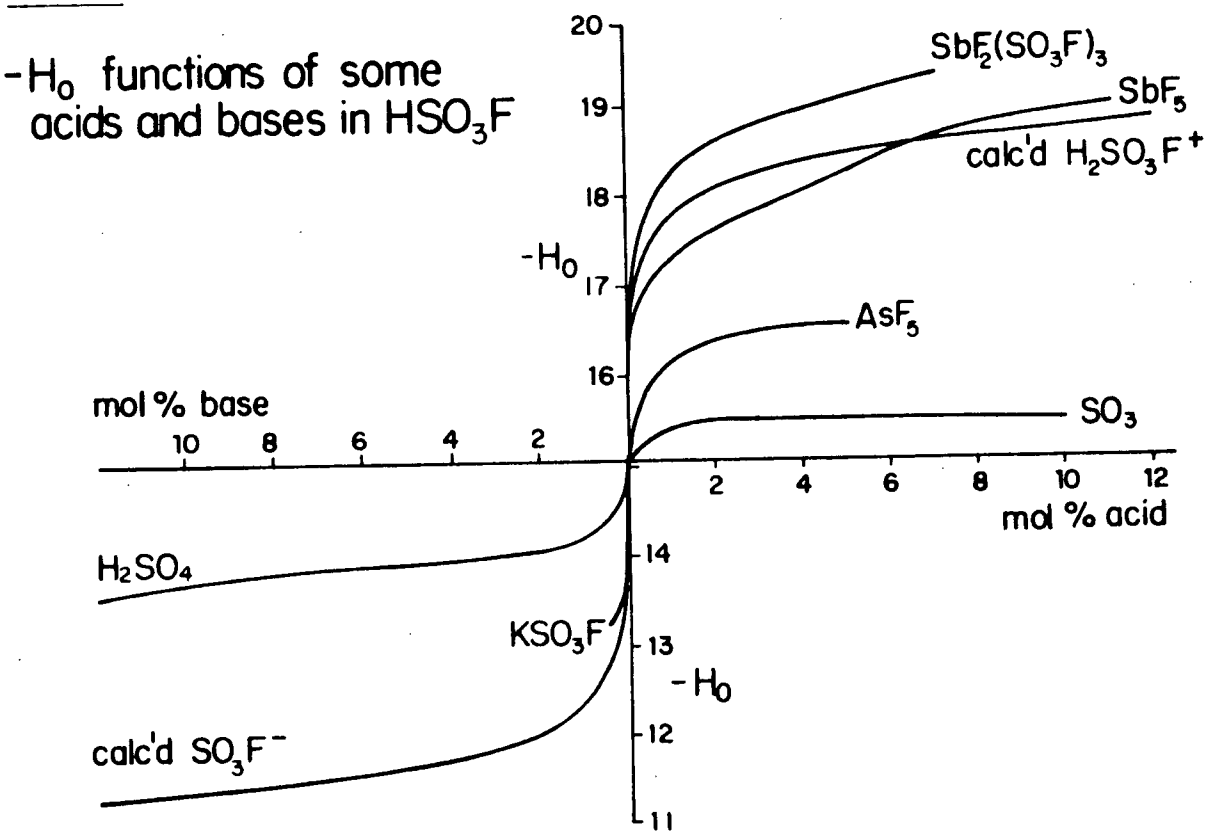
-H_0 functions of some acids and bases in HSO_3F
20
19
18
17
16
-H_0
$SbF_2(SO_3F)_3$
SbF_5
calc'd $H_2SO_3F^+$
AsF_5
SO_3
mol % base
10 8 6 4 2
2 4 6 8 10 12
mol % acid
H_2SO_4
KSO_3F
calc'd SO_3F^-
14
13
12
11
-H_0

on the increased viscosity of these strongly hydrogen bonded solutions containing high concentrations of SbF_5. Thus, this may not be a true measure of the protonating ability of such highly concentrated superacids. This could explain the conclusion reached in the study that HF-SbF_5 (which has a higher viscosity than HSO_3F-SbF_5) is the much more acidic medium of the two [52].

In any event, it should again be pointed out that the usefulness of a superacid system is reflected in the protonating ability, but also on the lack of basicity in the system. The greater charge delocalization in the HSO_3F based superacid is illustrated in the following basicity measurements.

b) The nucleophilicity, or basicity of a solution,determines the stability of a cationic species in it. An alkyl cation, for example, can rearrange with or without deprotonation during its lifetime in the acid, depending on the nucleophilicity of the acidic species. Using tritium-labelled alkanes, Krammer studied the extent of the isomerization and exchange reactions of alkanes in a series of acids containing different Lewis acids [53,54]. A selectivity parameter, I/E, defined as the ratio of:

$$k(\text{isomerization})/k(\text{exchange}) ,$$

was derived for each of the mixtures studied. The results, represented in Figure 1.2, show that I/E parallels H_o within a given acid, but the correlation is solvent dependent. Alternatively, a strong acid is usually also a weak base in a given solvent system.

FIG 1.2 RELATIONSHIP BETWEEN I/E AND $-H_o$[53]

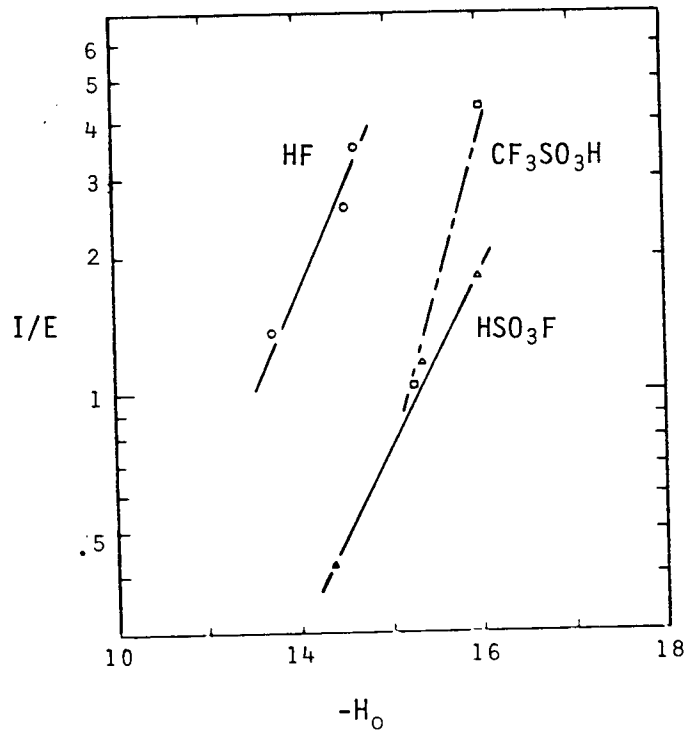

1.D APPLICATIONS OF SUPERACIDS

The low bascity of superacid systems has also been used to advantage in the study of highly electrophilic, non metallic polyatomic cations, in particular, polyhalogen cations [25,55]. The 'hardness' and electrophilicity of a particular cation are expected to increase with a decrease in its size. Thus, while I_7^+, I_5^+ and I_3^+ are stable in 100% H_2SO_4 [56], the smaller I_2^+ can only be obtained either in oleum [57] or in HSO_3F [56]. In the bromine system, the oxidation of Br_2 in the superacid medium of HSO_3F-SbF_5-SO_3 according to [28,58]:

$$3Br_2 + S_2O_6F_2 \longrightarrow 2Br_3^+ + 2SO_3F^- \quad , \qquad (1.21)$$

gives rise to Br_3^+, but, in the more basic HSO_3F, the cation disproportionates:

$$Br_3^+ + SO_3F^- \rightleftharpoons Br_2 + BrSO_3F \quad . \qquad (1.22)$$

Similarly, the smaller Br_2^+ ion is found to be unstable even in the extremely weakly basic medium of HSO_3F-SbF_5-SO_3 [28]:

$$2Br_2^+ + 2HSO_3F \rightleftharpoons Br_3^+ + BrSO_3F + H_2SO_3F^+ \quad . \qquad (1.23)$$

Contrary to earlier reports [59], there is no evidence for the existence of either Cl_2^+ or Cl_3^+ in superacid solutions [29]. However, Cl_3^+-containing salts have been identified in the reaction of a mixture of Cl_2 and ClF with either AsF_5 or HF-SbF_5 at -78°C [60].

The fact that strong protonic acids can catalyze rearrangement and nucleophilic substitution reactions involving large organic molecules has been known for a long time. Very recently,

Olah found that superacid systems, at high temperatures and pressures, can protonate small alkanes such as methane to form species like CH_5^+ [16]. The subsequent condensation of such cations to form larger, longer chained alkanes is a process of obvious industrial importance.

1.E PREPARATION OF METAL FLUOROSULFATES

Fluorosulfate chemistry displays a similarity to halogen chemistry in that the SO_3F group can be viewed as a pseudohalogen. Consequently, many of the synthetic methods used commonly in the synthesis of halides can be adapted to the fluorosulfate system with only minor changes.

1.E.1 SOLVOLYSIS OF ACID SALTS IN HSO_3F

As is common for the preparation of salts of a strong acid, fluorosulfates can be made by simple displacement reactions such as [2,21,61-63]:

$$HSO_3F + KCl \rightleftharpoons HCl + KSO_3F \ . \qquad (1.24)$$

The oxidation state of the metal involved remains unchanged and since this is an ionic reaction, it is especially applicable to the synthesis of alkali or alkali earth fluorosulfates. If the acid salt is polymeric, an incomplete reaction often occurs. For transition metal fluorosulfates that show limited solubilities in HSO_3F, such as $Cu(SO_3F)_2$, a complete reaction does not take place without the addition of KSO_3F to increase the basicity of

the medium [62]. As expected, the formation of a volatile acid such as HCl or HBr, as the by-products from the reaction greatly simplifies the preparation. Conversely, for carboxylates or other salts that give rise to non-volatile acids, the products, which need to be insoluble in HSO_3F in these cases, have to be separated by filtration. Furthermore, the solvolysis of compounds such as carbonates or nitrates will give H_2O as one of the products, and therefore cannot be used.

1.E.2 OXIDATION OF METALS BY HSO_3F

Hydrohalic acids are frequently used to react with metals to give metal halides directly. Just as some metals can reduce H_2SO_4 to SO_2, HSO_3F has been found to be reduced to SO_2 and even elemental sulfur. Besides, most metals are inert even in the boiling acid, either because HSO_3F cannot oxidize the metal or because an insoluble surface layer is formed [64].

1.E.3 INSERTION OF SO_3 INTO M-F BONDS

The formation of fluoride-fluorosulfates of As(V) and Sb(V) in HSO_3F by the insertion of SO_3 into the metal-fluorine bonds has been discussed [24,50]:

$$[SbF_5(SO_3F)]^- + nSO_3 \rightleftharpoons [SbF_{(5-n)}(SO_3F)_{n+1}]^- . \qquad (1.25)$$

Species with n of up to 3 have been identified in solution. When no acid is present, the substitution is incomplete, forming only one product when an excess of SO_3 is used [65].

$$SbF_5 + SO_3 \longrightarrow SbF_4(SO_3F) \ . \qquad (1.26)$$

When this method is applied to other metal fluorides, complete reaction is found only for alkali and alkaline earth metal fluorides [2,66,67]. For example, the difluorides of nickel and copper, when subjected to SO_3, yielded only about 20% conversions [68].

$$NiF_2 + 2SO_3 \longrightarrow Ni(SO_3F)_2 \ . \qquad (1.27)$$

The reaction of CrF_5 with SO_3 did not give a fluorosulfate of Cr(V), but did provide a novel synthesis of $S_2O_6F_2$ [69].

$$CrF_5 + 5SO_3 \longrightarrow S_2O_6F_2 + Cr(SO_3F)_3 \ . \qquad (1.28)$$

A final obstacle in these reactions is the tendency for SO_3 to polymerize, giving rise to asbestos-like materials of rather low volatility, making product separation difficult and awkward.

To summarize, the above three synthetic routes are of limited use in the synthesis of metal fluorosulfates. Furthermore, they do not provide a means to obtain metals in high oxidation states.

1.E.4 OXIDATIVE FLUOROSULFONATION WITH XSO_3F; X=Hal OR SO_3F

This general scheme combines fluorosulfate addition together with oxidation, analogous to the direct reaction of a metal or its salts with a halogen.

1.E.4.1 BIS(FLUOROSULFURYL) PEROXIDE

$S_2O_6F_2$, discovered by Cady and Dudley, is most efficiently prepared by the flow reaction of SO_3 with F_2 in the presence of

AgF_2 as a catalyst [70,71].

$$2SO_3 + F_2 \longrightarrow S_2O_6F_2 \ . \qquad (1.29)$$

It has a low dissociation energy of 22 kcal/mol, yielding SO_3F radicals, and can be regarded as a pseudohalogen in this respect [72,73]:

$$FO_2SO\text{-}OSO_2F \rightleftharpoons 2\cdot OSO_2F \ . \qquad (1.30)$$

Oxidative reactions with $S_2O_6F_2$ can give a variety of fluorosulfate-containing compounds, depending on the choice of starting materials. A few illustrative examples are given below:

a) Oxidative addition of SO_3F

$$MF_3 + S_2O_6F_2 \longrightarrow MF_3(SO_3F)_2 \quad M=As\ [74],\ Sb\ [26] \qquad (1.31)$$

$$CeF_3 + \tfrac{1}{2}S_2O_6F_2 \longrightarrow CeF_3(SO_3F)\ [75] \qquad (1.32)$$

b) Halogen displacement

$$MCl_x + \tfrac{x}{2}S_2O_6F_2 \longrightarrow M(SO_3F)_x + \tfrac{x}{2}Cl_2 \qquad (1.33)$$

M=Ga(III) [76], Sn(IV) [33].

c) Metal oxidation

$$Mo + 3S_2O_6F_2 \longrightarrow MoO_2(SO_3F)_2 + 2S_2O_5F_2\ [75]. \qquad (1.34)$$

$S_2O_6F_2$, being a nonionizing liquid, has very poor solvating properties towards ionic solids. Many metals are unreactive towards this strong oxidizing agent because of the rapid passivation of the metal surfaces. On the other hand, $S_2O_6F_2$ is easily transferred and handled in glass vacuum lines and it can be obtained readily and in good yields by reaction (1.29). The solubility problem mentioned previously may be solved by the availability of a suitable solvent to increase the reactivity

of $S_2O_6F_2$.

1.E.4.2 HALOGEN (I) MONOFLUOROSULFATES

Halogen (I) mono-fluorosulfates, formed by the direct reaction between the halogen and $S_2O_6F_2$,

$$Hal_2 + S_2O_6F_2 \longrightarrow 2HalSO_3F \quad Hal=F, Cl, Br, I \quad , \qquad (1.35)$$

are themselves also very strong oxidizing agents and should therefore be very useful in the preparation of metal fluorosulfates. Their relative effectiveness as the active reagents in such reactions is outlined below:

a) Fluorine (I) monofluorosulfate

FSO_3F is sometimes formed as a by-product during the synthesis of $S_2O_6F_2$ by reaction (1.29) when fluorine is present in excess. It is an extremely powerful oxidizing agent, and reactions with it usually lead to the simultaneous addition of fluorine and fluorosulfate, as in [26]:

$$SbF_3 + FSO_3F \longrightarrow SbF_4(SO_3F) \ . \qquad (1.36)$$

The major obstacle to the investigation of FSO_3F chemistry is its unpredictable tendency to detonate.

b) Chlorine (I) monofluorosulfate

Like FSO_3F, $ClSO_3F$ is the only binary fluorosulfate of the halogen. It can be made only by a high temperature (125°C) reaction which takes a week to complete. It must also be stored and handled in metal apparatus since it reacts with trace amounts of moisture in glass to give a red viscous liquid [77]. It has not

been used extensively in synthetic fluorosulfate chemistry also because of the ready availability of $BrSO_3F$ which can substitute for $ClSO_3F$ in most cases but does not have any of its disadvantages.

c) Bromine (I) monofluorosulfate

$BrSO_3F$, although extremely hygroscopic like the other halogen fluorosulfates, has been found to be an extremely versatile oxidative fluorosulfonating reagent. This easily synthesized red liquid appears to be associated and supports the solvation of ionic species [38,78]. It can be safely stored and handled in glass and can be distilled in vacuo at room temperature. $BrSO_3F$ reacts with chlorides or bromides to give the corresponding fluorosulfates [79] according to:

$$MCl_n + nBrSO_3F \longrightarrow M(SO_3F)_n + \tfrac{n}{2}Br_2 + \tfrac{n}{2}Cl_2 \quad . \qquad (1.37)$$

When alkali metal chlorides are used, complexation takes place and salts of the type $M(I)Br(SO_3F)_2$ are formed [80,81]. In the few reported reactions involving noble metals, $BrSO_3F$ was found to oxidize and dissolve the metals directly:

$$M + nBrSO_3F \longrightarrow M(SO_3F)_n + \tfrac{n}{2}Br_2 \qquad (1.38)$$

M=Au, Pt [82], Ag [83,84]. n=3, 4, 1.33 .

d) Iodine (I) monofluorosulfate

ISO_3F is expected to be only a mildly oxidizing and fluorosulfonating agent. Since it is a solid which is difficult to prepare, it has mainly been used for the study of poly- and interhalogen cations [37,85,86].

In conclusion, for the purpose of this study, all the previously described synthetic reagents have their advantages and disadvantages (either in terms of their physical or their chemical properties). It would be desirable to devise a general synthetic method which can be applied to specific compounds with only minor modifications needed.

1.F TRANSITION METAL FLUOROSULFATES

The chemistry of the 3d metals is, in general, better explored and understood than that of the heavier transition elements. It is therefore not surprising that most of the fluorosulfates of the 3d elements are known, with the metals in the normal oxidation numbers of +2 and +3 [5,87]. These are easily prepared by the solvolysis of the corresponding chloride or other salts in HSO_3F followed by filtration. These fluorosulfates are insoluble in the acid, indicating high degrees of polymerization in the solid state. This is supported by results from vibrational spectroscopy [62,87]. In addition, the oxyfluorosulfates $VO(SO_3F)_3$[88] and $CrO_2(SO_3F)_2$[34] have also been reported. These fluorosulfates are unsuitable as ansolvo-acids in HSO_3F.

For the heavier elements, the binary fluorosulfates of Cd [87] and Hg [89], prepared by:

$$Cd(C_6H_5COO)_2 + 2HSO_3F \longrightarrow Cd(SO_3F)_2 + 2C_6H_5COOH \qquad (1.39)$$

$$Hg + S_2O_6F_2 \longrightarrow Hg(SO_3F)_2 \qquad (1.40)$$

are also polymeric, with tridentate SO_3F groups [87]. Gold and platinum dissolve in $BrSO_3F$ and adducts have been isolated from

the reaction mixtures [82]. Oxyfluorosulfates with the metals usually in the highest attainable oxidation states are known; examples are: $NbO(SO_3F)_3$, $TaO(SO_3F)_3$, $ReO_3(SO_3F)$, $ReO_2(SO_3F)_3$ [88], $MoO_2(SO_3F)_2$ [90] and $WO(SO_3F)_4$ [27]. With the high positive charge on the metals in these compounds, they should be expected to possess Lewis acid properties. Since these compounds have not been fully characterized, a more detailed investigation of them and of related systems is also the intention of this study.

1.G VIBRATIONAL MODES OF THE SO_3F GROUP

The analysis of the vibrational spectrum of the SO_3F group can provide information regarding the type of coordination and the extent of interactions with the cations [91]. This is a distinct advantage a SO_3F group has over monatomic ligands such as F^- or Cl^-.

A free SO_3F^- ion has C_{3v} symmetry, but this can be reduced to C_s or even C_1 with a corresponding increase in the number of vibrational modes from 6, $(3A_1 + 3E)$, to 9, $(6A' + 3A'')$, when one or two oxygen atoms are coordinated. Coordination of all three oxygen atoms or even including the fluorine atom in a tridentate or tetradentate manner will restore C_{3v} symmetry to the ligand and reduce the number of bands back to six, $(3A_1 + 3E)$. All of the vibrational modes of SO_3F are both i.r. and Raman active.

Hence, the vibrational spectra of SO_3F groups can be divided into two main groups:

a) 6-band spectra produced from ionic, tridentate and tetradentate SO_3F groups with C_{3v} symmetry.

b) 9-band spectra produced from mono- and bi-dentate SO_3F groups which have C_s or C_1 symmetry.

Since there are three degenerate E modes when the fluorosulfate group has C_{3v} symmetry, these are susceptible to splittings by site symmetry or by aspherical cations producing polarization effects. The splittings can be seen in the SO_3 stretching region at ~1200 to 1300 cm^{-1}.

Within the two groups of 6- and 9-band spectra, a further distinction can be made based on the band positions. Firstly, coordination of oxygen or fluorine will weaken and thus lower the stretching frequencies of the S-O and S-F bonds. Secondly, electron withdrawal via the coordination of oxygen will strengthen the remaining S-O and S-F bonds. This, according to Cruickshank and Webster [92], is due to the increased back donation from the filled $p\pi$ orbitals of oxygen or fluorine to the empty $d\pi$ orbitals on sulfur now that the sulfur atom has become more positive. Hence the S-F stretching frequency can be used as a diagnosis to determine if coordination of the oxygen atom is present. Invariably, the S-F stretch shifts to a higher frequency for covalently bound SO_3F groups. Examples of the band patterns for the various types of coordination of the SO_3F group are shown in Fig 1.3 and discussed subsequently:

a) ionic ——— KSO_3F, being an ionic crystalline salt [93],

Fig 1.3 VIBRATIONAL BAND PATTERN FOR THE SO_3F GROUP

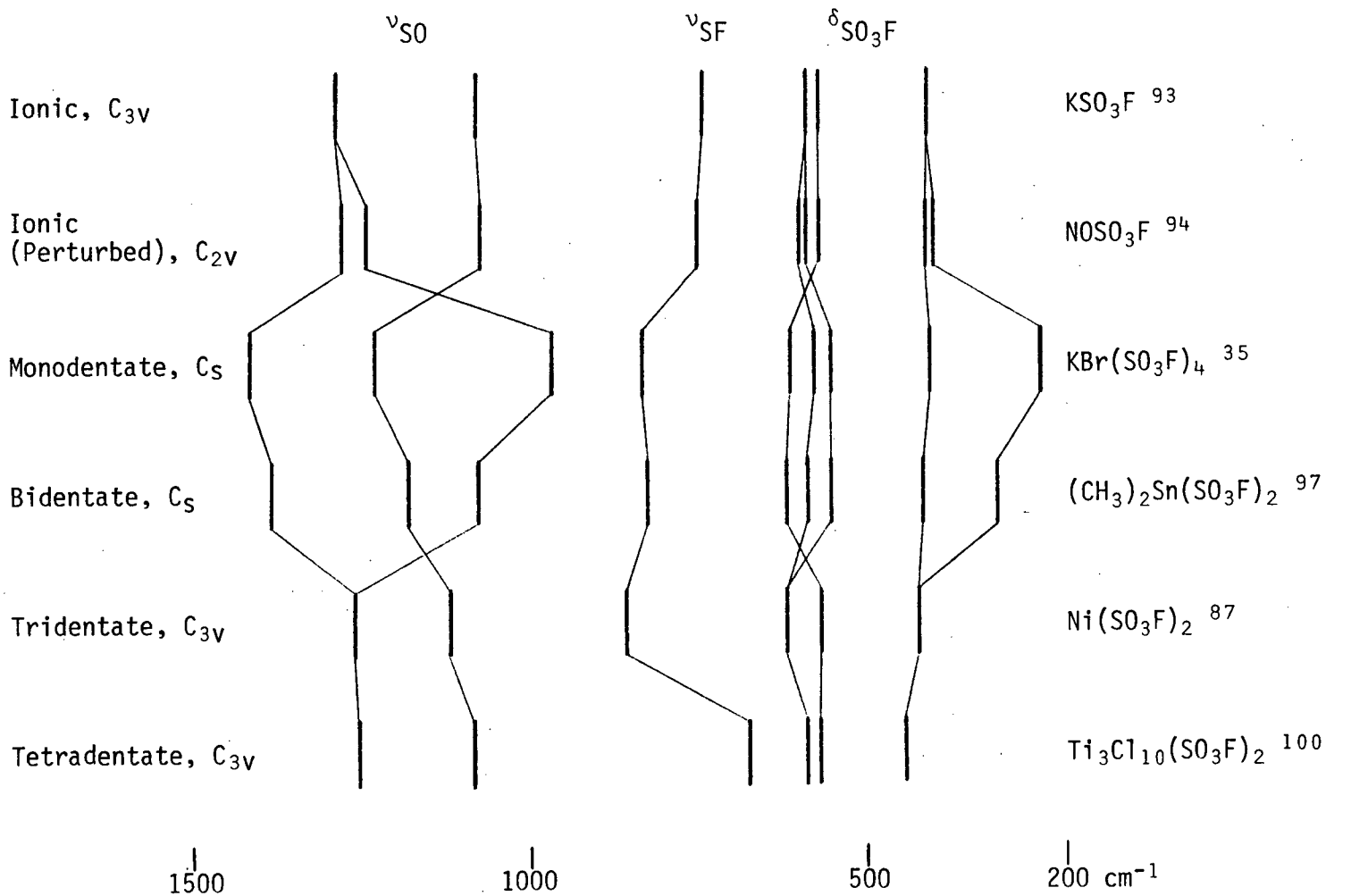

gives a vibrational spectrum representative of ionic fluorosulfate with bands at 1285, 1079, 745, (594, 586), 570 and 407 cm^{-1}.

b) ionic perturbed ——— With strongly polarizing and sometimes asymmetrical cations such as NO^+ and NO_2^+, splittings of the E modes are observed. For example, ν_4, (SO_3 stretch), becomes split by about 35 cm^{-1} in $NO(SO_3F)$ [94].

c) covalent monodentate ——— In Hal-SO_3F, the symmetry of the molecule is reduced to C_s, and the vibrational spectra show nine distinct bands. For example, in $ClSO_3F$, ν(S-F) is increased to 830 cm^{-1} and ν(S-O) are found at 1478, 1225 and 856 cm^{-1} [95].

d) covalent bidentate ——— As a bidentate ligand, the SO_3F group is usually found in the bridging mode between two metal ions, as in $(CH_3)_2Sn(SO_3F)_2$ [96,97]. For this type of coordination, ν(S-O) are found at ~1400, ~1150 and ~1070 cm^{-1}. While the example given here can be classified as containing bridging SO_3F groups spanning two identical metal ions, another type, which may be termed 'aniso-bidentate bridging' seem to occur in cases when the two metal ions have different charges. The spectra for such species, as in $M(II)[M(IV)(SO_3F)_6]$ [84,98] contain bands typical for both monodentate and bidentate SO_3F groups.

e) covalent tridentate ——— The 3d transition metal bis(fluorosulfates) are polymeric, each SO_3F ligand being coordinated to three different metal centres [87,99]. The symmetry of the anion is restored to C_{3v}. This type of coordination can be distinguished from the ionic C_{3v} situation by the high ν(S-F)

of about 850 cm^{-1} for these compounds.

f) covalent tetradentate ——— In the unique case involving $Ti_3Cl_{10}(SO_3F)_2$, the vibrational spectra for the compound indicate a C_{3v} symmetry for the SO_3F group. ν(S-F), however, is significantly lowered to 660 cm^{-1}, presenting evidence for the coordination of the fluorine atom as well [100].

Ionic fluorosulfates are not the only type that can show cation-anion interactions; in fact, most spectra of fluorosulfates have additional complexities caused by solid state splittings. Generally, vibrational spectra do provide useful information concerning the environment of the fluorosulfate group and the type of coordination. A number of diagnostic band positions together with their intensities normally allow a clear distinction between monodentate and bidentate coordinations, the two most commonly encountered types.

CHAPTER 2 EXPERIMENTAL

2.A INTRODUCTION

This chapter will deal only with general experimental techniques and the sources of starting chemicals used in this study; specific syntheses will be described in the appropriate chapters. Since most of the compounds involved are extremely moisture sensitive, an environment excluding air, (or more specifically,water), had to be employed.

Standard vacuum line techniques were used for the handling of volatile materials; all stop-cocks were of the greaseless teflon stem valve type from Kontes. Reactions were performed in one-part Pyrex reaction vials of about 30mL capacities, fitted with the teflon stop-cocks. Some typical glass apparatus used in this study is shown in Fig 2.1. When high gas pressures were anticipated in a reaction, 3mm thick-wall reactors were used in place of the standard 1mm-wall reactors.

In order to reduce the sources of contaminations, teflon coated stirring bars were used only when necessary. For the preparation of solutions for conductometric studies that required stirring, a glass-encapsulated stirring bar was used in a flat end reactor. In the course of the study, some specific situations required special modifications to the standard apparatus; a few are described in the appropriate chapters or shown in Fig 2.1.

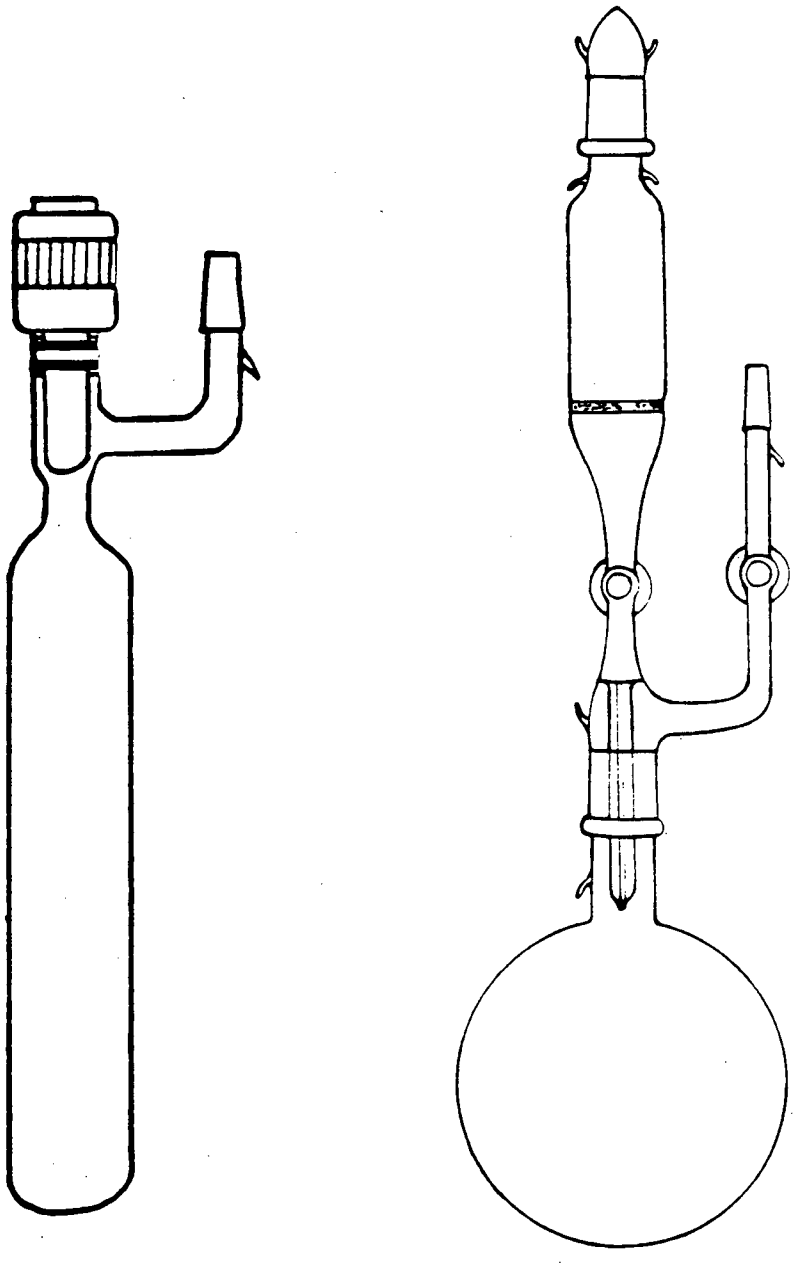

standard reactor

vacuum filter

FIG 2.1 EXAMPLES OF GLASS APPARATUS

All reactions were monitored by weight differences in the reaction vials. The removal of volatile materials after a reaction had completed usually proceeded by evacuating first at room temperature or below, followed by a further evacuation at ~40°C. The latter step was necessary especially in cases involving HSO_3F or $BrSO_3F$, as both have extremely low vapor pressures at room temperature.

Occasionally, the calculated yields from some reactions appeared to be low, with attack of the reaction vessel and the subsequent weight loss as SiF_4 the primary reason. In particular, high temperature reactions involving any fluorosulfate-containing reactants and extended reaction times were vulnerable to such an attack. Nevertheless, the reduction in the weights of the reactors were usually below 10mg and did not justify the use of less convenient vessels such as those made of fluoro-plastics (Kel-F) or metal. For reactions involving BrF_5 or fluorine at high pressure, Monel reactors were used.

2.B GENERAL EQUIPMENT

2.B.1 DRYBOX

The handling of hygroscopic materials that had limited volatilities at room temperature necessitated the use of a dry box — a Vacuum Atmosphere Corporation Dry-Lab, Model HE-43-2 fitted with a Dri-Train Model HE-93-B recirculating unit. The inert atmosphere of dry nitrogen gas was constantly drawn through

a molecular sieve chamber to maintain its purity.

2.B.2 ELECTRICAL CONDUCTIVITY

The conductivity cell, shown in Fig 2.2, is similar to the design of Barr et al [21]. This cell allowed the measurement on solutions with between ~7 to ~100mL of volumes. The platinum-black coating of the electrodes was renewed from time to time by electroplating from a solution of H_2PtCl_6 [101]. The cell constants were determined using aqueous KCl solutions of ~0.01M [102] and had values from (5.367 ± 0.007) to (5.353 ± 0.017) cm^{-1}.

The quantitative measurements of conductivity were carried out using a Wayne-Kerr Universal Bridge, Model B221A. The cell temperature of (25.00 ± 0.01)°C was maintained by immersion into an oil bath of ~35L capacity, regulated by a Sargent Thermonitor, Model ST. It was noted that after about 5 minutes, most of the solutions studied did not show any further variations in their conductivities. The equilibration period for all solutions was about 10 minutes in the oil bath after each addition of new materials to the cell.

In the beginning of this study, the addition of solutes or solvent to the cell was by the use of weight droppers, shown in Fig 2.3. It had previously been noted that the introduction of small amounts of moisture into the cell during the insertion and removal of the dropper led to a small but consistent rise in the conductivity of pure HSO_3F of the order of 10^{-5} $\Omega^{-1}cm^{-1}$ [103].

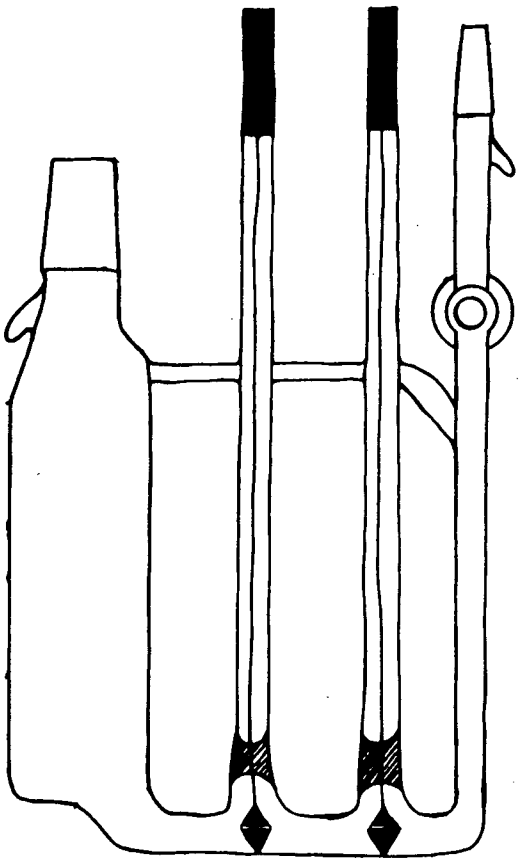

FIG 2.2 CONDUCTIVITY CELL

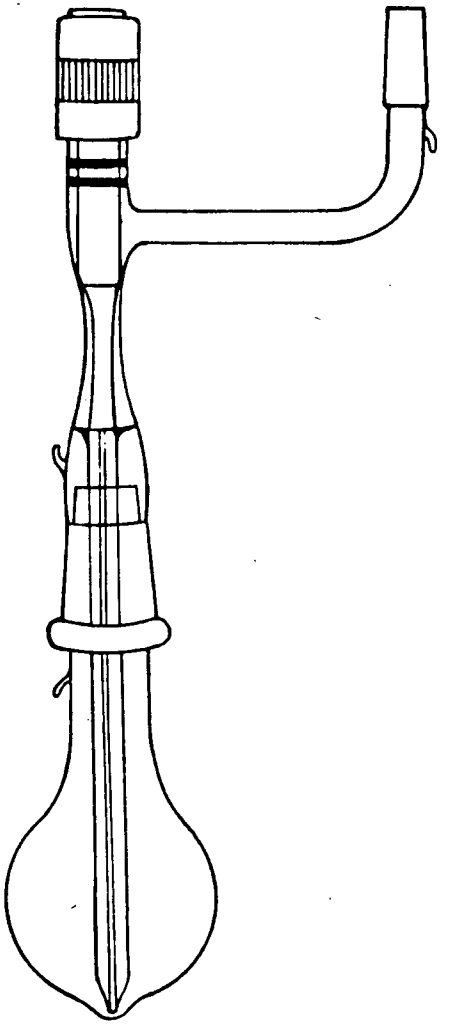

FIG 2.3 WEIGHT DROPPER

Because of the small quantities of solutes used in this study (~1 mmol), and the low molecular weight of water (18 $g \cdot mol^{-1}$), it was decided that this interference was not acceptable. Furthermore, the formation of HF and H_2SO_4 from the hydrolysis of HSO_3F would introduce two basic solutes in HSO_3F. Obviously, conductometric studies of acids in HSO_3F, the main objective of this study, would be adversely affected by this side reaction.

The volumetric addition of solutions, although limited in accuracy by the buret (±0.02 mL), provided an alternative that excluded the exposure to moisture. Such a buret is illustrated in Fig 2.4. Designed to be filled in the Dry box, which limited its maximum capacity to ~20mL, the buret's accuracy was maximized by using large volumes of dilute solutions. The actual measurement of the density of the solution to be added did not have to be performed as the buret was used as a fractionating device only. As long as the initial and final volumes and weights were known the intermediate quantities were calculated as a fraction of the total quantity. This also minimized errors due to the increase in the internal bore of the buret from etching, which would make any density measurements derived from other sources meaningless. This volumetric addition produced results that were better reproducible and less error prone than the method which monitors successive additions by weight.

FIG 2.4

VOLUMETRIC DROPPER

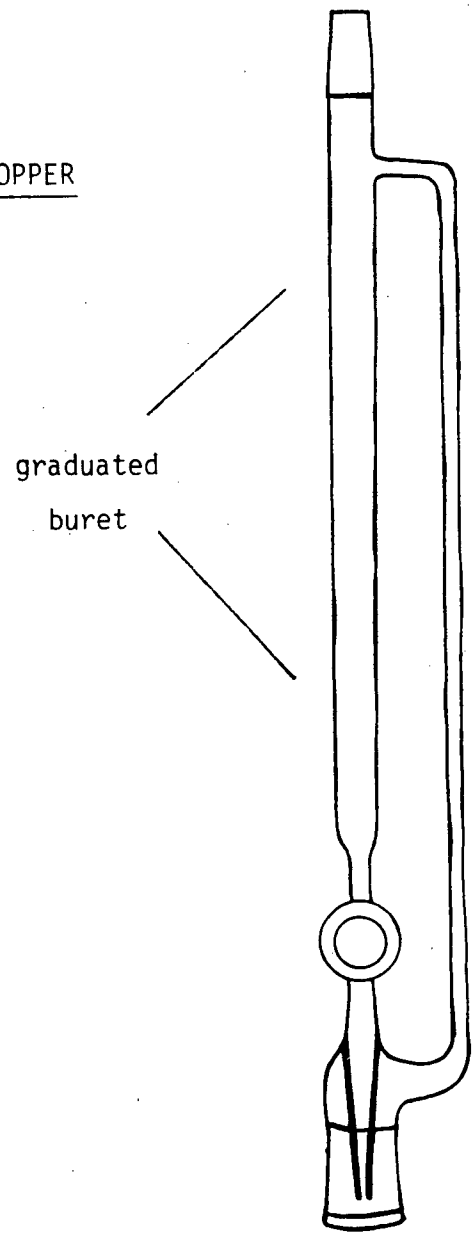

2.B.3 I.R. SPECTROMETRY

Routine i.r. spectra at room temperature were recorded on either a Perkin Elmer, Model 457,or a Pye Unicam Model SP1100, Grating Spectrophotometer, providing low frequency limits of 250 and 400 cm^{-1}, respectively. Spectra were taken on thin solid films pressed between AgBr, AgCl or BaF_2 windows with a transmission range down to ~250 cm^{-1}, ~400 cm^{-1} or ~800 cm^{-1}, respectively. The high reactivity of the fluorosulfates studied precluded the use of mulling agents or other window materials. For solution spectra in HSO_3F, thin teflon films were used to protect the windows, (only the O-H region was of interest).

For low temperature spectra at ~80K, a Perkin-Elmer Model 225 Grating Spectrophotometer with a low frequency limit of 200 cm^{-1} was used. The cell was of the Hörnig-Wagner design [114], consisting of an evacuable Pyrex Dewar with a pair of CsI windows. The Dewar cooled a brass sample window holder directly. Volatile samples could be condensed onto a cooled CsI window and solid samples could be directly deposited.

All spectra were calibrated with a polystyrene reference.

2.B.4 RAMAN SPECTROMETRY

Raman spectra were usually obtained with a Spex Ramalog 5 spectrophotometer equipped with a Spectra Physics Model 164 argon ion laser and using the 514.5 nm exciting line. The samples were contained in melting point capillaries. For compounds that were

brown or red, the green laser was found to cause local decomposition. Therefore, for these compounds, Raman spectra of reduced resolution were sometimes obtained using a Cary 81 spectrophotometer equipped with a Spectra Physics Model 125 He-Ne laser with a 632.8 nm exciting line. The samples were contained in 5 mm flat end Pyrex tubes.

A low temperature cell for the Ramalog 5, shown in Fig 2.5, was developed to enable the recording of spectra of compounds that were unstable to the laser at room temperature. The sample capillary was held in the brass sample holder (cooled to -80K) with grease. Generally, compared to spectra obtained at room temperature, better resolution was obtained. Shifts of bands to lower wavenumber, of the order of 3 to 5 cm^{-1}, were also noted.

2.B.5 ELECTRONIC SPECTROMETRY

Diffuse reflectance spectra of powdered solids from 350 to 740 nm were obtained on a Bausch and Lomb Spectronic 600 Spectrophotometer. For absorption spectra on mulls (in $C_8F_{17}SO_2F$ or fluorolube oil), or solutions in HSO_3F, a Cary 14 Spectrophotometer with a range from the near i.r. to 210 nm, was used. Standard silica solution cells used were of 1 or 10 mm path lengths. Solid mulls were pressed between quartz plates of 2.5 cm diameters and held inside a teflon sample holder.

FIG 2.5 LOW TEMPERATURE RAMAN CELL

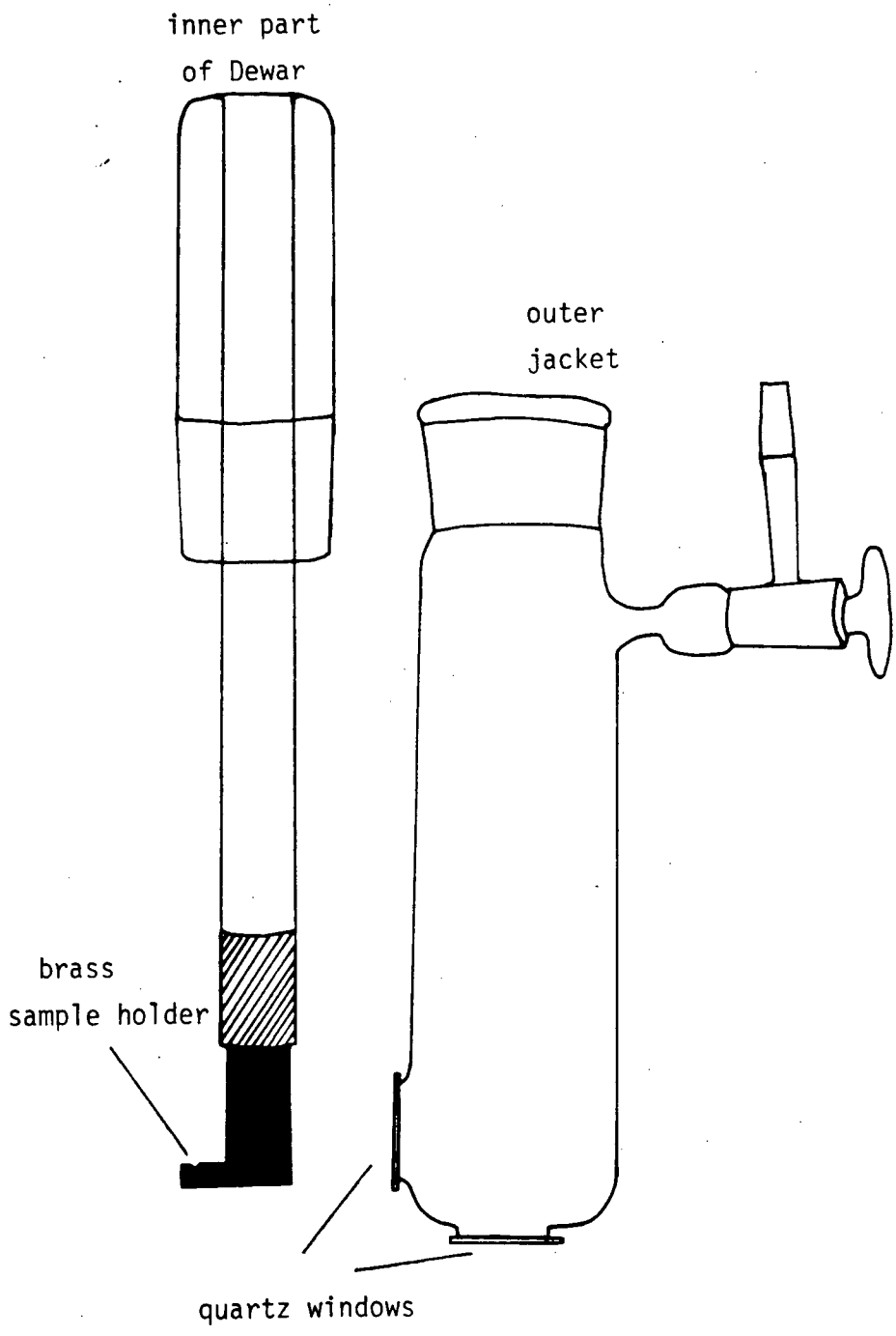

2.B.6 MAGNETOCHEMISTRY

Magnetic susceptibilities were measured using a Gouy apparatus described by Clark and O'Brien [105]. The calibration was performed using $Hg[Co(SCN)_4]$ [106]. The temperature of the sample was controlled by the rate of evaporation of liquid nitrogen around the chamber.

Diamagnetic corrections were taken from Landolt-Börnstein [107] and listed in Table 2.1.

2.B.7 NUCLEAR MAGNETIC RESONANCE

^{1}H — Using a Varian T-60 or a Varian EM-360, both operated at 60 MHz, spectra were recorded of solutions contained in 5 mm n.m.r. tubes and referenced to external TMS.

^{19}F — C.W. spectra were recorded on a Varian EM-360 operated at 56.45 MHz using 5 mm n.m.r. tubes. The lock signal was provided by either external $CFCl_3$ or internal HSO_3F. F.T. spectra were recorded on a Varian XL-100 operated at 94.1 MHz locked on external D_6-acetone. All ^{19}F-spectra are referenced to $CFCl_3$ with shifts to lower field considered negative.

^{119}Sn, ^{195}Pt — F.T. spectra were obtained on a Brüker Spectrospin 80 operated at 29.88 MHz for ^{119}Sn and 21.72 MHz for ^{195}Pt , 10 mm n.m.r. tubes were used, and the spectrometer was locked to external D_6-acetone. No specific references for the chemical shifts were used.

Table 2.1 DIAMAGNETIC SUSCEPTIBILITIES [107] (in cgs units)

Au^{3+} —— -27×10^{-6}
Cs^{+} —— -31×10^{-6}
Ir^{3+} —— -34×10^{-6}
Ir^{4+} —— -28×10^{-6}
Pd^{2+} —— -25×10^{-6}
Pd^{3+} —— -22×10^{-6}
Pd^{4+} —— -18×10^{-6}
Pt^{4+} —— -28×10^{-6}
Sn^{4+} —— -16×10^{-6}
SO_3F^{-} —— -40×10^{-6} (by analogy with SO_4^{2-})

Pascal constants : Br — -30.6×10^{-6}, Cl — -20.1×10^{-6}, O — $\sim-4\times10^{-6}$

Table 2.2 CHEMICALS USED WITHOUT PURIFICATION

Chemical	Source	Purity (%)
Au, -20 mesh	Alfa	99.995
Au_2O_3	Alfa	reagent grade
Ge, -325 mesh	Alfa	99.999
GeO_2	MCB	99.999
Ir, -60 mesh	Alfa	99.9
Mo, -200 mesh	Alfa	>99.9
Pd, -60 mesh	Alfa	99.9
Pt, -60 mesh	Alfa	99.9
$PtCl_2$	Strem	99.9
Sn, 20 mesh	BDH	99.97
W, -100 mesh	Alfa	99.98

2.C CHEMICALS

2.C.1 USED WITHOUT PURIFICATION

These are mostly metal powder of high purity for which no purification was necessary or practical. They are listed in Table 2.2 along with their purities and their sources.

2.C.2 PURIFICATION REQUIRED

a) The alkali metal chlorides were dried in a 120°C oven

KCl — 99.9% from MCB

CsCl — 99.5% from BDH

b) $BaCl_2$ was obtained by the dehydration of $BaCl_2 \cdot 2H_2O$ (99.0%, Analar, BDH) in a 120°C oven.

c) Br_2 from Milinkroft (AR grade) was purified by storage in a Pyrex vessel containing P_2O_5 to remove moisture and KBr to remove Cl_2.

d) Cl_2 from Matheson was passed through $KMnO_4$ to remove HCl and bubbled through concentrated H_2SO_4 to remove moisture.

e) SO_2 from Matheson, was liquidfied in a Pyrex vessel containing P_2O_5 as the desiccant.

f) NOCl from Matheson, was liquidfied and stored in a Pyrex vessel with $CaSO_4$ as the desiccant.

g) HSO_3F, from Allied Chemical, was purified by double distillations in a Pyrex apparatus at 1 atm. of dry nitrogen [21]. The constant boiling fraction at 163°C was either collected into a conductivity cell or into a large Pyrex storage vessel for

synthetic uses. The freshly distilled acid had a specific conductance of $1.1\text{-}1.3\times10^{-4}$ $\Omega^{-1}cm^{-1}$.

h) HSO_3CF_3 from Minnesota Mining and Manufacturing Company was distilled from concentrated H_2SO_4 at about 15 torr of dry nitrogen. The fraction with a boiling point of 120°C was collected.

2.C.3 SYNTHESIS REQUIRED

a) $S_2O_6F_2$ was prepared by the reaction between SO_3 and F_2 in a N_2 flow system catalyzed by AgF_2 [71]. The crude product was condensed as a liquid in Pyrex traps cooled by dry ice. Most of the FSO_3F was allowed to escape by warming the product to room temperature. Any excess SO_3 was removed by washing the crude product with concentrated H_2SO_4 followed by the subsequent separation of the two immiscible layers using a separation funnel. The product was then exacuated at dry ice temperature to remove the last traces of FSO_3F and then vacuum distilled into a large one-part Pyrex storage vessels stoppered with Kontes teflon stopcocks.

b) $BrSO_3F$ was prepared by reacting Br_2 with a slight excess of $S_2O_6F_2$ [78] in a long stem Pyrex reactor. The excess of $S_2O_6F_2$ was required to prevent the presence of unreacted Br_2. The crude product was pumped briefly to remove any oxygen formed and then stored.

c) $ClSO_3F$ was prepared by the reaction of a mixture of Cl_2 with $S_2O_6F_2$ in a Monel reactor at 125°C for 5 days [77]. Excess

reactants were removed by evacuation at dry ice temperature. The product was stored in the monel reactor.

d) ClO_2 was prepared from the reaction of $NaClO_3$ and H_2SO_4 in the presence of oxalic acid according to Brauer [118]. The product was used immediately for the preparation of ClO_2SO_3F.

e) ClO_2SO_3F was synthesized by distilling a large excess of $S_2O_6F_2$ into a thick wall reactor containing ClO_2 at -198°C [109]. The reactor was allowed to warm up slowly to room temperature. The resulting 2-layer liquid was pumped in vacuo to remove the excess $S_2O_6F_2$.

2.C.4 ELEMENTAL ANALYSES

These were performed by Analytische Laboratorien (formerly A. Bernhardt) Gummersbach, West Germany.

CHAPTER 3 PALLADIUM-FLUOROSULFATE

3.A INTRODUCTION

In the periodic group of Ni-Pd-Pt, the chemistry of palladium has received the least amount of attention in the past. As is commonly found in transition metal chemistry, a gradual increase in the stability of higher oxidation states of the metal is noted as one goes down the group [110]. Therefore, nickel is usually found in the +2 oxidation state, Ni(IV) being the highest one observed; platinum, on the other hand, exhibits both the +2 and +4 oxidation states, Pt(VI) being the highest one known. Both the +2 and +4 oxidation states of palladium are also quite common, but it is unlike platinum in that the divalent state is found to be more prevalent, examples for Pd(IV) being somewhat rare. The highest obtainable oxidation state of palladium is +5, and as is usually the case, it is found in a fluoride, the recently reported $O_2^+[PdF_6]^-$, and possibly $O_2^+[Pd_2F_{11}]^-$ [111]. While many organometallic compounds of palladium, like those of nickel and platinum, display oxidation states of 0 and +1, it is interesting to note that Pd(III), and also Pt(III), are exceedingly rare, and only a few examples such as the dicarbollyl of $Et_4N[Pd(\pi\text{-}2,3B_9C_2H_{11})_2]$ [112] have been reported. Generally, these compounds with palladium in the formal oxidation state of +3 are hard to make (electrochemical methods are often used), and require chelating or π bonding ligands to delocalize the metal's charge.

In the coordination chemistry of Ni(II), the d^8 ion usually exists in either one of three configurations: octahedral, e.g. $[Ni(H_2O)_6]^{2+}$; square planar, e.g. $[Ni(CN)_4]^{2-}$; or, tetrahedral, e.g. $[NiCl_4]^{2-}$. Magnetochemistry can provide an excellent means of differentiating between the three geometries: square planar complexes are diamagnetic while both octahedral and tetrahedral ones are paramagnetic, with magnetic moments that should correspond to two unpaired electrons. Because the tetrahedral configuration has a $^3T_1$ ground state, a large orbital contribution to its magnetic moment is expected, resulting in μ_{eff} values being much higher than the spin only value of 2.83 μ_B. This can also lead to a complex temperature dependence of the magnetic susceptibility, rather than the Curie-Weiss law behavior observed for octahedral compounds. For Pd(II) and Pt(II), diamagnetic square planar complexes are almost exclusively found. The increase in ligand field splitting for these two heavier elements of the group causes the $d_{x^2-y^2}$ orbital to be extremely high in energy, i.e., antibonding. Thus, a square planar configuration, in which the strongly antibonding $d_{x^2-y^2}$ can remain vacant, is favored. Also due to the large Δ_o, Pd(IV) and Pt(IV) are invariably octahedral, with a $^1A_{2g}$ electronic ground state.

The palladium-fluorine system represents some rather interesting anomalies and will be briefly reviewed because similarities between the corresponding fluoro- and fluorosulfato- compounds are to be expected.

PdF_2, formed by the reduction of the trifluoride by either SF_4 or SeF_4 [113], is the only paramagnetic binary Pd(II) compound. A magnetic moment of 1.84 μ_B, suggesting the presence of a magnetically concentrated system, is reported. The rutile structure of PdF_2 [104], with an octahedral coordination for Pd(II), and almost linear Pd-F-Pd bonds, allows antiferromagnetic coupling via the superexchange mechanism [115]. Therefore, it is not surprising to find that in mixed crystals of PdF_2-ZnF_2, the effective magnetic moment of Pd(II) increases with the amount of ZnF_2 diluent present, and at infinite dilution, an extrapolated μ_{eff} of ~3.2μ_B for PdF_2 is obtained [116]. Paramagnetism is also found for some derivatives of PdF_2, such as $CsPdF_3$ [117], $ZnPdF_4$ [116] and Pd(II)M(IV)F_6, with M=Ge, Sn, Pd, Pt [108]; but $BaPdF_4$ is reported to be diamagnetic [116]. Although PdO is diamagnetic [119], a compound which may be formulated as K_8Pd(II)Pd(IV)$_3O_{11}$ is paramagnetic, with a magnetic moment of 2.76μ_B for Pd(II) [120]. In contrast to the difluoride, the other palladium dihalides and their complexes are diamagnetic. For example, β-$PdCl_2$, isomorphous with the corresponding platinum chloride, consists of Pd_6Cl_{12} clusters with square planar [$PdCl_4$] units linked by chlorine-bridges [121].

While the other halogens form only the dihalides, fluorine, because of its high oxidizing power, is capable of supporting two additional binary fluorides: Pd_2F_6 and PdF_4. PdF_6, expected to be an even stronger oxidizing agent than PtF_6, has not been

successfully synthesized [122].

Palladium dibromide dissolves in BrF_3 to form a compound of the composition of $PdF_3 \cdot BrF_3$ which, upon heating, decomposes to form the trifluoride [123]. The trifluoride is paramagnetic, and its formulation as PdF_3 gives a magnetic moment of $2.04\mu_B$, suggesting a low spin d^7 electronic configuration for Pd(III) [124]. The absence of Jahn-Teller distortion in the solid state led Bartlett to invoke a mixed valency composition - Pd(II)Pd(IV)F_6, for the compound [108]. The recalculated magnetic moment of $2.88\mu_B$ for Pd_2F_6 is consistent with the presence of high spin d^8 Pd(II) and low spin d^6 Pd(IV), both in octahedral ligand fields. A recent neutron diffraction study shows Pd_2F_6 to be isomorphous with Pd(II)M(IV)F_6, with M=Ge, Sn, Pt [125], and M(II)Pd(IV)F_6, with M=Mg, Ca, Zn, Cd [126]. Although the two types of palladium species in the solid state cannot be distinguished in terms of their ionic radii, they can be found in two regular octahedral sites of different dimensions.

The tetrafluoride can be obtained by the direct fluorination of the trifluoride at 300°C and 7 atm. [127]. PdF_4 is diamagnetic[108], and a neutron diffraction study indicates octahedral coordination for Pd(IV) [128]. In view of the high oxidation state for palladium in PdF_4, the low spin d^6 electronic configuration found is not unexpected. Diamagnetic complexes of the type of $M_2[PdF_6]$, with M=K, Rb, Cs, can be readily obtained by the fluorination of the complex chloride with either fluorine [129] or BrF_3[130].

Both these Pd(IV)-containing fluorides are strong oxidizing agents, for example, they are capable of converting XeF_2 to XeF_4 [131]. This is consistent with the generally observed trend that Pd(IV) is usually more strongly oxidizing and more difficult to obtain than the corresponding Pt(IV) compounds. To summarize, the fluorides of palladium show some marked differences when compared to the other halides: a) higher oxidation states can be obtained in the fluoride system; and b) the difluoride and some of its derivatives deviate from the square planar geometry in favor of octahedral structures. Futhermore, the existence of $[PdHal_4]^{2-}$ and $[PdHal_6]^{2-}$, with Hal=F, Cl, indicates halide ion acceptor properties of the palladium halides. The formation of $[PdCl_6]^{2-}$ complexes is interesting in that the parent compound - $PdCl_4$, has not been prepared.

The investigation into the hitherto unknown palladium fluorosulfate system is expected to contribute further insights into both the halide and fluorosulfate systems [98,132].

3.B EXPERIMENTAL

3.B.1 SYNTHESIS OF PALLADIUM BIS(FLUOROSULFATE)

3.B.1.1 OXIDATION OF PALLADIUM METAL WITH $BrSO_3F$

$$Pd + 2BrSO_3F \longrightarrow Pd(SO_3F)_2 + Br_2 \qquad (3.1)$$

In a typical reaction, palladium metal (508 mg, 4.77 mmol), was allowed to react with an excess of $BrSO_3F$(~5 mL) at ~110°C for 2 weeks. This slow reaction led to the formation of a purple powder in the mixture. The removal of all volatile materials

yielded $Pd(SO_3F)_2$,(1.437 g, 4.72 mmol).

$Pd(SO_3F)_2$ is a light purple, hygroscopic, polycrystalline solid. It appears to lack any solubility in either $BrSO_3F$ or HSO_3F. When heated to above ~250°C, it decomposes, with condensations of SO_3-like crystals forming on the cooler part of the melting point capillary, suggesting a decomposition scheme of:

$$Pd(SO_3F)_2 \longrightarrow PdF_2 + 2SO_3 \qquad (3.2)$$

Analysis	Pd	S	F
Calculated %	35.10	21.15	12.49
Found %	34.94	21.06	12.47

3.B.1.2 THERMOLYSIS OF $Pd_2(SO_3F)_6$

$$Pd_2(SO_3F)_6 \longrightarrow 2Pd(SO_3F)_2 + S_2O_6F_2 \qquad (3.3)$$

The decomposition of $Pd_2(SO_3F)_6$, (323 mg, 0.343 mmol), at ~160°C in vacuo yielded $Pd(SO_3F)_2$, (277 mg, calc'd 244 mg), detected as the sole solid product by its Raman spectrum. $S_2O_6F_2$ was identified as the only volatile product (plus traces of SiF_4) by both i.r. and Raman spectroscopy. The reaction cannot be taken to completion because of the presence of small amounts of undecomposed $Pd_2(SO_3F)_6$ on the cooler part of the reaction vial inaccessible by heating.

3.B.1.3 REDUCTION OF $Pd_2(SO_3F)_6$ WITH Br_2

$$Pd_2(SO_3F)_6 + Br_2 \longrightarrow 2Pd(SO_3F)_2 + 2BrSO_3F \qquad (3.4)$$

Br_2, (~3 mL) was added to a sample of $Pd_2(SO_3F)_6$, (443 mg, 0.549 mmol), and the mixture was heated at 100°C for ½ hour.

The removal of all volatile material yielded $Pd(SO_3F)_2$, (339 mg, 1.113 mmol), identified by the i.r. spectrum of the purple solid obtained.

3.B.2 SYNTHESIS OF PALLADIUM TRIS(FLUOROSULFATE)

$$2Pd(SO_3F)_2 + S_2O_6F_2 \longrightarrow Pd_2(SO_3F)_6 \qquad (3.5)$$

An excess of $S_2O_6F_2$(~5 mL) was added to $Pd(SO_3F)_2$, (398 mg, 1.31 mmol). An immediate reaction was evident from the gradual darkening of the solid. The mixture was then heated at ~80°C for 12 hours to insure a complete conversion. After the removal of all volatile materials, $Pd_2(SO_3F)_6$ was obtained, (5.18 mg, 0.642 mmol).

$Pd_2(SO_3F)_6$ is a dark brown, hygroscopic powder. It displays no observable solubility in either $S_2O_6F_2$ or HSO_3F. It is thermally stable up to ~180°C at atmospheric pressure, although decomposition occurs at the lower temperature of ~120°C in vacuo according to equation (3.3).

Analysis	Pd	S	F
Calculated %	26.36	23.83	14.12
Found %	26.54	23.68	14.01

3.B.2.2 OXIDATION OF PALLADIUM METAL WITH $S_2O_6F_2/HSO_3F$

$$2Pd + 3S_2O_6F_2 \xrightarrow{HSO_3F} Pd_2(SO_3F)_6 \qquad (3.6)$$

A mixture of $S_2O_6F_2/HSO_3F$, (~5 mL), was distilled into a reactor containing palladium metal (215 mg, 2.02 mmol). After heating the mixture at ~100°C for 3 days, a reddish-brown solution

containing dark brown solids was formed, and all metal had reacted. The removal of all volatile materials yielded $Pd_2(SO_3F)_6$, (794 mg, 0.984 mmol).

3.B.3 SYNTHESIS OF HEXAKIS(FLUOROSULFATO)PALLADATE (IV) COMPLEXES

3.B.3.1 PREPARATION OF $Cs_2[Pd(SO_3F)_6]$

$$CsCl + HSO_3F \longrightarrow CsSO_3F + HCl \qquad (3.7)$$

$$2CsSO_3F + Pd + S_2O_6F_2 \xrightarrow{HSO_3F} Cs_2[Pd(SO_3F)_6] \qquad (3.8)$$

HSO_3F (~3 mL) was added to a mixture of palladium metal, (100 mg, 0.940 mmol), and CsCl, (316 mg, 1.877 mmol). After the removal in vacuo of all of the HCl formed from the initial solvolysis of CsCl, a mixture of $S_2O_6F_2/HSO_3F$, (~5 mL), was distilled into the reactor. An immediate reaction occurred at room temperature, with the color of the solution taking on a deep red color. Further heating of the reactants at ~100°C for 3 days led to the dissolving of all the metal powder. The removal of all volatile materials yielded a solid which analyzed as $Cs_2[Pd(SO_3F)_6]$, (902 mg, 0.933 mmol).

The compound can also be made by the reaction of a 2:1 ratio of CsCl and palladium metal with ~5 mL of $BrSO_3F$. A typical reaction requires about 14 days at ~100°C.

$Cs_2[Pd(SO_3F)_6]$ is a dark red, hygroscopic, crystalline solid which is soluble in both $BrSO_3F$ and HSO_3F. It decomposes at ~200°C.

Analysis	Cs	Pd	F
Calculated %	27.50	11.01	11.79
Found %	27.25	10.85	11.67

3.B.3.2 PREPARATION OF $Ba[Pd(SO_3F)_6]$

$$BaCl_2 + 2HSO_3F \longrightarrow Ba(SO_3F)_2 \qquad (3.9)$$

$$Ba(SO_3F)_2 + Pd + 2S_2O_6F_2 \xrightarrow{HSO_3F} Ba[Pd(SO_3F)_6] \qquad (3.10)$$

In a manner analogous to the preparation of $Cs_2[Pd(SO_3F)_6]$, a mixture of $Ba(SO_3F)_2$, formed from the solvolysis of $BaCl_2$, (310 mg, 1.490 mmol),in HSO_3F, and palladium metal, (158 mg, 1.490 mmol), was reacted with $S_2O_6F_2/HSO_3F$, (~5 mL). An immediate reaction also occurred at room temperature, with the formation of a bright red precipitate. The reaction mixture was heated at ~90°C for 7 days as the reaction was quite slow due to the insolubility of the product. The removal of all volatile materials yielded $Ba[Pd(SO_3F)_6]$, (1.233 g, 1.471 mmol).

An attempt to react a stoichiometric mixture of $BaCl_2$ and palladium metal with $BrSO_3F$ was unsuccessful as $Ba(SO_3F)_2$ was found to be insoluble in $BrSO_3F$.

$Ba[Pd(SO_3F)_6]$ is an orange-red, hygroscopic powder. It is slightly soluble in HSO_3F and is thermally stable up to ~200°C.

Analysis	Ba	Pd	S	F
Calculated %	16.39	12.70	22.95	13.60
Found %	16.24	12.64	22.89	13.82

3.B.3.3 PREPARATION OF $(ClO_2)_2[Pd(SO_3F)_6]$

$$2ClO_2SO_3F + Pd + 2S_2O_6F_2 \longrightarrow (ClO_2)_2[Pd(SO_3F)_6] \qquad (3.11)$$

Palladium metal, (129 mg, 1.212 mmol), was reacted with a mixture of ClO_2SO_3F (~0.5 mL) and $S_2O_6F_2$ (~5 mL). After maintaining a reaction temperature of ~70°C for 3 days, dark red crystals were formed together with the disappearance of all the metallic reactant. The removal of all volatile materials at ~60°C yielded $(ClO_2)_2[Pd(SO_3F)_6]$, (1.013 g, 1.212 mmol).

$(ClO_2)_2[Pd(SO_3F)_6]$,(749 mg, 0.896 mmol), was also prepared by the reaction of $Pd_2(SO_3F)_6$, (322 mg, 0.446 mmol), with a mixture of ClO_2SO_3F, (~0.5 mL), and $S_2O_6F_2$, (~2 mL), according to:

$$2ClO_2SO_3F + \tfrac{1}{2}Pd_2(SO_3F)_6 + \tfrac{1}{2}S_2O_6F_2 \longrightarrow (ClO_2)_2[Pd(SO_3F)_6] \qquad (3.12)$$

The product is a very dark red, hygroscopic, crystalline solid. It is soluble in both HSO_3F and ClO_2SO_3F, and melts with decomposition at ~200°C

Analysis	Cl	Pd	F
Calculated %	8.48	12.73	13.64
Found %	8.60	12.82	13.68

3.B.3.4 PREPARATION OF $(NO)_2[Pd(SO_3F)_6]$

$$4NOCl + Pd \longrightarrow (NO)_2[PdCl_4] + 2NO \qquad (3.13)$$

$$(NO)_2[PdCl_4] + 3S_2O_6F_2 \xrightarrow{HSO_3F} (NO)_2[Pd(SO_3F)_6] + 2Cl_2 \qquad (3.14)$$

By the reaction of palladium metal, (110 mg, 1.034 mmol), with a large excess of NOCl, (~3 mL), at room temperature for

12 hours, $(NO)_2[PdCl_4]$, (316 mg, 1.025 mmol), was obtained. This intermediate, insoluble in NOCl, was identified by its i.r. spectrum which has two bands at 2150, (νN-O), and 332 cm^{-1}, ($\nu PdCl_4$). This solid was then reacted with a mixture of $S_2O_6F_2/HSO_3F$, (~6 mL), at 80°C for 1 hour. The removal of all volatile materials at ~70°C yielded $(NO)_2[Pd(SO_3F)_6]$, (780 mg, 1.025 mmol).

It can also be obtained by the oxidation of $(NO)_2[PdCl_4]$ by $BrSO_3F$, according to:

$$(NO)_2[PdCl_4] + 6BrSO_3F \longrightarrow (NO)_2[Pd(SO_3F)_6] + 2Cl_2 + 3Br_2 \quad , \qquad (3.15)$$

although a large excess of $BrSO_3F$ has to be used for the formation of a pure product.

$(NO)_2[Pd(SO_3F)_6]$ is a bright red, hygroscopic, crystalline solid. It is soluble in HSO_3F and less so in $BrSO_3F$. It melts with decomposition at ~200°C.

Analysis	N	Pd	S	F
Calculated %	3.68	13.99	25.29	14.99
Found %	3.44	13.81	25.11	15.17

3.B.4 SYNTHESIS OF PALLADIUM(II) HEXAKIS(FLUOROSULFATO) METALLATES(IV)

3.B.4.1 PREPARATION OF Pd $Pt(SO_3F)_6$

$$Pd(SO_3F)_2 + Pt(SO_3F)_4 \xrightarrow{HSO_3F} Pd[Pt(SO_3F)_6] \qquad (3.16)$$

Platinum metal, (224 mg, 1.148 mmol), was converted into $Pt(SO_3F)_4$ by oxidation with a mixture of $S_2O_6F_2/HSO_3F$. $Pd(SO_3F)_2$,

formed by the reaction of palladium metal, (121 mg, 1.128 mmol), with a mixture of $S_2O_6F_2/HSO_3F$ followed by the subsequent reduction of $Pd_2(SO_3F)_6$ with Br_2, was added to a solution of the $Pt(SO_3F)_4$ in HSO_3F. No reaction was apparent at room temperature. After heating the mixture at ~50°C for 3 days, a green homogeneous precipitate formed. The solid obtained after a filtration of the suspension was washed with HSO_3F and dried at ~80°C in vacuo.

$Pd[Pt(SO_3F)_6]$ is a light green, hygroscopic powder. It appears to be insoluble in HSO_3F and is thermally stable up to ~200°C.

Analysis	Pd	S	F
Calculated %	11.88	21.80	12.72
Found %	11.62	21.74	12.88

3.B.4.2 PREPARATION OF Pd $Sn(SO_3F)_6$

$$Pd(SO_3F)_2 + Sn(SO_3F)_4 \xrightarrow{HSO_3F} Pd[Sn(SO_3F)_6] \qquad (3.17)$$

$Pd[Sn(SO_3F)_6]$ was prepared in a reaction similar to that for $Pd[Pt(SO_3F)_6]$. $Pd(SO_3F)_2$ (539 mg, 1.770 mmol) was mixed with a stoichiometric amount of $Sn(SO_3F)_4$ formed from the reaction of tin metal (210 mg, 1.770 mmol) with $S_2O_6F_2/HSO_3F$. No reaction occurred when HSO_3F was added to the mixture; when the reactor was heated at ~70°C, a slow reaction, evident from the gradual clearing of the initially cloudy solution, took place. After 7 days in this condition, all the purple $Pd(SO_3F)_2$ solids had changed into a blue powder, and the supernatant became clear.

The solids were filtered, washed with HSO_3F and dried at ~70°C in vacuo.

$Pd[Sn(SO_3F)_6]$ is a light blue, hygroscopic powder. It is apparently insoluble in HSO_3F and decomposes at ~250°C to a light purple solid.

Analysis	Pd	Sn	S	F
Calculated %	12.98	14.48	23.47	13.41
Found %	13.06	14.61	23.31	13.72

3.B.5 SYNTHESIS OF TETRAKIS(FLUOROSULFATO)PALLADATE(II) COMPLEXES

3.B.5.1 REDUCTION OF $Cs_2[Pd(SO_3F)_6]$ BY Br_2/SO_2

$$Cs_2[Pd(SO_3F)_6] + 2SO_2 \xrightarrow{Br_2} Cs_2[Pd(SO_3F)_4] + 2S_3O_8F_2 \quad (3.18)$$

$Cs_2[Pd(SO_3F)_6]$, was prepared by the reaction of palladium metal, (100 mg, 0.940 mmol), and CsCl, (316 mg, 1.877 mmol), with $S_2O_6F_2/HSO_3F$. After all volatile materials were removed in vacuo, SO_2(~4 mL) and Br_2(~1 mL) were added to the solid. The reaction mixture was stirred at room temperature for 1 day. The removal of all volatile materials gave a light brown material which analyzed as $Cs_2[Pd(SO_3F)_4]$, (721 mg, 938 mmol).

$Cs_2[Pd(SO_3F)_4]$ is a light brown hygroscopic powder which melts with decomposition at ~195°C. It is slightly soluble in HSO_3F, but deposits $Pd(SO_3F)_2$ immediately; the filtered solid shows only the i.r. spectrum of $Pd(SO_3F)_2$.

Analysis	Cs	Pd	S	F
Calculated %	34.59	13.85	16.69	9.89
Found %	34.68	13.66	16.54	10.01

3.B.5.2 REDUCTION OF $Ba[Pd(SO_3F)_6]$ BY Br_2/SO_2

$$Ba[Pd(SO_3F)_6] + 2SO_2 \xrightarrow{Br_2} Ba[Pd(SO_3F)_4] + 2S_3O_8F_2 \qquad (3.19)$$

In a manner analogous to the preparation of $Cs_2[Pd(SO_3F)_4]$, $Ba[Pd(SO_3F)_6]$ (196 mg, 0.941 mmol), prepared from the reaction of $BaCl_2$ and palladium metal (100 mg, 0.940 mmol) with $S_2O_6F_2/HSO_3F$, was reduced with a mixture of Br_2/SO_2 to give a compound suggesting the formulation of $Ba[Pd(SO_3F)_4]$, (602 mg, 0.941 mmol).

$Ba[Pd(SO_3F)_4]$ is a very light brown hygroscopic powder. It decomposes at ~200°C to a purple solid. It is insoluble in HSO_3F.

$(NO)_2[Pd(SO_3F)_4]$ can also be prepared likewise.

Analysis :	Ba	Pd	S	F
Calculated %	21.46	16.63	20.04	11.88
Found %	21.22	16.82	20.03	11.92

3.C DISCUSSION

3.C.1 SYNTHESIS AND GENERAL DISCUSSION

3.C.1.1 BINARY FLUOROSULFATES

$Pd(SO_3F)_2$ can be prepared by one of three methods:

a) the oxidation of palladium metal with $BrSO_3F$,

b) the reduction of $Pd_2(SO_3F)_6$ with Br_2, and

c) the controlled pyrolysis of $Pd_2(SO_3F)_6$.

Reaction a) has two precedents: the interaction of gold and platinum with $BrSO_3F$ is reported to yield the corresponding Au(III) and Pt(IV) fluorosulfates [82]. However, palladium metal is found to be much less reactive towards $BrSO_3F$, and long reaction times at high reaction temperatures of ~160°C are required. Further differences can be found in the solubilities of the three products in the reaction media: while both $Au(SO_3F)_3$ and $Pt(SO_3F)_4$ dissolve readily to form rather stable intermediates, $Pd(SO_3F)_2$ precipitates from the reaction mixture and no evidence of complex formation is evident. The high thermal stability, and its seeming insolubility in both $BrSO_3F$ and HSO_3F even at temperatures up to ~160°C, are consistent with $Pd(SO_3F)_2$ having a polymeric structure.

Although reaction a) provided the only direct synthesis of $Pd(SO_3F)_2$, the reduction of $Pd_2(SO_3F)_6$ by Br_2 was subsequently found to be the preferred method because of the ready availability of the trisfluorosulfate. Also, the product from reaction a) was found to contain traces of a brown substance, most likely

$Pd_2(SO_3F)_6$, which had to be decomposed by evacuation at ~120°C. The observation seems to imply that $BrSO_3F$ is capable of the oxidation of palladium metal to the tetravalent state, and this is indeed found in the preparation of soluble $[Pd(SO_3F)_6]^{2-}$ complexes. The successful reduction of $Pd_2(SO_3F)_6$ to $Pd(SO_3F)_2$ by Br_2, commonly used as an oxidizing agent, indicates the strong oxidizing ability of Pd(IV), in keeping with general observations regarding the chemistry of palladium [119,131].

The purple color of $Pd(SO_3F)_2$ provides an interesting comparison with other binary Pd(II) compounds: PdF_2 is also purple in color, but the other dihalides are brown. This may suggest an octahedral coordination for Pd(II) in the bis(fluorosulfate), as in the difluoride.

The facile preparation of $Pd_2(SO_3F)_6$ by the oxidation of the metal with a solution of $S_2O_6F_2$ in HSO_3F illustrates the importance of the presence of a suitable solvating medium in these reactions, even though the product may only be slightly soluble in HSO_3F. Without the addition of HSO_3F, the oxidation of the metal hardly proceed at all, even at ~160°C at a high pressure of $S_2O_6F_2$ in a Monel reactor.

An alternate formulation of the tris(fluorosulfate) as $Pd(SO_3F)_3$ would imply the presence of Pd(III), a very uncommon oxidation state and in contrast to the trifluoride, which is the mixed valency compound of Pd(II) $Pd(IV)F_6$ [108]. It is very likely that such an analogy exists in the fluorosulfate system, and

experimental evidence consistent with the formulation will be discussed subsequently.

3.C.1.2 FLUOROSULFATO COMPLEXES OF PALLADIUM

Both the binary fluorosulfates of palladium are insoluble in HSO_3F, thus precluding their uses as superacids in HSO_3F. However, the formulation of the tris(fluorosulfate) as a mixed valency compound suggests the existence of a $[Pd(IV)(SO_3F)_6]^{2-}$ species and a $Pd(II)[M(IV)(SO_3F)_6]$ species, much like $[PdF_6]^{2-}$ and $Pd[M(IV)F_6]$ in the fluoride system. Therefore, complexation reactions were attempted.

A general preparative route to complexes containing $[Pd(SO_3F)_6]^{2-}$ is the oxidation of the metal by $S_2O_6F_2/HSO_3F$ in the presence of a basic fluorosulfate. This method has also been used successfully in the preparation of complexes containing other metals in high oxidation state. The reaction involving ClO_2SO_3F did not require HSO_3F as a solvent because the former is a supercooled liquid at room temperature and can act as an ionizing solvent [134].

The synthesis of $(NO)_2[Pd(SO_3F)_6]$ by the reaction of $(NO)_2[PdCl_4]$ with $S_2O_6F_2$ illustrates the oxidation of Pd(II) to Pd(IV) with the replacement of Cl^- by SO_3F^-. The moderate reaction temperature of ~80°C minimized the formation of ClO_2SO_3F (by the oxidation of Cl_2 with $S_2O_6F_2$ in the presence of glass) although a small amount of a ClO_2SO_3F-like, red liquid was

detected as a by-product. The complete removal of this contaminant in vacuo at ~70°C is indicated by the agreement in the analytical result for the NO^+-complex. Since both the ClO_2^+- and the NO^+-complexes of $[Pd(SO_3F)_6]^{2-}$ have nearly identical thermal stabilities, the preferential formation of the latter may be due to:

a) the greater volatility of ClO_2SO_3F, and/or

b) the higher lattice energy expected for $(NO)_2[Pd(SO_3F)_6]$ due to the smaller size of the cation.

Although only four examples of complexes containing $[Pd(SO_3F)_6]^{2-}$ are reported here, other complexes containing M(I) and M(II) cations are expected to be obtainable using the general methods described here.

The synthesis of $Pd(II)[M(IV)(SO_3F)_6]$ involved the addition of a slight excess of $M(SO_3F)_4$, where M=Pt, Sn, to $Pd(SO_3F)_2$ followed by digestion in HSO_3F and subsequent filtration of the insoluble products. The excess is needed to ensure a stoichiometric ratio in the end products because of difficulties encountered in weighing the fluorosulfates accurately in the dry box. The rather low solubility of $Sn(SO_3F)_4$ in HSO_3F [33] dictated a rather long reaction time. However, in the reaction involving the very soluble $Pt(SO_3F)_4$, only a very slight increase in the reaction rate was noted; this provided more evidence for the extremely high degree of polymerization and insolubility for $Pd(SO_3F)_2$. The colors of these compounds (light blue for

$Pd[Sn(SO_3F)_6]$ and light green for $Pd[Pt(SO_3F)_6]$), also departed from the dark colors usually associated with square planar Pd(II) compounds. Thus the Pd(II) ion in these two fluorosulfato-complexes may be octahedrally coordinated.

In the preceeding reaction, $Pd(SO_3F)_2$ acts formally as a SO_3F^- donor, i.e., a base. Attempts were also made to involve the bis(fluorosulfate) in anionic complex formation; initially, these attempts were unsuccessful:

a) $CsSO_3F$ was found not to undergo any direct complexation reaction with $Pd(SO_3F)_2$, even after heating the mixture in HSO_3F at ~160°C. The solid obtained after filtration gave only an i.r. spectrum of unreacted $Pd(SO_3F)_2$.

b) The attempted solvolysis of $(NO)_2[PdCl_4]$ in HSO_3F at ~160°C produced an inhomogeneous mixture of white and brown solids (the starting material is brown). The i.r. spectrum taken of this mixture showed only bands due to $NOSO_3F$. The weight of the final product suggests that the solvolysis reaction must have occurred according to:

$$(NO)_2[PdCl_4] + 2HSO_3F \longrightarrow 2NOSO_3F + PdCl_2 + 2HCl \quad . \qquad (3.20)$$

Subsequently, a sample of $PdCl_2$ was indeed found not to react with HSO_3F at ~160°C, most likely a result of its high degree of polymerization.

c) The solvolysis of $(NO)_2[PdCl_4]$ in $BrSO_3F$ also led to the oxidation of Pd(II) to Pd(IV). This implies that the formation of $Pd(SO_3F)_2$ from the reaction of $BrSO_3F$ with the metal may be

due to the insolubility of $Pd(SO_3F)_2$ in the reaction medium rather than as a consequence of the limited oxidizing ability of $BrSO_3F$.

d) Because of the ability of Br_2 to reduce $Pd_2(SO_3F)_6$ to $Pd(SO_3F)_2$ at elevated temperature, the reduction of $Cs_2[Pd(SO_3F)_6]$, $Ba[Pd(SO_3F)_6]$ and $(NO)_2[Pd(SO_3F)_6]$ with Br_2 were attempted. But even at a reaction temperature of ~120°C, only $(NO)_2[Pd(SO_3F)_6]$ showed any signs of a reaction taking place, and the product is a mixture of unreacted $(NO)_2[Pd(SO_3F)_6]$, and some white/purple solids which could be $NOSO_3F$ and $Pd(SO_3F)_2$.

e) As the lack of a suitable solvent could have led to the demise of the above reduction attempt, a mixture of Br_2/HSO_3F was heated with $Ba[Pd(SO_3F)_6]$ at ~70°C for 1 day. The removal of volatile materials yielded a light brown product with a weight corresponding to the composition of $BaPd(SO_3F)_4$. An i.r. spectrum of the product, however, showed the presence of some bands due to $Pd(SO_3F)_2$, and therefore, although a reduction had taken place, some decomposition of the product had also occurred.

Since the reduction of a fluorosulfate with Br_2 usually leads to the formation of $BrSO_3F$, if it can be removed from an equilibrium, the reaction may be encouraged to proceed more effectively. SO_2 was used as such a $BrSO_3F$ scrubber. The successful reduction of $[Pd(SO_3F)_6]^{2-}$ complexes with a Br_2/SO_2 mixture at room temperature probably proceeds via the following scheme:

$$[Pd(SO_3F)_6]^{2-} + Br_2 \underset{\longleftarrow}{\overset{K<<1}{\longrightarrow}} [Pd(SO_3F)_4]^{2-} + 2BrSO_3F \qquad (3.21)$$

$$BrSO_3F + SO_2 \longrightarrow Br_2 + S_3O_8F_2 \quad . \qquad (3.22)$$

SO_2 alone, like Br_2 by itself, did not react with $Cs_2[Pd(SO_3F)_6]$ at temperatures up to ~100°C. Equation (3.21) appears to be shifted to the left, since the soluble $[Pd(SO_3F)_6]^{2-}$ complexes can be synthesized in a $Br_2/BrSO_3F$ mixture, By the careful removal of all the SO_2 and most of the Br_2, the slightly less volatile $S_3O_8F_2$ was identified by its gas i.r. spectrum.

This procedure employing Br_2/SO_2 as the reduction couple could be applied to the preparation of $Pd(SO_3F)_2$ from $Pd_2(SO_3F)_6$ and conceivably other systems in which the presence of $BrSO_3F$ may be unacceptable. The faster reaction time at a lower reaction temperature and the presence of relatively inert and volatile by-products are the major advantages of this method.

The difference in reactivity of the ionic $[Pd(SO_3F)_6]^{2-}$ complexes as compared to $Pd_2(SO_3F)_6$ may be attributed to their different thermal stabilities. While $Pd_2(SO_3F)_6$ decomposes at ~120°C in vacuo to give $S_2O_6F_2$, the ionic complexes are stable up to ~200°C, and their decomposition products contain SO_2F_2, identified by its i.r. spectrum. SO_2F_2 is also found in the gaseous thermolysis products of $Au(SO_3F)_3$ and $Pt(SO_3F)_4$, and is a result of complete breakdown of the compound rather than via step-wise reduction.

3.C.1.3 ATTEMPTED SYNTHESIS OF $Pd(SO_3F)_4$

The synthesis of $[Pd(SO_3F)_6]^{2-}$ strongly suggests that the

binary compound, $Pd(SO_3F)_4$, may be obtainable as well. Although solid $Pd(SO_3F)_4$ could not be isolated, some evidence for its existence in strongly oxidizing solution has been obtained:

a) $Pd_2(SO_3F)_6$ is virtually insoluble in HSO_3F, but the clear solution containing the solid immediately took on a dark red color when $S_2O_6F_2$ was added. The u.v. spectrum of the solution is identical to that produced by $(NO)_2[Pd(SO_3F)_6]$ in HSO_3F, with a λmax at 320 nm. As expected, the solubility of $Pd(SO_3F)_4$ in such a mixture increased with increasing proportion of HSO_3F (visually monitored), but even at a $S_2O_6F_2/HSO_3F$ ratio of less than 1/20, the solubility of $Pd_2(SO_3F)_6$ is less than a few mg per ~20 mL.

b) Using a Soxhlet type extraction device made of sintered-glass, the only product obtained after 21 days of extraction at ~70°C was $Pd_2(SO_3F)_6$, formed slowly in the filtered liquid.

c) The oxidation of palladium metal by $S_2O_6F_2/HSO_3F$ from ~25°C to ~100°C did not lead to the formation of $Pd(SO_3F)_4$. In order to minimize the decomposition of $Pd(SO_3F)_4$ at elevated temperature in vacuo, the removal of $S_2O_6F_2/HSO_3F$ was performed at room temperature (a very long process). Nevertheless the solid isolated afterwards was invariably $Pd_2(SO_3F)_6$.

d) The attempted high pressure oxidation of $Pd_2(SO_3F)_6$ at 200°C for 7 days with an excess of $S_2O_6F_2$ in a Monel reactor did not lead to a further oxidation of palladium.

To rationalize all the above observations, some speculations concerning the palladium-fluorosulfate system can be made:

a) There are many precedents where high oxidation states may be obtained in anionic complexes when the parent compounds are not known. Some pertinent examples are the $[PdCl_6]^{2-}$ complexes and $O_2^+[PdF_6]^-$, with neither $PdCl_4$ nor PdF_5 obtainable so far.

b) The decrease in decomposition temperatures from $Pd(SO_3F)_2$ (250°C) to $Pd_2(SO_3F)_6$ (120°C) indicates a marked drop in the thermal stability in the series. $Pd(SO_3F)_4$, if obtainable, may not be very stable at room temperature,

c) The equilibrium:

$$Pd_2(SO_3F)_6 + S_2O_6F_2 \underset{\longleftarrow}{\xrightarrow{HSO_3F}} 2Pd(SO_3F)_4 \quad , \qquad (3.23)$$

is expected to be strongly dependent on the relative concentrations of HSO_3F and $S_2O_6F_2$. In order to obtain a high concentration of the presumably soluble $Pd(SO_3F)_4$ in HSO_3F, a low $S_2O_6F_2$/HSO_3F ratio is required because $S_2O_6F_2$, being a covalent liquid, decreases the ionizing ability of the solvent. This in turn would almost certainly drive the equilibrium back to the left as the oxidizing strength of the solvent mixture is decreased. As an added disadvantage, the subsequent removal of both $S_2O_6F_2$ and HSO_3F at the end of the reaction favors the formation of the insoluble and more thermally stable $Pd_2(SO_3F)_6$.

d) The observed formation of $S_2O_6F_2$, presumably via $SO_3F\cdot$ radicals, in the pyrolysis of $Pd_2(SO_3F)_6$ is very unusual in terms of the thermal decomposition paths of metal fluorosulfates [62]. Only a few other examples can be found: $Xe(SO_3F)_2$, $XeF(SO_3F)$ [135,136] and $Ag(SO_3F)_2$ [84]; and all of these are extremely strong oxidizing

agents. Furthermore, although the $[Pd(SO_3F)_6]^{2-}$ complexes are very stable entities, they are extremely corrosive materials capable of oxidizing Br_2 to $BrSO_3F$ and producing the most serious attacks on AgCl i.r. windows of all the solid compounds examined in this study. All these observations point to an extremely strong oxidizing ability of Pd(IV), and the energy required for its formation must be recovered from sources such as increased lattice energy for the ionic complexes, and polymerization for $Pd_2(SO_3F)_6$.

In summary, the inability to obtain pure $Pd(SO_3F)_4$ may be attributed to its limited thermal stability, the lack of solubility of $Pd_2(SO_3F)_6$ in HSO_3F, and the high oxidizing power of Pd(IV).

3.C.2 VIBRATIONAL SPECTRA

3.C.2.1 $Pd(SO_3F)_2$

The i.r. and Raman data for $Pd(SO_3F)_2$ are listed in Table 3.1 and compared to the reported i.r. frequencies for $Ni(SO_3F)_2$ [87]. The spectra are assigned in terms of a C_{3v} symmetry for the SO_3F group except for the two low frequency bands. For $Ni(SO_3F)_2$, the 290 cm^{-1} band has been assigned to lattice modes [87]; for $Pd(SO_3F)_2$, the very weak band at 354 cm^{-1} could be due to impurities as it was not present in the i.r. The position of the S-F stretch at ~860 cm^{-1} implies a tridentate coordination mode for the anions rather than a true SO_3F^- ion. Thus, $Pd(SO_3F)_2$ is isostructural

TABLE 3.1: VIBRATIONAL FREQUENCIES OF $Pd(SO_3F)_2$

$Pd(SO_3F)_2$		$Ni(SO_3F)_2$ [87]	Assignment
R	IR	IR	
1231 m	1240 s,b	1262 vs	$\nu_4(E)$
1111 ms	1090 ms	1120 s	$\nu_1(A_1)$
869 m	860 s	859 s	$\upsilon_2(A_1)$
612 w	610 s	619 s	$\nu_5(E)$
552 w	565 m	568 m	$\nu_3(A_1)$
430 m	421 m	422 m	$\nu_6(E)$
354 vw			impurity
		290 m	Lattice mode

FIG. 3.1 PROPOSED STRUCTURE OF $Pd(SO_3F)_2$ [137]

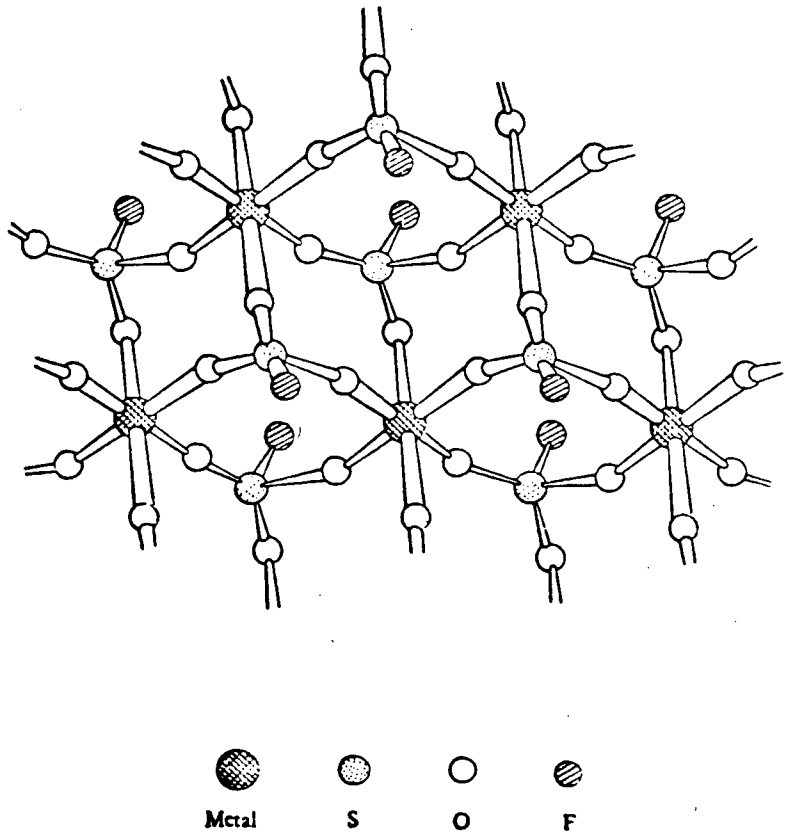

with a general class of bis(fluorosulfate)s which includes those of Ni, Mg, Ca, Zn, Cd, Hg, Fe and Co [87,99]. This highly polymeric structure is also consistent with the observed physical properties of $Pd(SO_3F)_2$, discussed in the previous section. The absence of splittings for the three degenerate E modes suggests a regular octahedral environment for Pd(II), in contrast to the extensive splittings observed in the spectra for $Cu(SO_3F)_2$ and $Mn(SO_3F)_2$ [62,87,99], which implies a distortion of the octahedral coordination spheres for the M(II) cations in these compounds. The proposed structure of $Pd(SO_3F)_2$, consistent also with its magnetic and electronic spectral information, is shown in Fig. 3.1 [137].

3.C.2.2 $[Pd(IV)(SO_3F)_6]^{2-}$ AND $Pd(II)[M(IV)(SO_3F)_6]$

Both i.r. and Raman spectra of the fluorosulfato complexes containing Pd(IV) were not easily obtainable for a number of reasons. The oxidizing ability of these compounds limited the use of i.r. window materials to BaF_2, with a transmission range down to only about 800 cm^{-1}. The dark colours of these compounds also interfered with the recording of Raman spectra at room temperature when the 514.4 nm line of the argon ion laser was used. Thus, sample cooling down to ~80K had to be employed in order to reduce laser induced decomposition. Alternatively, Raman spectra of rather low resolution were obtained on another spectrometer equipped with a He-Ne laser (623.8 nm).

For the two $Pd[M(IV)(SO_3F)_6]$ complexes, with M = Pt, Sn, i.r. spectra down to 450 cm^{-1} were obtained (AgCl plates). For $Pd[Sn(SO_3F)_6]$, because of the presence of strong fluoresence, a Raman spectrum could not be obtained.

The Raman spectra for $Pd_2(SO_3F)_6$ and $Pd[Pt(SO_3F)_6]$ are shown in Fig. 3.2 and Fig. 3.3, respectively. The observed vibrational frequencies for all the $[Pd(SO_3F)_6]^{2-}$ complexes and the two $Pd[M(IV)(SO_3F)_6]$ compounds are listed in Table 3.2 together with the literature values for $K_2[Sn(SO_3F)_6]$ [32]. With the exception of $Pd[Sn(SO_3F)_6]$, the Raman frequencies are reported, since they are generally of better resolution and extend to lower frequencies. The corresponding i.r. spectra show no major discrepancies in most of the band positions.

Except for a few additional features which will be discussed later, the spectra of these hexakis(fluorosulfato) complexes correlate well with each other and the main bands can be attributed to monodentate fluorosulfate groups in an anionic environment. A common, tentative assignment for these octahedral complexes is also attempted in Table 3.2.

As noted previously for the $[Sn(SO_3F)_6]^{2-}$ cases [32], band proliferation, especially in the SO_3F stretching region ($\gtrsim$800 cm^{-1}) is found. This is due, presumably, to solid state splittings and, probably more importantly, to extensive vibrational couplings suggesting, in turn, strong covalent bondings to the central M(IV) atoms. This is particularly true for the $[Pd(SO_3F)_6]^{2-}$

FIG. 3.2 RAMAN SPECTRUM OF $Pd_2(SO_3F)_6$

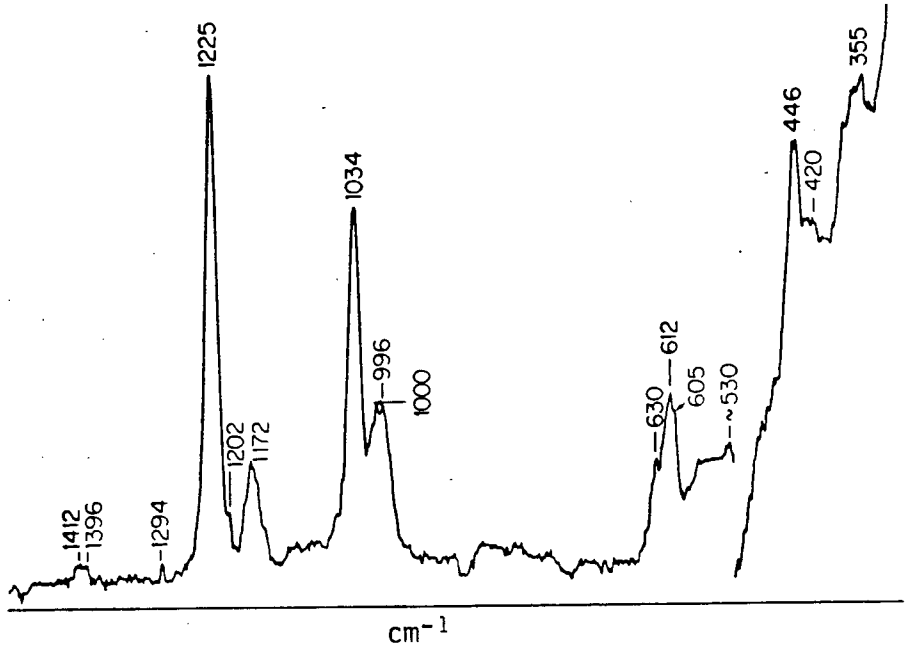

FIG. 3.3 RAMAN SPECTRUM OF $Pd[Pt(SO_3F)_6]$

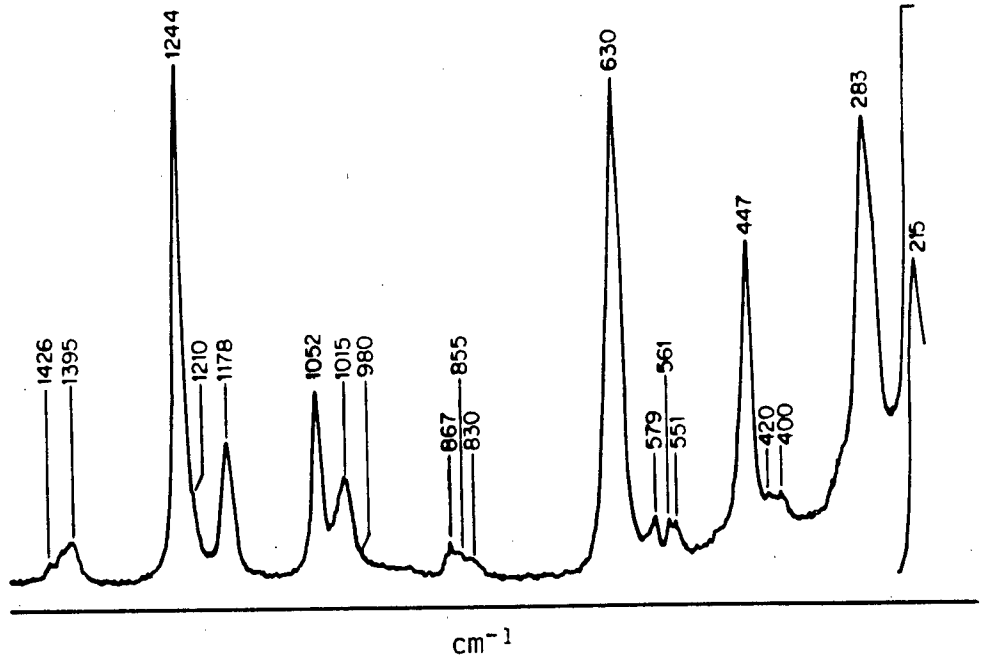

Table 3.2

Vibrational Spectra of $Cs_2[Pd(SO_3F)_6]$, $(NO)_2[Pd(SO_3F)_6]$, $(CrO_2)_2[Pd(SO_3F)_6]$ $Ba[Pd(SO_3F)_6]$, $Pd[Pd(SO_3F)_6]$, $Pd[Pt(SO_3F)_6]$ and $Pd[Sn(SO_3F)_6]$

$Cs_2[Pd(SO_3F)_6]$[a] Ra. $\Delta\nu[cm^{-1}]$ Int.	$(NO)_2[Pd(SO_3F)_6]$[a] Ra. $\Delta\nu[cm^{-1}]$ Int.	$(CrO_2)_2[Pd(SO_3F)_6]$[a] Ra. $\Delta\nu[cm^{-1}]$ Int.	$Ba[Pd(SO_3F)_6]$[a] Ra. $\Delta\nu[cm^{-1}]$ Int.	$Pd[Pd(SO_3F)_6]$ Ra. $\Delta\nu[cm^{-1}]$ Int.	$Pd[Pt(SO_3F)_6]$ Ra. $\Delta\nu[cm^{-1}]$ Int.	$Pd[Sn(SO_3F)_6]$ IR $\nu[cm^{-1}]$ Int.	Approximate Description
1405 w 1395 vw, sh	1407 vw 1388 mw	~1400 vw, b	1399 w, sh 1380 m	1412 w 1396 w	1426 w, sh 1395 ms	1425 ms, sh 1405 vs 1385 s	SO_2 asym. stretch
1300 vw 1236 vs 1212 m	1290 v 1235 vs 1209 ms	1293 w[b] 1240 vs 1215 m	1249 vs 1214 ms	1294 m 1225 vs 1202 w, sh 1172 m	1244 vs ~1210 sh 1178 ms	1250 m, sh 1195 vs, b 1105 w	SO_2 sym. stretch
1020 vs 995 ms 975 v, sh 960 vw, sh	1024 vs 1004 ms ~960 vw, sh	1050 m[b] 1020 s 1005 w 970 m	1013 vs 1001 ms, sh ~ 980 vw, sh	1034 s 1001 m 996 ms	1050 ms 1015 m, b ~960 vw	1028 vs, b	O-SO_2F stretch
835 vw 805 vw 785 w	852 mw 835 vw 823 w	841 w 828 w 805 w	857 ms 830 vw, sh	860 w 822 w	867 m 855 w ~850 vw	865 m, sh 855 vs	SF stretch
618 ms ~585 vw, sh 542 w 441 ms	622 s ~590 vw, sh 545 w 446 ms 420 vw	623 ms 607 m 590 vw 545 mw 444 ms	613 vs ~590 vw 551 w 459 ms 424 vw	630 ms 612 s 578 w 538 mw 446 ms 420 m	630 vs 579 vw 447 s 420 vw	648,632 ms 590 s 562,551 m 445 ms, sh	M-O stretch + M-O-S bend (see text) SO_2 bend SO_2 rock M-O stretch + M-OS bend
~400 vw 270 s 225 ms	~400 vw 264 s ~230 ms, sh	400 vw 272 vs ~230 m, sh	414 w 272 vs ~230 m,sh	360 m, sh	~400 w, sh 283 s 215 ms		S-O wagging MO deformation SO deformation

a) Spectrum recorded with sample at ~80K.

b) bands assigned to CrO_2^+

derivatives, in which strong Raman bands at ~1240 cm^{-1} (νSO_2 asym) and ~1020 cm^{-1} (νS-OPd) have weaker side bands at ~1210 and ~980 cm^{-1}, respectively, with the intensities reversed in the i.r. spectra.

The spectra for the three Pd(II) containing compounds have bands at ~1170 to 1190 and ~1040 to 1050 cm^{-1} that are not present in the spectra of the other complexes, including $Ba[Pd(SO_3F)_6]$. Bands in these regions, also reported for $Ag[Pt(SO_3F)_6]$ and $Ag[Sn(SO_3F)_6]$ [84], are usually associated with bidentate bridging fluorosulfate groups [33]. Their occurrence in the spectra of these particular compounds may be due to the strong polarizing abilities of the divalent transition metal cations. Ba^{2+} , although being a divalent cation, is not expected to have as great a polarizing effect on the fluorosulfate groups because it lacks the necessary d-orbitals. Further evidence in support of the coordination of Pd(II) will be presented in subsequent sections. This type of coordination, shown in Fig. 3.4, in which the fluorosulfate ligands are bonded primarily to M(IV) and coordinated weakly to M(II), can be considered as bridging anisobidentate. Hence, the ionic formulation of these compounds as consisting of discrete M(II) and $[M(IV)(SO_3F)_6]^{2-}$ units may be somewhat misleading. This highly polymerized structure is also inferred from the noted lack of solubility of these complexes, ($Ba[Pd(SO_3F)_6]$ is slightly soluble).

Strong Raman bands at ~620 to 640, ~400 to 460 and ~270 to

FIG.3.4 ANISOBIDENTATE BRIDGING MODE FOR SO_3F

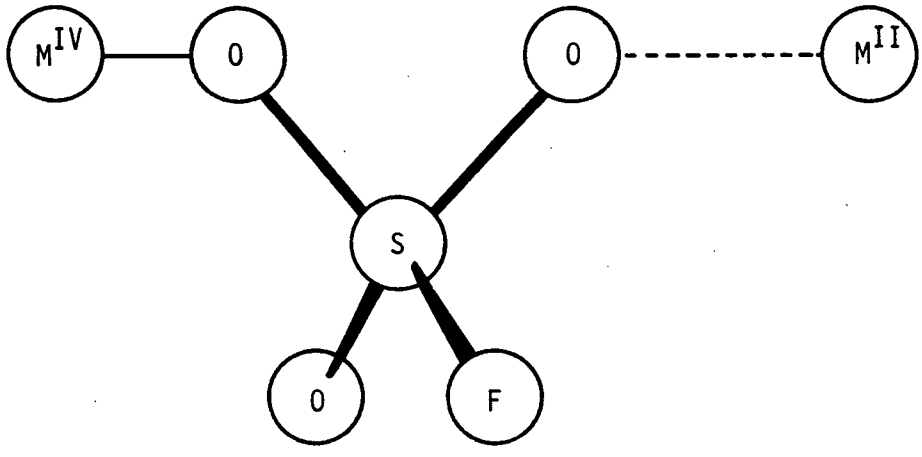

280 cm^{-1}, observed for all the anionic complexes are not assignable to absorptions due to the fluorosulfate groups alone. Their positions appear to show a slight dependence on the nature of both the M(IV) species and the counter-cations. These bands, occasionally split into doublets, are most likely due to M(IV)-O vibrations, possibly coupled with ligand deformation modes. The evidence for strong M(IV)-O bonds leading also to the coupling of S-O stretching modes has been discussed earlier.

For the complexes with polyatomic heterocations, additional bands due to the cations are observed and they compare favorably with previously reported data. For the NO^+ complex, the N-O stretch is found at 2330 cm^{-1} in the i.r.; in $(NO)_2[Sn(SO_3F)_6]$, the same vibration is found at 2325 cm^{-1} [32]. Bands due to ClO_2^+ are found at 1293 cm^{-1} (split into 1300 and 1290 cm^{-1} for the

stronger i.r. band) and 1050 cm^{-1}, consistent with literature values [32,138]. The bending mode for ClO_2^+, expected to be only weakly Raman active, and usually found at ~520 cm^{-1}, is not observable in this case.

To summarize, the apparent spectral similarities indicate strong structural similarities in these compounds. The formulation of the tris(fluorosulfate) as the ternary compound, Pd(II)[Pd(IV)$(SO_3F)_6$] is supported by its vibrational spectra. The strong vibrational coupling between the fluorosulfate groups and the [M(IV)O_6] skeleton confirms the covalent character of the M(IV)-O bond.

3.C.2.3 $[Pd(SO_3F)_4]^{2-}$

Because of the light brown color of the samples containing $[Pd(SO_3F)_4]^{2-}$, no Raman spectrum was obtainable. The i.r. frequencies are listed in Table 3.3. A good correlation can be made between the spectra of $[Pd(SO_3F)_4]^{2-}$ and those from the presumably square planar, $[Au(SO_3F)_4]^-$, suggesting structural similarities. The difference in the positions of a few diagnostic bands can be interpreted as being caused by the replacement of Au(III) by Pd(II). It has been hypothesized that the weakening of an S-O bond due to the coordination of the oxygen leads to the strengthening of the remaining S-F and S-O bonds [92]. The lowering of the S-F stretching frequency by about 20 cm^{-1} in the Pd(II) compound is significant, and must be attributed to a decrease in

TABLE 3.3: I.R. FREQUENCIES FOR $(NO)_2$-, Cs_2- AND Ba- $[Pd(SO_3F)_4]$

$Ba[Pd(SO_3F)_4]$	$(NO)_2[Pd(SO_3F)_4]$	$Cs_2[Pd(SO_3F)_4]$	$Cs[Au(SO_3F)_4]$	Assignment
	~2330 vw			ν N-O
1340 vs	1350 vs	1340 vs	1440 vs	ν_7 asymSO_3
1200 vs	1200 vs	1200 vs	1210 vs	ν_1 symSO_3
1030 vs	1020 vs	1000 vs	930 vs	ν_4 asymSO_3
800 s	800 s	795 s	~820 s	ν_2 S-F
640 s	660 s	655 s,sh 645 s	675 s	ν_3 SO_3F rock + ν MO sym
580 s	580 s	575 s	585 s	ν_5 SO_3F def
550 s	560 s	555 s	550 s	ν_8 SO_3F def
450 m	~420 m	~420 w	460 m	ν_9 SO_3F rock + ν MO asym

covalent nature of the Pd-O bond. This can also be illustrated by the decrease in the splitting in the asymmetric SO_3 stretch (ν_4 and ν_7) for $[Pd(SO_3F)_4]^{2-}$. (For $[Pd(SO_3F)_4]^{2-}$, $\nu_7-\nu_4=\sim340\ cm^{-1}$; for $[Au(SO_3F)_4]^-$, $\nu_7-\nu_4=\sim470\ cm^{-1}$). This seems to indicate that the three S-O bonds are more similar in the $[Pd(SO_3F)_4]^{2-}$ species than the ones in $[Au(SO_3F)_4]^-$, also not unexpected.

The colors of these Pd(II) complexes, together with evidence from vibrational spectroscopy, seem to indicate a square planar environment for the Pd(II). Magnetic susceptibility measurements, to be discussed later, support such a conclusion.

3.C.3 ELECTRONIC SPECTRA

The Pd(II) containing compounds of $Pd(SO_3F)_2$, $Pd[Sn(SO_3F)_6]$ and $Pd[Pt(SO_3F)_6]$ are purple, blue and green, respectively, quite in contrast to the usually brown colors of Pd(II) compounds with Pd(II) in a square planar environment. Similar blue or purple colors are also found for PdF_2, $CsPdF_3$ [107], $ZnPdF_4$ [116], and $Pd[M(IV)F_6]$ [103], with M = Ge, Sn, Pt, all with Pd(II) in an octahedral environment. However, a detailed analysis of their electronic spectra is not reported.

It is therefore not surprising that the magnetic results and the vibrational spectra also supported a regular octahedral environment for Pd(II) in $Pd(SO_3F)_2$ and $Pd[M(IV)(SO_3F)_6]$.

$Pd(SO_3F)_2$ shows a three-band electronic spectrum that can be assigned as due to d-d transitions. Although no extinction coefficients to support the assignment were obtainable because of the insolubility of all the compounds in HSO_3F, it appears that all the bands are of about the same intensities and the D_q and B values obtained from such an assignment are very reasonable.

The electronic ground state for a d^8 ion in an octahedral field is $^3A_{2g}$, and three d-d transitions are expected. The energy level diagram for a d^8 ion in an octahedral field is shown in Fig 3.5. The band positions of the observed electronic spectra and the calculated ligand field parameters of $Pd(SO_3F)_2$, $Pd[Sn(SO_3F)_6]$, $Pd[Pt(SO_3F)_6]$ and $Ni(SO_3F)_2$ [61] are listed in Table 3.4. There is generally a good correspondence between spectra obtained from mulls and those obtained by diffuse reflectance. In the platinum compound, ν_3 is not observed because the strong charge transfer band due to Pt(IV), with λ_{max} at 245 nm and ε of $\sim 1.5\times10^4$ $M^{-1}cm^{-1}$, extends well into the visible region. This further substantiates the premise that the remaining bands are due to the d-d transitions with lower intensities.

The good agreement in band positions for the spectra for the three compounds suggests a similar environment for Pd(II) and an $^3A_{2g}$ ground state in all cases. Although no splitting of any of the bands is observable, it does not confirm or deny the existence of distortion in the coordination sphere as the bands are quite broad. In any case, no distortion is evident from the vibrational

FIG. 3.5: ENERGY LEVEL DIAGRAM FOR A d^8 ION IN AN O_h FIELD

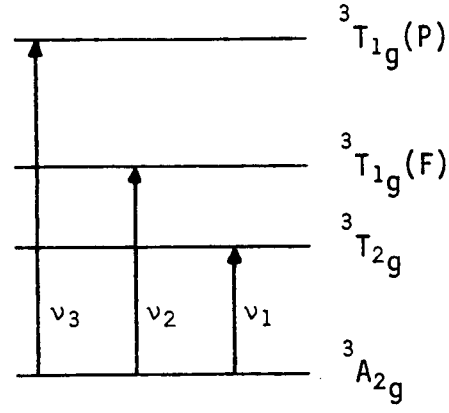

$\nu_1 = 10Dq$

$\nu_2 = \frac{1}{2}(15B + 30Dq) - \frac{1}{2}[(15B - 10Dq)^2 + 12B \cdot 10Dq]^{\frac{1}{2}}$

$\nu_3 = \frac{1}{2}(15B + 30Dq) + \frac{1}{2}[(15B - 10Dq)^2 + 12B \cdot 10Dq]^{\frac{1}{2}}$

TABLE 3.4: ELECTRONIC TRANSITIONS AND LIGAND FIELD PARAMETERS FOR SOME PALLADIUM (II) COMPOUNDS AND $Ni(SO_3F)_2$ (in cm^{-1})

	$Pd[Sn(SO_3F)_6]$	$Pd[Pt(SO_3F)_6]$	$Pd(SO_3F)_2$	$Ni(SO_3F)_2$ [61]
ν_1	11,050	11,400	11,770	
ν_2	16,950	16,950	17,400	
ν_3	26,850	26,480*	27,030	
Dq	1,105	1,140	1,177	734
B	717	642	633	905
B/B°	0.863	0.774	0.763	0.838

*calculated value
Diffuse reflectance values for ν_2 are 16,890 cm^{-1} for $Pd[Sn(SO_3F)_6]$ and 16,810 cm^{-1} for $Pd[Pt(SO_3F)_6]$

FIG. 3.5: ENERGY LEVEL DIAGRAM FOR A d^8 ION IN AN O_h FIELD

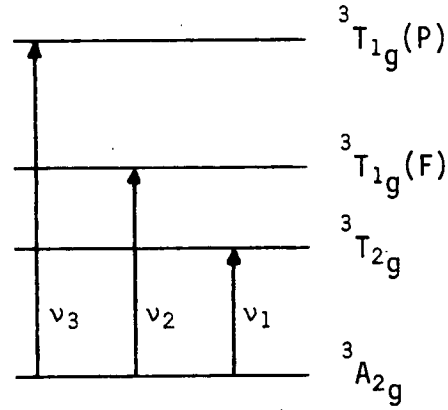

$$\nu_1 = 10Dq$$

$$\nu_2 = \tfrac{1}{2}(15B + 30Dq) - \tfrac{1}{2}[(15B - 10Dq)^2 + 12B \cdot 10Dq]^{\frac{1}{2}}$$

$$\nu_3 = \tfrac{1}{2}(15B + 30Dq) + \tfrac{1}{2}[(15B - 10Dq)^2 + 12B \cdot 10Dq]^{\frac{1}{2}}$$

TABLE 3.4: ELECTRONIC TRANSITIONS AND LIGAND FIELD PARAMETERS FOR SOME PALLADIUM (II) COMPOUNDS AND $Ni(SO_3F)_2$ (in cm^{-1})

	$Pd[Sn(SO_3F)_6]$	$Pd[Pt(SO_3F)_6]$	$Pd(SO_3F)_2$	$Ni(SO_3F)_2$ [61]
ν_1	11,050	11,400	11,770	
ν_2	16,950	16,950	17,400	
ν_3	26,850	26,480*	27,030	
Dq	1,105	1,140	1,177	734
B	717	642	633	905
B/B°	0.863	0.774	0.763	0.838

*calculated value
Diffused reflectance values for ν_2 are 16,890 cm^{-1} for $Pd[Sn(SO_3F)_6]$ and 16,810 cm^{-1} for $Pd[Pt(SO_3F)_6]$

analysis of the compounds. By using Tanabe-Sugano diagrams as suggested by Lever [139], the positions of all the bands are confirmed, and ν_3 for $Pd[Pt(SO_3F)_6]$ is calculated using this method. The octahedral splitting —— 10 D_q, and the interelectronic repulsion term —— B, are also obtained. The increase in D_q and the decrease in β, (defined as the ratio of B over B^o, the free ion value), in going from Ni(II), ($3d^8$), to Pd(II), ($4d^8$), are not unexpected in view of the higher nuclear charge and more spacially diffused 4d orbitals for palladium [110].

It appears that within the series of $Pd(SO_3F)_2$, $Pd[Pt(SO_3F)_6]$ and $Pd[Sn(SO_3F)_6]$, 10 D_q gradually decreases while β increases, with B approaching the B^o value of 830 cm^{-1} [141]. The presence of the M(IV) species, with their higher cationic charge, is expected to compete favorably for the coordination of the SO_3F ligands. A lessening of Pd-SO_3F interaction is expected to decrease 10 D_q and also increase the interelectronic repulsion as the orbitals are more confined to the metal. For the two complexes, the one that contains Sn(IV) has the lowest 10 D_q and the highest β value. This cannot be due to structural dissimilarities, because this was not noted in the vibrational spectra, and must be attributed to a greater ability of Sn(IV) to bond to the SO_3F groups. This has also been observed in the following two complexes —— $Ag(II)[M(IV)(SO_3F)_6]$, with M = Pt, Sn [84].

$(NO)_2[Pd(SO_3F)_4]$, $Cs_2[Pd(SO_3F)_4]$ and $Ba[Pd(SO_3F)_4]$ are light brown solids, and the bands of the diffuse reflectance spectra

of the latter two compounds are compared with those of $K_2[PdCl_4]$ [142] in Table 3.5. The energy level diagram for a d^8 ion in a square planar ligand field is shown in Fig. 3.6. As can be seen, a good comparison can be made between the spectra for the two types of compounds, suggesting the presence of species with similar electronic configuration. Strong absorptions are found for $K_2[PdCl_4]$ at 278 and 223 nm [142], and are assigned to L $\longrightarrow$ M charge transfer bands. For $[Pd(SO_3F)_4]^{2-}$, such absorptions were not observed as they are beyond the range of the instrument, but an extremely strong background was observed at the high energy end of the spectrum, giving rise to quite poor resolution for the two bands at ~450 nm. An assignment of the obtained spectra by analogy with $K_2[PdCl_4]$ gives $\Delta_1 \simeq 15{,}400$ cm^{-1}, $\Delta_2 \simeq 4600$ cm^{-} , and $\Delta_3 \simeq 2200$ cm^{-1}. Δ_1 is equivalent to 10 D_q if it can be assumed, (from a crystal field point of view at least), that a square planar structure is derived from the gradual elongation of an octahedron, and that the energy difference between $d(x^2-y^2)$ and $d(xy)$ remains 10 D_q [143]. A comparison to a Δ_1 of ~16,700 cm^{-1} for $K_2[PdCl_4]$, is reasonable on the basis that the fluorosulfate group is generally known to produce a weaker ligand field than a chloro group [61].

Some generalizations concerning the relative ability of a SO_3F group to coordinate to a metal ion depending on how the other two oxygen atoms are bonded can be made. For the Pd(II)-fluorosulfate system, three types of coordination of a SO_3F group are evident from results obtained in this study:

FIG. 3.6: d-ORBITAL ENERGY LEVEL FOR A SQUARE PLANAR COMPLEX [142]

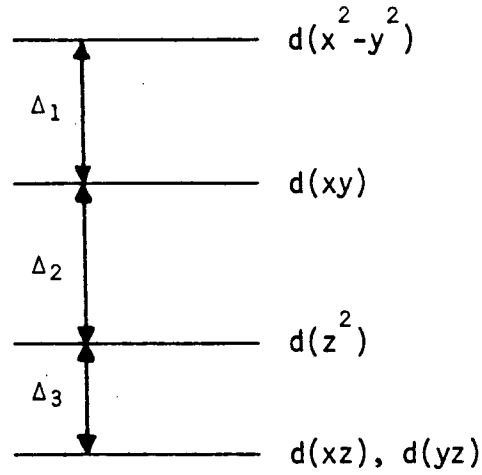

$\nu_1 = \Delta_1$

$\nu_2 = \Delta_1 + \Delta_2$

$\nu_3 = \Delta_1 + \Delta_2 + \Delta_3$

TABLE 3.5: ELECTRONIC SPECTRA AND LIGAND FIELD PARAMETERS FOR $[Pd(SO_3F)_4]^{2-}$ (in cm^{-1})

	$Cs_2[Pd(SO_3F)_4]$	$Ba[Pd(SO_3F)_4]$	$[PdCl_4]^{2-}$ [142]
ν_1, $^1A_{1g} \rightarrow {}^1A_{2g}$	~15,400 w	15,400 w	16,700
ν_2, $^1A_{1g} \rightarrow {}^1B_{1g}$	~20,000 s,sh	~20,000 s,sh	21,500
ν_3, $^1A_{1g} \rightarrow {}^1E_{1g}$	22,200 s	~22,700 s	23,300
Charge Transfer			36,000
Charge Transfer			44,900
Δ_1	15,400	15,400	16,700
Δ_2	4,600	4,600	4,800
Δ_3	2,200	2,500	1,800

a) monodentate, as in $[Pd(SO_3F)_4]^{2-}$,

b) aniso-bidentate bridging between Pd(II) and a M(IV) cation, as in $Pd[M(IV)(SO_3F)_6]$, and

c) bridging tridentate to three equivalent Pd(II) in $Pd(SO_3F)_2$.

Most likely a result of less competition for ligand electrons from another metal centre, a monodentate SO_3F produces the strongest ligand field. The withdrawal of electron density from a SO_3F group due to its bonding to a highly charged M(IV) cation can drastically reduce the ligands' coordinating ability to Pd(II). In fact, the reduction can make the SO_3F ligand in the former coordination mode bind more weakly to Pd(II) than does a tridentate SO_3F group. By extrapolation, a bidentate SO_3F group bridging two Pd(II) should produce a ligand field splitting somewhat between the ones present in $[Pd(SO_3F)_4]^{2-}$ and $Pd(SO_3F)_2$. Similar observations have been made for a number of transition metal trifluorides, MF_3, with M = Ti, V, Cr, Mn, Fe and Co, and their mixed ternary salts of the general formula of $M'_2M''[MF_6]$. The fluorine atoms in the binary fluorides are shared by two M(III) cations while in the $[MF_6]^{3-}$ complexes, the fluoride ligands are essentially coordinated to M(III) with weak interactions towards M", an alkali metal ion. An increase in Δ_o of ~7% is noted in going from MF_3 to $[MF_6]^{3-}$ [144].

For the $[Pd(SO_3F)_6]^{2-}$ containing compounds, less informative electronic spectra were obtained. $Pd_2(SO_3F)_6$ is a dark brown solid, and its u.v.-vis spectrum consists of a very intense,

featureless band which extends over most of the spectrum. This must be due to charge transfer because

a) the high cationic charge of Pd(IV) enhances L $\rightarrow$ M transfer, and

b) the mixed valency nature of the compound which can give rise to M $\rightarrow$ M' transfer.

As mentioned, the solution of $(NO)_2[Pd(SO_3F)_6]$ in HSO_3F shows a single absorption peak at 320 nm with an extinction coefficient of 1.3×10^4 $M^{-1}cm^{-1}$; charge transfer orgin of the L $\rightarrow$ M type is also suggested here.

3.C.4 MAGNETIC SUSCEPTIBILITY

As mentioned in the introduction, most palladium compounds, regardless of the oxidation state of palladium, are diamagnetic. This is because

a) both Pd(II) and Pd(IV) are even-electron species,

b) Pd(IV) is invariably octahedral low spin with high 10 D_q values, and

c) Pd(II) is usually in a square planar,and thus diamagnetic, environment.

Octahedral Pd(II), d^8, is expected to be paramagnetic, with two unpaired electrons corresponding to a $^3A_{2g}$ ground state. Therefore, a direct orbital contribution to the magnetic moment

is not expected, but through spin-orbital coupling, which is expected to be quite large for 2nd and 3rd series transition metals, the observed magnetic moment should be in excess of the spin-only value of 2.83 μ_B.

3.C.4.1 PARAMAGNETIC Pd(II) FLUOROSULFATES

Paramagnetism is found for $Pd(SO_3F)_2$, $Pd_2(SO_3F)_6$, $Pd[Pt(SO_3F)_6]$ and $Pd[Sn(SO_3F)_6]$, all with magnetic moments indicative of two unpaired electrons for Pd(II). As mentioned, the electronic spectra for these compounds have shown that a $^3A_{2g}$ ground state can best be assigned to Pd(II) in these compounds. The magnetic susceptibility of such a species can be represented by the following equation, according to Figgis [141]:

$$\chi_A = \chi_A^{s.o.}\left(1 - \frac{8k^2\lambda_o}{10\ D_q}\right) + \frac{8k^2N\beta^2}{10\ D_q} \qquad (3.24)$$

where $\chi_A^{s.o.}$ ≡ spin only susceptibility,

k ≡ electron delocalization factor,

λ_o ≡ spin-orbit coupling constant = $-\xi/2$ for d^8,

β ≡ Bohr Magneton,

N ≡ Avogardro's Number

$10\ D_q$ ≡ Ligand Field Splitting.

The first correction term involving λ_o, is due to the spin-orbital coupling, and the second (and much smaller) term arises from 2nd order Zeeman Effect and is usually called Temperature Independent Paramagnetism (T.I.P.). ξ, the spin-orbital coupling

parameter, has been estimated as 1460 cm^{-1} for Pd(II) [145]. Therefore, with λ_o negative, the observed magnetic susceptibility should be higher than the spin only value.

The magnetic susceptibilities of the four paramagnetic Pd(II) compounds are listed in Tables 3.6 to 3.9 and their Curie-Weiss Law dependence is represented diagrammatically in Fig 3.7. A comparison of these results with the corresponding fluoride system is made in Table 3.10. Having obtained the ligand field splitting parameter, D_q, from the electronic spectra of some of these compounds, it is possible to estimate the electron delocalization factor, k, and also to verify the value of the spin orbital coupling constant —— λ_o.

As can be seen, the four paramagnetic compounds all obey the Curie-Weiss Law in the temperature range of the investigation with very small Weiss constants as extrapolated from ~80 K. This suggests the presence of magnetically dilute systems in these cases, in contrast to the antiferromagnetic couplings observed in the fluoride system [104,108,116]. It is not expected that such couplings via the superexchange mechanism [115,146] can occur effectively through the polyatomic fluorosulfate ligands. The experimentally obtained magnetic susceptibilities and moments are very close to the ones calculated from the Curie-Weiss Law relationship. Small temperature dependence of the susceptibilities as a result of positive Weiss constants, can be decreased by applying T.I.P. to the two complexes containing Sn(IV) and Pt(IV).

TABLE 3.6 MAGNETIC PROPERTIES OF $Pd(SO_3F)_2$

T	χ_m^c	$1/\chi_m^c$	$1/\chi_m^c$ (calc)	μ_{eff}	μ_{eff} (calc)	μ_{eff} T
103	1.462×10^{-2}	68.40	67.43	3.47	3.50	3.45
125	1.163×10^{-2}	85.18	83.32	3.43	3.46	3.41
150	9.678×10^{-3}	102.2	101.4	3.43	3.44	3.40
183	8.119×10^{-3}	121.7	125.2	3.47	3.42	3.44
207	7.083×10^{-3}	139.1	142.5	3.45	3.41	3.42
225	6.313×10^{-3}	155.8	155.5	3.40	3.40	3.36
250	5.655×10^{-3}	173.6	173.6	3.39	3.39	3.35
274	5.067×10^{-3}	193.3	190.9	3.37	3.39	3.32
299	4.668×10^{-3}	209.5	209.0	3.38	3.38	3.33
K	cgs	cgs	cgs	μ_B	μ_B	μ_B units

$1/\chi_m^c$ (calc) = (T - 10)/1.38

TIP = 140×10^{-6} cgs units

k ~ 0.89

TABLE 3.7 MAGNETIC PROPERTIES OF $Pd_2(SO_3F)_6$

T	χ_m^c	$1/\chi_m^c$	$1/\chi_m^c$ (calc)	μ_{eff}	μ_{eff} (calc)	μ_{eff} T
334	4.419×10^{-3}	226.3	224.3	3.44	3.45	3.38
302	4.926×10^{-3}	203.0	202.2	3.45	3.46	3.40
279	5.410×10^{-3}	184.8	186.3	3.48	3.46	3.43
253	5.987×10^{-3}	167.0	168.3	3.48	3.47	3.44
229	6.616×10^{-3}	151.1	151.7	3.48	3.48	3.44
204	7.472×10^{-3}	133.8	134.4	3.49	3.48	3.46
179	8.621×10^{-3}	116.0	117.1	3.51	3.50	3.48
153	9.985×10^{-3}	100.2	99.12	3.50	3.51	3.47
131	1.185×10^{-2}	84.37	83.91	3.52	3.53	3.50
107	1.468×10^{-2}	68.13	67.30	3.54	3.57	3.53
K	cgs	cgs	cgs	μ_B	μ_B	μ_B units

$1/\chi_m^c$ (calc) = (T - 10)/1.45

TIP ~ 150×10^{-6} cgs units

k ~ 0.92 to 0.95

TABLE 3.8 MAGNETIC PROPERTIES OF $Pd[Pt(SO_3F)_6]$

T	χ_m	$1/\chi_m^c$	$1/\chi_m^c$ (calc)	μ_{eff}	μ_{eff} (calc)	μ_{eff} T
89	1.447×10^{-2}	69.09	69.82	3.21	3.19	3.20
119	1.106×10^{-2}	90.41	90.95	3.24	3.24	3.23
142	9.350×10^{-3}	107.0	107.1	3.26	3.26	3.24
167	7.975×10^{-3}	125.4	124.8	3.26	3.27	3.24
193	6.895×10^{-3}	145.0	143.1	3.26	3.29	3.23
222	6.122×10^{-3}	163.3	163.5	3.30	3.30	3.27
246	5.544×10^{-3}	180.4	180.4	3.30	3.30	3.27
278	4.934×10^{-3}	202.7	202.9	3.31	3.31	3.27
302	4.565×10^{-3}	219.1	219.8	3.32	3.32	3.28
K	cgs	cgs	cgs	μ_B	μ_B	μ_B units

$1/\chi_m^c$ (calc) = (T + 10)/1.42

TIP = 121×10^{-6}cgs units

k ~ 0.81

TABLE 3.9 MAGNETIC PROPERTIES OF $Pd[Sn(SO_3F)_6]$

T	χ_m^c	$1/\chi_m^c$	$1/\chi_m^c$ (calc)	μ_{eff}	μ_{eff} (calc)	μ_{eff} T
80	1.829×10^{-2}	54.69	55.41	3.42	3.40	3.40
107	1.407×10^{-2}	71.09	72.09	3.47	3.45	3.45
129	1.171×10^{-2}	85.38	85.68	3.48	3.47	3.45
154	9.833×10^{-3}	101.7	101.1	3.48	3.49	3.45
178	8.522×10^{-3}	117.3	116.0	3.48	3.50	3.45
203	7.564×10^{-3}	132.2	131.4	3.50	3.52	3.46
229	6.784×10^{-3}	147.4	147.5	3.53	3.52	3.48
252	6.121×10^{-3}	163.4	161.7	3.51	3.53	3.46
280	5.609×10^{-3}	178.3	179.0	3.54	3.54	3.49
306	5.172×10^{-3}	193.3	195.0	3.56	3.54	3.49
K	cgs	cgs	cgs	μ_B	μ_B	μ_B units

$1/\chi_m^c$ (calc) = (T + 10)/1.62

TIP = 185×10^{-6} cgs unit

k ~ 0.99

FIG 3.7 CURIE-WEISS PLOT FOR Pd(II)-FLUROUSULFATE DERIVATIVES

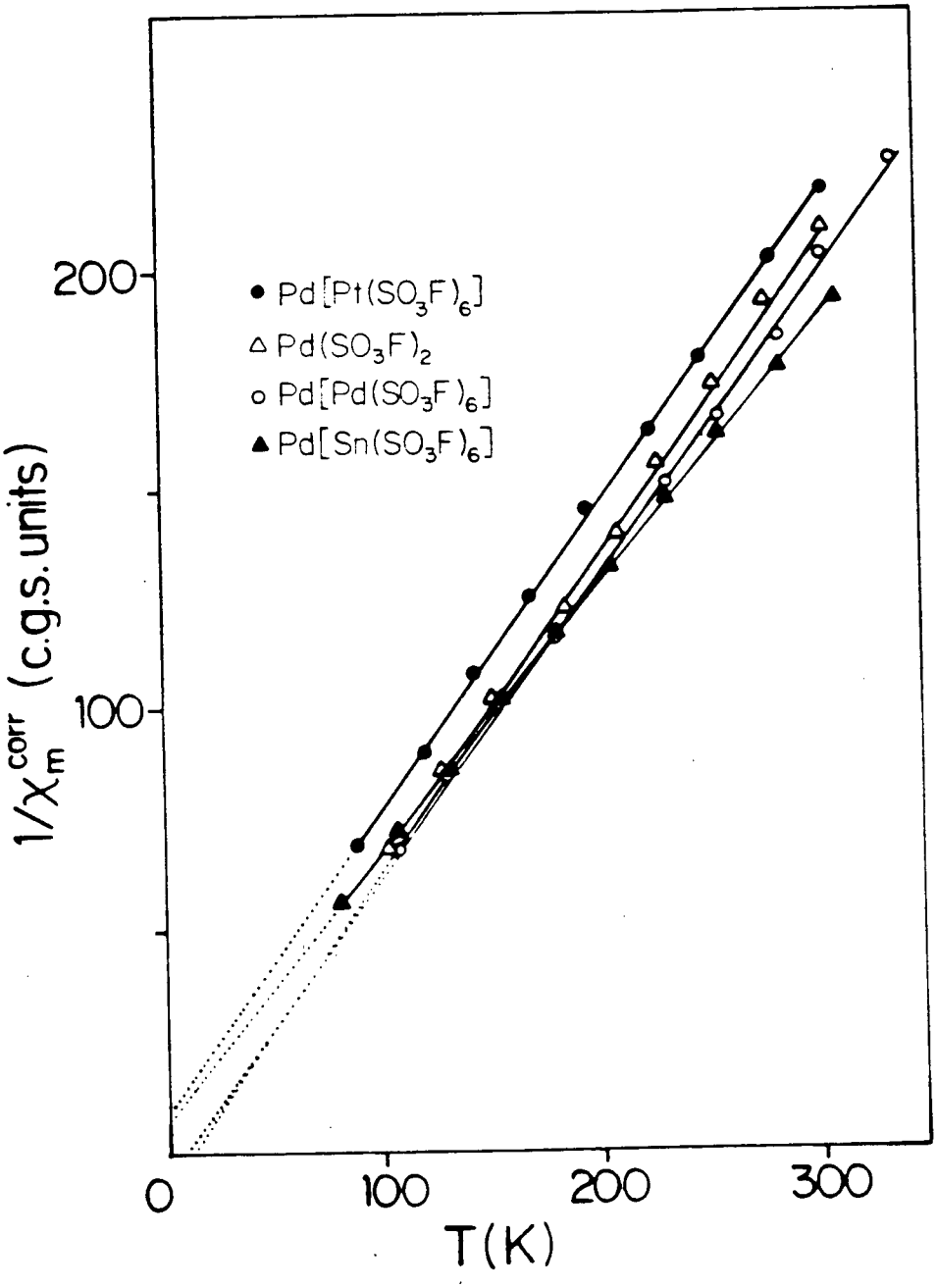

TABLE 3.10: MAGNETIC PROPERTIES OF SOME Pd(II) COMPOUNDS AT ROOM TEMPERATURE

	$10^3 \chi_m^c$	μ_{eff}	temperature dependence	Ref.
PdF_2	1.28	1.75	antiferromagnetic coupling	108,151
$Pd[PdF_6]$	3.31	2.81	θ = -28K	"
$Pd[PtF_6]$	3.10	2.72	θ = -1K	"
$Pd[GeF_6]$	3.34	2.82	θ = -31K	"
$Pd[SnF_6]$	3.37	2.83	θ = -28K	"
$Pd(SO_3F)_2$	4.80	3.38	$\chi_m^c = 1.38/(T-10)$	
$Pd[Pd(SO_3F)_6]$	5.01	3.46	$\chi_m^c = 1.45/(T-10)$	
$Pd[Pt(SO_3F)_6]$	4.61	3.32	$\chi_m^c = 1.42/(T+10)$	
$Pd[Sn(SO_3F)_6]$	5.26	3.54	$\chi_m^c = 1.62/(T+10)$	

For the two compounds with negative Weiss constants, no improvements could be expected from the T.I.P. adjustments, but still, the deviations are very small. No great significance should be attached to these small Weiss constants because they are extrapolated over a temperature range of close to 100 K. Magnetic orderings, should they occur, cannot be inferred from these measurements; ferromagnetic orderings have been found for Pd_2F_6 and $Pd[PtF_6]$ below 13 K and 21 K, respectively [147].

However, the similarity in the magnetic moments for all the four fluorosulfate-containing compounds indicates a similar environment for Pd(II) in all cases. It also shows, conclusively, that the tris(fluorosulfate) should be formulated as containing high spin, paramagnetic Pd(II), and low spin, diamagnetic, Pd(IV), in a mixed-valency configuration.

At first, the magnetic moments of these fluorosulfates appear to be much higher than the spin only value for Pd(II); however, an investigation into the isoelectronic nickel (II) system shows that even Ni(II), with a spin orbit coupling parameter —— ξ, of only ~630 cm^{-1} [145], can have magnetic moments as high as 3.5 μ_B. Some representative μ_{eff} values at 298 K are listed in Table 3.11.

As mentioned, although the magnetic moment of PdF_2 is lowered by antiferromagnetic exchange, at infinite dilution of the fluoride by ZnF_2, an extrapolated moment of 3.2 μ_B is obtained [116], quite close to the values for the fluorosulfate-

Table 3.11 MAGNETIC PROPERTIES OF SOME Ni(II) COMPOUNDS

	μ_{eff}	Temperature Dependence	Reference
$Ni(SO_3F)_2$	3.49	Curie-Weiss	148
$(NH_4)_2NiF_4 \cdot 2H_2O$	3.24	Curie-Weiss, θ = -13 K	149
$NiF_2 \cdot 4H_2O$	3.16	Curie-Weiss, θ = -19 K	149
$LiNiF_4$	3.19	Curie-Weiss, $\theta \sim 0$ K	149
NiF_2	2.85	Antiferromagnetic	149,150
NiF_2/MgF_2, 5.48 mol%Ni	3.04	Curie-Weiss, $\theta \sim -17$ K	150
$NiCl_2$	2.91	Ferromagnetic	150
$NiCl_2/MgCl_2$, 3.88 mol%Ni	3.20	Curie-Weiss, $\theta \sim 6$ K	150

containing compounds reported here.

The increase in the μ_{eff} at room temperature in the order of $Pd(SO_3F)_2 \sim Pd[Pt(SO_3F)_6] < Pd_2(SO_3F)_6 < Pd\ Sn(SO_3F)_6$ parallels a similar trend observed in the fluoride system [108,151]. Referring to equation (3.24), the only factors expected to have a dependence on individual Pd(II) compounds are 10 D_q —— the ligand field splitting, and k —— the electron delocalization factor which leads to an effective reduction of λ from the free ion value, λ_o. Although no ligand field parameters can be obtained from the electronic spectrum of $Pd_2(SO_3F)_6$, the similarity of its magnetic moment to those of the other compounds justifies using the known 10 D_q's for the three compounds to arrive at an estimate for k for Pd(II) in $Pd_2(SO_3F)_6$. The values of k obtained appear to increase in a similar trend as does μ_{eff}, approaching the free ion value of 1 for the Sn(IV) compound.

However, these differences which are obtained from small deviations in the magnetic measurements from Curie-Weiss Law

should not be overemphasized quantitatively since:

a) they are derived from values that test the limit of accuracy of the Gouy method, and

b) a purely Russell-Saunders coupling scheme, although assumed to apply in the calculations, may not accurately describe the behavior in heavy metal ions [141].

Nevertheless, the magnetic result from these Pd(II) compounds confirms the conclusions arrived at from electronic and vibrational spectroscopy. The Sn(IV) complex has the smallest 10 D_q, and both β and k are almost equal to 1, suggesting that of the four compounds, it most closely approaches a free-ion environment for Pd(II). An octahedral coordination for Pd(II), evident from vibrational spectroscopy, is also substantiated by these measurements.

3.C.4.2 DIAMAGNETIC FLUOROSULFATO COMPLEXES OF PALLADIUM

As expected, Pd(IV) was found to be diamagnetic, suggesting a $^1A_{1g}$ ground state. For $[Pd(SO_3F)_4]^{2-}$, diamagnetism was also observed, indicating a square planar coordination sphere —— the type usually encountered for Pd(II). The magnetic susceptibility results are listed in Table 3.12.

Table 3.12 MAGNETIC SUSCEPTIBILITIES FOR DIAMAGNETIC PALLADIUM FLUOROSULFATES (in c.g.s. units)

	χ_g	χ_m	$\Sigma\chi_{dia}$
$Ba[Pd(SO_3F)_6]$	$-3.15\pm0.27 \times 10^{-7}$	$-264\pm23 \times 10^{-6}$	-202×10^{-6}
$Cs_2[Pd(SO_3F)_4]$	$-2.78\pm0.24 \times 10^{-7}$	$-214\pm18 \times 10^{-6}$	-247×10^{-6}

3.C.5 SOLUTION STUDIES IN HSO_3F

Due to the observed lack of any appreciable solubility of most of the fluorosulfate-containing palladium compounds in HSO_3F, solution studies in these systems were rather limited.

Although $Cs_2[Pd(SO_3F)_4]$ and $(NO)_2[Pd(SO_3F)_4]$ are soluble in HSO_3F, the resulting solutions are very unstable, with a precipitation of $Pd(SO_3F)_2$ forming almost immediately upon the addition of the compounds. $Pd(SO_3F)_2$ was identified by i.r. spectroscopy as the only solid left after a filtration of the mixture. Presumably, the high lattice energy of the extensively polymerized $Pd(SO_3F)_2$ favored its formation and subsequent removal from the equilibrium of:

$$[Pd(SO_3F)_4]^{2-} \underset{\leftarrow}{\overset{HSO_3F}{\rightarrow}} Pd(SO_3F)_2 + 2SO_3F^- \quad . \qquad (3.25)$$

This is also consistent with the observation that no reversal of equation (3.25) takes place when alkali metal fluorosulfates are mixed with $Pd(SO_3F)_2$.

In order to provide further evidence for the existence of $[Pd(SO_3F)_6]^{2-}$ as an ionic entity, electrical conductivity measurements for solutions of $Cs_2[Pd(SO_3F)_6]$ in HSO_3F were undertaken. The results, shown in Fig 3.8, agree quite well with the literature values for an analogous compound, $K_2[Sn(SO_3F)_6]$ [32]. The basic dissociation for the anions $[M(SO_3F)_6]^{2-}$, where M = Pd, Pt, Ir, Sn, will be discussed in detail in Chapters 5 and 9. An ionization scheme, at least in a first approximation, can be

FIG. 3.8 CONDUCTIVITY OF $Cs_2[Pd(SO_3F)_6]$ IN HSO_3F

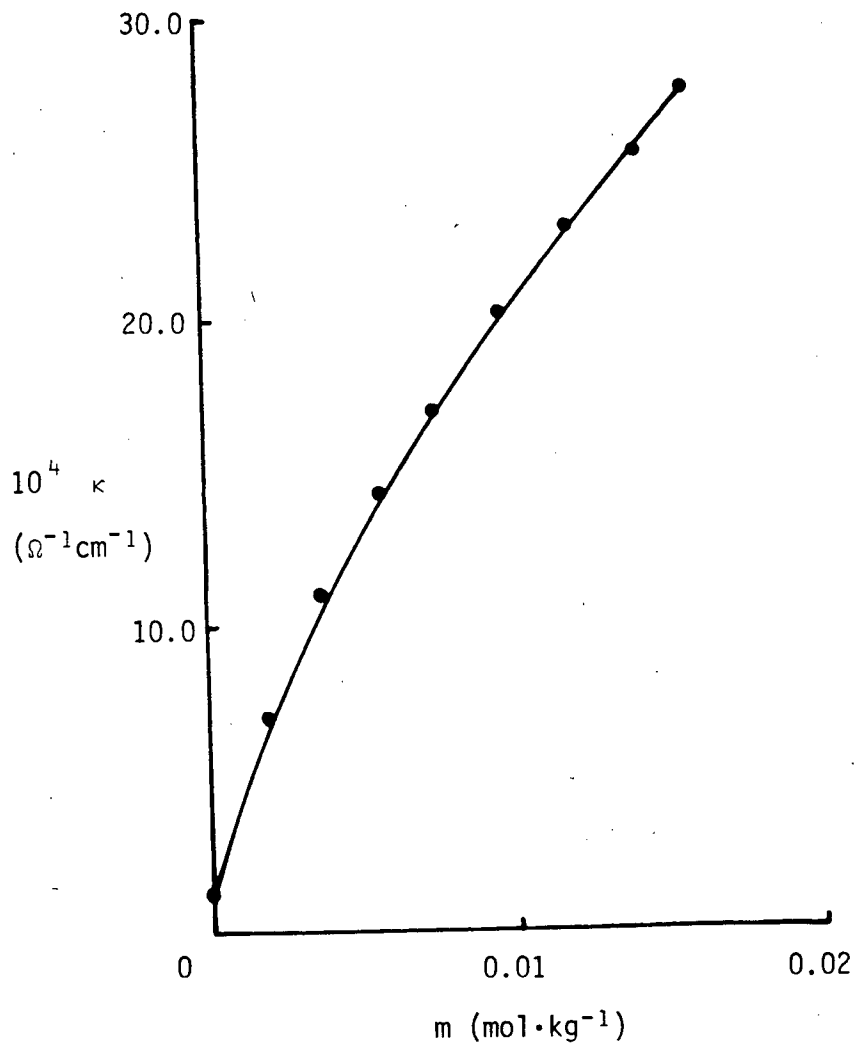

represented by:

$$Cs_2[Pd(SO_3F)_6] \xrightarrow{HSO_3F} 2Cs^+_{(solv)} + [Pd(SO_3F)_6]^{2-}_{(solv)} \qquad (3.26)$$

TABLE 3.13 CONDUCTIVITY OF $Cs_2[Pd(SO_3F)_6]$ IN HSO_3F (interpolated)

m	κ
0.0000	1.220
0.0020	7.275
0.0040	11.45
0.0060	15.02
0.0080	17.91
0.0100	20.48
0.0120	23.00
0.0140	25.14
$mol.kg^{-1}$	$10^{-4}\Omega^{-1}cm^{-1}$ units

3.D CONCLUSION

The study into the fluorosulfates of palladium yielded a number of new compounds with the metal in the +2 and the +4 oxidation states. Two binary fluorosulfates, $Pd(SO_3F)_2$, and the mixed valency compound, $Pd(II)Pd(IV)(SO_3F)_6$, were obtained and characterized.

$Pd(SO_3F)_2$ has the metal in the rather uncommon octahedral and thus paramagnetic environment. Dilute magnetic systems are also encountered for $Pd(II)[M(IV)(SO_3F)_6]$, where M = Pd, Pt, Sn. Ligand field parameters have also been determined for all the above compounds, except for $Pd_2(SO_3F)_6$, by electronic spectroscopy. Diamagnetic complexes containing the presumably square planar $[Pd(SO_3F)_4]^{2-}$ can also be obtained.

While a number of $[Pd(SO_3F)_6]^{2-}$ complexes can be synthesized and characterized, the parent compound —— $Pd(SO_3F)_4$ has thus far eluded all attempts. Indirect evidence seems to indicate its existence in $S_2O_6F_2/HSO_3F$ and that it has a strong fluorosulfate-accepting ability.

CHAPTER 4 GOLD-FLUOROSULFATE

4.A INTRODUCTION

Although gold is a member of the copper triad —— copper, silver and gold ——, unlike in most other groups, there is little resemblance between the chemistry of the three metals. While both the noble metals can exist in the monovalent state, Au(III) is the only commonly found high oxidation state. Both Ag(II) and Ag(III) are extremely strongly oxidizing and cannot be obtained easily. Compounds have frequently appeared in the literature in which gold has formally the oxidation number of +2. Most of them, however, are actually mixed valency compounds containing Au(I) and Au(III) because they are diamagnetic. A true Au(II) compound should be paramagnetic because of the presence of a d^9 electronic configuration for the metal. The few truly Au(II) compounds contain dithiolate-type ligands which are very effective in electron delocalization. These compounds are paramagnetic, as studied by bulk magnetic susceptibility measurements and e.s.r. [133,152].

The first example of a +5 oxidation state for gold is the $[AuF_6]^-$ complexes, formed by the fluorination/complexation reaction of AuF_3 according to [153,154]:

$$2XeF_2 + AuF_3 + 5F_2 \longrightarrow [Xe_2F_{11}]^+[AuF_6]^- \qquad (4.1)$$

The pentafluoride, AuF_5, can be prepared by the pyrolysis of $O_2[AuF_6]^-$ [155]. These fluorine coordinated compounds of Au(V) represent a frequent observation in transition metal chemistry

that the highest possible oxidation state of a metal is usually found in such systems.

The general chemistry of gold has been reviewed in a number of recent publications [156-159]. Again, some brief comments on the halide system of gold can provide some pertinent background information to the corresponding fluorosulfate system.

The monohalides, Au-Hal, with Hal=Cl, Br, I, the trihalides, $Au\text{-}Hal_3$, with Hal=F, Cl, Br, and the previously mentioned AuF_5, are known. All of these binary halides, because of their unsaturated coordination spheres, can exhibit Lewis acidity towards halide ions or other suitable donor ligands to form complexes. For examples, neutral adducts of the types Au(I)-Hal·L, and $Au(III)\text{-}Hal_3\cdot L$, where L=neutral ligands, and anionic complexes of the types of $[Au(I)\text{-}Hal_2]^-$, $[Au(III)\text{-}Hal_4]^-$ and $[AuF_6]^-$, can readily be prepared. The chemistry of the monohalides, by virtue of its similarities to those of Ag(I) and Cu(I), will not be discussed here.

The three trihalides are polymeric to varying degrees: Au_2Cl_6 and Au_2Br_6 are the species present in vapor, solid state and solutions in covalent solvents. AuF_3, on the other hand, is extensively polymerized, and consists of chains of fluorine-bridged $[AuF_4]$ units packed in a helical manner [160]. The tetrahalocomplexes, similar to the binary trihalides, are square planar and therefore diamagnetic [161]. Actually, all gold compounds, except for the very few that contains Au(II), are diamagnetic;

the rationale generally invoked to explain the diamagnetism of most Pd(II) compounds is even more applicable to Au(III) because of the latter's larger ligand field splitting.

$Au(SO_3F)_3$, first reported by Cady in 1972 [82], appears to be the only well documented binary oxyacid salt of Au(III). While the existence of the nitrate is questionable, its anionic complex, $K[Au(NO_3)_4]$, can be prepared and crystallographic results indicate the compound has monodentate nitrate group in a square planar configuration around Au(III) [162].

$Au(SO_3F)_3$ may behave as an ansolvo acid in the HSO_3F solvent system for the following reasons:

a) The reaction of gold metal with $BrSO_3F$, as reported by Cady et al[82], resulted in the formation of a solution. Since $BrSO_3F$ is an ionizing solvent [38], the solvation of the product indicates some type of dissociation process of the solvent taking place with $Au(SO_3F)_3$.

b) The product isolated from the reaction mixture described above is a solid of the approximate composition of $Au(SO_3F)_3 \cdot 2BrSO_3F$. This could be a donor-acceptor adduct, and since $BrSO_3F$ is not known to be a strong SO_3F acceptor [163], $Au(SO_3F)_3$ could be the acceptor, with the formation of a species which may be formulated as $[Br_2SO_3F]^+[Au(SO_3F)_4]^-$.

c) Solutions of AuF_3 in HSO_3F have been reported by Woolf to show acid behavior, although the actual nature of the species present in solution was not identified [164].

Therefore, a full investigation into the chemistry and solution behavior of $Au(SO_3F)_3$ in HSO_3F was undertaken, in the hope of establishing its existence as a novel superacid system [165,166]. The gold-trifluoromethylsulfate system was also studied for possible superacid behavior in HSO_3CF_3; the results are described in Appendix B.

4.B EXPERIMENTAL

4.B.1 SYNTHESIS OF $Au(SO_3F)_3$

4.B.1.1 OXIDATION OF GOLD METAL BY $S_2O_6F_2/HSO_3F$

$$2Au + 3S_2O_6F_2 \xrightarrow{HSO_3F} 2Au(SO_3F)_3 \qquad (4.2)$$

In a typical reaction, $S_2O_6F_2$ (~2 mL) and HSO_3F (~3 mL) were distilled into a reactor containing gold powder (579 mg, 2.940 mmol). The reaction proceeded slowly at room temperature, with the metal dissolving over a period of about 6 hours to give a yellow to orange solution. The removal of all volatile materials yielded $Au(SO_3F)_3$, (1.460 g, 2.955 mmol).

$Au(SO_3F)_3$ is a yellow to orange, hygroscopic, crystalline solid. It is sublimable at ~120°C in vacuo and melts with decomposition at ~140°C to a dark red liquid. It is very soluble in HSO_3F, with concentrations of up to ~7 m having been obtained. The elemental analysis of $Au(SO_3F)_3$ was reported by Cady et al [82].

4.B.1.2 SOLVOLYSIS OF $AuCl_3$ IN $BrSO_3F$

$$2AuCl_3 + 6BrSO_3F \longrightarrow 2Au(SO_3F)_3 + 3Br_2 + 3Cl_2 \qquad (4.3)$$

$AuCl_3$, (168 mg, 0.554 mmol), dissolved in $BrSO_3F$, (~6 mL), with gas evolution. The vapor had the appearance of Cl_2, which could be in equilibrium with BrCl. To ensure a complete reaction, the solution was heated at 60°C for 4 hours. After the removal of all volatile materials, $Au(SO_3F)_3$ was obtained, (276 mg, 0.599 mmol).

$Au(SO_3F)_3$ can also be obtained from,

a) the reaction of Au_2O_3 with $S_2O_6F_2/HSO_3F$:

$$Au_2O_3 + 3S_2O_6F_2 \xrightarrow{HSO_3F} 2Au(SO_3F)_3 + 3O_2 \ , \qquad (4.4)$$

or b) the reaction of gold metal with $BrSO_3F$ followed by the thermal decomposition of the intermediate as reported by Cady et al [82].

4.B.2 SYNTHESIS OF IONIC $[Au(SO_3F)_4]^-$ COMPLEXES

$$CsCl + HSO_3F \longrightarrow CsSO_3F + HCl \qquad (4.5)$$

$$2CsSO_3F + 2Au + 3S_2O_6F_2 \xrightarrow{HSO_3F} 2Cs[Au(SO_3F)_4] \qquad (4.6)$$

HSO_3F (~3 mL) was added to a mixture of CsCl (142 mg, 0.843 mmol) and gold powder (166 mg, 0.843 mmol). The HCl formed was removed by evacuating all the solvent. $S_2O_6F_2$, (~2 mL) and HSO_3F, (~4 mL), were then added to the solid mixture and the reactor was subsequently heated at ~60°C for 12 hours. After which time all the metal had reacted. The removal of all volatile materials yielded $Cs[Au(SO_3F)_4]$, (622 mg, 0.844 mmol).

An alternative synthetic route involves solvolysis/oxidation in $BrSO_3F$ according to:

$$CsCl + Au + 4BrSO_3F \longrightarrow Cs[Au(SO_3F)_4] + 2Br_2 + \tfrac{1}{2}Cl_2 \ . \qquad (4.7)$$

The equimolar mixture of CsCl and gold metal was heated in an excess amount of $BrSO_3F$ at ~60°C for 2 days, followed by the removal

of all volatile materials.

$Cs[Au(SO_3F)_4]$ is a yellow, crystalline, hygroscopic solid. It is soluble in both HSO_3F and $BrSO_3F$, and melts at 105°C into a deep orange liquid which decomposes at ~300°C.

Analysis	Cs	Au	F
Calculated %	18.30	27.13	10.47
Found %	18.14	26.98	10.30

4.B.2.2 PREPARATION OF $K[Au(SO_3F)_4]$

$$KCl + HSO_3F \longrightarrow KSO_3F + HCl \qquad (4.8)$$

$$2KSO_3F + 2Au + 3S_2O_6F_2 \xrightarrow{HSO_3F} 2Cs[Au(SO_3F)_4] \qquad (4.9)$$

In an analogous manner to the preparation of the corresponding Cs^+ salt, KCl (78 mg, 1.05 mmol) and gold powder (206 mg, 1.05 mmol) were reacted with a mixture of $S_2O_6F_2$ and HSO_3F to yield $K[Au(SO_3F)_4]$, (692 mg, 1.09 mmol).

Similarly, $K[Au(SO_3F)_4]$ can also be obtained from the co-solvolysis of KCl and $AuCl_3$ in an excess of $BrSO_3F$, followed by the removal of all volatile materials.

$K[Au(SO_3F)_4]$ is a yellow, crystalline, hygroscopic solid. It is soluble in both HSO_3F and $BrSO_3F$; it melts with decomposition at ~230°C.

Analysis	K	Au	F
Calculated %	6.18	31.15	12.02
Found %	6.22	30.80	12.28

4.B.2.3 PREPARATION OF $Li[Au(SO_3F)_4]$

$$Li_2CO_3 + S_2O_6F_2 \longrightarrow 2LiSO_3F + CO_2 + \tfrac{1}{2}O_2 \qquad (4.10)$$

$$2LiSO_3F + 2Au + 3S_2O_6F_2 \xrightarrow{HSO_3F} 2Li[Au(SO_3F)_4] \qquad (4.11)$$

An excess of $S_2O_6F_2$ (~1 mL) was added to a mixture of Li_2CO_3 (25 mg, 0.68 mmol) and gold powder (132 mg, 0.67 mmol). After the gas evolution from the first reaction had ceased, all volatile materials were removed and a mixture of $S_2O_6F_2$ (~2 mL) and HSO_3F (~2 mL) was distilled into the reactor. A slow reaction occurred, and the reactor had to be kept at 100°C for 2 days in order for all the metal to react. A precipitate formed, and the removal of all volatile materials yielded $Li[Au(SO_3F)_4]$, (406 mg, 0.68 mmol).

$Li[Au(SO_3F)_4]$ is a yellow, crystalline, hygroscopic solid which does not melt below 280°C. It is only slightly soluble in HSO_3F at room temperature.

Analysis	Li	Au	F
Calculated %	1.16	32.87	12.66
Found %	1.21	32.59	12.51

4.B.2.4 PREPARATION OF $(ClO_2)[Au(SO_3F)_4]$

$$ClO_2SO_3F + Au(SO_3F)_3 \longrightarrow (ClO_2)[Au(SO_3F)_4] \qquad (4.12)$$

$Au(SO_3F)_3$, (224 mg, 0.453 mmol), was dissolved in an excess of ClO_2SO_3F (~2 mL). The subsequent removal of all excess ClO_2-SO_3F yielded $(ClO_2)[Au(SO_3F)_4]$, (288 mg, 0.436 mmol).

The above compound can also be obtained from a reaction of gold metal with a $ClO_2SO_3F/S_2O_6F_2$ mixture, according to:

$$2ClO_2SO_3F + 2Au + 3S_2O_6F_2 \longrightarrow 2(ClO_2)[Au(SO_3F)_4] \quad . \qquad (4.13)$$

$(ClO_2)[Au(SO_3F)_4]$ is a yellow, crystalline, hygroscopic solid. It is soluble in ClO_2SO_3F at 25°C to give a light orange solution. It melts at 101 - 103°C to an orange liquid which decomposes at ~170°C.

Analysis	Cl	Au	S
Calculated %	5.23	29.81	19.41
Found %	5.23	30.00	19.24

4.B.2.5 PREPARATION OF $(NO)[Au(SO_3F)_4]$

$$2Au + 3Br_2 \longrightarrow 2AuBr_3 \qquad (4.14)$$

$$4NOCl + AuBr_3 \longrightarrow (NO)[AuCl_4] + 3NOBr \qquad (4.15)$$

$$(NO)[AuCl_4] + 4BrSO_3F \longrightarrow (NO)[Au(SO_3F)_4] + 2Br_2+2Cl_2 \qquad (4.16)$$

Gold powder (112 mg, 0.569 mmol) was reacted with Br_2 at 80°C for 12 hours to give $AuBr_3$, (247 mg, 0.565 mmol), which was reacted with an excess of NOCl (~5 mL) at 80°C for ½ day. The insoluble, light brown, powder was identified as $(NO)[AuCl_4]$, (209 mg, 0.567 mmol), by its Raman spectrum which had bands at 2205 and 2183 cm^{-1}, (νN-O), and also at 345 and 321 cm^{-1}, ($\nu[AuCl_4]$). $(NO)[Au(SO_3F)_4]$, (348 mg, 0.558 mmol) was prepared by reacting the $(NO)[AuCl_4]$ with an excess of $BrSO_3F$, (~2 mL), and heating the reaction mixture at 80°C for ½ hour. The product was

isolated after the removal of all volatile materials.

$(NO)[Au(SO_3F)_4]$ is a yellow, crystalline, hygroscopic solid. It is soluble in both $BrSO_3F$ and HSO_3F. It melts at 192 - 195°C to an orange liquid which decomposes at ~260°C.

Analysis	N	Au	F
Calculated %	2.25	31.61	12.19
Found %	2.10	31.85	12.32

4.B.3 SYNTHESIS OF $[Au(SO_3F)_4]$ COMPLEXES CONTAINING HALOGENO-FLUOROSULFATO CATIONS

4.B.3.1 PREPARATION OF $[Br(SO_3F)_2][Au(SO_3F)_4]$

$$Br_2 + 3S_2O_6F_2 \longrightarrow 2Br(SO_3F)_3 \qquad (4.17)$$

$$2Br(SO_3F)_3 + 2Au + 3S_2O_6F_2 \longrightarrow 2[Br(SO_3F)_2][Au(SO_3F)_4] \qquad (4.18)$$

Br_2, (37 mg, 0.231 mmol) and gold powder (90 mg, 0.457 mmol) were reacted with $S_2O_6F_2$ (~3 mL) at 70°C for ½ day. The oxidation of Br_2 proceeded quickly, as evident by the formation of a yellow solution. Soon afterwards, the gold metal dissolved to form two immiscible, light yellow layers, with the top layer presumably containing mostly $S_2O_6F_2$. The bottom layer crystallized when the mixture was cooled at 0°C for 3 days. The removal of all volatile materials at room temperature yielded $[Br(SO_3F)_2][Au(SO_3F)_4]$, (408 mg, 0.468 mmol).

$[Br(SO_3F)_2][Au(SO_3F)_4]$ is a light yellow, hygroscopic, cry-

stalline solid that has a tendency towards supercooling at room temperature. It melts at 52 - 55°C.

Analysis	Br	Au	S	F
Calculated %	9.17	22.61	22.08	13.08
Found %	9.26	22.45	21.84	13.13

4.B.3.2 PREPARATION OF $[I(SO_3F)_2][Au(SO_3F)_4]$

$$I_2 + 3S_2O_6F_2 \longrightarrow I(SO_3F)_3 \qquad (4.19)$$

$$2I(SO_3F)_3 + 2Au + 3S_2O_6F_2 \longrightarrow 2[I(SO_3F)_2][Au(SO_3F)_4] \qquad (4.20)$$

In a manner similar to the last preparation, I_2 (92 mg, 0.363 mmol) and gold powder (143 mg, 0.726 mmol) were allowed to react with $S_2O_6F_2$ (~3 mL) at ~80°C for 12 hours. After all the metal had reacted, crystalline $[I(SO_3F)_2][Au(SO_3F)_4]$ was formed upon cooling the mixture to room temperature (650 mg, 0.708 mmol).

$[I(SO_3F)_2][Au(SO_3F)_4]$ is a light orange to yellow, hygroscopic crystalline solid. It has a melting range of 70 - 73°C.

Analysis	I	Au	F
Calculated %	13.82	21.45	12.41
Found %	14.04	21.61	12.67

4.B.4 SYNTHESIS OF $[Au(SO_3F)_4]^-$ COMPLEXES CONTAINING POLYBROMINE CATIONS

4.B.4.1 PREPARATION OF $(Br_3)[Au(SO_3F)_4]$

$$Au + 4BrSO_3F \longrightarrow (Br_3)[Au(SO_3F)_4] + \tfrac{1}{2}Br_2 \qquad (4.21)$$

An excess of $BrSO_3F$ (~3 mL) was distilled onto gold powder, (293 mg, 1.488 mmol), contained in a reaction vial. A vigorous, exothermic reaction occurred at room temperature. To ensure a complete reaction, the mixture was heated at 60°C for 6 hours. The removal of all volatile materials at room temperature yielded a compound that analyzed as $(Br_3)[Au(SO_3F)_4]$, (1.239 g, 1.488 mmol).

$(Br_3)[Au(SO_3F)_4]$ is a dark brown, hygroscopic, polycrystalline solid. It decomposes at 105°C to form $Au(SO_3F)_3$. It is soluble in $BrSO_3F$ and HSO_3F.

Analysis	Br	Au	F
Calculated %	28.78	23.65	9.12
Found %	28.64	23.89	9.15

4.B.4.2 PREPARATION OF $(Br_5)[Au(SO_3F)_4]$

$$(Br_3)[Au(SO_3F)_4] + Br_2 \longrightarrow (Br_5)[Au(SO_3F)_4] \qquad (4.22)$$

Gold powder (175 mg, 0.888 mmol) was converted into (Br_3)-$[Au(SO_3F)_4]$ as described above. Br_2 (~5 mL) was distilled onto the intermediate and the mixture was heated at 70°C for 6 hours. The removal of all volatile materials at room temperature yielded $(Br_5)[Au(SO_3F)_4]$, (875 mg, 0.882 mmol).

The same compound can also be obtained by

a) the addition of excess Br_2 to a 2:1 mixture of $Au(SO_3F)_3$ and $S_2O_6F_2$, according to:

$$5Br_2 + 2Au(SO_3F)_3 + S_2O_6F_2 \longrightarrow 2(Br_5)[Au(SO_3F)_4] \ , \qquad (4.23)$$

or b) the addition of excess Br_2 to $[Br(SO_3F)_2][Au(SO_3F)_4]$:

$$[Br(SO_3F)_2][Au(SO_3F)_4] + 3Br_2 \longrightarrow (Br_5)[Au(SO_3F)_4] + 2BrSO_3F \ . \qquad (4.24)$$

$(Br_5)[Au(SO_3F)_4]$ is a dark brown, polycrystalline, hygroscopic solid. It is insoluble in Br_2, and melts with decomposition at ~65°C. The compound shows a slight decomposition pressure at room temperature in vacuo but is stable if kept in 1 atm nitrogen.

Analysis	Br	Au	F
Calculated %	40.25	19.84	7.66
Found	40.20	20.07	7.79

4.C DISCUSSION

4.C.1 SYNTHESIS AND GENERAL DISCUSSION

4.C.1.1 $Au(SO_3F)_3$

For the intended solution study on $Au(SO_3F)_3$ in HSO_3F, a convenient and fast synthetic route to very pure samples of the compound was needed. The original synthesis, described by Cady et al [82], involved the oxidation of the metal with $BrSO_3F$ followed by the pyrolysis of the intermediate with the reported composition of $Au(SO_3F)_3 \cdot 2BrSO_3F$, led to slightly impure products. Samples of $Au(SO_3F)_3$ obtained by this method were found to be slightly paramagnetic, with a magnetic moment of ~0.5 μ_B and displaying Curie-Weiss law behavior from ~300 to ~100K. Interestingly, the original synthesis of AuF_3 by an almost parallel method, represented below:

$$Au + 2BrF_3 \longrightarrow AuF_3 \cdot BrF_3 + \tfrac{1}{2}Br_2 \qquad (4.25)$$

$$AuF_3 \cdot BrF_3 \xrightarrow{\Delta} AuF_3 + BrF_3 \quad , \qquad (4.26)$$

also produced weakly paramagnetic materials [167], while pure AuF_3 obtained from the direct fluorination of $AuCl_3$ is diamagnetic [160,168]. Although the presence of Au(II) or paramagnetic bromine-containing species such as Br_2^+ may be the cause of the observed paramagnetism, a detailed investigation was considered beyond the intent of this study.

The reaction of gold metal with $S_2O_6F_2$ resulted in only a slow surface attack and required a reaction temperature of ~160°C for ~14 days. The addition of HSO_3F as the solvent allows the

synthesis of pure and diamagnetic $Au(SO_3F)_3$ in a fast and efficient manner. As an added advantage, this method allows the direct preparation of solutions of $S_2O_6F_2$ in HSO_3F because the excess $S_2O_6F_2$ can be removed readily. As shown by Raman spectroscopy of the resulting solutions, for an initial 1:1 $S_2O_6F_2/HSO_3F$ mixture, no trace of $S_2O_6F_2$ (detected by νO-O at 900 cm^{-1}) [95] was left after about 70% of the solution was removed by vacuum.

The alternative synthetic route to $Au(SO_3F)_3$ by the solvolysis of $AuCl_3$ in $BrSO_3F$ offers no distinct advantage over the $S_2O_6F_2/HSO_3F$ method. The attempted solvolysis of $AuCl_3$ in HSO_3F did not proceed even at ~110°C.

4.C.1.2 IONIC $[Au(SO_3F)_4]^-$ COMPLEXES

The preparation of these complexes utilizes the various synthetic methods described in Chapter 3 for the preparation of Pd(IV) complexes. Due to the lack of reactivity of gold metal towards HSO_3F [64], stoichiometric mixtures of gold and an alkali metal chloride can be solvolysed to give the corresponding $M(I)(SO_3F)$. The addition of $S_2O_6F_2/HSO_3F$ results in the oxidation of gold and the formation of the alkali metal tetrakis(fluorosulfato) aurate(III) salts. Because of the deliquescent nature of LiCl, the carbonate was used instead; but because the solvolysis of CO_3^{2-} in HSO_3F would lead to water being one of the products, according to:

$$CO_3^{2-} + 2HSO_3F \longrightarrow H_2O + CO_2 + 2SO_3F^- \quad , \qquad (4.27)$$

$S_2O_6F_2$ was used as the fluorosulfonating agent. These pseudo-one-step reactions are very reliable synthetic routes which exclude the handling of hygroscopic intermediates.

$NO[AuCl_4]$ is usually prepared by the reaction between NOCl and $AuCl_3$ in the presence of a solvent such as diethyl ether or THF [169]. To avoid having to dry and use such hygroscopic solvents, an alternative synthetic method was chosen, involving the solvolysis and subsequent complexation of $AuBr_3$ in NOCl.

A very interesting trend can be noted in the melting points of a few of these complexes: ClO_2^+, (~102°C), ~Cs^+, (~105°C), < NO^+, (~193°C), K^+, (~230°C), Li^+, (~280°C).

This may be due to lattice energy effects which depend on the size of the cation, and anion-polarization by the cation resulting in anion-cation interactions. The effect of NO^+ is very similar to that of K^+; this is consistent with crystallographic results from other studies which have shown that the two cations have almost identical effective ionic radii in the solid state [94].

4.C.1.3 COMPLEXES CONTAINING POLYBROMINE CATIONS

In order to characterize the intermediate of $Au(SO_3F)_3 \cdot 2BrSO_3F$ from the Au + $BrSO_3F$ reaction, thought to contain a $[Br_2(SO_3F)]^+$ ion, the published formation reaction was reinvestigated [82]. While interhalogen cations such as Br_2Cl^+, I_2Cl^+ and I_2Br^+ [85] are known, such an analogy does not exist in the form of

$[Br_2(SO_3F)\ ]^+$. Although the auto-ionization of $BrSO_3F$ has been postulated as [38]:

$$3BrSO_3F \rightleftharpoons [Br_2(SO_3F)]^+ + [Br(SO_3F)_2]^- \quad , \qquad (4.28)$$

only thermally unstable salts containing $[Br(SO_3F)_2]^-$ are known [80,81,163].

The oxidation of gold with an excess of $BrSO_3F$ did yield a dark brown polycrystalline material: however, its chemical analysis revealed its composition as $Br_3Au(SO_3F)_4$, suggesting a formulation as $Br_3^+[Au(SO_3F)_4]^-$.

The Br_3^+ cation has been identified in solid compounds of the type of $Br_3^+EF_n^-$, where EF_n^- = AsF_6^- [170], BF_4^- and SbF_6^- [171], and in solutions of strong protonic acids [25,28,55]. The addition of Br_2 to $BrSO_3F$ giving Br_3^+ was also shown by low temperature i.r. spectroscopy [172].

The formation of Br_3^+ in the reaction of gold with $BrSO_3F$ may proceed via the following reaction scheme:

$$Au + 3BrSO_3F \longrightarrow Au(SO_3F)_3 + {}^3/_2Br_2 \qquad (4.29)$$

$$Br_2 + BrSO_3F \rightleftharpoons Br_3^+ + SO_3F^- \qquad (4.30)$$

$$Br_3^+ + SO_3F^- + Au(SO_3F)_3 \overset{BrSO_3F}{\rightleftharpoons} Br_3^+[Au(SO_3F)_4]^- \quad , \qquad (4.31)$$

with the precipitation of the final product a necessary driving force to its formation. Evidence for reaction (4.30) has been found in superacid solutions [28] and low temperature i.r. study [172]. Unlike the previously reported Br_3^+-containing compounds, which all show appreciable decomposition pressures at 25°C, $Br_3^+[Au(SO_3F)_4]^-$ is found to be thermally stable at room temperature,

with no decomposition evident in a dynamic vacuum at 25°C.

The thermal decomposition of $Br_3^+[Au(SO_3F)_4]^-$ at ~100°C in vacuo to give slightly paramagnetic $Au(SO_3F)_3$ may proceed via a Br_2^+-containing species. The $^2\Pi_{3/2g}$ ground state would give rise to the observed paramagnetism. Therefore, attempts were made to synthesize $Br_2^+[Au(SO_3F)_4]^-$, by reacting Br_2 with stoichiometric amounts of $BrSO_3F$ or $S_2O_6F_2$ and $Au(SO_3F)_3$, according to:

$$\tfrac{1}{2}Br_2 + BrSO_3F + Au(SO_3F)_3 \longrightarrow Br_2^+[Au(SO_3F)_4]^- \qquad (4.32)$$

$$Br_2 + \tfrac{1}{2}S_2O_6F_2 + Au(SO_3F)_3 \longrightarrow Br_2^+[Au(SO_3F)_4]^- \quad . \qquad (4.33)$$

However, both these reactions led to the formation of rather inhomogeneous products, even when $C_8F_{17}SO_2F$ was used as the inert reaction medium for Br_2. The observation of a strong resonance Raman spectrum of Br_2^+, with the principle band at 360 cm^{-1}, indicates the cation was present [25,28], but an analytically pure product of the desired composition was not isolable.

The further addition of bromine to $Br_3[Au(SO_3F)_4]$ resulted in the formation of $Br_5[Au(SO_3F)_4]$, a compound of relatively low thermal stability (although the decomposition at room temperature is rather slow, thus allowing its isolation). A formulation invoking the hitherto unknown Br_5^+ ion is possible. In the iodine system, I_5^+ has been reported in solid I_5AlCl_4 [173] as well as in HSO_3F solution together with I_7^+ [56]. The limited thermal stability of Br_5^+ is not unexpected, and the compound can only be formed in a large excess of Br_2, whether the starting material is $Br_3[Au(SO_3F)_4]$ or $[Br(SO_3F)_2][Au(SO_3F)_4]$. Being an easily oxidiz-

able species, with a formal oxidation number of +1/5 for bromine, Br_5^+ is unstable in the presence of any significant quantities of $BrSO_3F$; for example, when gold is reacted with a mixture of Br_2/$BrSO_3F$ of approximately 1:1 by volume, the only product isolated is the tribromine species.

4.C.1.4 COMPLEXES CONTAINING HALOGENO-FLUOROSULFATO CATIONS

There is only one precedent reported for complexes containing $[Hal(SO_3F)_2]^+$ cations, with Hal = Br and I, — those of $[Sn(SO_3F)_6]^{2-}$ [31]. The synthesis of the corresponding $[Au(SO_3F)_4]^-$ containing complexes was undertaken to gain more insights into this group of compounds and to compare the SO_3F^- acceptor abilities of $Au(SO_3F)_3$ and $Hal(SO_3F)_3$. The successful synthesis of $[Hal(SO_3F)_2]^+[Au(SO_3F)_4]^-$ would establish $Au(SO_3F)_3$ as the stronger ansolvo acid and confirm the amphoteric behavior of the halogen trifluorosulfates.

The reaction of stoichiometric amounts of bromine or iodine and gold with an excess of $S_2O_6F_2$ resulted in the formation of the corresponding $[Hal(SO_3F)_2][Au(SO_3F)_4]$, with the formulation supported by a characterization of the compounds. $S_2O_6F_2$ acts as both the oxidizing agent and the solvent in these reactions by dissolving the halogen tris(fluorosulfate) formed in the initial reactions. The reaction can be viewed as between a Lewis acid and a Lewis base, according to:

$$Hal(SO_3F)_3 + Au(SO_3F)_3 \longrightarrow [Hal(SO_3F)_2][Au(SO_3F)_4] \quad . \quad (4.34)$$

The alternative reaction scheme involving $Au(SO_3F)_3$ as the base is not supported by vibrational spectroscopy.

As the compound originally thought to be a 2:1 adduct between $BrSO_3F$ and $Au(SO_3F)_3$ turned out to contain the Br_3^+ cation instead, attempts were made to synthesize the adduct by alternate methods. Although $Au(SO_3F)_3$ was found to be soluble in $BrSO_3F$, the only product isolated upon the removal of all volatile materials was $Au(SO_3F)_3$. It therefore appears that the $[Br_2(SO_3F)]^+$ cation has very limited stability with respect to dissociation in vacuo at room temperature.

4.C.1.5 REACTION OF $Au(SO_3F)_3$ WITH NEUTRAL DONOR MOLECULES

$$Au(SO_3F)_3 + :L \longrightarrow Au(SO_3F)_3 \cdot L \qquad (4.35)$$

Although many attempts were made to synthesize adducts of the type of $Au(SO_3F)_3 \cdot L$ according to equation (4.35), no stable products could be isolated.

$Au(SO_3F)_3$ was found to be slightly soluble in SO_2, and the resulting solution was investigated by Raman spectroscopy, but the removal of all SO_2 at 0°C yielded only unreacted $Au(SO_3F)_3$. The use of other Lewis bases such as pyridine, dimethylsulfoxide, and acetonitrile all led to the reduction of $Au(SO_3F)_3$ to gold metal.

It therefore appears that:

a) With the formation of $SbF_5 \cdot SO_2$ [174], SbF_5 is a stronger Lewis acid towards SO_2 than $Au(SO_3F)_3$ is, although this could be

due to the inability of SO_2 to compete favorably against the bridging SO_3F groups in the $Au(SO_3F)_3$ polymer. In any case, SO_2 is a very weak Lewis base; $SbF_5 \cdot SO_2$ has only limited thermal stability [174] and SO_2 has been used effectively as a diluent in superacid systems [45].

b) The observed reduction of $Au(SO_3F)_3$ by the ligands with stronger Lewis basicity may proceed by the displacement of the coordinating SO_3F group followed by a reductive decomposition of the Au(III) species to Au(0). The substitution of SO_3F groups in transition metal bis(fluorosulfate)s by pyridine and bipyridine to form ionic fluorosulfates have been reported [83,84,175].

4.C.1.6 ATTEMPTS TO STABILIZE OTHER POLYHALOGEN AND INTERHALOGEN CATIONS

The only reported example for a polychlorine cation is Cl_3^+, found in thermally unstable complexes with $[AsF_6]^-$ or $[SbF_6]^-$ as the counter-anion [60]. The reasonable thermal stability of $Br_3[Au(SO_3F)_4]$ suggests that the chlorine analogue may exist as well. Also, interhalogen cations formed between bromine and chlorine are uncommon, with $BrCl_2^+$ and Br_2Cl^+ identifiable only in SbF_5 solutions [176]; the interaction of Br_3^+ and Br_5^+ with Cl_2 may be a possible synthetic route to such compounds.

Unfortunately, both $Br_3[Au(SO_3F)_4]$ and $Br_5[Au(SO_3F)_4]$, when reacted with chlorine gas at room temperature, or with liquid chlorine at ~-78°C, resulted in the formation of a product with

the characteristics of $AuCl_3$ as followed by weight and i.r. spectroscopy. No compounds containing mixed chloro-bromo cations were isolated from these reactions. $AuCl_3$ reacted with $ClSO_3F$ to give a mixture identified by Raman spectroscopy as consisting of $ClO_2[Au(SO_3F)_4]$ and $Au(SO_3F)_3$, with the former arising as a result of $ClSO_3F$'s reaction with traces of moisture in the quartz reactor [77]. The attempted reductive replacement of $(ClO_2)^+$ in $ClO_2[Au(SO_3F)_4]$ with Cl_3^+ by reaction with liquid chlorine was unsuccessful; an analogous reaction using Br_2 yielded $Br_3[Au(SO_3F)_4]$. No reaction was evident either when $AuCl_3$ was mixed with a ~1:3 mixture of $ClSO_3F/Cl_2$ at ~-23°C. Therefore, the basicity of the $[Au(SO_3F)_4]^-$ anion may not be low enough for the stabilization of Cl_3^+, $BrCl_2^+$ or Br_2Cl^+; all of them are expected to be more electrophilic than Br_3^+. The borderline stability of Br_2^+ in the Au(III)-SO_3F system may be due to a similar explanation.

4.C.1.7 ATTEMPTED FURTHER OXIDATION OF GOLD

Although the most common oxidation state of gold is Au(III), Au(V) can be found in the fluoride system [153-155]. Considering the strong similarity between fluorides and fluorosulfates, the possibility of such an analogy in the fluorosulfate system was explored.

Neither $Au(SO_3F)_3$ nor $Cs[Au(SO_3F)_4]$, when exposed to unfiltered u.v. radiation from a Hg-discharge lamp in the presence of $S_2O_6F_2$ at temperatures up to ~100°C, was found to react. The

addition of O_2 to the above reactor containing $Au(SO_3F)_3$ and $S_2O_6F_2$ did not yield any O_2^+ containing products. FSO_3F, a very powerful oxidant, was added to $Cs[Au(SO_3F)_4]$ and warmed up to room temperature; no fluoride-fluorosulfate of Au(V) was obtained from the reaction.

4.C.2 VIBRATIONAL SPECTRA

4.C.2.1 IONIC $[Au(SO_3F)_4]$-COMPLEXES AND $Au(SO_3F)_3$

The Raman spectra of $K[Au(SO_3F)_4]$ and $(ClO_2)[Au(SO_3F)_4]$ are shown in Fig. 4.1 and 4.2, respectively. As can be illustrated in the figures, these complexes are excellent Raman scatterers, and spectra of extremely high signal to noise ratio and good resolution are generally obtained even with laser powers of ~15 mW. The Raman frequencies of $M[Au(SO_3F)_4]$, with M = Cs, K, Li, NO, and ClO_2, are listed in Table 4.1 and are compared with those of $K[I(SO_3F)_4]$ [35]. The i.r. frequencies of $Cs[Au(SO_3F)_4]$ are also included in the table to illustrate the intensity difference between the two types of spectra.

Except for occasional small splittings, identical spectra are obtained for all the complexes discussed here. Both band positions and relative intensities agree well with the previously reported spectra for $[I(SO_3F)_4]^-$ and $[Br(SO_3F)_4]^-$, suggesting some structural similarities and similar vibrational mode assign-

FIG. 4.1

Raman Spectrum of $K[Au(SO_3F)_4]$

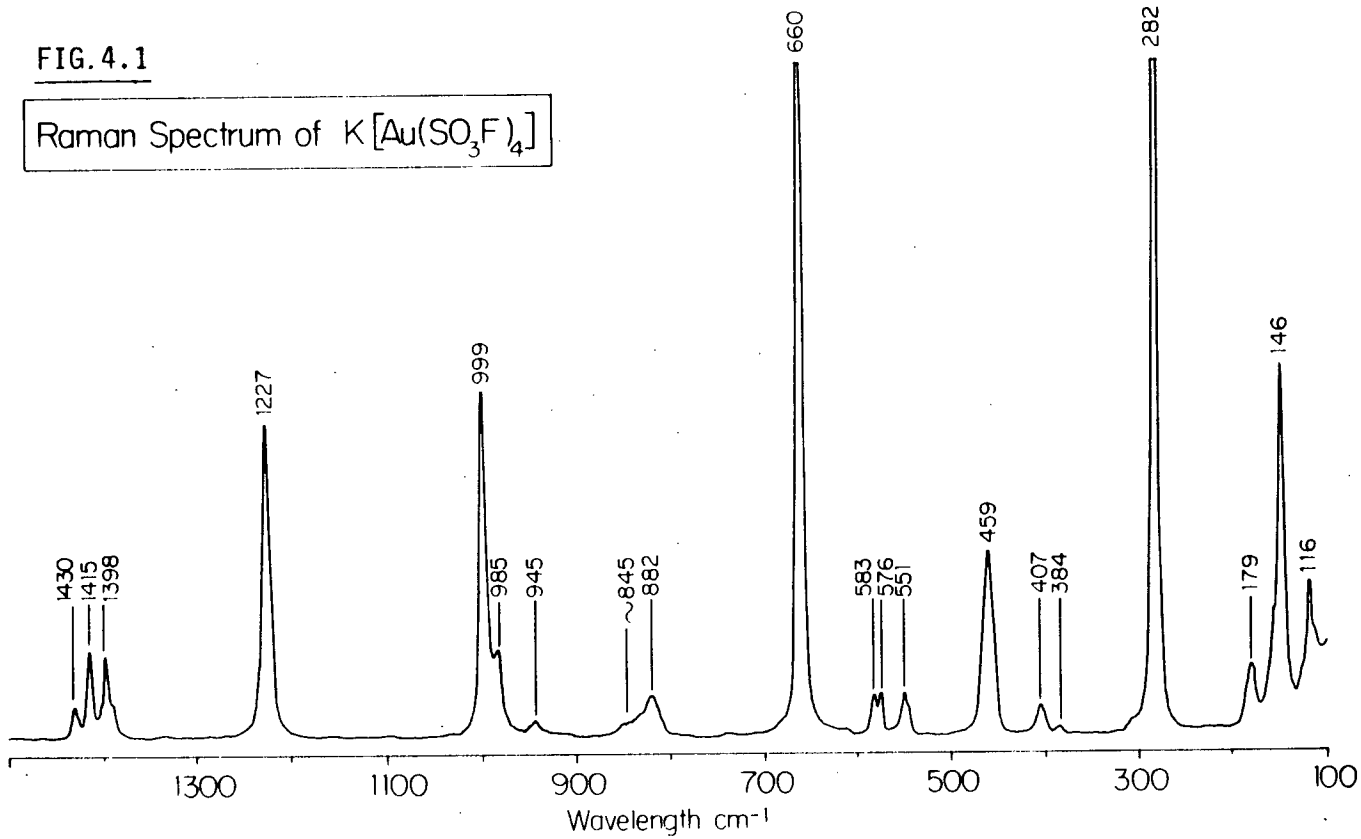

FIG.4.2

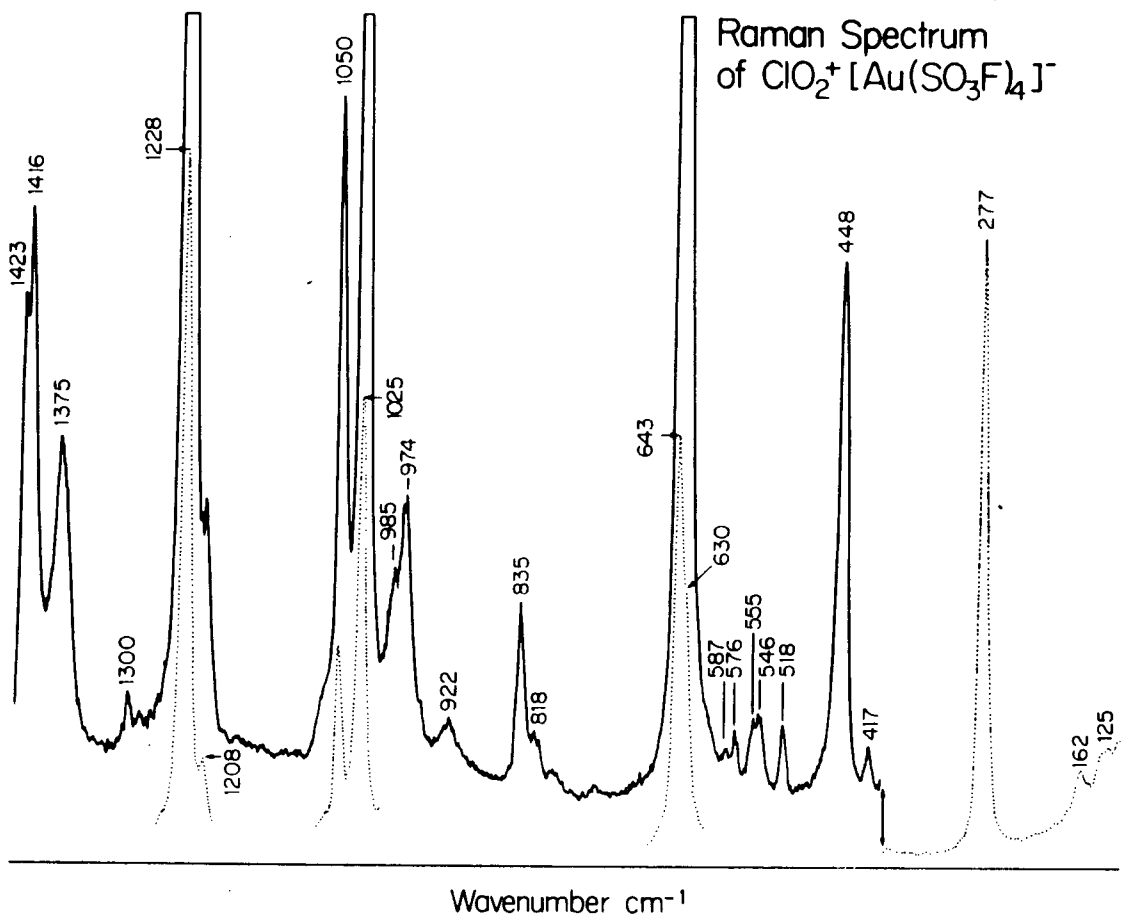
Raman Spectrum
of $ClO_2^+[Au(SO_3F)_4]^-$
1423
1416
1375
1300
1228
1208
1050
1025
985
974
922
835
818
643
630
587
576
555
546
518
448
417
277
162
125
Wavenumber cm^{-1}

TABLE 4.1: VIBRATIONAL FREQUENCIES OF $M[Au(SO_3F)_4]$

$K[I(SO_3F)_4]$ [35] R	M = $C\ell O_2$ R	M = NO R	M = Li R	M = K R	M = Cs R	M = Cs IR	Assignment
		2331 w					νNO^+
	1423 m		1434 w	1430 w			
1409 m	1416 m	1417 m	1409 w,sh	1415 m	1404 m	1400 s,b	$\nu_{as}SO_3$
	1375 w	1395 m	1400 w	1398 m	1380 w,sh		
			1390 w,sh				
	1300 vw						$\nu_{as}C\ell O_2^+$
1250 s	1228 vs	1231 vs	1242 vs	1227 s	1239 vs	1240 s	ν_sSO_3
1222 w,sh	1208 w	1204 w	1210 w,sh		1205 w,sh	1208 vs	
	1050 m						$\nu_sC\ell O_2^+$
1002 m	1025 s	1018 s	1029 s	999 s	1011 s	1010 w,sh	
	985 m,sh						
	974 m	978 w	985 w	985 w	960 vw	970 s,sh	$\nu_{as}SO_3$
	922 vw	933 vw	950 vw	945 vw		930 vs,b	
837 m	835 m	846 m	835 w	845 vw	830 w	830 s	
	818 m	818 m	815 m	828 w	814 w	810 s	νSF
						678 s	
620 vs	643 vs	651 s	642 vs	660 vs	649 vs		νMO + def
		643 s					
582 m	587 w	580 w	582 w	583 w	580 w	585 s	
	576 w	573 w		576 w			δSO_2bend
554 m	555 w	546 w	555 w	551 w	550 w	550 s	δSO_2
	546 w						
							$\delta C\ell O_2^+$
	518 w						
442 s	448 s	455 m	453 s	459 m	452 s	456 s	νMO + def
		455 m					
407 w	417 w	402 vw	415 w	407 w	405 w		
397 w			391 w	384 vw	391 w		ρSO_3
260 s	277 vs	278 vs	280 vs	282 vs	282 s		
239 vs					279 vs		νMO + def
	162 w	150 w,sh	151 w	179 w	150 m		
	125 w	133 m		146 s	127 m		Lattice Modes
				116 m			

ments [35]. The position of the SO_3 - stretching modes at ~1400, ~1220, and ~1000 cm^{-1} indicate monodentate SO_3F groups in an overall anionic environment [32,35]. The reversal of the intensities of these bands in the i.r. and Raman spectra, best illustrated by the two groups at ~(1240, 1200 cm^{-1}) and ~(1010, 950 cm^{-1}), are presumably due to vibrational couplings between identical SO_3F groups through the $[AuO_4]$ skeleton to produce in-phase and out-of-phase vibrations, as discussed in Chapter 3.

An extreme case of intensity reversal in the two types of spectra can be found in the 640-680 cm^{-1} region, where internal fluorosulfate modes are commonly not expected for monodentate SO_3F groups. Strong contributions from $[AuO_4]$ stretching vibrations coupled to ligand deformation modes may explain the mutual exclusion of i.r. and Raman bands in this region. In addition, strong Raman bands are found at ~450 and ~280 cm^{-1} for all the complexes; they may have their origins in the same sort of vibrational couplings discussed for the ~650 cm^{-1} band, not entirely unexpected for such a complex molecule with a cation of +3 charge.

A Raman spectrum was taken of the melt of $Cs[Au(SO_3F)_4]$ at ~150°C; except for the presence of line broadening, the spectrum obtained was identical to that at room temperature. Depolarization ratio measurements revealed all the stronger bands, for which ρ, the depolarization ratio, could be obtained, have a large contribution from asymmetric vibrations, with all ρ values of the order of 0.1 (for a totally symmetric vibration ρ should be close to

zero). This is expected for a molecule with such a low symmetry (C_s) and supports the argument for the presence of strong vibrational couplings.

An interesting comparison of the $[AuO_4]$ vibrations can be made with the vibrational spectrum of $K[Au(NO_3)_4]$, which has an extremely intense and depolarized Raman band at 360 cm^{-1} assignable to $[\nu_s\text{-}AuO_4]$ [177]. Furthermore, the splittings in the NO_3-stretching modes can best be explained as due to solid state effects since the intensities after splitting are very similar. On the contrary, as previously mentioned, in the fluorosulfate system, some of the bands are split into strong/weak pairs, evident of strong vibrational couplings. The crystal structure of $K[Au(NO_3)_4]$ [162] indicates a significant lengthening of the $AuO\text{-}NO_2$ bond to 1.37 Å from 1.25 Å in $Ni(NO_3)_2 \cdot 4H_2O$ [178], in which NO_3^- is uncoordinated. The other two N-O bond lengths are (1.20±0.03) Å, shorter than that found in free nitrates. As a comparison, in $(CH_3)_2Sn(SO_3F)_2$, in which the SO_3F groups are bidentate bridging, all the SnO-S bond lengths are equivalent within experimental error [97]. Therefore, as far as vibrational analysis is concerned, $[Au(NO_3)_4]^-$ may be viewed as consisting of $[AuO_4]\text{---}[NO_2]$, whereas in $[Au(SO_3F)_4]^-$, a much closer association between the two units is evidently present, giving rise to the observed extensive vibrational couplings.

For the complexes containing the alkali metal ions, the additional splittings observed in the SO_3-stretching region are most

likely due to anion-cation interaction, which can be a form of solid state effects; the degree of splitting appears to increase with decreasing cation sizes, suggesting an increase in the polarizing power of the cation. The manifestation of these effects in producing splittings in the SO_3 stretching modes rather than in producing any significant frequency shifts provides further evidence for a very stable $[Au(SO_3F)_4]$ unit.

The presence of ionic species in all the complexes is supported by the almost invariable band position of the anion and the agreement of the vibrational frequencies for the two heterocations, ClO_2^+ and NO^+, with published values. The fundamentals for the chloronium cation are found at 1300, 1050 and 518 cm^{-1} [179]; similarly, the N-O stretching frequency is found at 2331 cm^{-1}, compared to ~2300 cm^{-1} for $NOSO_3F$ [94]. Splittings in the vibrational spectra due to the aspherical nature of these two multiatomic cations are not unexpected.

Finally, the similarities in the vibrational spectra extend also to $Au(SO_3F)_3$ and the halogen tris(fluorosulfate)s, $Br(SO_3F)_3$ and $I(SO_3F)_3$, illustrated in Table 4.2. The spectra contain contributions from both monodentate and bridging bidentate fluorosulfate groups. The diagnostic band for the bidentate bridging SO_3F ligand is found at 1135 cm^{-1} [180], and also in the SO_3-stretching, a strong doublet is present at 1442 and 1425 cm^{-1} in the i.r. spectrum, indicating two types of SO_3F coordinations. The splittings in the $[AuO_4]$ related vibrational modes at (682, 670 cm^{-1}),

Table 4.2 VIBRATIONAL FREQUENCIES OF $Au(SO_3F)_3$

$Au(SO_3F)_3$ R	$Au(SO_3F)_3$ IR	$I(SO_3F)_3$ [35] R
1449 m 1423 m,sh	1442 vs 1425 s,sh	1469 m 1381 w
1227 vs	1240 s 1220 s,sh	1233 vs 1182 w,sh
1102 w 1053 m 955 m,sh 936 s 899 s	1135 ms 1055 s 960 s,b 920 s,sh 895 s,b	1076 w,sh 1050 m 963 s
873 m,sh 822 w	820 s	869 s 826 w
650 vs 610 w	682 s 670 s,sh 610 w	642 vs 619 w
583 w	590 s 582 s	580 m,sh
546 m	550 s	540 m,sh
465 m 444 w	460 m	457 s 430 w
		412 m 386 m
348 m 327 w,sh		
292 vs 285 s		290 vs 270 s,sh
189 170 149		181 m 148 m

(465, 444 cm^{-1}) and (292, 285 cm^{-1}) are most likely the result of the presence of non-identical SO_3F groups around Au(III) and the coupling of AuO_4 vibrations of adjacent $[AuO_4]$ units through bridging SO_3F ligands. While splittings previously assigned to solid state effects are observed in the Raman spectra of some $[Au(SO_3F)_4]$ complexes in the same regions, they are of much smaller magnitudes and are not present in their i.r. spectra. The proliferation of low frequency bands for $Au(SO_3F)_3$, especially in the i.r. spectrum, must be a result of structural complexities leading to a reduced local symmetry for the $[AuO_4]$ unit. A band of medium intensity at 348 cm^{-1} in the Raman spectrum of $Au(SO_3F)_3$ may be assigned as due to νAu-O, which, because of the distortion in the AuO_4 skeleton from square planar geometry, becomes a separate vibration in addition to those that are coupled to ligand deformations.

Thus, it can be concluded that $Au(SO_3F)_3$ contains both bridging- and terminal-fluorosulfate groups, in possibly a polymerized structure with a distorted square planar environment for Au(III).

4.C.2.2 $[X(SO_3F)_2][Au(SO_3F)_4]$, X=Br, I

Both the title compounds are excellent Raman scatterers when sample cooling to ~80 K is employed; the spectra thus obtained are of extremely high resolution. They were found to either melt or decompose at room temperature upon their exposure to laser radiation. Their vibrational frequencies are compared with those

of $[Br(SO_3F)_2][Sn(SO_3F)_6]$ [31] and $Cs[Au(SO_3F)_4]$ in Table 4.3. As can be seen, both new compounds give rather complex vibrational spectra, and a complete band assignment is therefore not possible.

It is evident that the strong characteristic Raman bands for $[Au(SO_3F)_4]^-$ are present in the spectra of the two compounds; on the other hand, referring to the spectrum of $K[I(SO_3F)_4]$ listed in Table 4.1, bands due to $[I(SO_3F)_4]^-$ could not be found in the iodine-containing complex discussed here. For example, the strong $[I(SO_3F)_4]^-$ bands at 1250, 1002, 620, 442, 260 and 239 cm^{-1} are absent in the gold-containing complex. This argues against the alternative formulation for these compounds as $[Au(SO_3F)_2]$-$[X(SO_3F)_4]$, with $Au(SO_3F)_3$ formally acting as the SO_3F-donor. This is also consistent with the observation that while both halogen fluorosulfates —— $I(SO_3F)_3$ [36] and $Br(SO_3F)_3$, are weak electrolytes in HSO_3F, $Au(SO_3F)_3$ forms highly conducting solutions in HSO_3F and as will be discussed in the following section, has been found to be a strong SO_3F acceptor.

Further supporting evidence for the suggested formulation can be found in the bromine-containing complex. By comparison to the reported spectra for $Br(SO_3F)_3$ [35] and $[Br(SO_3F)_2][Sn(SO_3F)_6]$ [31], characteristic bands due to $[Br(SO_3F)_2]^+$ are readily recognized in the $[Au(SO_3F)_4]^-$ complex. In particular, the pair of bands at 1050 and 1491 cm^{-1}, assigned to an asymmetric SO_3-stretch, are found in other cases at such a high frequency only for volatile SO_3F-derivatives such as $S_2O_6F_2$ [95], $S_2O_5F_2$ and $S_3O_8F_2$ [181]. It

TABLE 4.3: VIBRATIONAL FREQUENCIES OF $[X(SO_3F)_2]\cdot[Au(SO_3F)_4]$

$[Br(SO_3F)_2]$-$[Sn(SO_3F)_6]$ [31]	X = Br	X = I	X = I	$Cs[Au(SO_3F)_4]$
R	R,~80K	R,~80K	IR	R
1500 ms	1505 ms	1476 w	1458 w,sh	
1487 mw,sh	1491 w,sh			
	1479 w	1460 w	1440 w,sh	
1420 mw	1425 ms	1413 ms	1410 s,sh	1404 ms
	1416 m	1400 m		
	1400 mw	1388 vw	1388 s	
1387 ms	1389 mw	1380 w	1382 vs	1380 vw
	1252 m,sh			
1248 s	1235 s	1237 m,sh		1239 vs
	1220 ms	1227 ms	1225 s,sh	1205 w
1197 s	1195 ms	1217 vs	1198 vs	
1145 s	1174 m	1174 ms	1175 s,sh	
	1130 m,sh	1135 m	1130 m,sh	
1092 s				
		1039 ms		
1020 ms	1022 s	1022 ms	1025 w	1011 s
	1008 m,sh	990 vw		
985 m	963 mw,b	964 ms	960 s,b	960 vw,b
	921 vw	930 vw	925 vs	
	887 vw	865 w	860 m	
865 vs	864 m	855 w		
850 ms	852 m	842 w	840 m,sh	830 mw
830 w	817 w,b	830 vw		
745 s	745 ms	813 ms	815 vs	814 w
		773 vw		
640 s	648 vs	651 vs	670 m,sh	
		646 vs		649 vs
		631 s,sh	635 s	
596 mw	581 w	589 w	579 s	580 w
	571 w	569 w		
558 m	549 w	553 mw	555 m,sh	550 w
530 m	530 vw	548 w,sh	542 s	
464 s	452 s	453 s	452 s	452 s
430 vw				
414 ms	410 vw	399 vw		405 w
386 m	390 vw	390 vw		391 w
309 s	308 vs	298 s,sh		
	296 vw	290 s,sh		
264 ms	281 vs	278 vs		282 vs
	213 w	210 vw		
		205 w		
		181 w		
	151 m	159 w		150 m
	108 w	135 w		127 m
	100 w,sh	109 m		

also appears that the increase in positive charge on the bromine atom increases the frequency of this vibrational mode, as can be illustrated below for the three compounds:

	$[Br(SO_3F)_2]^+[Au(SO_3F)_4]$	$Br(SO_3F)_3$ [35]	$K[Br(SO_3F)_4]$ [35]
ν =	1505	1490	1424

A speculation as to the cause of this trend could be the strengthening of the Br-O bond upon the removal of a SO_3F group as the positive charge becomes more concentrated on the bromine atom.

Nevertheless, an ionic formulation of these compounds consisting of $[X(SO_3F)_2]^+$ and $[Au(SO_3F)_4]^-$ moieties may be an oversimplification. Prominent bands in the region of ~1150 cm^{-1}, characteristic for bidentate bridging fluorosulfate groups [180], indicate the presence of covalent cation-anion interaction in both the $[Au(SO_3F)_4]^-$- and $[Sn(SO_3F)_6]^{2-}$-derivatives. Such an interaction is not unexpected between these large anions and cations; in the molecular structure of the related interhalogen cation complexes of $[BrF_2][SbF_6]$ [182] and $[ICl_2][SbCl_6]$ [86], short interionic distances suggest the presence of strong interactions, but not to the extent that the compounds could be classified as covalent solids.

4.C.2.3 $Br_n[Au(SO_3F)_4]$, n=3, 5

Because of their dark colors, both polybromine-containing complexes gave rather poorly resolved Raman spectra, even when the samples were cooled to ~80 K. Their i.r. spectra at room

temperature show a band pattern typical of $[Au(SO_3F)_4]^-$, with no cation bands observable down to ~450 cm^{-1}. Low temperature i.r. spectra using CsI windows allowed the extension of the transmission range down to ~200 cm^{-1}; but because the sample could only be deposited as a powder, the spectra have peaks with broad contours due to the Christiansen effect. The vibrational frequencies of the two polybromine complexes are compared with the Raman frequencies of $Cs[Au(SO_3F)_4]$ in Table 4.4.

As mentioned previously, it becomes evident from the vibrational spectra that the only fluorosulfate-containing species is $[Au(SO_3F)_4]^-$. The band positions of the spectra from the two compounds are very similar, consistent with the almost invariant spectra observed for the ionic $[Au(SO_3F)_4]^-$-complexes. Unfortunately, a clear identification and assignment of bands due to the two polybromine cations are rather difficult. The low frequency range expected for ν Br-Br (<300 cm^{-1}) presented an instrumentation problem combined with the possible confusion of bands observed at such low frequencies with lattice modes. Furthermore, the very intense Raman band at ~282 cm^{-1} observed for the $[Au(SO_3F)_4]^-$ ion is in the same region where the stretching fundamentals for Br_3^+ are expected. (In superacid solutions, only one peak at ~290 cm^{-1} was reported for Br_3^+, attributed to a coincidence of the two stretching modes) [55,183]. A relatively strong Raman band at 220 cm^{-1} observed for $Br_3[Au(SO_3F)_4]$ may be due to the bending mode of Br_3^+. Two other weak bands are found at 188 and 178 cm^{-1}

Table 4.4 VIBRATIONAL FREQUENCIES OF $Br_n[Au(SO_3F)_4]$

$Br_3[Au(SO_3F)_4]$		$Br_5[Au(SO_3F)_4]$		$Cs[Au(SO_3F)_4]$
R, ~80 K	IR, ~80 K	R, ~80 K	IR, ~80 K	R, ~298 K
1408 ms 1386 m	1410 vs,sh 1392 vs	1409 m 1392 m	1380 s,b	1404 m 1380 w,sh
1218 s 1192 m	1220 s 1190 s,sh	1224 s 1201 mw	1200 s,b	1239 vs 1205 w
1016 m 960 vw	1020 w 955 vs,sh 930 vs	1020 m 1014 m	960 s,sh 920 s,b	1011 s 960 vw
829 mw 814 w	830 s,b	820 vw	800 s	830 mw 814 w
645 s	678 s	650 s 645 s,sh	670 s	649 vs
590 vw	585 s		575 s	580 w
545 w	548 s		540 m	550 w
520 w	520 vw			
454 s	462m	452 ms	450 m	452 s
	405 w	400 vw		405 w 319 w
286 vs	300 ms 285 w	304 m 294 m 282 m	305 m 295 m	
275 s,sh	267 m	279 vs	260 w	282 vs
220 s 188 w 178 w,sh 167 w 150 w		205 ms,b 150 m		150 m

in the Raman spectrum, with a band at 300 cm^{-1} observable also in the i.r. spectrum. The assignment of these weak bands is most likely lattice modes.

Br_5^+, because of its low symmetry (C_2 or even C_1), is expected to have nine vibrational modes, all i.r. and Raman active. (VSEPR predicts a linear Br_3 unit with bent terminal bromine attachments at each end free to rotate). For $Br_5[Au(SO_3F)_4]$, bands that may be due to Br_5^+ are found at 304, 295, 267 and 205 cm^{-1} in the Raman spectrum, and at 305, 295 and 260 cm^{-1} in the i.r. spectrum. It is noteworthy that the Raman spectrum does not provide any evidence for the presence of free Br_2, with ν(Br-Br) expected at 320 cm^{-1} [28].

Therefore, the presence of Br_5^+ can best be arrived at by default of all the other possibilities that the five bromine atoms can exist in, especially since there is no evidence for a breakdown of the $[Au(SO_3F)_4]^-$ anion and an involvement of bromine in the formation of Au-Br bonds. Unfortunately, both the polybromine-containing complexes are polycrystalline and all attempts at a crystal structure determination have been unsuccessful.

4.C.3 MAGNETIC SUSCEPTIBILITY

Except for a paramagnetic contaminant present in samples of $Au(SO_3F)_3$ prepared by the pyrolysis of $Br_3[Au(SO_3F)_4]$, the

tris(fluorosulfate) is diamagnetic. Diamagnetism is also observed for the two polybromine-containing complexes, further confirming the presence of a square planar low-spin electronic configuration for Au(III). The magnetic susceptibility results are listed below in Table 4.5.

Table 4.5 MAGNETIC SUSCEPTIBILITIES OF $Au(SO_3F)_3$ AND $Br_n[Au(SO_3F)_4]$

	χ_g(cgs units)	χ_m(cgs units)	$\Sigma \chi_{dia}$
$Au(SO_3F)_3$	$-(2.94\pm0.03)\times10^{-7}$	$-(147\pm2)\times10^{-6}$	-152×10^{-6}
$Br_3[Au(SO_3F)_4]$	$-(2.88\pm0.03)\times10^{-7}$	$-(240\pm3)\times10^{-6}$	-284×10^{-6}
$Br_5[Au(SO_3F)_4]$	$-(3.34\pm0.15)\times10^{-7}$	$-(331\pm15)\times10^{-6}$	-345×10^{-6}

4.C.4 SOLUTION STUDIES IN HSO_3F

With the exception of $Li[Au(SO_3F)_4]$, all complexes containing $[Au(SO_3F)_4]^-$ are very soluble in HSO_3F at room temperature. As expected for a polymeric material, $Au(SO_3F)_3$ dissolves only very slowly; but when the initially produced suspension is allowed to stand for several hours at room temperature, or if heating is applied at ~100°C for ~1 h, clear solutions can be formed. In addition, when $Au(SO_3F)_3$ is prepared from $S_2O_6F_2$/HSO_3F, the removal of all $S_2O_6F_2$ results in the formation of very concentrated solutions of $Au(SO_3F)_3$ in HSO_3F (~7 m) and these can be easily diluted for solution studies.

4.C.4.1 ELECTRONIC SPECTRA

With the exception of the polybromine complexes, all solutions containing the gold-fluorosulfato species are yellow to deep orange in color, depending on the concentration. Both $Au(SO_3F)_3$ and $Cs[Au(SO_3F)_4]$ give rise to identical absorption spectra in HSO_3F, with λ_{max} at 278 nm and ε of 1.5×10^4 $M^{-1}cm^{-1}$. This rather broad band, best interpreted as due to charge transfer, extends well into the visible region and obscures any band which may be due to d-d transitions (the half-width of the band is about 120 nm).

In $[Pd(SO_3F)_4]^{2-}$, the charge transfer bands are higher in energy, presumably due to the lower effective nuclear charge on the metal, and therefore bands arising from d-d transitions are observed.

Solutions of the polybromine-cation-containing complexes, although reddish brown in color when they are concentrated, gave identical spectra with λ_{max}=278 nm. Bands due to bromine containing species, (Br_3^+ at 375 nm, Br_2 at 410 nm, and Br_2^+ at 510 nm) [28,58], all with ε of the order of ~1600 $M^{-1}cm^{-1}$, could not be detected.

4.C.4.2 CONDUCTIVITY MEASUREMENTS

The results of electrical conductivity measurements on dilute solutions of $K[Au(SO_3F)_4]$ and $Au(SO_3F)_3$ in HSO_3F are shown

in Fig. 4.3 and 4.4 respectively. While both solutes behave as strong electrolytes in HSO_3F, as indicated by the almost linear concentration dependence of the specific conductance, their effects on the dissociation equilibrium of the solvent are quite different.

It appears that the ionization of $K[Au(SO_3F)_4]$ in HSO_3F can best be described according to:

$$K[Au(SO_3F)_4] \xrightarrow{HSO_3F} K^+_{(solv)} + [Au(SO_3F)_4]^-_{(solv)} \qquad (4.36)$$

Although the basic dissociation of $[Au(SO_3F)_4]^-$ according to:

$$[Au(SO_3F)_4]^-_{(solv)} \rightleftharpoons Au(SO_3F)_{3(solv)} + SO_3F^-_{(solv)} \qquad (4.37)$$

is possible, the conductometric titration of $Au(SO_3F)_3$ with KSO_3F, (the reverse of the above reaction) giving a minimum conductance at a mole ratio of 1:1, does not provide any supporting evidence for such a dissociation occurring to any great extent; furthermore, the equilibrium constant for equation (4.37) thus calculated is of the order of 10^{-6}.

On the other hand, $Au(SO_3F)_3$ exhibits a much higher conductivity in HSO_3F, and as can be seen from Fig 4.4, it approaches the conductivity observed for solutions of $SbF_2(SO_3F)_3$ [24]. Since this can only be due to the presence of large amounts of either $H_2SO_3F^+$ or SO_3F^-, as they possess very high ionic mobilities in HSO_3F [11], $Au(SO_3F)_3$ is therefore either a strong acid or a strong base. With preliminary information concerning the Lewis acidity of $Au(SO_3F)_3$ obtained from the synthesis of complexes containing

FIG. 4.3 CONDUCTIVITY OF $[Au(SO_3F)_4]$-COMPLEXES IN HSO_3F

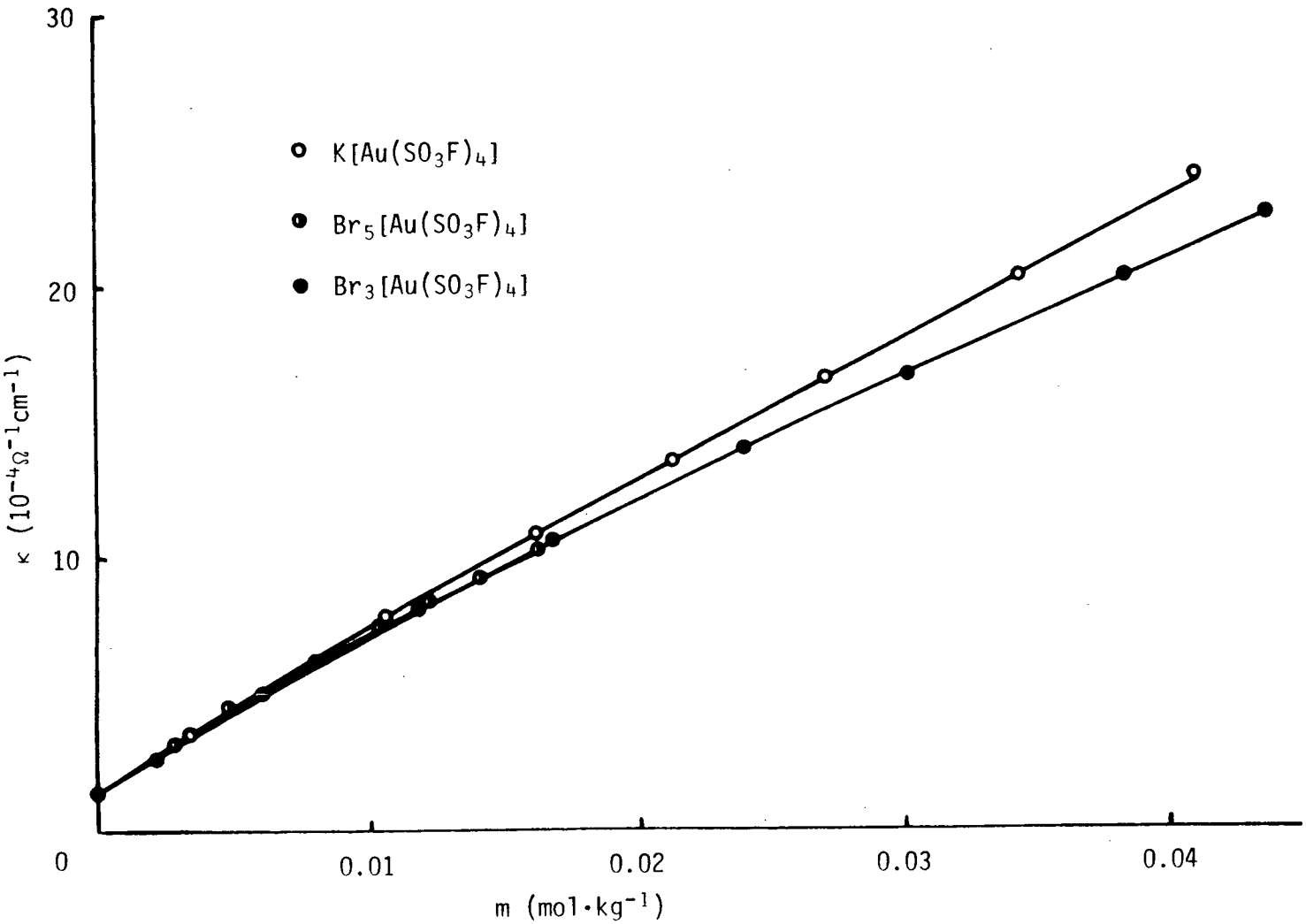

FIG.4.4 CONDUCTIVITY OF $Au(SO_3F)_3$ IN HSO_3F

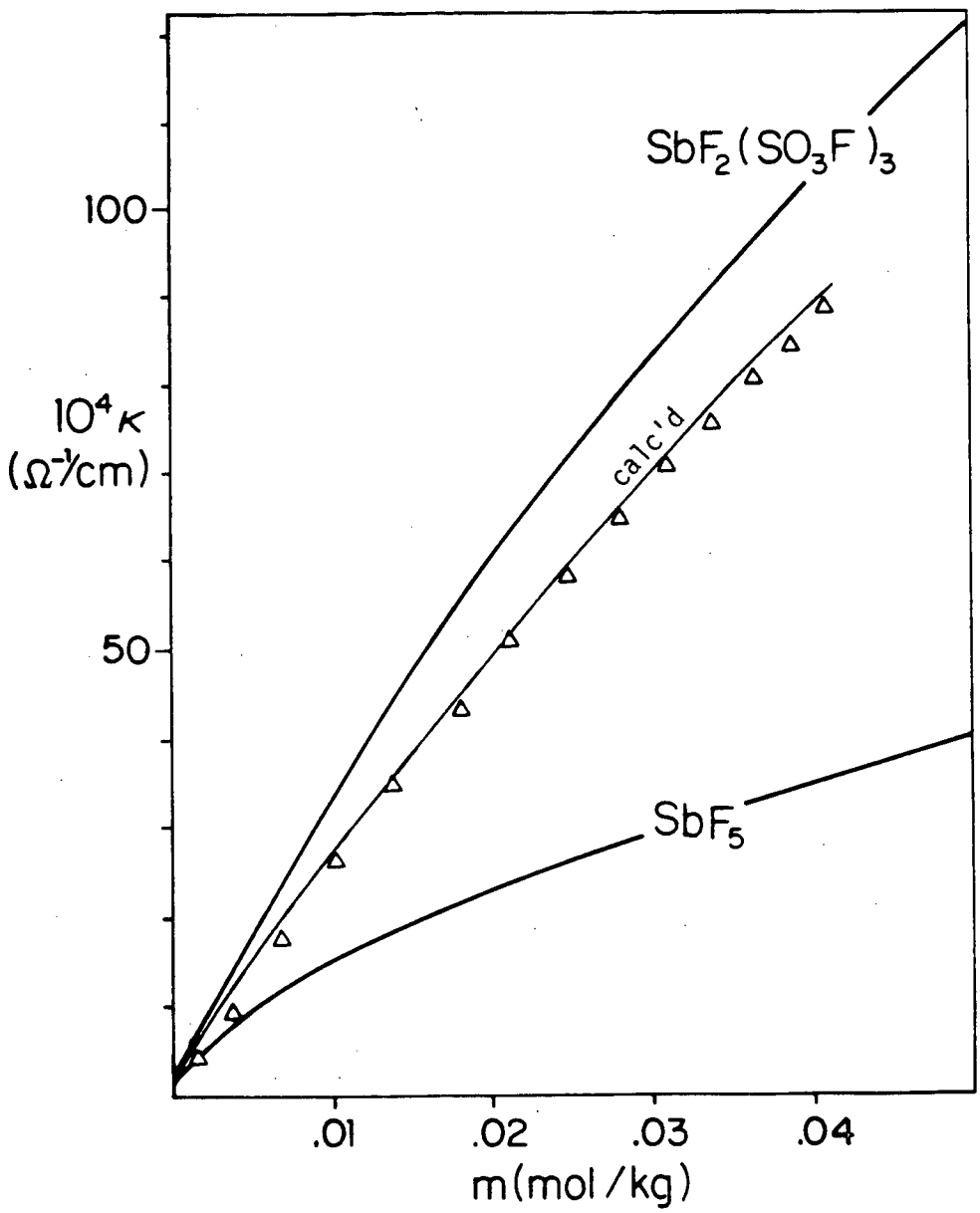

$[Au(SO_3F)_4]$, it is not surprising therefore to find that $Au(SO_3F)_3$ behaves as a strong acid by its conductometric titration with KSO_3F solutions, shown in Fig. 4.5 and Table 4.6. As expected for the titration of a strong acid (the only other example of such a moiety in HSO_3F being $SbF_2(SO_3F)_3$) [24], with a strong base, the conductance decreases gradually upon the addition of KSO_3F, until the endpoint at the $KSO_3F/Au(SO_3F)_3$ ratio of 1 is reached. The coincidence of the endpoint with the point of lowest conductance is typical for a strong, monoprotic acid in a protonic solvent. In comparison, SbF_5, a weaker acid, reaches its minimum conductance in a titration at a KSO_3F/SbF_5 ratio of ~0.4, and the region of low conductance is broad and ill-defined [24].

The titration can be formulated as the neutralization of a strong acid —— $H[Au(SO_3F)_4]$ or its equivalent, with a strong base —— KSO_3F, according to:

$$KSO_3F + H[Au(SO_3F)_4] \longrightarrow K[Au(SO_3F)_4] + HSO_3F \quad . \qquad (4.38)$$

Whether $H[Au(SO_3F)_4]$ or solvated $Au(SO_3F)_3$ is actually the acid present in solution is immaterial to this discussion, since they are both nonconducting species.

Since KSO_3F solutions were used in the titration instead of solid KSO_3F, the total concentration of the system decreased as the titration proceeded. This is the major factor contributing to the curvature of the conductivity plot; a correction, although not entirely theoretically justified, can be made and is also shown in Fig. 4.5. It can be seen that this second curve, in

FIG. 4.5

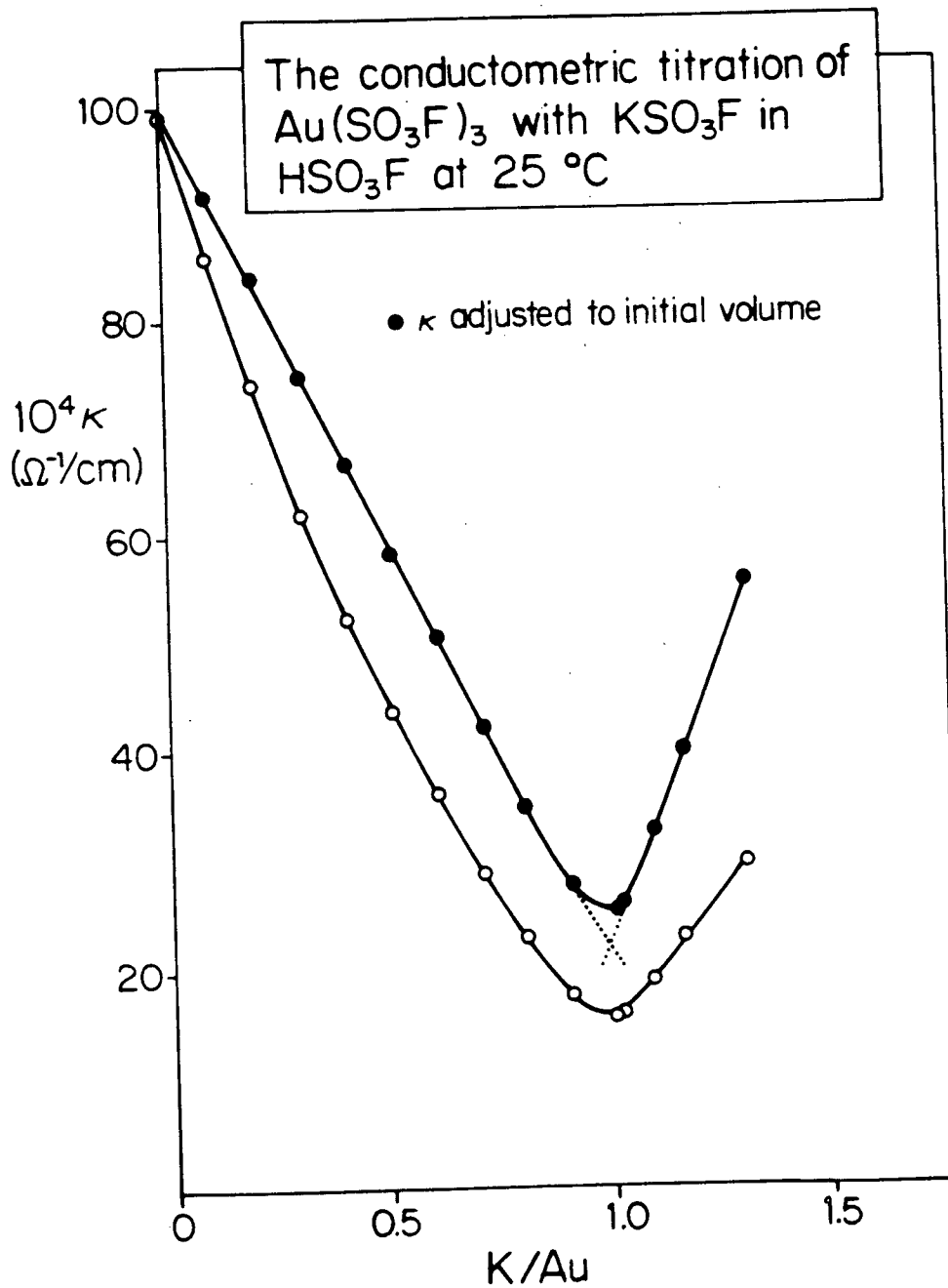
The conductometric titration of $Au(SO_3F)_3$ with KSO_3F in HSO_3F at 25 °C
● κ adjusted to initial volume
$10^4 \kappa$ (Ω^{-1}/cm)
100
80
60
40
20
0
0.5
1.0
1.5
K/Au

TABLE 4.6 CONDUCTOMETRIC TITRATION OF $Au(SO_3F)_3$ WITH KSO_3F IN HSO_3F

R	κ_{obs}	κ_{calc}	$\lvert\kappa_{obs}-\kappa_{calc}\rvert$	I (calc)
0	99.92	99.92	0	0.031
0.1	86.82	86.72	0.10	0.030
0.2	75.21	75.04	0.16	0.030
0.3	64.84	64.64	0.20	0.030
0.4	55.52	55.30	0.22	0.030
0.5	47.09	46.88	0.21	0.030
0.6	39.43	39.23	0.20	0.030
0.7	32.42	32.26	0.16	0.029
0.8	25.99	25.88	0.11	0.029
0.9	20.07	20.01	0.06	0.029
1.0	15.60	15.60	0	0.029
	$10^{4}\Omega^{-1}cm^{-1}$	$10^{-4}\Omega^{-1}cm^{-1}$	$10^{-4}\Omega^{-1}cm^{-1}$	$mol.kg^{-1}$

which the conductance has been corrected to correspond to the initial concentration of $Au(SO_3F)_3$, is almost a straight line, especially at the initial points.

The fact that the concentration corrected curve is not a straight line can be caused by:

a) the polymerization of $Au(SO_3F)_3$,

b) the dependence of molal conductivity, λ^*, with respect to concentration, and/or

c) the incomplete ionization of the superacid in solution.

The polymerization of the ansolvo acid, found in SbF_5 and $SbF_2(SO_3F)_3$ [24], does not seem to occur in the HSO_3F-$Au(SO_3F)_3$ system, at least not in the dilute solution (~0.04 m) range that the titration was performed in.

For an ionic electrolyte in dilute solutions, the molal conductivity is expected to decrease as the ionic strength, I, which can be approximated by molality for a 1:1 electrolyte ($I \equiv \frac{1}{2}\sum_0^i m_i z_i^2$, where z is the ionic charge), increases. This relationship, which is really only applicable at ionic strengths of less than 10^{-3} m, can be represented below [184] :

$$\lambda^* = \lambda_o^* - kI^{\frac{1}{2}}$$

where $\lambda_o^* \equiv \lambda^*$ as $I \longrightarrow 0$

and $k = \text{func}(\lambda_o^*, \varepsilon, T, \eta, z)$.

At higher ionic strengths, λ^* decreases much faster than can be described by the above equation. In this particular titration, by coincidence, the ionic strength remains relatively constant

throughout the titration, and therefore the variation of λ^* due to changes in I is not very serious.

Assuming K^+ and $[Au(SO_3F)_4]^-$ are the only conducting species in solution at the endpoint, (this is not entirely correct and a solvent conductivity of 1×10^{-4} $\Omega^{-1}cm^{-1}$ has been subtracted from the interpolated κ of 1.56×10^{-3} $\Omega^{-1}cm^{-1}$ at the endpoint), some estimates concerning the λ^* values and the equilibrium constant for the acid dissociation of $H[Au(SO_3F)_4]$ according to:

$$H[Au(SO_3F)_4] + HSO_3F \xrightarrow{K_a} H_2SO_3F^+ + [Au(SO_3F)_4]^-, \qquad (4.40)$$

can be made. Using the literature value of 320 for $\lambda_o^*(H_2SO_3F^+)$ and a value of 30 for $\lambda_o^*(K^+)$ [21], and applying the λ^* correction procedure described in Appendix A, a value of 24 is obtained for $\lambda_o^*([Au(SO_3F)_4]^-)$, together with K_a of 0.051 mol/kg. The λ_o^* value for the anion is in a reasonable range for a singly charged ion in HSO_3F; by comparison, $\lambda^*([SbF_2(SO_3F)_4]^-)$ is ~13 at 0.086 m [24]. This latter low value may be attributed to it having been obtained from a solution of much higher ionic strength and perhaps, more importantly, the larger degree of solvent-solute interaction in the antimony system, as illustrated by its tendency towards dimerization.

The correspondence between the calculated conductance, using the above parameters, and the experimentally obtained data is quite good, considering the crude adjustments made to the λ^* values. The remaining deviations, which are also listed in Table 4.6, are quite small and can be rationalized in terms of non-

idealities in the solution behavior of the species.

An earlier conductometric titration of AuF_3 in HSO_3F with KSO_3F gave a conductivity minimum at a KSO_3F/AuF_3 ratio of ~0.4 [164]. It is likely that the titration is not between KSO_3F and AuF_3, but between KSO_3F and a series of mixed fluoride-fluorosulfate of of Au(III) formed by the solvolysis of AuF_3 in HSO_3F:

$$AuF_3 + HSO_3F \rightleftharpoons AuF_2(SO_3F) + HF \text{ , etc.} \qquad (4.41)$$

The HF formed, being a base in HSO_3F [21], would increase the basicity of the solution according to:

$$HF + HSO_3F \rightleftharpoons H_2F^+ + SO_3F^- \text{ .} \qquad (4.42)$$

The conductivity result on the $Br_n^+[Au(SO_3F)_4]$ species is also shown in Fig. 4.3. As can be seen, they have an almost identical conductance/concentration dependence as $K[Au(SO_3F)_4]$ in HSO_3F. This observation is not totally unexpected for either of the two complexes, if they ionize as 1:1 electrolytes; for $Br_3[Au(SO_3F)_4]$, the following dissociation is most likely:

$$Br_3[Au(SO_3F)_4]_{(s)} \xrightarrow{HSO_3F} Br_3^+{}_{(solv)} + [Au(SO_3F)_4]^-{}_{(solv)} \text{ .} \qquad (4.43)$$

However, for $Br_5[Au(SO_3F)_4]$, although a similar dissociation is consistent with the observed conductivity, it is not expected to occur for a number of reasons. Firstly, Br_5^+ has never been observed in solution, and excess Br_2 can be reportedly removed from superacid solutions containing Br_3^+ by evacuation [28]. Secondly, when $Br_5[Au(SO_3F)_4]$ is dissolved in HSO_3F, the evolution of Br_2 is evident from the color of the gas phase above the solution. This suggests a dissociation of Br_5^+ into Br_3^+ and Br_2,

the latter being a non-electrolyte, would give rise to a similar conductivity as $Br_3[Au(SO_3F)_4]$ solutions:

$$Br_5[Au(SO_3F)_4]_{(s)} \xrightarrow{HSO_3F} Br_{2(solv)} + Br_3^+{}_{(solv)} + [Au(SO_3F)_4]^-_{(solv)}. \quad (4.44)$$

4.C.4.3 N.M.R. SPECTRA

The ^{19}F-n.m.r. spectra of solutions of $Au(SO_3F)_3$ and $Cs[Au(SO_3F)_4]$ are shown in Fig. 4.6. All spectra show the presence of two resonances: the strong one at ~-40 ppm due to HSO_3F and a weaker one slightly downfield assigned to Au(III)-fluorosulfate-containing species.

The spectrum for the $Cs[Au(SO_3F)_4]$ solution is very straight forward, with the weaker peak due to $[Au(SO_3F)_4]^-$ arising as a result of a dissociation similar to the type of equation (4.36). The presence of two very sharp signals indicates negligible exchange in the system. This is most likely a consequence of the formation of a coordinatively saturated species with little or no dissociation giving rise to other SO_3F-containing moieties. This hypothesis is also supported by the observation that the solvent peak at -40.8 ppm is not shifted from that of pure HSO_3F (-40.6 ppm) within experimental errors.

For $Au(SO_3F)_3$, the n.m.r. spectra of its solutions in HSO_3F also show two resonances, but they seem to indicate a much more complex solution behavior. The spectrum for the dilute solution already shows line broadening for both resonances. When the con-

FIG 4.6 ^{19}F-N.M.R. SPECTRA OF $Au(SO_3F)_3$ AND $Cs[Au(SO_3F)_4]$ IN HSO_3F

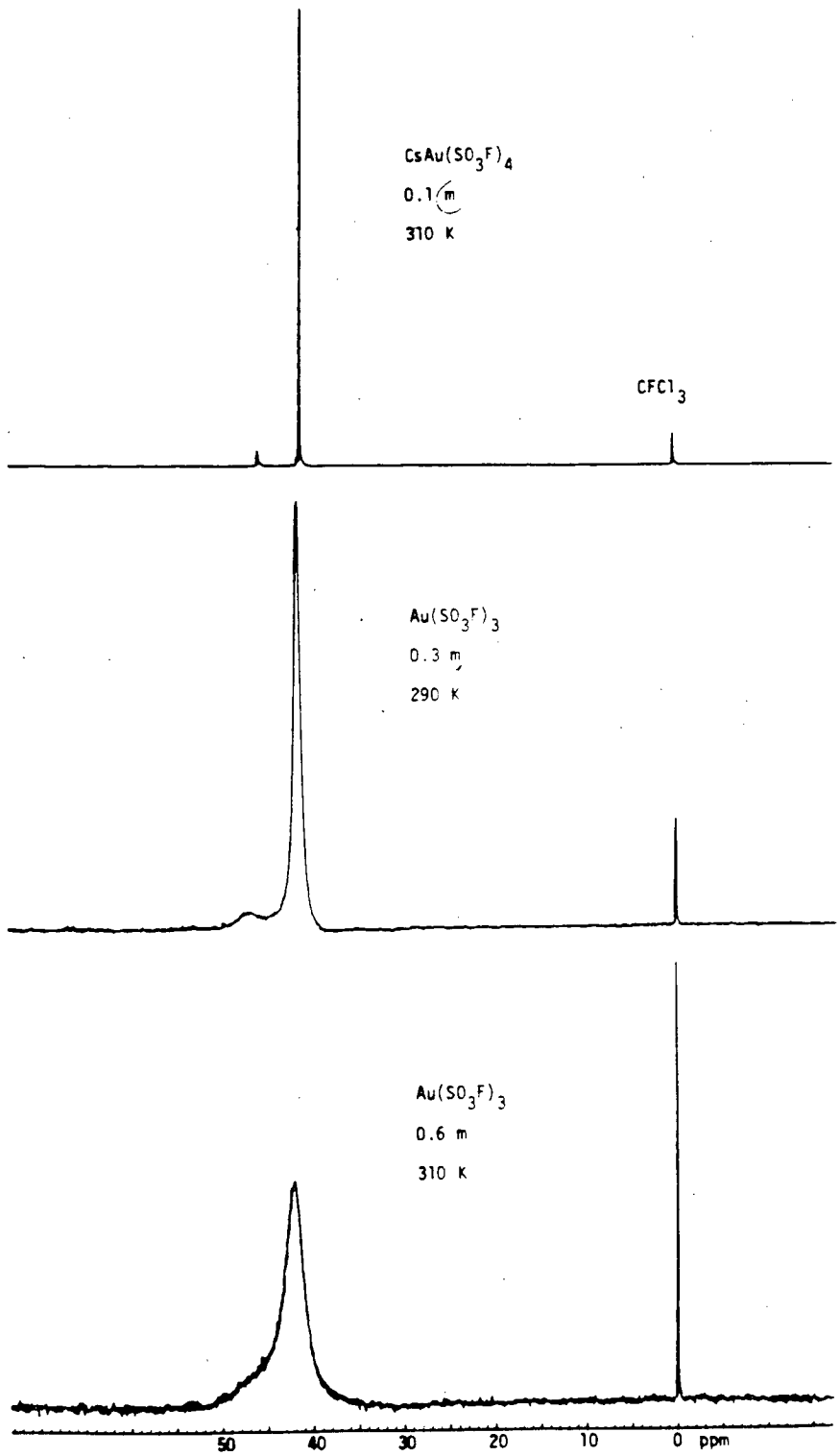

centration is increased the position of the solute resonance becomes increasingly uncertain due to line broadening, and ~2 m, the peaks are found at -41.2 and ~-46.5 ppm.

For a more concentrated solution (~7 m), the two resonances collapse into a single, extremely broad, (half width of ~5 ppm) and asymmetric peak. Although this concentration dependence is also partly due to viscosity effects, the presence of two separate resonances for dilute solutions and the asymmetric single resonance in the concentrated solution argues against a rapid exchange rate for equation (4.40). Since it is not expected that the exchange of a proton would drastically alter the magnetic environment for fluorine in a fluorosulfate group, its effect on line broadening is not as great as that obtained if a SO_3F group actually dissociates from $[Au(SO_3F)_4]^-$. The latter process presumably takes place rapidly in the HSO_3F-$I(SO_3F)_3$ system, as a single resonance was observed in its ^{19}F- n.m.r. spectrum even at -90°C [36].

The appearance of a single ^{19}F-resonance for the solute in the HSO_3F-$Au(SO_3F)_3$ is consistent with the presence of a monomeric species (at least in dilute solutions), rather than SO_3F bridged species. Again, due to line broadening, combined with the expectation that the chemical environment for the fluorine atoms in both configurations should not be very different, such a conclusion may not be warranted from these results alone.

In addition, a downfield shift of the solvent resonance to

10.30 ppm was observed in the ^1H- n.m.r. spectrum of the concentrated solutions, while for dilute solutions, the resonance remains unchanged at 9.93 ppm. Since the resonance for the pure solvent is already broad due to extensive hydrogen bonding, no further broadening was discernable. The downfield shift of the resonance, however, has a precedence in the H_2SO_3F-$H[B(SO_3H)_4]$ superacid system [185].

4.C.4.4 VIBRATIONAL SPECTRA

Raman spectra were obtained on solutions of $Au(SO_3F)_3$ and $Cs[Au(SO_3F)_4]$ in HSO_3F. The observed Raman shifts are listed in Table 4.7.

As expected for solution spectra, the bands are rather broad, and since the fluorosulfate group is common to both the solvent and solute, some overlap is encountered. However, the Au-SO_3F species in solution is found to be an excellent Raman scatterer, allowing the observation of bands at quite low concentrations. For more concentrated solutions, suppression of the solvent bands occurs, leading to the observed trend in relative intensities.

The spectra of $Au(SO_3F)_3$ in solution are very similar to that obtained for $Cs[Au(SO_3F)_4]$ in both the solid state and HSO_3F solution. This suggests a breakdown of the binary fluorosulfate's polymeric structure once it becomes solvated. Any polymeric fluorosulfate bridged species, observed in the solid state vibrational spectra of $Au(SO_3F)_3$, are not evident in even very

TABLE 4.7: RAMAN FREQUENCIES FOR $Cs[Au(SO_3F)_4]$, $Br_3[Au(SO_3F)_4]$ and $Au(SO_3F)_3$ IN HSO_3F

HSO_3F	$Cs[Au(SO_3F)_4]$ ~1 m	$Br_3[Au(SO_3F)_4]$* ~1 m	$Au(SO_3F)_3$ ~0.15 m	$Au(SO_3F)_3$ ~2.3 m	$Au(SO_3F)_3$ ~7 m	
1440 ms	1440 m,b		1430 ms			
	1420 m	1417 w	1420 m,sh	1412 m,b	1420 m,b	
				~1360 m,b	~1360 vw	
1230 ms,b	1232 s	1230 vw	1228 vs	1227 vs	1226 vs	
1178 m	1190 m,sh	1175 s	1185 s,sh	~1190 vw		
		1060 w			~1090 vw	$3\nu,Br_2^+$
		1020 w			997 m,sh	
960 s	958 m	968 m	960 vw	960 w,b	960 m	
	910 vw		910 vw	910 w,b	912 m	
850 vs	849 s	850 ms	848 s	846 m	840 m	
	~820 m,sh			830 m,sh	820 m,sh	
		718 w				$2\nu,Br_2^+$
	649 vs	652 ms	647 vs	647 vs	647 vs	
560 vs	~570 s,sh		~570 s,sh	580	~570 m,sh	
555 sh	553 s	553 m	550 s	547 m	546 s	
	453 s	456 m	455	457 s	457 s	
405 s	406 s	400 w	~395 ms,b	~400 w,b	~400 w,b	
393 s,sh	392 s	391 w				
		362 m				ν,Br_2^+
					~350 vw,b	
	278 vs	284 vs	276 vs	276 vs	276 vs	
		206 w				δ,Br_3^+
	150 m	156 m	150 mw	151 mw	148 mw	

*Frozen solution at ~80K

highly concentrated solutions of $Au(SO_3F)_3$ in HSO_3F. Very weak new bands at ~1360, ~1090 and 350 cm^{-1} for the almost saturated (~7 m) solution may be due to combination bands, the presence of small amounts of bridged species or laser induced decomposition products. It should also be mentioned that the most prominent bands at ~645, ~450 and ~275 cm^{-1}, previously assigned to modes containing Au-O vibrations, are all present in the solution spectra as single bands with no noticeable splittings. Overall, the solution spectra of $HSO_3F/Au(SO_3F)_3$ can best be regarded as the composite of HSO_3F and $[Au(SO_3F)_4]^-$.

The concentration range covered by the Raman experiment overlaps well with those used to obtain n.m.r. spectra. However, more dilute solutions were used to obtain conductivity measurements. Nevertheless, it seems rather unlikely that polymerization of $Au(SO_3F)_3$ should exist at such low concentrations, evidence for such a process can hardly be detected in very concentrated solutions. The results presented here suggest that the species in solution can best be described as $H[Au(SO_3F)_4]$ in equilibrium with $[Au(SO_3F)_4]^-$.

Finally, as previously reported for pure HSO_3F [8], bands due to the O-H stretching vibration could not be detected in the solution Raman spectra obtained here. I.R. spectra, obtained by using Teflon films between BaF_2 plates, show a shift of the solvent band from 3125 cm^{-1} [186] to ~2950 cm^{-1} for a 2.3 m solution. However, the extreme broadness of the band (half width ~700 cm^{-1})

makes it difficult to attach much significance to the frequency shift.

For the two polybromine-containing species, only $Br_3^+[Au(SO_3F)_4]^-$ was found to be stable in HSO_3F solutions, and even for this solution, the sample had to be cooled to ~80 K in order to obtain a Raman spectrum. The Raman frequencies are also listed in Table 4.7. The peaks are generally quite broad, like in a typical solution spectrum. All the bands due to $[Au(SO_3F)_4]^-$ and HSO_3F can be distinguished, along with a series of resonance Raman bands originating at 362 cm^{-1}, and assignable to Br_2^+. The concentration of Br_2^+ must be very low, as bands due to this species are extremely intense due to the resonance Raman effect. The source of Br_2^+ may be due to the dissociation of Br_3^+ according to:

$$Br_3^+(solv) \rightleftharpoons Br_2^+(solv) + \tfrac{1}{2}Br_2(solv) \quad , \qquad (4.45)$$

with the equilibrium lying mostly to the left.

The strong band at 284 cm^{-1}, usually found at 276 cm^{-1} for other $[Au(SO_3F)_4]$ complexes, may contain some contribution from Br_3^+ vibrations, expected at ~290 cm^{-1} [28]. This upward shift in band position is also noted in its solid state spectrum. Finally, the weak band at 206 cm^{-1} may be due to δ Br_3^+, which, because of the solvation of the cation by HSO_3F, becomes shifted to a lower frequency from 220 cm^{-1} in the solid.

4.C.5 RAMAN STUDIES OF $Au(SO_3F)_3$ IN LIQUID SO_2

Sulfur dioxide, owing partly to its low Lewis acidity and basicity, is commonly used as a solvent in superacid systems, since it is a relatively poor ionizing solvent which can dissolve organic compounds. It was originally thought that because of the observed high Lewis acidity of $Au(SO_3F)_3$ towards SO_3F^-, adduct-formation according to:

$$Au(SO_3F)_3 + SO_2 \longrightarrow [Au(SO_3F)_3 \cdot SO_2] \quad , \qquad (4.46)$$

may be possible. Although no such adduct could be isolated, it was hoped that Raman spectroscopy may provide some evidence for its existence in ℓ-SO_2 solutions. The spectra were recorded in high pressure capillaries containing saturated solutions of $Au(SO_3F)_3$ in ℓ-SO_2 at room temperature. The solubility of $Au(SO_3F)_3$ in ℓ-SO_2 is quite low, but solute peaks with intensities comparable to the two weaker solvent peaks at 1337 and 521 cm^{-1} can be obtained. The Raman frequencies for such a solution are listed in Table 4.8.

Most compounds containing SO_2 as a ligand are very unstable with respect to SO_2 elimination [187]. The Lewis acid-Lewis base adduct of $SbF_5 \cdot SO_2$, with an oxygen-bonded SO_2 ligand, is only thermally stable up to ~50°C [188]. The i.r. spectrum of this complex has bands at 1625(w), 1323(s), 1145(w, sh), 1100(m), 696(s), and 480 cm^{-1}(w) [174]. It has also been detected in the HSO_3F-SbF_5-SO_2 superacid system by the presence of a band at 1106 cm^{-1} in the Raman spectrum [22]. It seems that in the presence

Table 4.8 RAMAN FREQUENCIES FOR $Au(SO_3F)_3$ IN SOLID STATE AND IN ℓ-SO_2 SOLUTION AT 298 K

solid state	ℓ-SO_2 solution	Assignment
1449 m 1423 m,sh	1427 m 1385 m	
	1337 s	ν_{as} ℓ-SO_2
 1227 vs	1276 vw 1224 vs	
	1145 vvs 1122 m	ν_s ℓ-SO_2 ν_s ℓ-$SO^{16}O^{18}$
1102 w 1053 m 955 m,sh 936 s 899 s	1071 w 1031 w 970 m 915 m	
822 w	820 w	
650 vs	657 m,sh	
610 w 583		
546 m	543 w,sh	
	521 s	δ ℓ-SO_2
465 m 444 w	458 m	
348 m 327 w,sh	365 w	
292 vs 285 s	286 vs 272 vs	

of liquid SO_2 as the solvent, the only diagnostic Raman band for O-bonded SO_2 is a band at ~1100 cm^{-1}.

Most transition metal -SO_2 complexes are S-bonded, for $[Ru(NH_3)_4(SO_2)Cl]Cl$, the SO_2 vibrations are found at 1301(s), 1278(s), 1110(s), and 555 cm^{-1}(m), in the i.r. [189].

A comparison of the Raman frequencies of solid $Au(SO_3F)_3$ and its solution in ℓ-SO_2 reveals that except for some small shifts in band positions, the spectra are almost identical. The band at 1122 cm^{-1} is due to the isotope effect of $S^{16}O^{18}O$ and is confirmed by its presence in the Raman spectrum of pure ℓ-SO_2. This band, although expected to be ~10^{-3} times as intense as the band due to the more abundant $S^{16}O_2$, arises because this symmetric mode is ~10^3 times more intense than the bands in the rest of the spectrum.

Some increased splittings in the $[AuO_4]$ related vibrations are observed and may be interpreted in two opposite ways:

a) In the formation of smaller oligomers such as $Au_2(SO_3F)_6$, the coupling between the $[AuO_4]$ vibrations in adjacent $[Au(SO_3F)_4]$ units via SO_3F bridging groups may be stronger than in the solid state where increased cross-linkage serves to diffuse the coupling.

b) If $Au(SO_3F)_3 \cdot SO_2$ is formed, the replacement of a bidentate SO_3F group by SO_2 will lead to a greater distortion in the AuO_4 unit from D_{4h} symmetry, leading to an increased splitting in the bands.

The band at 365 cm^{-1} can conceivably be due to νAu-OSO or

νAu-SO_2, but the position of νAu-(SO_3F bridging) at 348 cm^{-1} in $Au(SO_3F)_3$ makes such an assignment rather ambiguous. In the SO_3-stretching region for bridging SO_3F group at ~1000 cm^{-1}, the relative intensity of the three bands at 1031,970, and 915 cm^{-1} is very similar to that found for solid $Au(SO_3F)_3$; quite unlike that observed for monodentate SO_3F groups such as $[Au(SO_3F)_4]^-$. Therefore, it does not appear that the relative proportion of monodentate/bidentate SO_3F groups changes upon the dissolution of $Au(SO_3F)_3$ in ℓ-SO_2.

With direct evidence supporting the formation of an adduct absent, it must be concluded that if it does exist, it must be present in quite a low concentration, The species most likely to be present in ℓ-SO_2 are smaller oligomers of $Au(SO_3F)_3$, such as $Au_2(SO_3F)_6$.

4.D CONCLUSION

$Au(SO_3F)_3$ has been shown to act as a strong ansolvo-acid in HSO_3F, giving rise to a new superacid system. From conductivity measurements and the conductometric titration of $H[Au(SO_3F)_4]$ with KSO_3F, the acidity of the new superacid is found to be comparable to that of $H[SbF_2(SO_3F)_4]$. However, unlike the antimony system, no extensive polymerization of the ansolvo-acid is evident in solution, although $Au(SO_3F)_3$ itself is a polymer, with bridging SO_3F groups.

A series of ionic salts containing the $[Au(SO_3F)_4]^-$ anion can be synthesized with alkali metal ions, NO^+ and ClO_2^+. These have been characterized using vibrational spectroscopy.

The Lewis acidity of $Au(SO_3F)_3$ with respect to SO_3F abstraction can be demonstrated in its reaction with the halogen tris-(fluorosulfate)s of $Br(SO_3F)_3$ and $I(SO_3F)_3$,to give the corresponding $[Hal(SO_3F)_2]^+$ cations; in this system, extensive anion-cation interaction is evident from the proliferation of bands in the vibrational spectra, suggesting the presence of bridging SO_3F groups.

The low oxidizing power of $Au(SO_3F)_3$ is illustrated by the successful synthesis of polybromine cations-Br_3^+ and Br_5^+, stabilized by $[Au(SO_3F)_4]^-$. The stability of Br_3^+ in the gold complex with respect to dissociation is higher than all previously reported examples of Br_3^+ complexes, and the Br_5^+ cation is the only such example so far. The stability of solutions of $Br_3[Au(SO_3F)_4]$

in HSO_3F also points to the low basicity of the $[Au(SO_3F)_4]^-$ anion in solution, a property essential to any further attempts in the stabilization of other novel cations.

$Au(SO_3F)_3$, $[Au(SO_3F)_4]^-$, and the two polybromine cations are all diamagnetic, suggesting a square planar coordination of SO_3F for Au(III) giving rise to a $^1A_{1g}$ electronic ground state.

CHAPTER 5 PLATINUM-FLUOROSULFATE

5.A INTRODUCTION

The chemistry of platinum has been studied extensively in the past and is one of the earliest systems investigated in coordination chemistry. The principle oxidation states of platinum are +2 and +4; the higher states of +5 and +6 occur only in fluorine-containing compounds. The investigation into the chemistry of PtF_6, one of the most powerful oxidizing and fluorination agents, led to the discovery of the first noble gas compound.

Platinum forms a wide variety of complexes with platinum in both very high and very low oxidation states. Simple anionic complexes containing $[Pt\text{-}Hal_4]^{2-}$ and $[Pt\text{-}Hal_6]^{2-}$, together with $[PtF_6]^-$ and $[Pt_2F_{11}]^-$ are known and can be easily obtained. Their existence suggests halide ion accepting properties of the binary platinum halides.

In contrast to palladium, the relative ease with which the +4 oxidation state can be accessed is illustrated by the existence of $PtBr_4$ and PtI_4, formed by direct halogenation of the metal. The reaction takes place even when neither Br_2 nor I_2 are usually considered to be strong oxidizing agents [190]. Some structural aspects and some principle features of the halides of platinum will be reviewed briefly.

As mentioned before, most of the compounds in the series of $Pt\text{-}Hal_2$, $Pt\text{-}Hal_3$ and $Pt\text{-}Hal_4$ are known but in keeping with the

trend observed for palladium, the trivalent oxidation state of platinum is very uncommon and the trihalides are best regarded as mixed valency compounds of Pt(II)Pt(IV)-Hal_6. Not unexpected, the di- and tetra-halides are all diamagnetic, implying a square planar d^8 electronic configuration for Pt(II) and an octahedral low-spin d^6 configuration for Pt(IV). In general, Pt(IV) compounds are diamagnetic because of the high ligand field splitting possible with the 5d metal in such a high oxidation state. The 'trihalides', with the exception of Pt_2F_6, only recently synthesized [191], are also diamagnetic, providing one the most conclusive evidence for the mixed valency nature of the compounds (Pt(III), d^7, with an odd number of electron, must be paramagnetic). Pt_2F_6, a black solid whose existence was suggested at a very early time in fluorine chemistry by Moissan, is the only example for Pt(II) in an octahedral environment with a $^3A_{2g}$ electronic ground state and a magnetic moment of 3.05 μ_B. PtF_2 has not been successfully synthesized so far, and it has been suggested that this fluoride may not be stable with respect to a disproportionation into platinum metal and PtF_4 [192].

The two higher-valent fluorides, $[PtF_5]_4$ and PtF_6, are obtained by the fluorination of platinum, or lower-valent platinum halides, at different conditions [192,193]. Both have found use as fluorinating agents in the synthesis and stabilization of easily reduced and novel cations such as O_2^+, XeF^+ and ClF_6^+ [122,194]. Fluorination reactions involving PtF_6 usually lead to the forma-

tion of $[PtF_6]^-$ or $[Pt_2F_{11}]^-$, both are anions of low basicity.

The solution behavior of PtF_4 in HSO_3F, like that of AuF_3, was studied by Woolf; however, due to the extremely low solubility of PtF_4 in HSO_3F, no quantitative results were obtained, even though acidic behavior was suggested [164]. The only known fluorosulfate of platinum, $Pt(SO_3F)_4$, was synthesized in a method analogous to the preparation of $Au(SO_3F)_3$ —— from a reaction between the metal and $BrSO_3F$ [82]. The initial product from the above reaction with $BrSO_3F$ is likewise reported to give an adduct of the approximate composition of $Pt(SO_3F)_4 \cdot 4BrSO_3F$. These rather preliminary results raise the possibility that $Pt(SO_3F)_4$ may act as a SO_3F^- acceptor, leading to the formation of $[Pt(SO_3F)_6]^{2-}$ and therefore a superacid system in HSO_3F.

5.B EXPERIMENTAL

5.B.1 PREPARATION OF $Pt(SO_3F)_4$

$$Pt + S_2O_6F_2 \xrightarrow{HSO_3F} Pt(SO_3F)_4 \qquad (5.1)$$

In a typical reaction, platinum powder (233 mg, 1.19 mmol) was reacted with a mixture of $S_2O_6F_2/HSO_3F$ at 120°C for 2 days. The orange colored solution gave, after the removal of all volatile materials, dark yellow crystals of $Pt(SO_3F)_4$, (692 mg, 1.07 mmol).

$Pt(SO_3F)_4$ is a deep yellow to light orange crystalline, hygroscopic solid. It melts with decomposition at 220°C and is very soluble in HSO_3F. The micro-analysis of the compound had been reported previously [82].

$Pt(SO_3F)_4$ can also be prepared by the reaction of platinum metal with $BrSO_3F$ followed by the pyrolysis of the intermediate as reported earlier by Cady et al [82].

5.B.2 SYNTHESIS OF COMPLEXES CONTAINING $[Pt(SO_3F)_6]^{2-}$

5.B.2.1 PREPARATION OF $Cs_2[Pt(SO_3F)_6]$

$$CsCl + HSO_3F \longrightarrow CsSO_3F + HCl \qquad (5.2)$$

$$2CsSO_3F + Pt + 2S_2O_6F_2 \xrightarrow{HSO_3F} Cs_2[Pt(SO_3F)_6] \qquad (5.3)$$

$CsSO_3F$, formed by the solvolysis of CsCl (302 mg, 1.80 mmol) in HSO_3F, was mixed with a stoichiometric amount of platinum metal powder (175 mg, 0.897 mmol) and reacted with $S_2O_6F_2$ (~3 mL)

and HSO_3F (~5 mL). The reaction required heating at 80°C for 3 days, after which time a light yellow solution had formed. The evacuation of all volatile materials yielded crystalline $Cs_2[Pt(SO_3F)_6]$.

$Cs_2[Pt(SO_3F)_6]$ is a light yellow, crystalline, hygroscopic solid. It is soluble in HSO_3F and melts with decomposition at ~260°C.

Analysis	Cs	Pt	S	F
Calculated %	25.19	18.49	18.23	10.80
Found %	25.03	18.39	18.32	10.72

5.B.2.2 PREPARATION OF $(ClO_2)_2[Pt(SO_3F)_6]$

$$2ClO_2SO_3F + Pt(SO_3F)_4 \longrightarrow (ClO_2)_2[Pt(SO_3F)_6] \qquad (5.4)$$

ClO_2SO_3F (~1 mL) was added to a sample of $Pt(SO_3F)_4$ (828 mg, 1.400 mmol). A portion of $Pt(SO_3F)_4$ was found to dissolve in the liquid which was heated at ~60°C for 1 day. The removal of all volatile materials at ~70°C gave $(ClO_2)_2[Pt(SO_3F)_6]$.

The compound can also be prepared by the reaction of platinum metal with a mixture of $S_2O_6F_2$ and ClO_2SO_3F according to:

$$Pt + 2ClO_2SO_3F + 2S_2O_6F_2 \longrightarrow (ClO_2)_2[Pt(SO_3F)_6] \qquad (5.5)$$

at 160°C for 2 days followed by the removal of all volatile materials at 70°C.

$(ClO_2)_2[Pt(SO_3F)_6]$ is a light yellow, crystalline, hygroscopic solid. It is soluble in HSO_3F and melts with decomposition at ~195-200°C.

Analysis	Cl	Pt	F
Calculated %	7.67	21.11	12.33
Found %	7.60	21.24	12.42

5.B.2.3 PREPARATION OF $Ba[Pt(SO_3F)_6]$

$$BaCl_2 + 2HSO_3F \longrightarrow Ba(SO_3F)_2 \qquad (5.6)$$

$$Ba(SO_3F)_2 + Pt + 2S_2O_6F_2 \longrightarrow Ba[Pt(SO_3F)_6] \qquad (5.7)$$

Anhydrous $BaCl_2$ (88 mg, 0.423 mmol) was converted into the fluorosulfate by the reaction with HSO_3F (~5 mL). After the removal of the HCl evolved, $S_2O_6F_2$ (~2 mL) was distilled onto the equimolar mixture of $Ba(SO_3F)_2$ and platinum metal powder (82 mg, 0.420 mmol) in HSO_3F. After heating at 140°C for 3 days, all the metal had dissolved and a light yellow precipitate had formed. The removal of all volatile materials yielded $Ba[Pt(SO_3F)_6]$.

$Ba[Pt(SO_3F)_6]$ is a light yellow, hygroscopic powder. It is only sparingly soluble in HSO_3F and melts with decomposition at ~190°C.

Analysis	Ba	Pt	F
Calculated %	14.82	21.05	12.03
Found %	14.83	21.03	12.27

5.B.2.4 PREPARATION OF $(Br_3)_2[Pt(SO_3F)_6]$

$$Pt + 6BrSO_3F \xrightarrow{Br_2} (Br_3)_2[Pt(SO_3F)_6] \qquad (5.8)$$

Platinum metal powder (157 mg, 0.805 mmol) was reacted with a large excess of $BrSO_3F$ (~10 mL) at 140°C for 7 days. About 1 mL

of Br_2 was added into the mixture which was heated at ~70°C for about 5 minutes. The subsequent removal of all volatile materials at room temperature yielded a compound analyzed as $(Br_3)_2[Pt(SO_3F)_6]$ (998 mg, 0.787 mmol).

$(Br_3)_2[Pt(SO_3F)_6]$ is a dark brown, polycrystalline, and hygroscopic solid. Prolonged standing at room temperature in vacuo causes the slow evolution of Br_2, but the compound is reasonably stable in an atmosphere of nitrogen where it decomposes at ~90°C.

Analysis	Br	Pt	F
Calculated %	37.78	15.37	8.98
Found %	38.05	15.36	8.84

5.B.3 PREPARATION OF $CsPt(SO_3F)_5$

$$CsCl + HSO_3F \longrightarrow CsSO_3F + HCl \qquad (5.9)$$

$$CsSO_3F + Pt + 2S_2O_6F_2 \xrightarrow{HSO_3F} CsPt(SO_3F)_5 \qquad (5.10)$$

Stoichiometric amounts of CsCl (102 mg, 0.606 mmol) and platinum metal powder (118 mg, 0.605 mmol) are mixed in a reactor. HSO_3F (~2 mL) is added to solvolyze the CsCl, and the resultant solution evacuated to remove all HSO_3F. A mixture of $S_2O_6F_2/HSO_3F$ (~4 mL) is then added and the reaction vial held at 80°C for 3 days, after which time all the metal had dissolved and a light orange solution had formed. The removal of all volatile materials yielded a compound which analyzed as $CsPt(SO_3F)_5$ (503 mg, 0.608 mmol).

$CsPt(SO_3F)_5$ is a light yellow crystalline solid, soluble in HSO_3F. It melts with decomposition at ~154°C to an orange liquid.

Analysis	Cs	Pt	F
Calculated %	16.11	23.35	11.53
Found %	15.93	23.41	11.63

5.C DISCUSSION

5.C.1 SYNTHESIS AND GENERAL DISCUSSION

5.C.1.1 PLATINUM TETRAKIS(FLUOROSULFATE)

$Pt(SO_3F)_4$ can be prepared, in a manner analogous to the synthesis of $Au(SO_3F)_3$, by the reaction of platinum metal with a) $S_2O_6F_2$ /HSO_3F, or b) $BrSO_3F$ followed by the subsequent decomposition of the bromine-containing intermediate. Method a) is the preferred synthetic route as $Pt(SO_3F)_4$ is formed directly. Samples of the compound obtained via b) were always darker in color (Cady reported the color of $Pt(SO_3F)_4$ as being dark brown) and contained paramagnetic impurities. It seems that the high temperature (~120°C) involved in the pyrolysis of the intermediate (although the intermediate show signs of decomposition at ~90°C, a higher temperature was needed in order to shorten the time for the reaction), may also lead to the thermal decomposition of the desired product. This intermediate, again similar to the $Au(SO_3F)_3$-$BrSO_3F$ system, is best regarded as $(Br_3)_2[Pt(SO_3F)_6]$ instead of an adduct between $Pt(SO_3F)_4$ and $BrSO_3F$.

There are, however, a few major differences between the synthesis of $Pt(SO_3F)_4$ and $Au(SO_3F)_3$. While both metals can be synthesized by the same methods, platinum displays a much lower degree of reactivity towards either $BrSO_3F$ or $S_2O_6F_2/HSO_3F$. Furthermore, the removal of HSO_3F from solutions containing $Pt(SO_3F)_4$ proceeds only with difficulties at room temperature, suggesting possibly a greater degree of solvent-solute interac-

tion in the platinum system.

5.C.1.2 COMPLEXES CONTAINING $[Pt(SO_3F)_6]^{2-}$

The synthesis of the three ionic complexes containing Ba^{2+}, ClO_2^+ and Cs^+ follows a general scheme to the preparation of transition metal fluorosulfato complexes. Their synthesis provides the first evidence for the fluorosulfate-accepting property of $Pt(SO_3F)_4$. Complexes of a less ionic nature, exemplified by $Pd[Pt(SO_3F)_6]$, discussed in Chapter 3, and $Ag[Pt(SO_3F)_6]$ [84], can also be readily prepared.

The reaction of $BrSO_3F$ with platinum metal leads to the formation of a complex containing the Br_3^+ cation. Although this reaction supposedly proceeds via an analogous mechanism as the corresponding reaction in the gold system, some differences exist. The formation of $(Br_3)_2[Pt(SO_3F)_6]$ according to equation (5.8) requires that all the bromine formed from the reduction of $BrSO_3F$ be used up, while in the reaction involving gold metal, and excess of half a mole of Br_2 is left per mole of gold reacted. Since Br_3^+ is not expected to be very stable in the presence of $BrSO_3F$, a strong oxidizing agent, the complete conversion of all Br_2 into the complex may not occur. Experimentally, yields corresponding to as low as a 1:1 mixture of $Pt(SO_3F)_4$ and $(Br_3)_2[Pt(SO_3F)_6]$ have been obtained for reactions involving large excess of $BrSO_3F$. The situation is further aggrevated by the observed low thermal stability of the complex in vacuo. The synthesis of analytically

pure $(Br_3)_2[Pt(SO_3F)_6]$ therefore requires the introduction of a small quantity of Br_2 (~1 mL) into the reaction mixture after all the metal had dissolved. The preparation can also be accomplished by the in situ synthesis of $BrSO_3F$ in the reaction vial using $S_2O_6F_2$ and a slight excess of Br_2. This latter method eliminates the initial vacuum distillation of $BrSO_3F$, which has a low vapor pressure at room temperature.

The thermal stability of $(Br_3)_2[Pt(SO_3F)_6]$ is comparable to that of $Br_5 Au(SO_3F)_4$, both showing signs of decomposition, giving off Br_2, at room temperature in vacuo. It is therefore not surprising that further addition of bromine to Br_3^+, forming longer chained polybromine cations, does not occur in this system. It is possible that the large number of bromine atoms, already six in $(Br_3)_2[Pt(SO_3F)_6]$, will drastically reduce the lattice energy in a complex such as $(Br_5)_2[Pt(SO_3F)_6]$. If this postulation is correct, then the lower thermal stability of $(Br_3)_2[Pt(SO_3F)_6]$ as compared to $Br_3[Au(SO_3F)_4]$ is not necessarily a consequence of the lower Lewis acidity of $Pt(SO_3F)_4$.

5.C.1.3 SYNTHESIS OF $CsPt(SO_3F)_5$

The synthesis of $CsPt(SO_3F)_5$ was sought as supporting evidence for the polymerization of $Pt(SO_3F)_4$ as inferred from the conductometric titration of the fluorosulfate with KSO_3F solutions. Being a SO_3F^- acceptor, forming $[Pt(SO_3F)_6]^{2-}$ in the presence of an excess of SO_3F^-, $CsPt(SO_3F)_5$ is made in a reaction

essentially between $CsSO_3F$ and $Pt(SO_3F)_4$, all the HCl formed in the initial solvolysis of CsCl in HSO_3F having been removed by evacuating the $CsSO_3F$ solution to dryness (the formation of a mixture of complexes containing Cs^+ and ClO_2^+ is a likely occurrence if any chlorine-containing substance was present). This complex appears to be a dimeric species from an analysis of its vibrational spectra.

5.C.1.4 ATTEMPTED SYNTHESIS OF FLUOROSULFATES CONTAINING PLATINUM IN OTHER OXIDATION STATES

The ease with which Pt(IV) could be obtained suggests that Pt(V) fluorosulfate or fluorosulfato complexes might be obtainable. This was found not to be the case, and no reaction was observed when $Pt(SO_3F)_4$ was heated at 100°C with $S_2O_6F_2$. It seems logical to assume that, with the reactivity of $S_2O_6F_2$ greatly enhanced when it is dissolved in HSO_3F, the oxidation of a transition metal in $S_2O_6F_2/HSO_3F$ should lead to the highest oxidation state attainable in the metal-fluorosulfate system.

The attempted synthesis of $Pt(SO_3F)_2$ by the solvolysis of $PtCl_2$ in HSO_3F, consistent with attempted reactions involving other noble metal chlorides examined in this study, with or without the presence of KSO_3F, did not give rise to any reaction product. The heating of a sample of K_2PtCl_4 in HSO_3F at ~80°C for 2 days led to the decomposition of the sample , although an ionic fluorosulfate, probably KSO_3F, identified by its i.r. spectrum,

was the only fluorosulfate-containing species present. The residue gave a positive chloride ion test. Furthermore, the extremely polymeric nature of $PtCl_2$ can be illustrated by an unsuccessful chloride abstraction reaction with $Sn(SO_3F)_4$, which shows no signs of any reaction after 3 days at ~90°C.

While the reduction of $Pd_2(SO_3F)_6$ with Br_2 gave rise to $Pd(SO_3F)_2$, such an analogous reaction involving $Pt(SO_3F)_4$ or any of its complexes may not be too likely. The formation of $(Br_3)_2$-$[Pt(SO_3F)_6]$, containing bromine in the +1/3 formal oxidation state and in the presence of an excess of bromine, seems to indicate that the fluorosulfate of Pt(IV), likewise Au(III), is compatible with Br_2, and therefore no reduction should be expected to take place.

5.C.2 VIBRATIONAL SPECTRA

5.C.2.2 PLATINUM TETRAKIS(FLUOROSULFATE)

Due to the low Raman scattering efficiency of $Pt(SO_3F)_4$ coupled with its limited stability in the laser beam, only poorly resolved Raman spectra could be obtained. The vibrational frequencies of $Pt(SO_3F)_4$ are compared to the i.r. frequencies of $Au(SO_3F)_3$ in Table 5.1.

As can be seen, a good correspondence between the major bands in the spectra of the two compounds can be made, indicating

Table 5.1 VIBRATIONAL FREQUENCIES OF $Pt(SO_3F)_4$ and $Au(SO_3F)_3$

$Pt(SO_3F)_4$ R.	$Pt(SO_3F)_4$ I.R.	$Au(SO_3F)_3$ I.R.	$Sn(SO_3F)_4$ [33] R.	Assignment
1445 m	~1400 vs,b	1442 vs 1425 s,sh	1431 s 1420 s,sh	$\nu_{as}SO_3$
1230 vs	1225 vs	1240 s 1220 s,sh	1233 s	$\nu_{s}SO_2$
	~1150 s,vb	1135 ms	1124 s	
1060 w	~1070 vs,vb	1055 s	1075 s	
	~1000 vs,vb	960 s,b	986 w	$\nu_{as}SO_3$
		920 s,sh	911 m	
900 s,b	~900 vs,vb	895 s,b		
~822 vw	~820 s,vb	820 s,b	845 m	ν_{S-F}
			827 m	
		682 s		
	~670 s,b	670 s,sh		
640 s	~640 s,b	~650 w,sh	640 w,sh	ν_{SM-O} + MO-S def.
~615 w,sh		610 w	632 s	
		590 s	589 s	
	580 s	582 s		SO_3F def
545 w	540 m	550 s	552 m	SO_3F rock
454 m		460 m	427 s	$\nu_{as}M-O$ + MO-S def.
293 s			320 w	
268 s				$\nu_{s}M-O$ + SO_3F rock

the presence of similar bonding modes for SO_3F groups in them. In the i.r. spectrum of $Pt(SO_3F)_4$, a very strong and broad peak extends from ~800 to ~1150 cm^{-1}; some minor features are discernable only when very thin-film samples are used. This is in contrast to $Au(SO_3F)_3$, for which relatively well resolved bands can be observed in this same region. This complexity in the S-O and S-F stretching modes of $Pt(SO_3F)_4$ may not be totally unexpected. If the coordination of Pt(IV) is octahedral, for each Pt(IV), there will be two monodentate and two bridging bidentate SO_3F groups. By comparison, $Au(SO_3F)_3$ would have only two monodentate and one bridging bidentate SO_3F groups for each Au(III). This increased proportion of bridging SO_3F groups would give rise to a proliferation of vibrational modes, in particular in the SO-stretching region, unless their local symmetry is identical, as in $Sn(SO_3F)_4$.

In contrast to $Pt(SO_3F)_4$, $Sn(SO_3F)_4$ has relatively well-resolved bands in the ~800 to ~1100 cm^{-1} region in its i.r. spectrum [33], while both compounds are expected to give the same monodentate to bidentate SO_3F ligand ratio. The reason may lie in the proposed structure for $Sn(SO_3F)_4$, which has trans-monodentate SO_3F groups and a square planar arrangement for the bridging SO_3F groups. This would mean that all the bridging SO_3F groups are well ordered and in relatively similar structural arrangements. Conversely, in $Pt(SO_3F)_4$, the bridging may not lead to the formation of such a well ordered polymeric structure. This may be

illustrated by a difference in the physical properties of two tetrakis(fluorosulfates). While $Sn(SO_3F)_4$ is virtually insoluble in HSO_3F, $Pt(SO_3F)_4$ is extremely soluble, although the break down of the polymer in the latter case is very slow.

5.C.2.2 COMPLEXES CONTAINING $[Pt(SO_3F)_6]^{2-}$

Unlike the parent compound, the three ionic complexes containing the $[Pt(SO_3F)_6]^{2-}$ anion were found to be excellent Raman scatterers, giving rise to well resolved spectra. $(Br_3)_2[Pt(SO_3F)_6]$, however, presented a similar problem as the analogous Au(III) complex; as a result of its dark color and low Raman-scattering efficiency, only poorly resolved Raman spectra could be obtained, even when the sample was cooled to ~80 K. The Raman frequencies of the four $[Pt(SO_3F)_6]^{2-}$ complexes are listed in comparison with those of $Cs_2[Pd(SO_3F)_6]$ in Table 5.2. The i.r. spectrum of $(ClO_2)_2[Pt(SO_3F)_6]$ is shown in Fig. 5.1. The vibrational spectra of $Pd[Pt(SO_3F)_6]$ have already been discussed in Chapter 3, and are consistent with the presence of anisobidentate bridging SO_3F groups spanning Pd(II) and Pt(IV), both in octahedral coordination spheres.

A comparison of the vibrational spectra of $[Pt(SO_3F)_6]^{2-}$ and $[Pd(SO_3F)_6]^{2-}$ reveals that the compounds both contain monodentate SO_3F groups, and that they appear to be isostructural. Slight shifts at ~630, ~450 and ~280 cm^{-1} are presumably due to the different M(IV) cations, supporting the assignment of these

TABLE 5.2: RAMAN FREQUENCIES OF $[Pt(SO_3F)_6]^{2-}$ COMPLEXES

$X = (C\ell O_2)_2$	$X = Cs_2$	$X = Ba$	$X = (Br_3)_2$	$Cs_2[Pd(SO_3F)_8]$	Assignment
1406 m	1416 w,sh	1397 w	~1400 vw	1405 w	$\nu_{as}SO_2$
1375 m	1410 m	1386 m	~1377 w	1395 vw,sh	
1300 vw					$\nu_{as}C\ell O_2^+$
1250 vs	1250 vs	1258 vs	1229 m	1236 vs	
1220 vw,sh					ν_sSO_2
1208 m	1219 m	1218 m	1199 w	1212 m	
1045 s					$\nu_sC\ell O_2^+$
1022 w	1043 s	1033 m	1045 w	1020 vs	
1003 w	1010 m	1012 w	~1005 vw	995 ms	$\nu_{as}SO_2$
852 w		857 w		835 vw	
826 vw		838 vw		805 vw	νS-F
807 vw	~800 w,b			785 w	
631 s	634 vs	629 vs	634 w	618 ms	ν_sM-O + SO_3F def
580 vw	579 vw	583 vw		~585 vw,sh	def SO_3F
546 vw	550 vw	549 vw		542 w	
517 w					$\delta C\ell O_2^+$
445 m	444 m	460 m	450 w	441 ms	$\nu_{as}M$-O + SO_3F def
		422 vw			
~410 vw,b		411 w		~400 vw	SO_3F def
			295 m		Br_3+
283 s	280 vs	283 vs	272 m	270 s	ν_sM-O + SO_3F
273 s					

FIG 5.1

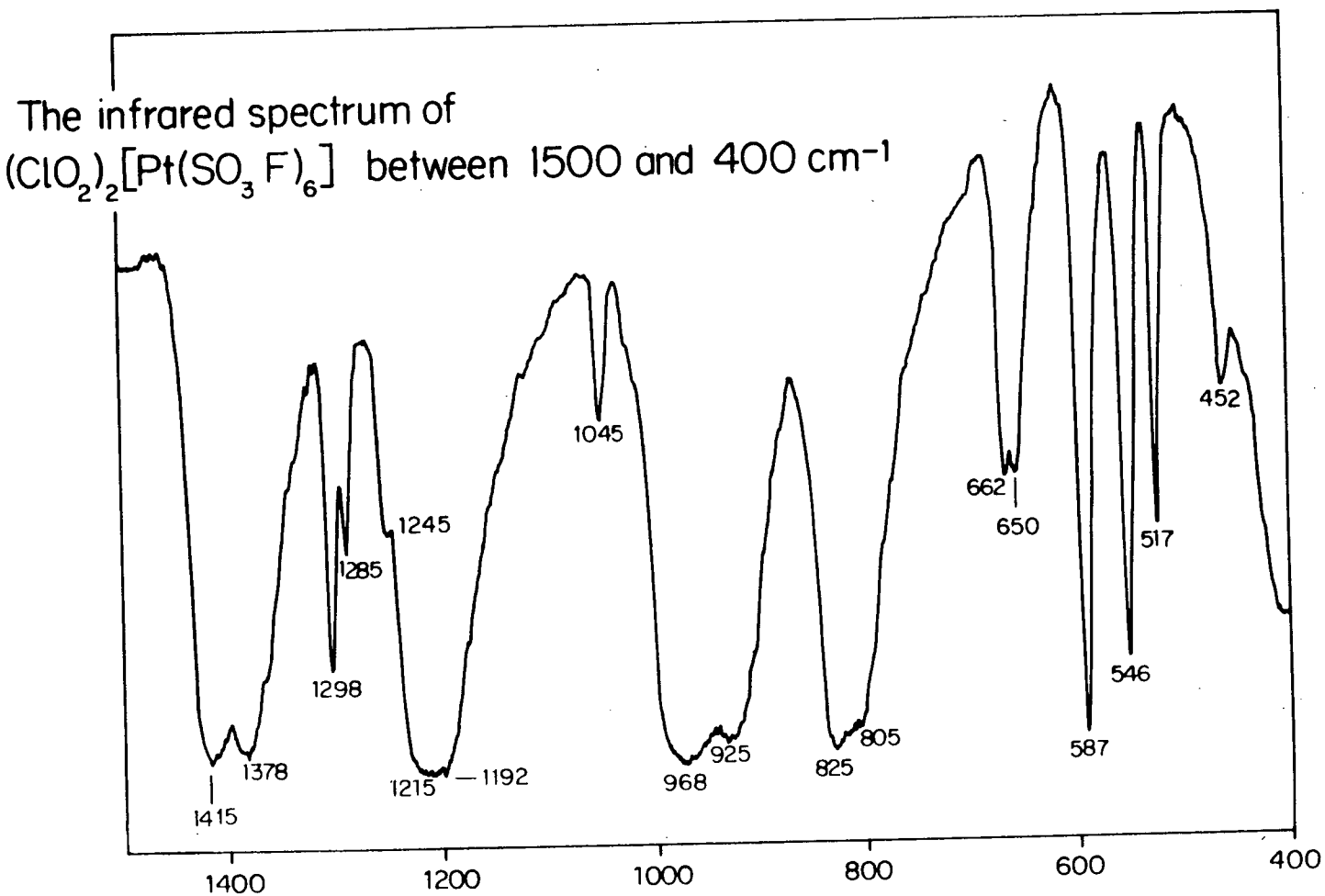
The infrared spectrum of
$(ClO_2)_2[Pt(SO_3F)_6]$ between 1500 and 400 cm^{-1}
1415
1378
1298
1285
1245
1215
1192
1045
968
925
825
805
662
650
587
546
517
452
1400
1200
1000
800
600
400

vibrational modes as having substantial contributions from the $[MO_6]$ skeletal vibrations. The i.r. spectrum of $(ClO_2)_2[Pt(SO_3F)_6]$ shows almost a mutual exclusion of the SO_3F stretching modes and the MO vibrations with the Raman frequencies listed, especially in the ~1050 to ~900 cm^{-1} region. Extensive couplings within the same vibrational modes between different SO_3F groups must be present to account for the intensity differences.

For the ClO_2^+-containing complex, ν_{as} ClO_2^+ are found at 1298 and 1285 cm^{-1} in the i.r. spectrum, split by the two naturally occurring isotopes of ^{37}Cl and ^{35}Cl. ν_s- and δ- ClO_2^+ are found at 1045 and 517 cm^{-1} respectively, supporting an ionic formulation for the compound.

The i.r. spectrum of $(Br_3)_2[Pt(SO_3F)_6]$, down to the low frequency limit of ~400 cm^{-1} for the AgCl windows used, indicates the presence of bands due only to the $[Pt(SO_3F)_6]^{2-}$ anion. In the low temperature Raman spectrum, all the major bands due to the anion are also present, together with new features at 295, 355 and ~700 cm^{-1}. The two higher frequency bands show an intensity difference that may be due to the Resonance Raman effect of Br_2^+, and the peak at 295 cm^{-1} compares well with the value of 290 cm^{-1} in superacid solutions [28] and the band at 280 cm^{-1} in $Br_3[Au(SO_3F)_4]$, both assigned as due to Br_3^+. The presence of Br_2^+ seems to be suggested in all the Raman spectra of Br_3^+-containing complexes studied here; it may be a decomposition product or in equilibrium with Br_3^+ in these systems.

5.C.2.3 $CsPt(SO_3F)_5$

Both the Raman and i.r. spectra of this compound have features that can be ascribed to the presence of both monodentate and bidentate SO_3F groups. The vibrational frequencies of $CsPt(SO_3F)_5$ are listed in Table 5.3 together with those of $CsSn(SO_3F)_5$ and $CsRu(SO_3F)_5$.

It is evident from the Table that the characteristic strong Raman band at 900 cm^{-1} for $Pt(SO_3F)_4$ is missing from the Raman spectrum of $CsPt(SO_3F)_5$, and a general simplification of the S-O stretching region in the i.r. spectrum of the latter compound is also noticed. This argues against the possibility that the compound is simply a mixture of $Pt(SO_3F)_4$ and $Cs_2[Pt(SO_3F)_6]$. Not surprisingly, the spectra are still quite complex, as even for a dimeric $[Pt_2(SO_3F)_{10}]^{2-}$ species, there exists three different types of SO_3F groups —— equatorial bridging, equatorial monodentate and terminal monodentate.

A good agreement between the vibrational frequencies of the compounds listed in Table 5.3 suggests the presence of similar SO_3F groups in all three cases. The i.r. active asymmetric SO-stretching vibration for $CsSn(SO_3F)_5$ is at ~1000 cm^{-1}, almost 80 cm^{-1} higher than that found for the other complexes. An analogous observation is also found for $[Sn(SO_3F)_6]^{2-}$ [32]; whereas in $[M(SO_3F)_6]^{2-}$, with M=Pd, Pt, Ir, and $[Au(SO_3F)_4]^-$, the band is shifted to ~930 cm^{-1}. A slightly different mode of electronic interaction may take place in the complexes involving transition

TABLE 5.3: VIBRATIONAL FREQUENCIES OF $CsPt(SO_3F)_5$ AND RELATED COMPOUNDS

$CsPt(SO_3F)_5$		$CsRu(SO_3F)_5$ [209]	$CsSn(SO_3F)_5$		
R	IR	IR	R	IR	
1442 vw,sh			1430 vw		
1412 m	1400 vs	1405 vs,b	1418 w	~1400 vs,b	$\nu_{as}SO_3$
1390 vw					
1250 vw,sh					
1240 s			1265 m	1260 m	ν_sSO_2
1225 w,sh	1210 vs	1215 vs	~1220 w,b	1220 vs	
				1190 s,b	
	1120 s	1140 m	1130 w	1125 s,b	ν_sSO_2 bridge
			1112 w		
1080 vw				1080 s,b	
1058 w			1062 w		
1050 w,sh	1040 m	1045 m			
1005 m			~1002 vw		
980 w,b					$\nu_{as}SO_3$
967 w,b	950 vs,b			~1000 vs,b	
930 w	920 vs,b	925 vs,b			
				880 w	
835 w			850 w	~830 w,sh	
817 w	800 vs,b	810 s,b	820 w	800 vs,b	νSF
658 w	670 w,sh				
635 s	650 m,b	660 m	630 m	625 m,b	$\nu_sM\text{-}O + SO_3F$ def
605 w			605 vw		
590 vw				595 w	
580 vw	580 m	580 ms	585 w	587 m	
547 w	540 m	550 ms	560 w	560 m	SO_3F def
510 vw	515 vw,sh				
447 m	~400 w,sh	440 mw	~430 w,sh	~450 vw,sh	$\nu_{as}M\text{-}O + SO_3F$ def
410 vw					
275 s					$\nu_sM\text{-}O + SO_3$ bend

metals. The vibrational spectra of $CsSn(SO_3F)_5$ will be discussed in more detail in Chapter 9.

Therefore, it appears that the existence of monomeric $[Pt(SO_3F)_5]^-$ with monodentate SO_3F groups is not supported by the vibrational spectra of the compound. A polymeric structure, containing $[Pt(SO_3F)_5]_n^{-n}$, must therefore be present, as there is no evidence that the compound is a mixture of $Pt(SO_3F)_4$ and $[Pt(SO_3F)_6]^{2-}$. A dimer would have two $[Pt(SO_3F)_6]$ octahedra joined by a common edge, a trimer or high oligomers would be a cyclic structure joined via cis-corners of the octahedra. The exact structure cannot be elucidated by vibrational spectroscopy alone and an X-ray diffraction study is required.

5.C.3 MAGNETIC SUSCEPTIBILITY

All the Pt(IV)-SO_3F compounds investigated in this study are diamagnetic, suggesting a low-spin octahedral ligand field for the d^6 Pt(IV) and a $^1A_{1g}$ electronic ground state. The experimentally obtained susceptibilities at room temperature are listed in Table 5.4. As it was required for a dilution experiment in Chapter 6, the temperature dependence of the magnetic susceptibility of $(ClO_2)_2[Pt(SO_3F)_6]$ was investigated from 300 to 81 K. The diamagnetic susceptibility of $-(250 \pm 15)\times10^{-6}$ cgs units was found to have no discernable temperature dependence. The sum

of the Pascal constant for ClO_2^+ and the diamagnetic correction for $[Pt(SO_3F)_6]^{2-}$ [107] is -320×10^{-6} cgs units. Therefore, $(70 \pm 15)\times10^{-6}$cgs units of paramagnetic susceptibility must be due to Temperature Independent Paramagnetism, expected to be only about 50×10^{-6} cgs units for Pt(IV) [141]. The presence of T.I.P. is also evident for the other compounds listed in Table 5.4.

Table 5.4 DIAMAGNETIC SUSCEPTIBILITY FOR SOME Pt(IV)-FLUOROSULFATE COMPOUNDS (IN cgs UNITS) AT ROOM TEMPERATURE

	χ_g	χ_m	$\Sigma\chi_{dia}$
$Pt(SO_3F)_4$	$-(1.52\pm31)\times10^{-7}$	$-(81\pm17)\times10^{-6}$	-188×10^{-6}
$Ba[Pt(SO_3F)_6]$	$-(2.95\pm7)\times10^{-7}$	$-(271\pm6)\times10^{-6}$	-292×10^{-6}
$(ClO_2)_2[Pt(SO_3F)_6]$ *	$-(2.70\pm16)\times10^{-7}$	$-(250\pm15)\times10^{-6}$	-320×10^{-6}
$(Br_3)_2[Pt(SO_3F)_6]$	$-(3.47\pm16)\times10^{-7}$	$-(440\pm20)\times10^{-6}$	-454×10^{-6}

* $81 \leq T \leq 300$ K

5.C.4 SOLUTION STUDIES IN HSO_3F

5.C.4.1 ELECTRONIC SPECTRA

Solutions of $Pt(SO_3F)_4$ and $Cs_2[Pt(SO_3F)_6]$ have identical absorption spectra when dissolved in HSO_3F, supporting the presence of similar Pt(IV)-fluorosulfate species. The spectrum consists of a strong broad peak at 245 nm (half width of ~70 nm), $\varepsilon\sim1.5\times10^4$ $M^{-1}cm^{-1}$. This band must be of charge transfer origin; no other absorptions due to d-d transition could be observed.

5.C.4.2 ELECTRICAL CONDUCTIVITIES

Both $(ClO_2)_2[Pt(SO_3F)_6]$ and $Pt(SO_3F)_4$ dissolve in HSO_3F to give conducting solutions, and, as in the HSO_3F-$Au(SO_3F)_3$ system, the binary fluorosulfate gives rise to strongly conducting solutions. $CsPt(SO_3F)_5$ also dissolves in HSO_3F to give solutions with conductivities slightly higher than those of $(ClO_2)_2[Pt(SO_3F)_6]$, when the conductivities are calculated for equivalents of cations, i.e. Cs^+ and ClO_2^+. The conductivities of solutions of $(ClO_2)_2[Pt(SO_3F)_6]$ and $CsPt(SO_3F)_5$ are shown in Fig. 5.2 and listed in Table 5.5. Those of $Pt(SO_3F)_4$ are shown in Fig. 5.3 and Table 5.6.

The conductivities of solutions of $(ClO_2)_2[M(SO_3F)_6]$, where M=Pt, Sn [32], Ir, Pd, are all very similar, indicating a similar dissociative process in HSO_3F. A qualitative titration using small amounts of KSO_3F indicates no acidic property for $(ClO_2)_2[Pt(SO_3F)_6]$.

If $(ClO_2)_2[Pt(SO_3F)_6]$ undergoes a simple ionic dissociation in solution, like $K[Au(SO_3F)_4]$, according to:

$$(ClO_2)_2[Pt(SO_3F)_6] + HSO_3F \longrightarrow 2ClO_2^+{}_{(solv)} + [Pt(SO_3F)_6]^{2-}{}_{(solv)} \quad , (5.11)$$

the conductivity of the resultant solution should be about 1.5 times that of a solution of $K[Au(SO_3F)_4]$ at the same concentration. This is expected because

a) $\lambda_o^*(K^+)=30$, while $\lambda_o^*([Au(SO_3F)_4]^-)=24$,

b) $\lambda_o^*(K^+)$ seems to be slightly higher than $\lambda_o^*(ClO_2^+)$ [109], and,

FIG 5.2

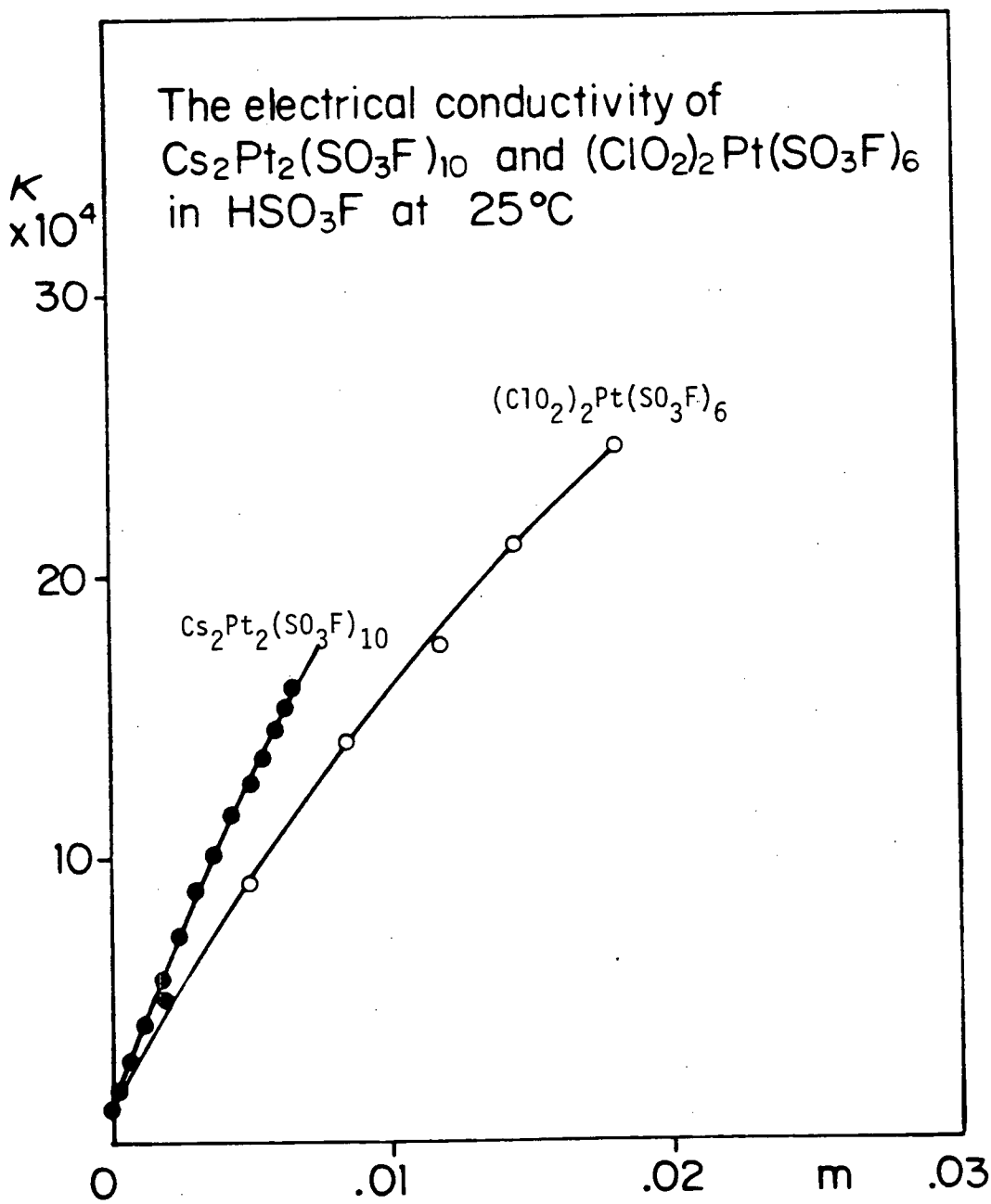
The electrical conductivity of
$Cs_2Pt_2(SO_3F)_{10}$ and $(ClO_2)_2Pt(SO_3F)_6$
in HSO_3F at 25°C
K
x10⁴
30
20
10
0
.01
.02
m
.03
$(ClO_2)_2Pt(SO_3F)_6$
$Cs_2Pt_2(SO_3F)_{10}$

Table 5.5 CONDUCTIVITY OF $(ClO_2)_2[Pt(SO_3F)_6]$ AND $CsPt(SO_3F)_5$ IN HSO_3F

m*	$(ClO_2)_2[Pt(SO_3F)_6]$	$[Cs(Pt(SO_3F)_5]$
0.000	1.720	1.148
0.002	5.185	5.925
0.004	7.986	10.62
0.006	10.59	14.64
0.008	13.54	
0.010	15.54	
0.012	17.82	
0.014	20.11	
0.016	22.29	
0.018	24.59	
0.020	27.46	
0.022	30.43	
0.024	32.86	
0.026	34.10	
$mol \cdot kg^{-1}$	$10^{-4}\Omega^{-1}cm^{-1}$	$10^{-4}\Omega^{-1}cm^{-1}$ units

* For comparison purposes, the molality of $CsPt(SO_3F)_5$ is calculated for two cations, i.e., $[CsPt(SO_3F)_5]_2$

FIG 5.3 CONDUCTIVITY OF $Pt(SO_3F)_4$ IN HSO_3F

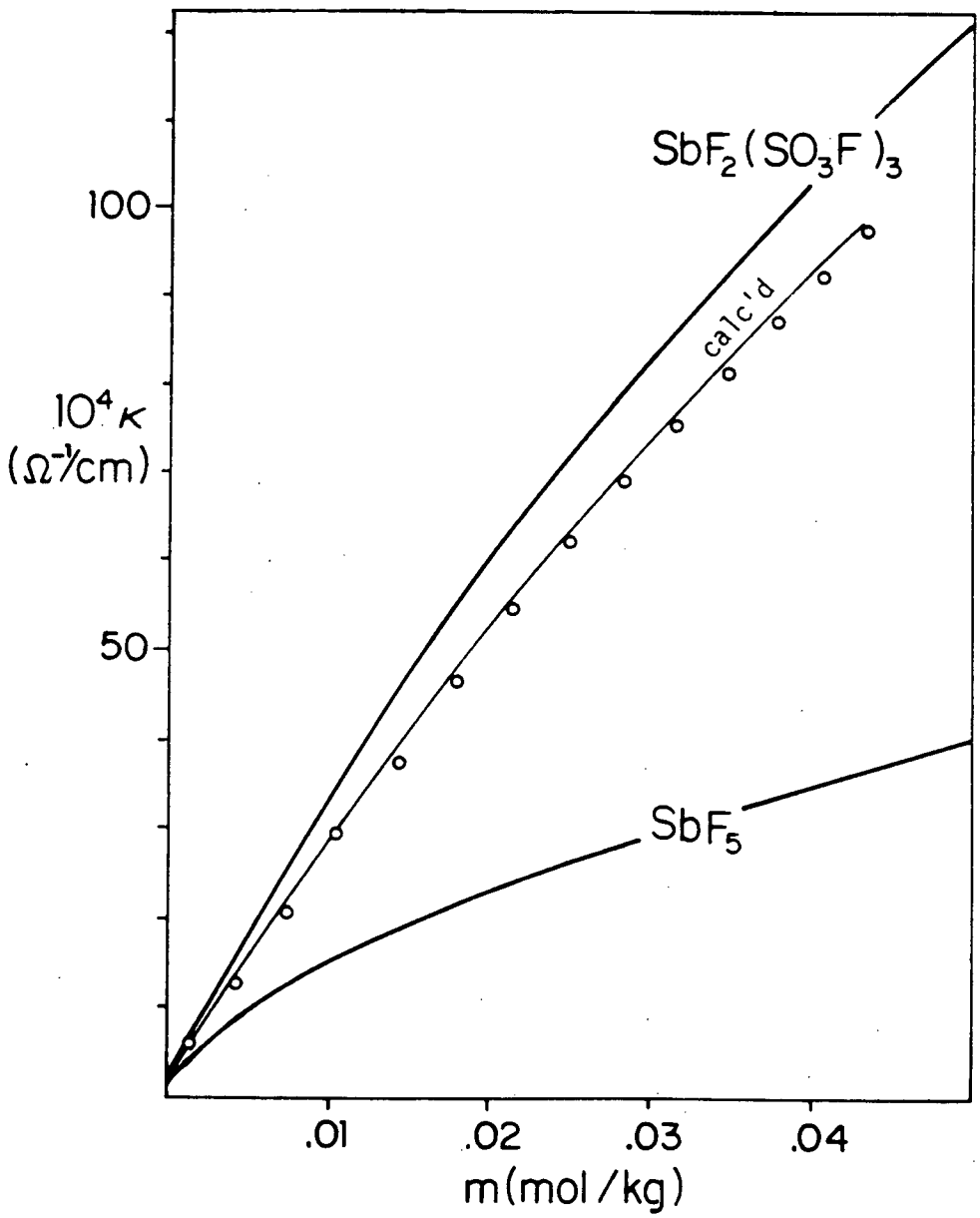

Table 5.6 CONDUCTIVITY OF $Pt(SO_3F)_4$ IN HSO_3F

m	κ(obs)	κ(calc)
0.000	1.134	1.100
0.002	11.83	6.75
0.004	12.43	13.09
0.006	16.05	19.08
0.008	22.05	24.77
0.010	28.05	30.20
0.012	32.85	35.40
0.014	37.08	40.38
0.016	41.73	45.18
0.018	46.78	49.81
0.020	51.58	54.29
0.022	56.03	58.62
0.024	60.25	62.82
0.026	64.41	66.90
0.028	68.50	70.87
0.030	72.44	74.73
0.032	76.31	78.50
0.034	80.14	82.17
0.036	83.96	85.76
0.038	87.77	89.27
0.040	91.57	92.70
$mol \cdot kg^{-1}$	$10^{-4}\Omega^{-1}cm^{-1}$	$10^{-4}\Omega^{-1}cm^{-1}$ units

c) $\lambda_o^*[Pt(SO_3F)_6]^{2-}$ should be less than $\lambda_o^*([Au(SO_3F)_4]^-)$ due to its double negative charge which may result in more extensive solution. This, however,is not found for $(ClO_2)_2[Pt(SO_3F)_6]$ or any of the $[M(SO_3F)_6]^{2-}$ complexes; on the contrary, the conductivity of these solutions is about twice that of $K[Au(SO_3F)_4]$, at the same concentration. Furthermore, whereas the molal conductivity of $K[Au(SO_3F)_4]$ remains relatively constant with respect to concentration, the same is not true for the $[M(SO_3F)_6]^{2-}$ complexes; these seem to decrease much faster as the concentration increases.

The high conductivity, the large concentration dependence of the molal conductivity and the lack of acidic behavior for the solutions seem to suggest the existence of an equilibrium giving rise to SO_3F^- in the process, i.e., a basic dissociation for $[M(SO_3F)_6]^{2-}$. Further evidence for this will be presented in the titration of $Pt(SO_3F)_4$ with KSO_3F.

As can be seen from Fig 5.3, the conductivity of $Pt(SO_3F)_4$ in HSO_3F is comparable to that of $Au(SO_3F)_3$, which has been shown to be a superacid in HSO_3F; but being a solute that can conceivably give rise to two acidium ions per mole of $Pt(SO_3F)_4$ dissolved, the conductivity appears quite low, or about a half as expected for a complete dissociation.

As with any diprotic acid, $H_2[Pt(SO_3F)_6]$, the hypothetical solvated acid in HSO_3F, should undergo the following two-step deprotonation reaction:

$$HSO_3F + H_2[Pt(SO_3F)_6] \underset{\leftarrow}{\xrightarrow{K_1}} H_2SO_3F^+ + H[Pt(SO_3F)_6]^- \qquad (5.12)$$

$$HSO_3F + H[Pt(SO_3F)_6]^- \underset{\leftarrow}{\xrightarrow{K_2}} H_2SO_3F^+ + [Pt(SO_3F)_6]^{2-} \quad . \quad (5.13)$$

K_1 should also be expected to be much larger than K_2, by analogy with multiprotic acids in the aqueous system, such as H_2SO_4 and H_3PO_4. With the high conductivity of solutions of HSO_3F-$Pt(SO_3F)_4$, $H_2[Pt(SO_3F)_6]$ must be almost completely dissociated via equation (5.12), and the almost identical conductivity of HSO_3F-$Pt(SO_3F)_4$ with that of HSO_3F-$Au(SO_3F)_3$ suggests an almost monoprotic system, or $K_1 >> K_2$.

The conductometric titration of $H_2[Pt(SO_3F)_6]$ with KSO_3F, a typical plot of which is shown in Fig 5.4, supports both the above suggestions. In the beginning of the titration, and up to a K/Pt ratio of about 1, the conductance decreases almost linearly with the addition of KSO_3F, indicating that a strong acid is present. But further into the titration, a gradual increase in the slope of the titration curve occurs, and a broad conductivity minimum is found at a K/Pt ratio of ~1.5. The titration curve crosses the equivalent point of 2 without any changes in the slope that would suggest that it is reached. This indicates a very weakly acidic solution, and $K_2[Pt(SO_3F)_6]$, the empirical formula of the species present at the endpoint, is a base in HSO_3F. The titration was repeated 6 times, using both weight- and volume-buret addition of KSO_3F, and the result is reproducible.

Using the procedure described in Appendix A, a theoretical titration curve was calculated; this is shown in Fig 5.4 and

FIG. 5.4

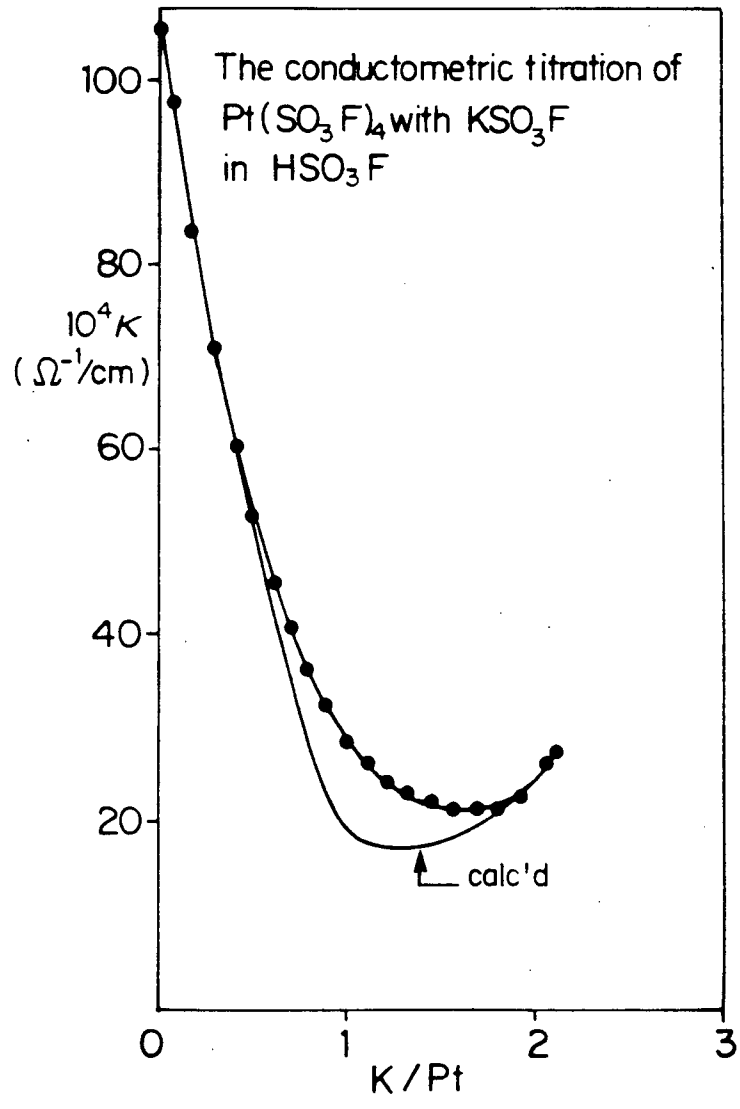
The conductometric titration of
Pt(SO3F)4 with KSO3F
in HSO3F
100
80
60
40
20
10^4 κ
(Ω^-1/cm)
calc'd
0
1
2
3
K/Pt

listed in Table 5.7. The following parameters were used:

$\lambda_o^*(H_2SO_3F^+)$ = 320,
$\lambda_o^*(SO_3F^-)$ = 227,
$\lambda_o^*(K^+)$ = 29,
$\lambda_o^*(H[Pt(SO_3F)_6]^-)$ = 29,
$\lambda_o^*([Pt(SO_3F)_6]^{2-})$ = 32,
K_1 = 6.3×10^{-2} mol/kg,
K_2 = 5.0×10^{-5} mol/kg, and
$K_{ap} = [H_2SO_3F^+]\cdot[SO_3F^-]$ = 3.8×10^{-8} mol/kg.

This would give a basic dissociation, K_{-2}, for $[Pt(SO_3F)_6]^{2-}$ in HSO_3F, according to:

$$[Pt(SO_3F)_6]^{2-} + HSO_3F \underset{\longleftarrow}{\xrightarrow{K_{-2}}} H[Pt(SO_3F)_6]^- + SO_3F^- \quad , \qquad (5.14)$$

of $1.2\ 10^{-3}$ mol/kg, i.e., $[Pt(SO_3F)_6]^{2-}$ is a reasonably strong base when dissolved in HSO_3F. This is consistent with the high conductivity of solutions of $[Pt(SO_3F)_6]^{2-}$ and the basic behavior of the solution near the endpoint of the $Pt(SO_3F)_4/KSO_3F$ titration. By analogy, the other $[M(SO_3F)_6]^{2-}$, where M=Sn, Pd, Ir, because of the similarity in the conductivity of their solutions, should have very similar K_{-2} values and thus are strong bases in HSO_3F.

The fit between the calculated and observed titration points is acceptable at the ratios K/Pt at ~0 and at ~2, the deviation increases quite rapidly as K/Pt approximates 1, a higher acidity than can be accounted for by equations (5.12) and (5.13) was observed. The λ_o^* values are in the range expected for the various species, although the apparently high mobility of $[Pt(SO_3F)_6]^{2-}$

Table 5.7 CONDUCTOMETRIC TITRATION OF $Pt(SO_3F)_4$ WITH KSO_3F IN HSO_3F

R	κ(obs)	κ(calc)*	I
0.00	104.8	104.8	0.032
0.20	79.43	79.78	0.031
0.40	60.09	59.48	0.031
0.60	45.51	42.77	0.030
0.80	35.40	28.93	0.030
1.00	28.71	19.03	0.031
1.20	24.75	17.33	0.038
1.40	22.73	17.81	0.045
1.60	21.69	18.93	0.051
1.80	21.62	20.95	0.056
2.00	24.61	24.61	0.060
	$\Omega^{-1}cm^{-1}$	$\Omega^{-1}cm^{-1}$	$mol \cdot kg^{-1}$ units

* calculated using the following parameters:

$\lambda_o^*(H_2SO_3F^+) = 320$

$\lambda_o^*(SO_3F^-) = 227$

$\lambda_o^*(K^+) = 29$

$\lambda_o^*(H[Pt(SO_3F)_6]^-) = 29$

$\lambda_o^*([Pt(SO_3F)_6]^{2-}) = 32$

$[H_2SO_3F^+] \cdot [SO_3F^-] = 3.8 \times 10^{-8}\ mol^2 \cdot kg^{-2}$

$K_1 = 0.063\ mol \cdot kg^{-1}$

$K_2 = 5.0 \times 10^{-5}\ mol \cdot kg^{-1}$

should require some explanation. Although one would normally expect that a doubly charged ion would have a less mobility than its singly charged counterpart because of the increased size of the former's solvation sphere, such a phenomenon may not be very important when the ion itself is already very large, like the $[M(SO_3F)_6]^{2-}$ studied here, and the charge can be delocalized more efficiently than a point charge such as K^+. K^+ may be extensively solvated in HSO_3F since $\lambda_o^*(Ba^{2+})$ is about 35 in $Ba(SO_3F)_2$ solutions ($\lambda_o^*(K^+) = 29$) [21]. For similarly solvated ions of different charges, the higher the charge on the ion, the higher its mobility should be, since it would experience an increased force from the electric field.

At the intermediate K/Pt ratios during the titration, the excess acidium ion may be indirectly due to a dimerization of $[Pt(SO_3F)_6]$-containing species according to:

$$H_2[Pt(SO_3F)_6] \underset{}{\overset{K_{d1}}{\rightleftharpoons}} \tfrac{1}{2}H_2[Pt_2(SO_3F)_{10}] + HSO_3F \qquad (5.15)$$

$$H[Pt(SO_3F)_6]^- \overset{K_{d2}}{\rightleftharpoons} \tfrac{1}{2}H_2[Pt_2(SO_3F)_{10}] + SO_3F^- \qquad (5.16)$$

$$[Pt(SO_3F)_6]^{2-} \overset{K_{d3}}{\rightleftharpoons} \tfrac{1}{2}[Pt_2(SO_3F)_{10}]^{2-} + SO_3F^-. \qquad (5.17)$$

All these dimerization reactions have the result of decreasing the acidity of the system; two also have a strong dependence on $[SO_3F^-]$ and conversely $[H_2SO_3F^+]$. At the initial conditions of high acidity, if the hypothesis is correct, dimerization or even higher oligomer formation is favored. But as the titration proceeds (by the addition of KSO_3F solution which also dilutes the system), the initially formed oligomers will gradually depoly-

merize, and increase the acidity of the solution by the reverse reaction which can be represented by:

$$\tfrac{1}{2}H_2[Pt_2(SO_3F)_{10}] + 3HSO_3F \underset{\leftarrow}{\overset{K_{-1}}{\rightarrow}} [Pt(SO_3F)_6]^{2-} + 2H_2SO_3F^+ \quad . \qquad (5.18)$$

The net effect of this extra quantity of $H_2SO_3F^+$ would contribute to an increase in conductivity of the system. Furthermore, the actual K_1 would be higher than the one calculated here and the actual K_2 would be lower. This is because of the calculation procedure used; also because of this, $\lambda_o^*([Pt(SO_3F)_6]^{2-})$ would be lowered, but since the calculated value is so high to start with, this should not be a problem. This extra set of equilibria serves to buffer the system when the acidity is not very high, and the observed broad conductivity minimum seems to be consistent with this. It is possible to include equations (5.15) to (5.17) into the calculation, but the procedure outlined in Appendix A already involves four variables and the addition of three more is certainly beyond the intent of this study. Qualitatively, the addition of equations (5.15) to (5.17) appears to be able to shift the calculated curve closer to the observed one.

It is now necessary to present some evidence for polymerization in the platinum(IV)-fluorosulfate system. $Pt(SO_3F)_4$ is a polymer in the solid state, much like $Au(SO_3F)_3$ is, and both dissolve in HSO_3F only with difficulties, although very concentrated solutions can be formed. $Pt(SO_3F)_4$ shows a much greater reluctance to dissolve, and this has been discussed in the vibrational

spectra section. Solutions of $Pt(SO_3F)_4$ obtained in this manner all show lower conductivity than those obtained without first isolating $Pt(SO_3F)_4$ as a solid (i.e., formed from platinum metal and $S_2O_6F_2/HSO_3F$). The complete removal of all $S_2O_6F_2$ in the latter case is shown by Raman spectroscopy for one such sample. It therefore appears that oligomers, possibly of a much higher degree of polymerization than 2, may be present when solid $Pt(SO_3F)_4$ is dissolved in HSO_3F. Furthermore, as mentioned before, the apparent molal conductivity of $(ClO_2)_2[Pt(SO_3F)_6]$, and also those of $CsPt(SO_3F)_5$, $CsSn(SO_3F)_5$ and $Pt(SO_3F)_4$ all show a large concentration dependence. This is especially evident for $CsSn(SO_3F)_5$, for which a larger concentration range was investigated. A detailed discussion on the conductivity of $CsM(SO_3F)_5$ and $[M(SO_3F)_6]^{2-}$, M=Pt, Sn, will be presented in Chapter 9. All these observations suggest the occurrence of polymerization in solutions containing these species.

Supporting evidence can also be found in the vibrational spectra of $CsPt(SO_3F)_5$ (also $CsSn(SO_3F)_5$), which indicate the presence of both monodentate and bidentate SO_3F groups. It can be visualized that $CsPt(SO_3F)_5$ is the compound isolated at K/Pt=1 during the titration, and that it is formed either by the desolvation-dimerization of $H[Pt(SO_3F)_6]^-$ according to:

$$2H[Pt(SO_3F)_6]^- \longrightarrow [Pt_2(SO_3F)_{10}]^{2-} + 2HSO_3F \quad , \qquad (5.19)$$

or, if $[Pt_2(SO_3F)_{10}]^{2-}$ is the predominant species present at that condition, by a desolvation process. The n.m.r. and vibrational

spectra evidence to be presented later seem to indicate quite a low extent of polymerization in solution, and favors equation (5.19) (this does not negate its contribution to the conductivity though, because the deviation between the two curves in Fig 5.4 is quite small).

$CsPt(SO_3F)_5$ dissolves in HSO_3F to give a solution which shows acidic conductivity. Its higher conductivity than solutions of $(ClO_2)_2[Pt(SO_3F)_6]$ (Fig 5.2) is consistent with $H_2SO_3F^+$ having a greater ionic mobility than SO_3F^-.

5.C.4.3 SOLUTION VIBRATIONAL SPECTRA

It was hoped that Raman spectra of solutions of $Pt(SO_3F)_4$ would show signs of polymerization. This, however, was not observed up to a concentration of about 0.12 mol/kg. Actually, the only bands that are definitely due to $Pt(SO_3F)_4$ are at 638, 455 and 276 cm^{-1}, as all other bands are overlapped by broad solvent bands. This suggests that solutions of $Pt(SO_3F)_4$ are not as efficient Raman scatterers as those of $Au(SO_3F)_3$. In addition, because of the broadness of the peaks, splittings observed in the solid state spectra of $CsPt(SO_3F)_5$ are not evident here.

5.C.4.4 SOLUTION N.M.R.

All three species, $Pt(SO_3F)_4$, $CsPt(SO_3F)_5$ and $Cs_2[Pt(SO_3F)_6]$ gave identical ^{19}F-n.m.r. spectra in HSO_3F solutions. This is

in sharp contrast to what was observed in the $Au(SO_3F)_3$-HSO_3F system. A typical ^{19}F-n.m.r. spectrum of $Pt(SO_3F)_4$-HSO_3F is shown in Fig. 5.5.

One of the natural occurring isotope of platinum, ^{195}Pt, has a nuclear spin of ½, and its coupling to ^{19}F supposedly gives rise to the splitting of the fluorine resonance with J(Pt-F) = 31 Hz. Since ^{195}Pt is present in only 33.8% natural abundance, about $^2/_3$ of the fluorine signal should not be affected, and this was shown by an integration of the peaks. Therefore, the coupling occurs via a sulfur and an oxygen atom. $[PtF_6]^{2-}$ on the other hand, presumably due to the proximity of the two atoms, has a large J(Pt-F) coupling constant of ~2000 Hz [195].

For the species $[Pt_2(SO_3F)_{10}]^{2-}$, the coupling scheme for that ion alone will be a 1:8:2:8:1 pattern, each separated by ~15 Hz. This is expected since the chemical environment for a fluorosulfate group should not be very different whether the SO_3F ligand is monodentate or bidentate. However, no satellites on either side of the triplet was observed, at concentrations up to ~0.12 mol/kg. This indicates that even if the dimer is present, it must be in quite a low concentration.

The sharpness of the resonances does not necessarily mean a lack of exchange between the platinum-fluorosulfate-containing solute (at -47.8 ppm) and the solvent (at -40.8 ppm), as these resonances are 7 ppm apart, and proton exchange evidently does occur in this system.

FIG. 5.5

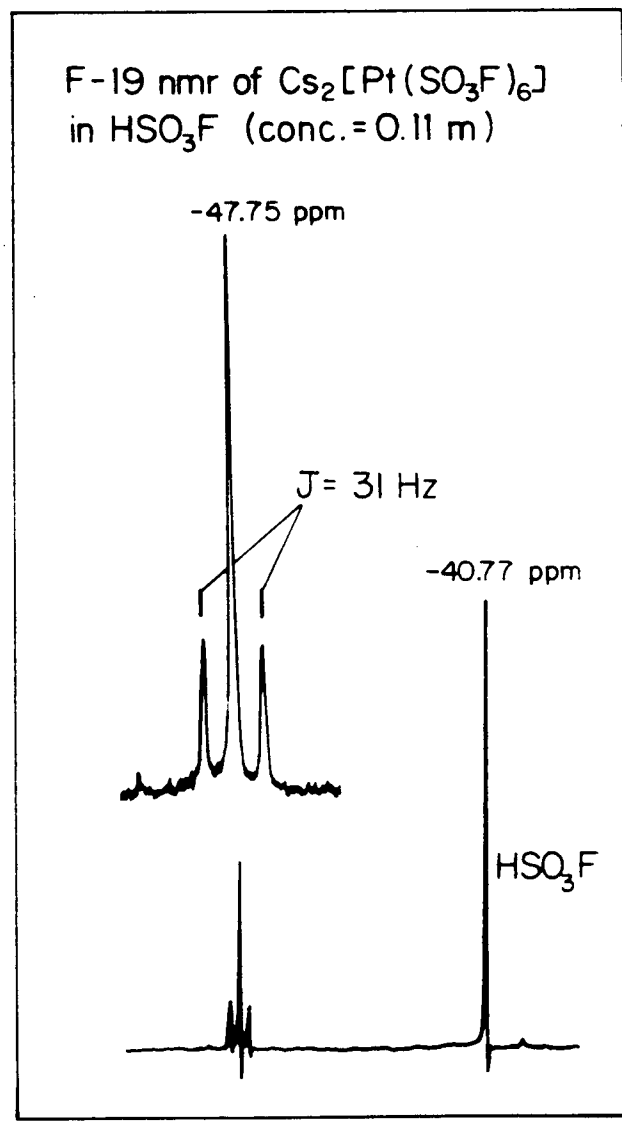
F-19 nmr of $Cs_2[Pt(SO_3F)_6]$
in HSO_3F (conc. = 0.11 m)
-47.75 ppm
J = 31 Hz
-40.77 ppm
HSO_3F

These ^{19}F-n.m.r. results show that identical species containing platinum and fluorosulfate groups are present in solution, whether the starting solid is the binary fluorosulfate or either of its two types of complexes.

Since ^{195}Pt is a nucleus accessible by n.m.r. spectroscopy, attempts were made to obtain ^{195}Pt-n.m.r. spectra of these solutions. For the spectrum of $[Pt(SO_3F)_6]^{2-}$, a septet of the relative intensity of 1:6:15:20:15:6:1 and separated by J(Pt-F)=31 Hz is expected, while for $[Pt_2(SO_3F)_{10}]^{2-}$, two groups of septets separated by J(Pt-Pt) should be present if Pt-Pt coupling occurs. The observation of the latter group of peaks should provide the most conclusive evidence for the existence of the dimer in solution.

This, unfortunately, did not occur, and no ^{195}Pt-n.m.r. spectra was obtainable for any one of the fluorosulfates, even when solutions of up to ~1 mol/kg concentration were used, although a resonance from a $[PtCl_6]^{2-}$ test solution was obtained. The wide range of chemical shifts possible in ^{195}Pt-n.m.r. spectra (~7000 ppm from $[PtF_6]^{2-}$ to $[PtCl_6]^{2-}$) combined with its low sensitivity (only ~0.3 % that of proton when natural abundance is included) [40] probably contributed to this experiment's demise.

5.D CONCLUSION

HSO_3F-$Pt(SO_3F)_4$ has been found to be a superacid in the HSO_3F solvent system. In a per-mole basis, its acidity is comparable to that of HSO_3F-$Au(SO_3F)_3$ and slightly less than that of HSO_3F-SbF_2-$(SO_3F)_3$. The decrease in acidity in the system, similar to other diprotic acids, is due to the low equilibrium constant for the dissociation of the second proton. In addition, the oligomer-formation of the $[Pt(SO_3F)_6]$-containing species is also a contributing factor. These have been shown by conductometric titrations of the superacid with KSO_3F.

As expected, complexes containing $[Pt(SO_3F)_6]^{2-}$ can readily be formed, including one which contains the tribromine cation — $(Br_3)_2[Pt(SO_3F)_6]$. The anion dissociates in HSO_3F to give basic conducting solutions, and appears to be isostructural with a general class of $[M(IV)(SO_3F)_6]^{2-}$ anions. A complex with the empirical formula of $CsPt(SO_3F)_5$ can also be synthesized this is a weak acid in HSO_3F and is not monomeric in the solid state.

The Pt(IV)-fluorosulfate system investigated here is diamagnetic, thus indicating a $^1A_{1g}$, low-spin electronic ground state for the d^6 metal ion in an octahedral ligand field.

CHAPTER 6 IRIDIUM-FLUOROSULFATE

6.A INTRODUCTION

Iridium is one of the rarest members of the platinum metals, but because of its possible role in homogeneous catalysis, especially with Ir in the lower oxidation states, the chemistry of iridium has been a field of active research [198,196]. Iridium can exist in a variety of oxidation states, from -1 to +6, the possible exception being Ir(II), which is isoelectronic with Pd(III) and Pt(III). As far as the halogen chemistry of iridium is concerned, it is much like that of platinum, with IrF_6, $[IrF_5]_4$ and $Ir\text{-}Hal_3$, Hal=F, Cl, Br, I, all having been synthesized. Although the binary tetrahalides of iridium are unknown, it forms many very stable $[Ir\text{-}Hal_6]^{2-}$ complexes [190]. The instability of $Ir\text{-}Hal_4$, at least in the case of IrF_4, cannot be attributed to the lack of oxidative ability of the halogen, and may be due to the more favorable formation of either IrF_3 or $[IrF_5]_4$. The normal product of the fluorination of iridium metal, depending on the reaction condition, is IrF_6 or $[IrF_5]_4$; IrF_3 can only be obtained by the reduction of the higher fluorides.

While the gold and the platinum systems discussed in previous chapters provided some interesting solution chemistry, and novel superacid systems in HSO_3F, they are lacking in having any paramagnetic compounds. One of the most easily accessible oxidation states of iridium, at least in anionic complexes, is Ir(IV), which

is d^5. So regardless of whether the ion is high spin or low spin, this should provide a paramagnetic species.

The high ligand field splitting expected for Ir(IV) would almost certainly force the electronic state to be $^2T_{2g}$, low-spin. Although this would imply quite complicated temperature dependent magnetic behavior for Ir(IV), this is sometimes not very noticeable due to the inherent small magnitude of the magnetic susceptibility itself. However, antiferromagnetic coupling is prevalent in this system, and $[Ir\text{-}Hal_6]^{2-}$ complexes,with Hal=Cl, Br, have low moments of about 1.5 μ_B at room temperature [197]. It was of interest to see if the replacement of a halide ion with a SO_3F group would lead to a drastic increase in the magnetic moment of the species, as was observed in the palladium system.

Therefore, the investigation into iridium-fluorosulfate is not so much in terms of solution studies, but rather as a study into the magnetic behavior of fluorosulfates containing a transition metal in a high oxidation state and to collect more information as to the coordination properties of the fluorosulfate group.

6.B EXPERIMENTAL

6.B.1 SYNTHESIS OF IRIDIUM TRIS(FLUOROSULFATE)

$$Ir + 2S_2O_6F_2 \xrightarrow{HSO_3F} Ir(SO_3F)_4 \qquad (6.1)$$

$$Ir(SO_3F)_4 \xrightarrow[\Delta]{} Ir(SO_3F)_3 + \tfrac{1}{2}S_2O_5F_2 + \tfrac{1}{4}O_2 \qquad (6.2)$$

In a typical reaction, iridium metal (158 mg, 0.822 mmol) was reacted with an excess of $S_2O_6F_2/HSO_3F$ (~10 mL) at ~140°C. Parts of the metal initially dissolved to form a brown solution containing $Ir(SO_3F)_4$; after 3 days of heating, a deep purple solution together with unreacted metal was formed. After the removal of most of the $S_2O_5F_2$ and oxygen formed from the reaction, more $S_2O_6F_2$ (~3 mL) was added to the mixture which was subsequently reheated at ~140°C. After 3 days, all metal had dissolved and the solution again changed back into having a deep purple color. All volatile materials were removed in vacuo and a solid which analyzed as $Ir(SO_3F)_3$ was obtained (398 mg, 0.813 mmol). $Ir(SO_3F)_3$ can also be obtained by the thermal decomposition of $Ir(SO_3F)_4$ at ~120°C in vacuo according to equation (6.2). In a typical pyrolysis experiment, $Ir(SO_3F)_4$ (294 mg, 0.500 mmol) was converted into $Ir(SO_3F)_3$ (239 mg, 0.488 mmol) after 12 hours of heating.

$Ir(SO_3F)_3$ is a very deep bluish purple, hygroscopic solid. It is soluble in HSO_3F and decomposes at ~200°C with the evolution of a colorless gas which was not identified.

Analysis	Ir	S	F
Calculated %	39.27	19.66	11.65
Found %	39.10	19.46	11.48

6.B.2 SYNTHESIS OF IRIDIUM TETRAKIS(FLUOROSULFATE)

$$Ir(SO_3F)_3 + \tfrac{1}{2}S_2O_6F_2 \longrightarrow Ir(SO_3F)_4 \qquad (6.3)$$

$Ir(SO_3F)_4$ can be prepared in a reaction similar to that discussed for $Ir(SO_3F)_3$. Iridium metal (198 mg, 1.030 mmol), was reacted with $S_2O_6F_2/HSO_3F$ (~4 mL) and was taken through the same cycles of $S_2O_6F_2$ addition. When all the metal had dissolved and most of the $S_2O_5F_2$ had been removed, $S_2O_6F_2$ (~2 mL) was added to the solution of essentially $Ir(SO_3F)_3$ in HSO_3F. This was heated at ~60°C for 6 hours, after which time a deep brown solution had formed. The removal of all volatile materials by the usual method yielded $Ir(SO_3F)_4$ with traces of the blue $Ir(SO_3F)_3$ (the weight of the product was slightly lower than expected for $Ir(SO_3F)_4$ also). More $S_2O_6F_2$ (~2 mL) was added to the impure product which was heated at ~60°C for another 6 hours. The removal of all excess $S_2O_6F_2$ (and traces of $S_2O_5F_2$ and oxygen) at room temperature yielded pure $Ir(SO_3F)_4$ (607 mg, 1.032 mmol).

$Ir(SO_3F)_4$ is a deep brown, almost black, hygroscopic solid which is very soluble in HSO_3F. It decomposes into $Ir(SO_3F)_3$ according to equation (6.2) at ~100°C in vacuo but is stable up ~150°C in an atmosphere of N_2.

Analysis	Ir	S	F
Calculated %	32.66	21.80	12.92
Found %	32.50	21.60	12.69

6.B.3 SYNTHESIS OF $[Ir(SO_3F)_6]^{2-}$ COMPLEXES

6.B.3.1 PREPARATION OF $(ClO_2)_2[Ir(SO_3F)_6]$

$$2ClO_2SO_3F + Ir + 2S_2O_6F_2 \xrightarrow{HSO_3F} (ClO_2)_2[Ir(SO_3F)_6] \qquad (6.4)$$

A mixture of ClO_2SO_3F (~1 mL), and $S_2O_6F_2/HSO_3F$ (~6 mL) was allowed to react with iridium metal (289 mg, 1.505 mmol) at ~120°C for 3 days. All the metal by that time had dissolved and the solution took on a dark brown color. The removal of all volatile materials at ~70°C yielded a compound which analyzed as $(ClO_2)_2$-$[Ir(SO_3F)_6]$ (1.362 g, 1.478 mmol).

$(ClO_2)_2[Ir(SO_3F)_6]$ can also be prepared by:

a) replacing ClO_2SO_3F with $ClSO_3F$ in equation (6.4) and performing the reaction under the same conditions, or

b) a reaction between $IrCl_3$ and $S_2O_6F_2/HSO_3F$ at ~120°C for 4 days.

In both these alternative synthetic routes, the required ClO_2SO_3F is generated by an attack of $ClSO_3F$ (formed from the reaction of $IrCl_3$ with $S_2O_6F_2$ in (b)) on the glass reactor.

$(ClO_2)_2[Ir(SO_3F)_6]$ is a dark orange-brown, hygroscopic solid. It is soluble in HSO_3F and melts with decomposition at ~190°C to form a dark brown liquid.

Analysis	Cl	Ir	F
Calculated %	7.69	20.86	12.37
Found %	7.51	21.04	12.44

6.B.3.2 PREPARATION OF $Cs_2[Ir(SO_3F)_6]$

$$CsCl + HSO_3F \longrightarrow CsCl + HCl \quad (6.5)$$

$$2CsSO_3F + Ir + 2S_2O_6F_2 \xrightarrow{HSO_3F} Cs_2[Ir(SO_3F)_6] \quad (6.6)$$

$Cs_2[Ir(SO_3F)_6]$ was prepared by the oxidation of iridium metal (398 mg, 2.071 mmol) with $S_2O_6F_2/HSO_3F$ (~10 mL) in the presence of CsCl (798 mg, 4.146 mmol) at ~150°C for 10 days. The removal of all volatile materials at ~70°C yielded a product with a weight corresponding to that expected for $Cs_2[Ir(SO_3F)_6]$, (2.121 g, 2.015 mmol).

$Cs_2[Ir(SO_3F)_6]$ is a pale orange, hygroscopic solid. It is soluble in HSO_3F and melts with decomposition at ~150°C.

6.B.3.3 PREPARATION OF $Ba[Ir(SO_3F)_6]$

$$BaCl_2 + 2HSO_3F \longrightarrow Ba(SO_3F)_2 \quad (6.7)$$

$$Ba(SO_3F)_2 + Ir + 2S_2O_6F_2 \xrightarrow{HSO_3F} Ba[Ir(SO_3F)_6] \quad (6.8)$$

A mixture of dried $BaCl_2$ (198 mg, 0.951 mmol) and iridium metal (183 mg, 0.952 mmol) was reacted with $S_2O_6F_2/HSO_3F$ (~10 mL) at ~100°C for 2 weeks and, after replenishing the largely decomposed $S_2O_6F_2$, at ~160°C for another 2 weeks. The removal of all volatile materials at ~70°C yielded a product with a weight suggesting the composition of $Ba[Ir(SO_3F)_6]$ (788 mg, 0.853 mmol). The low yield is due to the visually evident etching of the glass reactor by the solution.

$Ba[Ir(SO_3F)_6]$ is a light orange, hygroscopic solid. It appears to be almost insoluble in HSO_3F, and decomposes at ~200°C.

6.C DISCUSSION

6.C.1 SYNTHESIS AND GENERAL DISCUSSION

6.C.1.1 BINARY FLUOROSULFATES

Iridium was found to be much less reactive than platinum towards fluorosulfonation, whether the starting material is the metal itself or $IrCl_3$. Although, as pointed out in previous chapters, these noble metal chlorides are not susceptible to displacement reactions in HSO_3F, they are usually quite reactive towards $S_2O_6F_2/HSO_3F$.

All the preparative reactions described could take up to 1 month for completion, while some had actually been aborted eventually. The preparation of the binary fluorosulfates has one of the most serious difficulties that a synthetic reaction could encounter —— the decomposition of both the reactant ($S_2O_6F_2$) and the product ($Ir(SO_3F)_4$). Since $S_2O_6F_2$ is not known to decompose into $S_2O_5F_2$ and O_2 at a temperature of only ~120°C, the path that it takes must be via $Ir(SO_3F)_4$, in a catalytic manner. A higher reaction temperature was not feasible since it was found that the decomposition took place much faster than the conversion of the metal to either Ir(III) or Ir(IV). The $S_2O_5F_2$ formed, identified by i.r. spectroscopy, had to be removed before the $S_2O_6F_2$ could be replenished because its presence would reduce the ionizing ability of the solvent. Because of the extremely dark colors of the solutions, the addition of the oxidant was usually repeated

at least twice after all the metal had reacted, to ensure a complete reaction.

The decomposition of $Ir(SO_3F)_4$ to form $S_2O_5F_2$ and oxygen is unlike that found for $Pd_2(SO_3F)_6$, $Au(SO_3F)_3$ or $Pt(SO_3F)_4$. While the latter two compounds break down completely to form SO_2F_2, the decomposition of palladium tris(fluorosulfate) giving $S_2O_6F_2$ has been used as an evidence for Pd(IV)'s strong oxidizing ability. It therefore appears that Ir(IV) is not a very strong oxidizing agent. Although the compound is not very thermally stable, it is one of the few examples of binary Ir(IV) compounds, another example of which is IrO_2 [199].

6.C.1.2 $[Ir(SO_3F)_6]^{2-}$ COMPLEXES

As with the synthesis of the binary fluorosulfates of iridium, these reactions are very time consuming. Although the thermal stability of the anionic Ir(IV) complexes appears to be greater than that of $Ir(SO_3F)_4$, the formation of the complexes, for some inexplicable reasons, is very slow. An attempt to synthesize $Na_2[Ir(SO_3F)_6]$ was terminated after six months, at which time the reactor had become badly etched. The above reaction was actually thought to proceed quickly by the following reasonings.

a) The decomposition of $[Ir(SO_3F)_6]^{2-}$ is faster when it is solvated, and for the almost insoluble $Ba[Ir(SO_3F)_6]$, a higher reaction temperature of ~160°C could be used, but, because of the insolubility of the product, the reaction

proceeded slowly.

b) An inspection of the solubility of the various alkali metal hexachloroplatinates(IV) reveals that $Na_2[PtCl_6]$ has a very low solubility and $Na_2[Ir(SO_3F)_6]$ may be expected to behave similarly. This was later found to be the case during the course of the reaction, but the formation of the complex was exceedingly slow, and it more than compensated for the presumably slower decomposition of the product.

6.C.2 VIBRATIONAL SPECTRA

For both the binary fluorosulfates, vibrational spectroscopy had been of very limited help in their investigation. Being deeply colored compounds, no Raman spectra could be obtained, even at ~80 K. The i.r. spectra obtained were of extremely poor resolution. Using a variety of mulling agents such as fluorolube oil, hexachlorobutadiene and silicone oil, separate regions of the spectrum could be 'pieced' together for $Ir(SO_3F)_3$. The i.r. frequencies of $Ir(SO_3F)_3$ and $Ir(SO_3F)_4$ are listed in Table 6.1 and compared to those of $Pt(SO_3F)_4$. All three spectra are very similar, especially in the region of ~800 - 1200 cm^{-1}, where the large number of bands probably leads to overlaps and thus the observed unresolvability. This suggests that the two iridium

TABLE 6.1 i.r. FREQUENCIES OF $Ir(SO_3F)_3$ AND $Ir(SO_3F)_4$

$Ir(SO_3F)_3$	$Ir(SO_3F)_4$	$Pt(SO_3F)_4$
1400 s	1390 s	~1400 vs,b
1210 s	1210 s	~1225 vs
		~1150 s,vb
1100 vs,	1070 s,sh	~1070 vs,vb
1020 vs,sh	1020 s,b	~1000 vs,vb
950 s,vb		~900 vs,vb
	870 s,b	
800 s,vb	820 s,b	~820 s,vb
		~670 s,b
630 s	640 m,b	~640 s,b
575	580 m	580 s
540	540 m	540 m
450		

fluorosulfates are extensively SO_3F-bridged species. Because of the increased complexity of the i.r. spectrum of $Ir(SO_3F)_3$ over that of $Au(SO_3F)_3$, the former may not be square planar, but rather octahedral. This may be resolved with the synthesis of anionic complexes of either $[Ir(SO_3F)_4]^-$ or $[Ir(SO_3F)_6]^{3-}$, although this was not persued. In the halide system, the trihalides contain octahedrally coordinated Ir(III) with, as expected, a low spin d^6 electronic configuration.

For the $[Ir(SO_3F)_6]^{2-}$ complexes, i.r. spectra of reasonable resolution could be obtained, but due to the samples' deep yellow color, Raman spectra of only relatively poor quality was recorded at ~80 K. The vibrational frequencies of these compounds are listed in Table 6.2 in comparison with the Raman frequencies of $Cs_2[Pt(SO_3F)_6]$. The three iridium complexes all have spectra that are similar to that of $Cs_2[Pt(SO_3F)_6]$, suggesting a similar type of metal-ligand interaction and a monodentate coordination of the SO_3F groups. The positions of the three vibrational modes of ClO_2^+ at (1310, 1295), 1060 and 522 cm^{-1} in the i.r. spectrum also indicate an ionic formulation for the compound can be made.

In summary, it appears that all the iridium species involved in this study have octahedral coordination for iridium, with bidentate SO_3F groups evident for the two binary fluorosulfates.

TABLE 6.2 VIBRATIONAL FREQUENCIES OF $[Ir(SO_3F)_6]^{2-}$

$(C\ell O_2)_2[Ir(SO_3F)_6]$		$Cs_2[Ir(SO_3F)_6]$		$Ba[Ir(SO_3F)_6]$	$Cs_2[Pt(SO_3F)_6]$
IR	R†	IR	R	IR	R
1400s,b	1400,1380w	1390sb	1415w	1390s	1416w,sh
					1410m
1310s*					
1295s*					
	1250vs		1255m		1250vs
1200s	1200w	1195s,b	1212w	1200s	1219m
1050w*	1047*				
			1057m		1043s
950vs,vb		950vs,b	978w	950s,b	1010m
		920vs,b	950w	900s,b	
820s	840,810w	~800s,b	~802w,b	820s	~800w,b
660s	640w	645m	630w	630w	634vs
590s	580w	570s	575w	575m	579vw
550s	548w	540s	550w	540m	550vw
522m*	520w*				
	460w	460vw		460w,sh	
	443w	440m	440vw	447m	440m
	286m		287w		280vs
	268m				

*denotes bands due to $C\ell O_2^+$

†obtained at ~80K

6.C.3 MAGNETIC SUSCEPTIBILITY

According to Figgis, the magnetic susceptibility of Ir(IV), a d^5 low spin system with a $^2T_{2g}$ electronic ground state can be represented by the following equation [141]:

$$\mu^2 = \frac{8 + (3x - 8)\exp(-3x/2)}{x[2 + \exp(-3x/2)]} \qquad (6.9)$$

where $x = \lambda/kT$

$\lambda = -\xi = -5000\ cm^{-1}$ for Ir(IV) [196]

k = Boltzmann's constant = $0.6950\ cm^{-1}$

Therefore, as $x \rightarrow -\infty$ (for large $|\lambda|$ or low temperature), $\mu \rightarrow \sqrt{3}$, and as $x \rightarrow 0$, $\mu \rightarrow \sqrt{5}$. In the temperature range accessible in this study (~100 - 330 K), μ should have values from 1.76 μ_B at 100 K to 1.84 μ_B at 330 K. For the hexachloro- and hexabromo-complexes of Ir(IV), μ_{eff} was found to generally decrease with temperature, but in most cases they were lower than $\sqrt{3}$, the minimum value predicted by equation (6.9). The moments also showed marked drops at temperatures below ~150 K to ~1.3 μ_B; this had been attributed to antiferromagnetic couplings in the system [197].

The magnetic susceptibility results on $(ClO_2)_2[Ir(SO_3F)_6]$, $Cs_2[Ir(SO_3F)_6]$ and $Ir(SO_3F)_4$ are listed in Tables 6.3 to 6.5, respectively. The temperature dependence of their μ_{eff} is shown in Fig 6.1.

In all three cases, the observed magnetic moments are lower than the expected values (the estimated uncertainty in μ is about $\pm 0.02\ \mu_B$, contributions from temperature and weighing errors considered). μ_{eff} ranges from 1.55 to 1.71 μ_B for $Cs_2[Ir(SO_3F)_6]$,

TABLE 6.3 MAGNETIC PROPERTIES OF $(ClO_2)_2[Ir(SO_3F)_6]$

T	χ_m^c	$1/\chi_m^c$	$1/\chi_m^c$ (calc'd)	μ_{eff}	μ_{eff} (calc'd)
78	4.348×10^{-3}	230	234	1.64	1.63
108	3.236×10^{-3}	309	314	1.67	1.66
130	2.653×10^{-3}	377	371	1.66	1.67
155	2.294×10^{-3}	436	436	1.68	1.68
178	2.000×10^{-3}	500	498	1.69	1.69
203	1.770×10^{-3}	565	563	1.70	1.70
227	1.585×10^{-3}	631	626	1.70	1.70
251	1.447×10^{-3}	691	689	1.70	1.71
276	1.326×10^{-3}	754	755	1.71	1.71
300	1.238×10^{-3}	808	816	1.72	1.71
K	cgs	cgs	cgs	μ_B	μ_B units

$$1/\chi_m^c \text{ (calc'd)} = (T + 12)/0.382$$

TABLE 6.4 MAGNETIC PROPERTIES OF $Cs_2[Ir(SO_3F)_6]$

T	χ_m^c	$1/\chi_m^c$	$1/\chi_m^c$ (calc)	μ_{eff}	μ_{eff} (calc)
78	3.831×10^{-3}	261	269	1.55	1.52
106	3.003×10^{-3}	333	339	1.59	1.58
129	2.494×10^{-3}	401	399	1.60	1.61
154	2.141×10^{-3}	467	462	1.62	1.63
179	1.880×10^{-3}	532	524	1.64	1.65
203	1.681×10^{-3}	595	586	1.65	1.66
229	1.536×10^{-3}	651	651	1.68	1.68
252	1.410×10^{-3}	709	709	1.68	1.68
277	1.290×10^{-3}	775	773	1.69	1.69
302	1.214×10^{-3}	824	836	1.71	1.70
K	cgs	cgs	cgs	μ_B	μ_B units

$$1/\chi_m^c \text{ (calc)} = (T + 28)/0.395$$

TABLE 6.5 MAGNETIC PROPERTIES OF $Ir(SO_3F)_4$

T	χ_m^c	$1/\chi_m^c$	$1/\chi_m^c$ (calc)	μ_{eff}	μ_{eff} (calc)
284	9.06×10^{-4}	1104	1155	1.43	1.40
254	9.63×10^{-4}	1039	1040	1.40	1.40
230	1.028×10^{-3}	972.9	948.9	1.38	1.39
205	1.102×10^{-3}	907.7	853.5	1.34	1.39
177	1.320×10^{-3}	757.5	746.7	1.37	1.38
154	1.556×10^{-3}	642.8	659.0	1.38	1.37
130	1.758×10^{-3}	569.1	567.5	1.35	1.35
107	2.044×10^{-3}	489.3	479.8	1.32	1.34
78	2.963×10^{-3}	337.5	369.1	1.36	1.30
K	cgs	cgs	cgs	μ_B	μ_B

$1/\chi_m^c$ (calc) = (T + 19)/0.262

FIG 6.1 MAGNETIC MOMENTS OF $(ClO_2)_2[Ir(SO_3F)_6]$ AND $Cs_2[Ir(SO_3F)_6]$

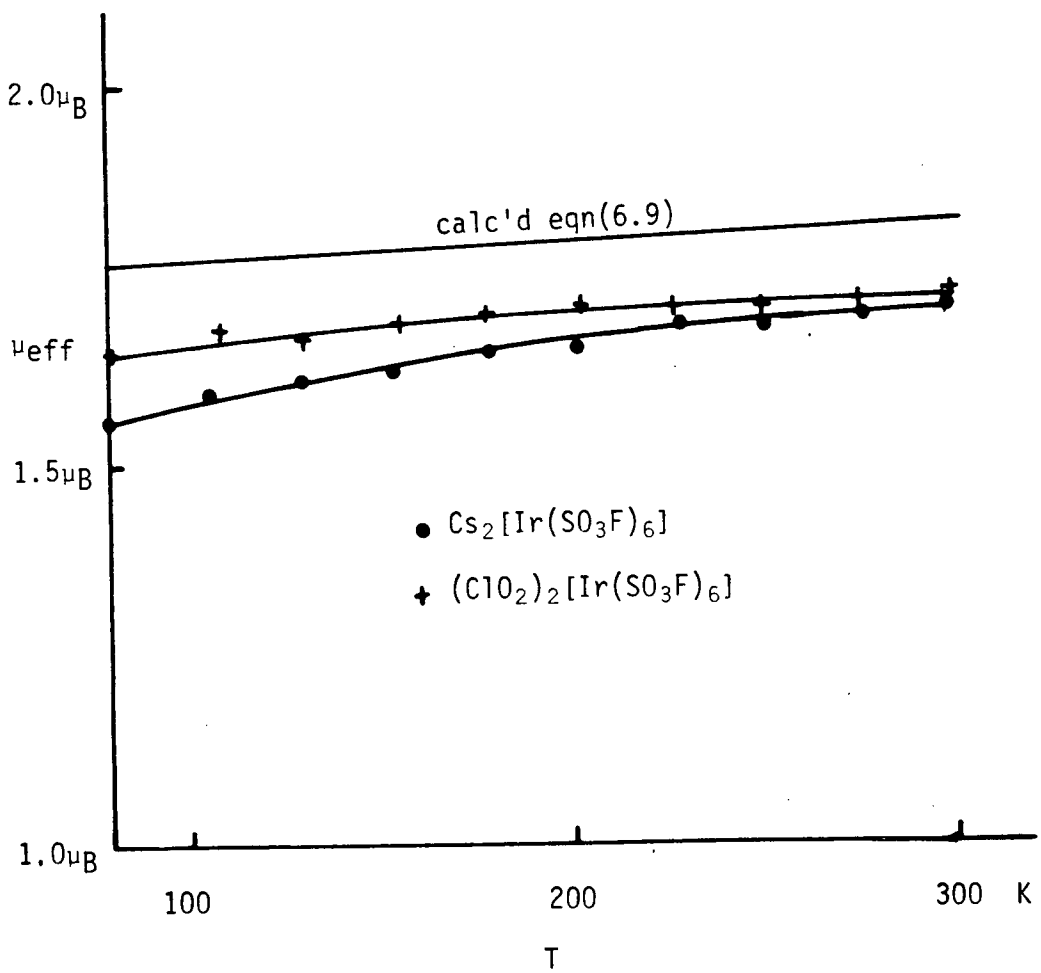

1.64 to 1.72 μ_B for $(ClO_2)_2[Ir(SO_3F)_6]$ and 1.32 to 1.43 μ_B for $Ir(SO_3F)_4$. At high temperature, the moments remain relatively constant and appear to obey the Curie-Weiss Law. This suggests either the presence of antiferromagnetic coupling in these systems, or perhaps, a slight departure of the coordination sphere around Ir(IV) from cubic symmetry.

Jahn-Teller distortion in a low-spin d^5 system is predicted from theory, and results in an axial elongation of the coordination sphere. However, since the splitting occurs in the orbitals not directly facing the ligands, a distortion of this type is usually very small compared to that present in species such as Cu^{2+}, d^9, which can give rise to severe axial elongations leading to the formation of square planar complexes. For Ti^{3+}, d^1, which has a $^2T_{2g}$ electronic ground state but with a positive spin-orbital coupling constant, λ, (resulting in a drop of μ_{eff} from $\sqrt{5}$ as $x \rightarrow 0$ to zero as $x \rightarrow \infty$, i.e., a larger range of variation in the moment as compared to a d^5 system), the magnetic behavior of $CsTi(SO_4)\cdot 12H_2O$ has been interpreted in terms of a large distortion of about 3.6 times the magnitude of the spin-orbital coupling [141]. Because the effect of low symmetry on the magnetic moment of a compound is inversely proportional to λ, the spin orbital coupling constant, Jahn-Teller distortion may not be explicit in Ir(IV), which has a λ_o value almost 33 times that of Ti(III). In any case, a distortion would lead to an increase of the magnetic moment, at the temperature of this study, to about

1.8 μ_B, and this is certainly not observed here. Besides, the vibrational spectra do not offer any suggestion that a large distortion from O_h symmetry occurs. Therefore, it must be concluded that Jahn-Teller distortion, although it should be present in the iridium compounds studied here, does not appear to contribute to the observed lowering of the magnetic moment to below 1.73 μ_B.

The other likely alternative —— antiferromagnetic coupling, was therefore investigated. As the vibrational spectra of the $[Ir(SO_3F)_6]^{2-}$- and $[Pt(SO_3F)_6]^{2-}$- complexes show great similarities, and it is not really expected that they would be structurally very different, a dilution experiment involving a mixture of $(ClO_2)_2[M(SO_3F)_6]$, M=Ir, Pt, was undertaken.

Starting with a mixture of metal powders containing 8.85 mole % of iridium, the mixed chloronium salt was prepared by reacting the metals with ClO_2SO_2F and $S_2O_6F_2/HSO_3F$. The resulting product corresponded to the expected weight and had the appearance of $(ClO_2)_2[Pt(SO_3F)_6]$. The result of a bulk magnetic susceptibility measurement on the mixture is listed in Table 6.6 and shown in Fig 6.2.

The ClO_2-containing complexes were used because, in the case of $[Ir(SO_3F)_6]^{2-}$, it is the only iridium complex that can be prepared comparatively easily. The presence of an excess reactant —— ClO_2SO_3F, also ensure the formation of a product of high purity. The diamagnetic correction of $(250\pm15)\times10^{-6}$ cgs units, obtained for $(ClO_2)_2[Pt(SO_3F)_6]$ over a temperature range of 81 to

Table 6.6 MAGNETIC PROPERTIES OF $(ClO_2)_2[Ir(SO_3F)_6]$ DILUTED IN $(ClO_2)_2[Pt(SO_3F)_6]$ (8.85 mol% Ir)

T	χ_m^c	$1/\chi_m^c$	$1/\chi_m^c$ (calc)	μ_{eff}	μ_{eff} (calc)	
303	1.506	664	728	1.91	1.82	
277	1.515	660	675	1.83	1.81	
251	1.435	697	621	1.70	1.80	
229	1.616	619	575	1.72	1.78	
204	1.911	523	523	1.77	1.76	
179	2.201	454	472	1.78	1.74	
154	2.416	414	420	1.73	1.71	
129	2.745	364	369	1.68	1.67	
106	3.073	325	320	1.61	1.62	
78	4.049	247	263	1.59	1.54	
K	10^{-3}cgs	cgs	cgs	μ_B	μ_B	UNITS

$1/\chi_m^c(calc) = (T + 49)/0.484$

FIG 6.2 MAGNETIC MOMENT OF $(ClO_2)_2[Ir(SO_3F)_6]$ DILUTED IN $(ClO_2)_2[Pt(SO_3F)_6]$ (8.85 mol% Ir)

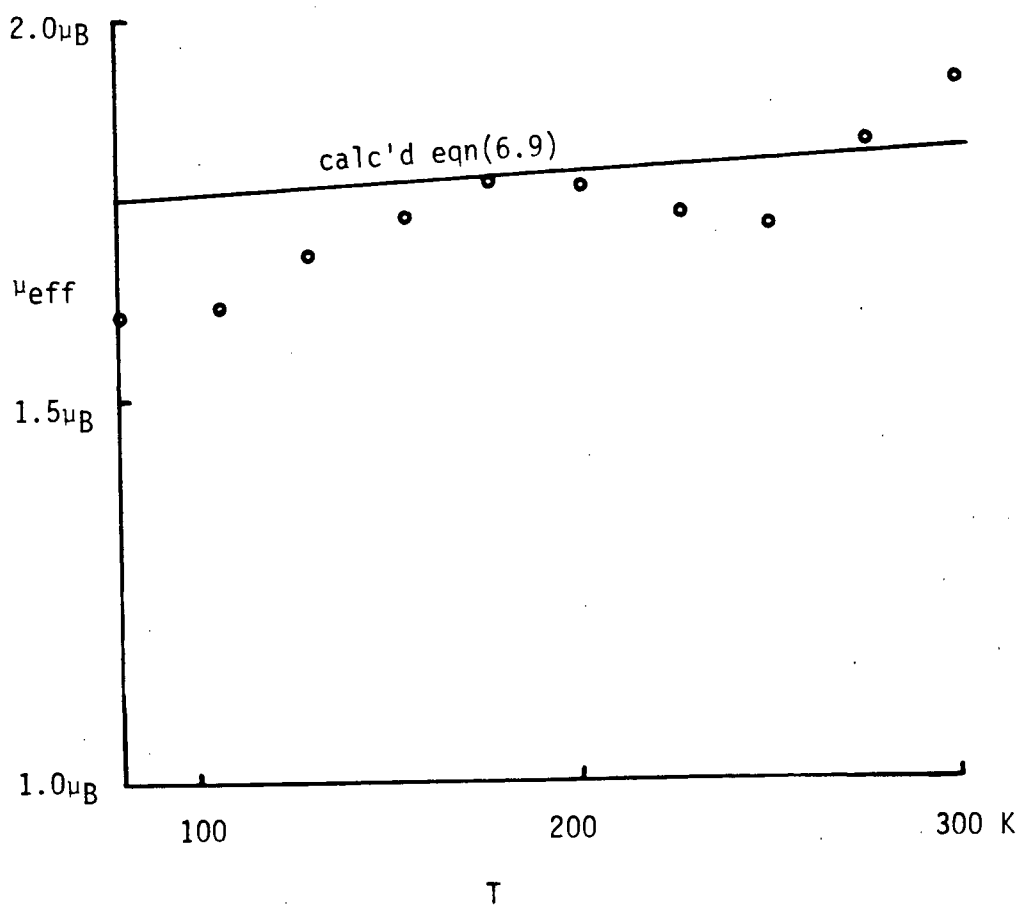

300 K, was used for both the complexes. Any Temperature Independent Paramagnetism present in these systems, estimated to be of the order of only 50×10^{-6} cgs units [141], should be compensated for by this procedure.

Although the accuracy of the measurements is greatly reduced by the introduction of $(ClO_2)_2[Pt(SO_3F)_6]$, a diamagnetic species, as the majority constituent (the estimated uncertainty, arising mainly from weight measurements, ranges from ±0.12 μ_B at ~300 K to ±0.05 μ_B at ~80 K), it can be seen that the μ_{eff} obtained agree quite well with those calculated from equation (6.9), and in general, are consistently higher than those of pure $(ClO_2)_2$-$[Ir(SO_3F)_6]$. This shows that antiferromagnetic coupling does occur in the Ir(IV) fluorosulfate system, and is the most likely cause contributing to a lowering of μ_{eff} in these compounds. A similar explanation has been invoked for the hexahalo-complexes of Ir(IV), although in this latter class of compounds, a much more extensive coupling must be present as their magnetic moments are much lower than what is found here. This is consistent with the conclusion arrived at in Chapter 3 on the paramagnetic Pd(II) compounds that SO_3F is a much poorer medium for the superexchange to occur than monatomic ligands such as the halide ions.

For $Ir(SO_3F)_3$, diamagnetism is observed, with χ_m of $-(80\pm30)$ $\times10^{-6}$ cgs units, compared to a sum of diamagnetic correction of -154×10^{-6} cgs units. It therefore appears that Ir(III) in the fluorosulfate is a spin-paired, d^8 system, not surprising in

view of the high 10 D_q expected for a 5d metal in the +3 oxidation state. The coordination for Ir(III) in $Ir(SO_3F)_3$ can either be octahedral or square planar in order to explain the diamagnetism, but there appears to be no reason why a square planar geometry should prevail over an octahedral one for a d^6 system, unless by stereochemical restrictions which should not be present here. Therefore, the ligand configuration for $Ir(SO_3F)_3$ is most likely octahedral, or conversely, all fluorosulfate groups present in the compound must be bidentate, leading to the great complexity observed in the S-O stretching region in the i.r. spectrum.

6.C.4 SOLUTION STUDIES IN HSO_3F

6.C.4.1 CONDUCTIVITY MEASUREMENTS

Iridium-fluorosulfate was not intended to be investigated for its possible use as a superacid system in HSO_3F, although there exist indications that it may be one, at least for $Ir(SO_3F)_4$.

The conductivity measurements of solutions of $(ClO_2)_2[Ir(SO_3F)_6]$ in HSO_3F were undertaken to further establish its similarity to the corresponding platinum complex, and to provide evidence for the existence of $[Ir(SO_3F)_6]^{2-}$-containing species in solution. The results are shown in Fig 6.3 and listed in Table 6.7. From

FIG 6.3 CONDUCTIVITY OF $(ClO_2)_2[Ir(SO_3F)_6]$ IN HSO_3F

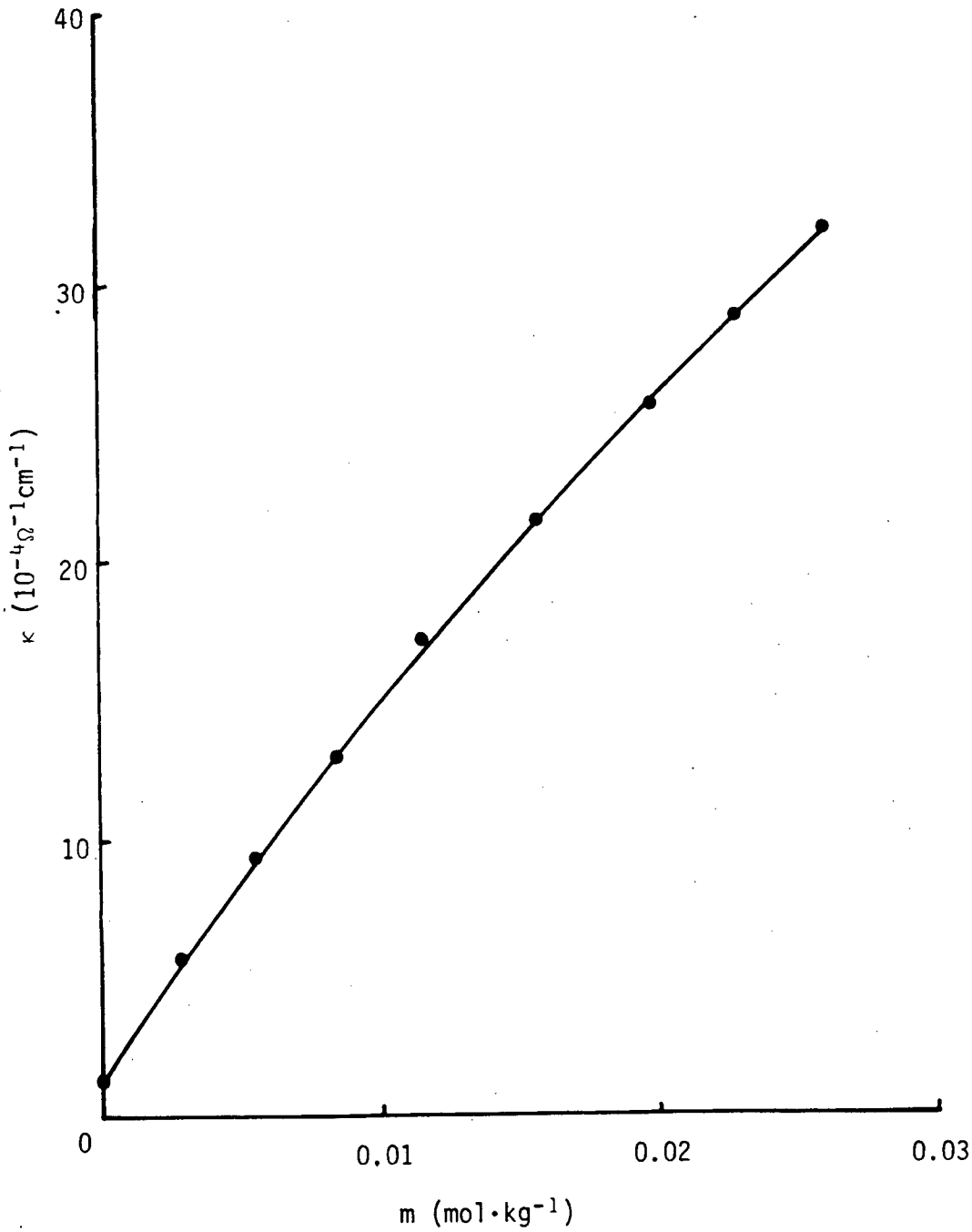

TABLE 6.7 CONDUCTIVITY OF $(C\ell O_2)_2[Ir(SO_3F)_6]$ IN HSO_3F*

m	κ
0.00	0.280
0.20	3.801
0.40	7.581
0.60	9.885
0.80	12.20
1.00	14.92
1.20	17.56
1.40	19.60
1.60	21.50
1.80	23.60
2.00	25.63
2.20	27.49
2.40	30.06
2.60	32.22
10^{-2}mol.kg^{-1}	$10^{-4}\Omega^{-1}$cm^{-1} unit

* interpolated

the plot, it becomes evident that the ionization of $(ClO_2)_2[Ir(SO_3F)_6]$ in HSO_3F is very similar to that of the other $[M(SO_3F)_6]^{2-}$ complexes, M=Pd, Pt, Ir, Sn, and a similar solution behavior must be present for all these solutes, i.e., $[Ir(SO_3F)_6]^{2-}$ undergoes a basic dissociation in HSO_3F according to:

$$[Ir(SO_3F)_6]^{2-} + HSO_3F \rightleftharpoons H[Ir(SO_3F)_6]^{-} + SO_3F^{-} \quad , \qquad (6.10)$$

with an equilibrium constant of the order of 10^{-3}, by comparison with the conductivity of the other hexafluorosulfato-complexes, described in detail in Chapters 5 and 9.

6.C.4.2 ELECTRONIC SOLUTION SPECTRA

All the compounds, with the exception of the insoluble $Ba[Ir(SO_3F)_6]$, form deeply colored solutions in HSO_3F. $Ir(SO_3F)_3$ dissolves to form a bluish purple solution with an absorption maximum at 563 nm, $\varepsilon \sim 1\times10^4$ $M^{-1}cm^{-1}$. Both $Ir(SO_3F)_4$ and $(ClO_2)_2[Ir(SO_3F)_6]$, although they are differently colored in the solid state, form solutions with an identical λ_{max} at 200 nm, $\varepsilon \sim 1\times10^4$ $M^{-1}cm^{-1}$, suggesting the presence of similar species in solution. The high ε values imply that these absorptions must be due to charge transfer, most likely from L $\longrightarrow$ M.

6.D CONCLUSION

The Ir(IV)-fluorosulfate system has been shown to be a paramagnetic analogue of the Pt(IV)-fluorosulfate system, although no attempts were made to test the iridium fluorosulfates' possible acidity in HSO_3F. The d^5 low-spin electronic configuration of Ir(IV) resulted in some very interesting magnetic properties. From a dilution experiment involving the presumably isomorphous compounds of $(ClO_2)_2[M(SO_3F)_6]$, M=Ir, Pt, antiferromagnetic exchange has been shown to be present in $(ClO_2)_2[Ir(SO_3F)_6]$, although to a lesser extent than in the halide system. The contention that the superexchange mechanism cannot operate effectively through a fluorosulfate ligand, first suggested in the Pd(II)-fluorosulfate system, is supported by the results here.

$Ir(SO_3F)_3$ is diamagnetic, and therefore, most likely octahedral. This system was not investigated in much detail as it was not the original intention of studying iridium chemistry.

CHAPTER 7 MOLYDENUM(VI)-FLUOROSULFATE

7.A INTRODUCTION

The investigation into the molydenum-fluorosulfate system is guided mostly by interests on synthetic and structural aspects. For a binary or ternary metal fluorosulfate, all previous work indicates that the highest oxidation state obtainable by the metal appears to be +4, although the coordination sphere around the central metal ion may be octahedral. This may be due to the limited oxidizing power of $S_2O_6F_2$, the strongest oxidant in the fluorosulfate system, or due to the steric crowding in the coordination sphere if a highly charged M(V) or M(VI) species is present.

For molydenum, as well as tungsten, the +6 oxidation state is readily attainable, even when relatively weak oxidizing agents are used [140]. Mo(VI) and W(VI) are found in binary halides, MX_6, and their complexes, as well as in oxyhalides mainly of the two types MOX_4 and MO_2X_2, with X=F and Cl. With the possible exception of MoO_2F_2 and MF_8^{2-}, which are octa-coordinated, and MF_7^-, which is seven-coordinated, these compounds have octahedral structures. In most of the oxyhalides, an octahedral geometry is obtained by using bridging oxygen to form highly polymerized compounds, whereas $MoOF_4$ and WOF_4 appear to have bridging fluorine [200-204].

Complexes containing terminal M=O bonds generally show

strong Raman and i.r. absorptions in the region of 900-1100 cm^{-1}, which can be assigned to metal oxygen stretching [200,205,206]. With the absence of detailed crystallographic data, vibrational spectra of the oxyhalides have been used frequently to elucidate structures. The substitution of a fluorosulfate group for a halide ligand in the oxyhalides introduces a potential bridging group and diminishes the importance of oxygen bridging. The reason for this expectation is the larger SO_3F ligand would increase the distance between intermolecular M=O groups and make bridging via the smaller oxygen atoms more difficult. Vibrational spectroscopy should be very helpful in this case because ν M-O is readily detected and the conformation of the SO_3F group is also evident from vibrational spectroscopy.

Previously published work in this area is represented by the synthesis of $WO(SO_3F)_4$ and a report on its ^{19}F-n.m.r. and Raman spectra [211]. The compound is a clear liquid at room temperature and appears to be polymeric with both bridging and terminal SO_3F groups; bands at ~960 cm^{-1} in its Raman spectrum has been assigned to the terminal W=O stretch. The reaction of Mo or $Mo(CO)_6$ with $S_2O_6F_2$ is reported to give rise to two products: $MoO_2(SO_3F)_2$, a white solid, and a red liquid that analyzed as $MoO(SO_3F)_2$ [90]. Since the chemistries of Mo(VI) and W(VI) are very similar, it was decided to characterize the two previously reported molydenum oxyfluorosulfates and to attempt complex formation reactions on these compounds.

7.B EXPERIMENTAL

7.B.1 PREPARATION OF $MoO_2(SO_3F)_2$

$$Mo + xsS_2O_6F_2 \longrightarrow MoO_2(SO_3F)_2 + MoO(SO_3F)_4 + S_2O_5F_2 \qquad (7.1)$$

$MoO_2(SO_3F)_2$ was prepared by a method based on the original synthesis described by Shreeve and Cady. Molydenum metal (~0.5 g) was allowed to react with an excess of $S_2O_6F_2$ (~5 mL) in the temperature range from ~25 to ~70°C, resulting in the formation of a white solid and a red liquid. The mixture was vacuum filtered and washed with $S_2O_6F_2$. The removal of all volatile materials from the solid residue yielded $MoO_2(SO_3F)_2$.

$MoO_2(SO_3F)_2$ is an extremely hygroscopic white solid which decomposes at ~230°C into a blue solid.

Analysis	Mo
Calculated %	29.42
Found %	29.55

$MoO_2(SO_3F)_2$ can also be conveniently prepared by reacting Mo metal with $ClSO_3F$ in a quartz reactor at ~40°C. In a typical reaction, Mo metal powder (386 mg, 4.02 mmol) was reacted with $ClSO_3F$ (~4 mL) for 2 weeks, giving $MoO_2(SO_3F)_2$ (1.315 g, 4.03 mmol) without contamination from $MoO(SO_3F)_4$.

$$Mo + 6ClSO_3F \longrightarrow MoO_2(SO_3F)_2 + 2S_2O_6F_2 + 3Cl_2 \ . \qquad (7.2)$$

$S_2O_6F_2$ was detected by its i.r. spectrum.

7.B.2 PREPARATION OF $MoO(SO_3F)_4$

The red filtrate from the reaction of Mo with $S_2O_6F_2$ was subjected to a dynamic vacuum with the sample held at ~40°C. After 12 hours, an orange-red liquid of very high viscosity was obtained. The sample analyzed as $MoO(SO_3F)_4$.

$MoO(SO_3F)_4$ appears to show a large range of miscibility with $S_2O_6F_2$ at room temperature. Upon heating at ~100°C, $MoO(SO_3F)_4$ decomposes according to:

$$MoO(SO_3F)_4 \longrightarrow MoO_2(SO_3F)_2 + S_2O_5F_2 \quad , \tag{7.3}$$

with $S_2O_5F_2$ detected by its i.r. spectrum.

Analysis	Mo	S	F
Calculated %	18.88	25.24	14.95
Found %	19.13	24.82	15.13

7.C DISCUSSION

7.C.1 SYNTHESIS AND GENERAL DISCUSSION

The reaction of molydenum metal with $S_2O_6F_2$ resulted in the formation of two Mo(VI)-containing compounds — a white solid, and a red liquid which analyzed as $MoO(SO_3F)_4$, instead of the previously reported Mo(IV)-containing species. Different ratios of the two oxyfluorosulfates seem to be obtainable under different reaction temperatures. If the reaction is performed at room temperature, most of the product is $MoO(SO_3F)_4$, but if the reaction temperature is raised to ~70°C, $MoO_2(SO_3F)_2$ is the main product. Furthermore, the thermal decomposition of $MoO(SO_3F)_4$ giving $MoO_2(SO_3F)_2$, although this does not constitute a viable synthetic route, because of relatively high volatility of $MoO(SO_3F)_4$, also suggests a similar thermal stability trend. A scheme of formation of the two compounds, consistent with the above observations, may be presented:

$$Mo + 3S_2O_6F_2 \longrightarrow \text{'}Mo(SO_3F)_6\text{'} \qquad (7.4)$$

$$\text{'}Mo(SO_3F)_6\text{'} \longrightarrow MoO(SO_3F)_4 + S_2O_5F_2 \qquad (7.5)$$

$$MoO(SO_3F)_4 \longrightarrow MoO_2(SO_3F)_2 + S_2O_5F_2 \ . \qquad (7.6)$$

The formation of molydenum hexakis(fluorosulfate) as the initial oxidation product is followed by the elimination of $S_2O_5F_2$, giving the two oxyfluorosulfates. The energetically favorable formation of a Mo=O bond, coupled with the resulting reduction in the steric crowding around Mo(VI),are most likely the contributing factors. This is also consistent with the general reaction

chemistry of $S_2O_6F_2$, where the initial reaction of $\cdot OSO_2F$ radicals leads to the formation of a fluorosulfate. The ability of molybdenum to form Mo=O bonds with p_π-d_π donation from filled oxygen orbitals probably promotes the decomposition.

Whereas $WO(SO_3F)_4$ was reported to be obtainable by the reaction of the metal with $S_2O_6F_2$ at ~100°C, it appeared to be the sole product [27]. When the synthesis was repeated in this study, the removal of all volatile materials yielded a small amount of white precipitate. This could possibly be $WO_2(SO_3F)_2$, but no attempts were made to identify this solid or to increase its yield.

In order to test the complex formation ability of the Mo(VI)-oxyfluorosulfate, a slight excess of ClO_2SO_3F was added to a mixture of $MoO_2(SO_3F)_2$ and $MoO(SO_3F)_4$ in $S_2O_6F_2$. The removal of all volatile materials at ~50°C did not lead to any weight increase and therefore, no complex formation was evident. If a complex was formed, it must have been of a rather low thermal stability.

7.C.2 VIBRATIONAL SPECTRA

7.C.2.1 $MoO_2(SO_3F)_2$

The vibrational spectra of $MoO_2(SO_3F)_2$ show a distinct pair of sharp peaks at ~994 and 955 cm^{-1}, with inverted intensities in the Raman and i.r.. These vibrations are assigned to stretching

vibrations of the O=M=O group, and their positions compare well with those found for liquid or gaseous MoO_2Cl_2, in which terminal Mo=O bonds have been postulated [200]. Therefore, it appears that terminal Mo=O bonds are present, and the relatively high intensity of the symmetric mode at 994 cm^{-1} in the i.r. spectrum is consistent with a non linear O=Mo=O arrangement. The vibrational frequencies for $MoO_2(SO_3F)_2$ are shown in Table 7.1 in comparison with those of $SnCl_2(SO_3F)_2$ [33].

There are three possible geometries for the compound:

a) tetrahedral with monodentate SO_3F groups,

b) trigonal bipyramidal with one monodentate-and one bridging SO_3F group, or,

c) octahedral with only bridging SO_3F groups and cis-M=O bonds.

The vibrational spectra indicate the absence of monodentate SO_3F groups, thus ruling out the first two possibilities. The observed spectra are most consistent with the presence of bidentate SO_3F groups in the compound, as indicated by the characteristically strong asymmetric SO_2 stretch at ~1170 cm^{-1} in the i.r. spectrum.

Strong vibrational couplings within the $MoO_2(SO_3F)_2$ moiety and best reflected in the SO_2 stretching vibrations at ~1000 and ~1200 cm^{-1}, and between ν M-O and δ O-SO_2F vibrations producing Raman intensity enhancements at ~650, ~450 and ~280 cm^{-1}, as found in anions of the type $[M(SO_3F)_n]^{m-}$, seem to be absent. The position of ν SF is found at 873-885 cm^{-1}, indicating a strong

Table 7.1 VIBRATIONAL FREQUENCIES OF $MoO_2(SO_3F)_2$

$MoO_2(SO_3F)_2$		$SnCl_2(SO_3F)_2$ [33]	
R.	I.R.	R.	Assignment
1420 w 1394 w	1390 s,b	1389 s	$\nu_{as}SO_3$
1244 v w	1247		
1175 m 1088 w	1170 s,b	1125 w 1089 vs	$\nu_{s}SO_3$
1038 w	1040 s,b	1061 m	$\nu_{as}SO_3$
994 vs	990 m		$\nu_{s}O{=}Mo{=}O$
955 s	955s		$\nu_{as}O{=}Mo{=}O$
873 w	850 s,b	870 s	$\nu S{-}F$
630 w	630 m	632 s	$\delta O{=}Mo{=}O$
596 w 561 vw	590 m 555 m	587 m 552 m	$\delta_{as}SO_3$
~450 vw,sh	445 m	442 s	$\delta O{=}Mo{=}O$
402 m	410 w	424 m	δ rock
		356 vs	$\nu_{s}SnCl$
		312 s	$\delta Sn{-}(OSO_2F)_4$ + def S-O
260 w			$\delta Mo{-}(OSO_2F)_4$

Mo(VI)-OSO_2F interaction [92]. In general, the vibrational bands assigned to the SO_3F group correspond closely to a pattern shown by $SnCl_2(SO_3F)_2$, also listed in Table 7.1; however, in the latter case, a linear Cl-Sn-Cl grouping is evident from both vibrational and ^{119}Sn Mössbauer spectroscopy. For this compound, the presence of bidentate bridging SO_3F groups has been proposed [33].

For $MoO_2(SO_3F)_2$, an arrangement consisting of two oxygen atoms on one side of the molecule and four bridging SO_3F groups on the other side of the distorted octahedron can be proposed here.

7.C.2.2 $MoO(SO_3F)_4$

The vibrational frequencies of $MoO(SO_3F)_4$ are listed in comparison with Raman data of $WO(SO_3F)_4$ [211] in Table 7.2 (the relative intensities of the Raman bands of $WO(SO_3F)_4$ were not given in the reference). As can be seen, a good correspondence can be made between the spectra of the two compounds, suggesting structural similarities. The terminal Mo=O stretch is assigned to a sharp Raman band at 933 cm^{-1}. The presence of both bridging and terminal SO_3F groups is indicated by the band positions. The band at ~700 cm^{-1}, present also in the spectrum of $WO(SO_3F)_4$, is presumably due to bridging SO_3F groups in a specific comformational mode. Again, strong vibrational couplings are not observed for $MoO(SO_3F)_4$.

Table 7.2 VIBRATIONAL FREQUENCIES OF $MoO(SO_3F)_4$

$MoO(SO_3F)_4$		$WO(SO_3F)_4$ [211]
R.	I.R.	R.
1460 m	1450 s,sh	1464
1410 m	1400 vs,b	1416
1243 vs	1200 vs,b	1240
1165 w,b		1163
1045 s,sh		1044
1028 s	1025 vs	
933 s	950 s	964
		944
850 vw,b	840 s	873
		853
		826
		801
735 m	720 s	707
		700
636 m	630 m	644
582 vw	580 m,sh	
550 m	555 s	552
451 w		455
		421
275 w		280
		273

7.C.3 ^{19}F-n.m.r. SPECTRA OF $MoO(SO_3F)_4$

Since $MoO(SO_3F)_4$ is very soluble in $S_2O_6F_2$, solution ^{19}F-n.m.r. spectra of the compound were obtained. The spectrum of a ~10 mol% solution in $S_2O_6F_2$ consists of a single broad peak at -42.3 ppm (Fig 7.1). The peak is highly asymmetric, with a shoulder definitely present on the low-field side. When the concentration of $MoO(SO_3F)_4$ is increased to almost 100%, with only a trace of $S_2O_6F_2$ as the reference, two definite resonances become evident at -42.0 and -41.4 ppm, although they are extremely broad and overlapping.

FIG. 7.1

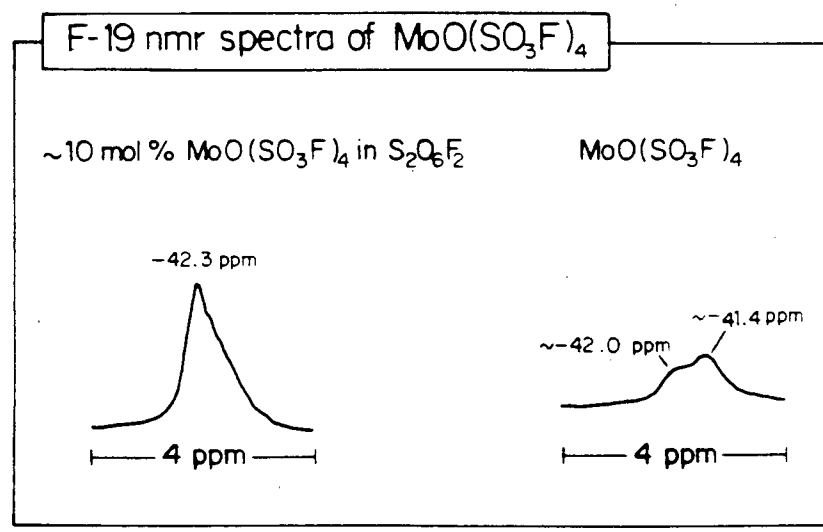

A dilution of $MoO(SO_3F)_4$ with $S_2O_6F_2$ is expected to lead to a break down of the polymer and thus a decrease in the number of bridging SO_3F groups. Therefore, the resonance at -42.0 ppm can be assigned as due to monodentate SO_3F groups while the one at -41.4 ppm must be due to bridging SO_3F groups. The extreme broadness of the peaks indicates an exchange process involving the inter-convertion of the two types of SO_3F groups or possibly a random polymerization process.

The broadness of the peaks also prevented any attempts at quantitative measurements on the relative abundance of the two types of SO_3F groups, but it appears that in almost pure $MoO(SO_3F)_4$, the resonance due to the bridging species is slightly more prominent. If the coordination around Mo(VI) is octahedral, the ratio of bridging to terminal SO_3F groups should be 1:3. The observation here implies an almost equal population for both types of ligands, or an increase in the coordination number. Octa-coordination for Mo(VI) has been suggested for MoO_2F_2 [200] and MoF_8^{2-} [201]. It is also likely, from the broadness of the resonance and the lack of appreciable vibrational couplings between ν Mo-O and ν SO_3F, that dynamic species with possibly various coordination numbers from six to eight, or even higher, may be present.

7.D CONCLUSION

Two Mo(VI) oxyfluorosulfates have been characterized mainly by vibrational spectroscopy. For $MoO_2(SO_3F)_2$, a white solid, hexa-coordination of molydenum with a cis-O=Mo=O bond and bridging SO_3F groups is suggested. For $MoO(SO_3F)_4$, both bridging and terminal SO_3F groups are present, with a terminal Mo=O bond evident. From ^{19}F-n.m.r., $MoO(SO_3F)_4$ appears to undergo intermolecular exchange reactions between the two types of differently bonded SO_3F ligands, possible resulting in the compound's existence as a liquid at room temperature.

The presence of $Mo(SO_3F)_6$ as a possible intermediate in the synthesis of these two compounds is suggested, although it could not be isolated. Neither oxyfluorosulfates appear to have any tendency towards accepting SO_3F^- to form anionic complexes.

CHAPTER 8 GERMANIUM- AND TIN- FLUOROSULFATE

8.A INTRODUCTION

The group IV halides are potential halide ion acceptors because of the possibility of the expansion of their coordination spheres to six (carbon is an exception due to its lack of available low energy d-orbitals). The covalency of the bond between the element and electronegative atoms such as oxygen and the halogens increases as the element becomes more non-metallic, with the result that the lighter halides are volatile whereas PbF_4 is a high-melting crystal. The fluorosulfates of C(IV) [79], Sn(IV) [33] and Pb(IV) [207], and the adduct of $Si(SO_3F)_4 \cdot 2CH_3CN$ [96] have been reported, but only $Sn(SO_3F)_4$ is known to form anionic complexes [32]. The other fluorosulfates are either unstable at room temperature or dissociate in HSO_3F solutions.

During the investigation into the palladium-fluorosulfate system, described in Chapter 3, it became apparent that $Sn(SO_3F)_4$ could have a SO_3F-accepting ability comparable to that of $Pt(SO_3F)_4$. Unfortunately, $Sn(SO_3F)_4$ reportedly is insoluble in HSO_3F [33], thus ruling out its usefulness as a superacid in that solvent system. As $Pb(SO_3F)_4$ was reported to exhibit basic behavior in HSO_3F [207], it was decided to investigate the hitherto unknown germanium-fluorosulfate system as possibly an easily obtainable superacid in HSO_3F.

$Sn(SO_3F)_4$ is similar to $Pt(SO_3F)_4$ in that in both systems,

the hexakis(fluorosulfato)-complexes can be synthesized. A complex of the empirical formula of $CsPt(SO_3F)_5$ was used as an illustration of the polymerization of the platinum-fluorosulfate system in solution, although little structural information could be obtained from vibrational spectra analysis other than that it was polymeric in the solid state. By using ^{119}Sn Mössbauer spectroscopy, which had been applied to the study of $Sn(SO_3F)_4$ and $[Sn(SO_3F)_4]^{2-}$, it may be possible to provide more insights into the structure of the analogous $[Sn(SO_3F)_5]_x^{x-}$ complex, if it can be synthesized. The solution behavior of the tin-fluorosulfate system will also be investigated and compared to those of other M(IV)-fluorosulfates.

8.B EXPERIMENTAL

8.B.1 Sn(IV)-FLUOROSULFATE

8.B.1.1 PREPARATION OF $Sn(SO_3F)_4$

$$Sn + 2S_2O_6F_2 \xrightarrow{HSO_3F} Sn(SO_3F)_4 \qquad (8.1)$$

In a typical reaction, tin metal granules (121 mg, 1.019 mmol) were reacted with a mixture of $S_2O_6F_2$ (~3 mL) and HSO_3F (~2 mL) at room temperature. A rapid reaction occurred and after 3 days, all of the metal had reacted and a white precipitate had formed. The removal of all volatile materials yielded a product identified by vibrational spectroscopy as $Sn(SO_3F)_4$ (530 mg, 1.029 mmol).

8.B.1.2 PREPARATION OF $KSn(SO_3F)_5$

$$KCl + HSO_3F \longrightarrow KSO_3F + HCl \qquad (8.2)$$

$$KSO_3F + Sn + 2S_2O_6F_2 \xrightarrow{HSO_3F} KSn(SO_3F)_5 \qquad (8.3)$$

Tin metal granules (402 mg, 3.387 mmol) were added to a reactor containing solid KSO_3F obtained from the solvolysis of KCl (251 mg, 3.366 mmol) in HSO_3F. After a mixture of $S_2O_6F_2/HSO_3F$ (~3 mL) was distilled into the reactor, a violent reaction occurred at room temperature. The reaction mixture was subsequently kept at ~50°C for 12 hours to ensure completion. The removal of all volatile materials yielded a glass-like material which has a weight corresponding to that of $KSn(SO_3F)_5$ (2.201 g, 3.370 mmol).

$KSn(SO_3F)_5$ is a clear, hygroscopic crystalline solid which

may be a supercooled glass at room temperature. It is very soluble in HSO_3F.

8.B.1.3 PREPARATION OF $CsSn(SO_3F)_5$

$$CsCl + HSO_3F \longrightarrow CsSO_3F + HCl \qquad (8.4)$$

$$CsSO_3F + Sn + 2S_2O_6F_2 \xrightarrow{HSO_3F} CsSn(SO_3F)_5 \qquad (8.5)$$

In a manner analogous to the preparation of $KSn(SO_3F)_5$, tin metal granules (566 mg, 4.769 mmol) were allowed to react with $CsSO_3F$ formed from the solvolysis of CsCl (802 mg, 4.764 mmol) in HSO_3F, giving a white, crystalline, hygroscopic product which analyzed as $CsSn(SO_3F)_5$ (3.492 g, 4.675 mmol).

$CsSn(SO_3F)_5$ is soluble in HSO_3F.

Analysis	S	F
Calculated %	21.47	12.72
Found %	21.11	12.39

8.B.1.4 PREPARATION OF $Cs_2[Sn(SO_3F)_6]$

$$2CsCl + Sn + 3S_2O_6F_2 \xrightarrow{HSO_3F} Cs_2[Sn(SO_3F)_6] + Cl_2 \qquad (8.6)$$

A mixture of dried CsCl (839 mg, 4.983 mmol) and tin metal granules (296 mg, 2.494 mmol) is reacted with $S_2O_6F_2/HSO_3F$ (~5 mL) at ~90°C for 1 day. After the removal of all volatile materials from the solution at 90°C, a white solid which corresponds to $Cs_2[Sn(SO_3F)_6]$ (2.444 g, 2.497 mmol) was obtained.

$K_2[Sn(SO_3F)_6]$ can be prepared similarly.

8.B.2 GERMANIUM-FLUOROSULFATE

8.B.2.1 PREPARATION OF $GeF_2(SO_3F)_2$

$$Ge + 2S_2O_6F_2 \xrightarrow{HSO_3F} GeF_2(SO_3F)_2 + 2SO_3 \qquad (8.7)$$

Germanium metal powder (129 mg, 1.777 mmol) was reacted with a mixture of $S_2O_6F_2/HSO_3F$ (~2 mL) at ~80°C for 3 days. A white sublimate formed on the cooler parts of the reactor and the product was vacuum filtered, washed with $S_2O_6F_2$ and dried by evacuation at room temperature for 30 minutes. A white powder which analyzed as $GeF_2(SO_3F)_2$ (428 mg, 1.386 mmol) was obtained; the yield was very low due to the loss of the product by removal in vacuo.

$GeF_2(SO_3F)_2$ can also be obtained by the reaction of germanium metal powder with $S_2O_6F_2$ at ~150°C for 1 week. This method, although takes longer to complete, eliminates the filtration process.

$GeF_2(SO_3F)_2$ is a white, hygroscopic, flaky solid which is insoluble in HSO_3F. It is sublimable at room temperature in vacuo.

Analysis	Ge	S	F
Calculated %	23.52	20.77	24.62
Found %	21.06	18.68	22.12

Although the analytical result appears to be low, the calculated mole ratio for Ge:S:F is 1.000:2.009:4.014, an excellent comparison with the expected 1:2:4 ratio.

8.B.2.2 PREPARATION OF $(ClO_2)_2[Ge(SO_3F)_6]$

$$2ClO_2SO_3F + Ge + 2S_2O_6F_2 \xrightarrow{HSO_3F} (ClO_2)_2[Ge(SO_3F)_6] \qquad (8.8)$$

A mixture of ClO_2SO_3F (~1 mL) and $S_2O_6F_2$ (~4 mL) was distilled into a reactor containing germanium metal powder (130 mg, 1.791 mmol). An exothermic reaction occurred at room temperature, and the metal dissolved into the deep red ClO_2SO_3F layer. After keeping the reaction mixture at ~50°C for 1 day to ensure a complete reaction, the excess liquid reactants were removed by pumping at ~80°C for 12 hours. A light yellow solid, which analyzed as $(ClO_2)_2[Ge(SO_3F)_6]$ (126 mg, 0.157 mmol) was obtained; again, the low yield was caused by the volatility of the product.

$(ClO_2)_2[Ge(SO_3F)_6]$ is a light yellow, hygroscopic solid. It is sublimable in vacuo at room temperature, but melts at ~145°C under an atmosphere of nitrogen, giving off a ClO_2SO_3F-like gas.

Analysis	Ge	F
Calculated %	9.05	14.22
Found %	8.75	14.22

8.C DISCUSSION

8.C.1 SYNTHESIS AND GENERAL DISCUSSION

The synthesis of $Sn(SO_3F)_4$, using the medium of $S_2O_6F_2/HSO_3F$, is an improvement over the original synthesis using $SnCl_4$ [33], both in terms of speed and purity of the product. Because of the possibility of HSO_3F being reduced by tin metal, a larger than normal ratio of $S_2O_6F_2$ (~75 %) was used as a precaution, and the reaction mixture had to be shaken from time to time to ensure no local depletion of $S_2O_6F_2$. When $S_2O_6F_2$ was omitted from the reaction, the glass reactor became badly etched and the solution took on a blue color, most likely due to sulfur cations [25]. For the same reason, the solvolysis of CsCl or KCl in HSO_3F cannot be performed in the presence of metallic tin, which must be added to the alkali-metal fluorosulfate in the dry-box. Although $Sn(SO_3F)_4$ is insoluble in HSO_3F, the reactivity of tin metal towards $S_2O_6F_2$ is greatly enhanced by the addition of the acid, suggesting a very slight solubility, combined with the energetically highly favorable formation of $Sn(SO_3F)_4$ from Sn.

$CsSn(SO_3F)_5$ does not precipitate $Sn(SO_3F)_4$ in solutions in HSO_3F; this argues against the complex as being a mixture of $Sn(SO_3F)_4$ and $Cs_2[Sn(SO_3F)_6]$. Furthermore, highly concentrated solutions can be obtained at room temperature ($\gtrsim$1.3 mol/kg). $KSn(SO_3F)_5$ is extremely soluble in HSO_3F, and at high concentrations, results in the formation of a glass-like material which

loses HSO_3F very slowly.

The attempted synthesis of $Ge(SO_3F)_4$ resulted in the formation of a compound that analyzed as $GeF_2(SO_3F)_2$. The systematic lowering of the analytical results for the compound seems to suggest the presence of an inert impurity in the sample; small fragments of glass in the germanium metal powder could be the source of such an error. Mixed halide-fluorosulfate compounds of Sn(IV) such as $SnF_2(SO_3F)_2$ [208] and $SnCl_2(SO_3F)$ [33] are known; ^{119}Sn Mössbauer and vibrational spectroscopy suggest the presence of terminal halide ligands and bridging SO_3F groups in these compounds. $SnF_2(SO_3F)_2$ can be prepared by the replacement of chlorine in SnF_2Cl_2 by $S_2O_6F_2$ or $ClSO_3F$ [208], and $SnCl_2(SO_3F)_2$ can be obtained by a ligand redistribution reaction involving $SnCl_4$ and $Sn(SO_3F)_4$ [33]. The existence of $GeF_2(SO_3F)_2$ instead of $Ge(SO_3F)_4$ as a stable compound at room temperature provides a transition between the $Si\text{-}SO_3F$ and the $Sn\text{-}SO_3F$ systems. Due to the preferential formation of a Si-F covalent bond over a $Si\text{-}OSO_2F$ bond, the product obtained from the fluorosulfonation of silicon compounds is invariably SiF_4, and the compound $Si(SO_3F)_4 \cdot 2CH_3CN$ requires stabilization by the two coordinated nitriles [66]. $Sn(SO_3F)_4$, on the other hand, is a crystalline solid stable up to 216°C [33]. In view of this, and the expectation that the electronegativity of germanium is between that of silicon and tin, it is not surprising to find the observed stability of the $Ge\text{-}OSO_2F$ bond with respect to replacement by a Ge-F bond.

$Ge(SO_3F)_4$, however, can be stabilized by the formation of $[Ge(SO_3F)_6]^{2-}$ complexes, but these also exhibit quite low thermal stabilities, subliming or decomposing in vacuo at room temperature. Attempts to prepare $Cs_2[Ge(SO_3F)_6]$ resulted in the formation of a $CsSO_3F$-rich product, as shown by Raman and i.r. spectroscopy. $(ClO_2)_2[Ge(SO_3F)_6]$ could be obtained as a pure product because the ClO_2SO_3F formed from the decomposition is also volatile, but in order to ensure the complete removal of the excess ClO_2SO_3F used in the reaction, a large quantity of the desired product was also lost. An alternative method may be to use filtration instead of evacuation as a means of removing excess reactants, followed by washing with liquid SO_2 which can be evaporated at room temperature without the application of a vacuum.

8.C.2 VIBRATIONAL SPECTRA

8.C.2.1 $CsSn(SO_3F)_5$

As mentioned in Chapter 5, the vibrational spectra of $CsSn(SO_3F)_5$ are very similar to those of $KRu(SO_3F)_5$ [209] and $CsPt(SO_3F)_5$, suggesting structural similarities. Only a relatively poorly resolved Raman spectrum could be obtained for $CsSn(SO_3F)_5$ due to the sample's fluorescence in the laser radiation. The Raman frequencies of $CsSn(SO_3F)_5$ are compared to the literature values

Table 8.1 RAMAN FREQUENCIES OF $CsSn(SO_3F)_5$

$CsSn(SO_3F)_5$	$Sn(SO_3F)_4$ [33]	$K_2[Sn(SO_3F)_6]$ [32]
1430 w	1431 s	1407 m
1406 w	1420 s,sh	1390 m
1265 m		1278 ms
1220 w	1233 s	1228 m
		1208 w
1130 w	1124 s	
1112 w		
1060 w	1075 s	1096 s
1055 w		
1000 w	986 w	1002 m
	911 m	
850 w	845 m	859 m
820 w	827 m	836 m
		823 m
	640 w,sh	
630 m	632 s	625 s
605 vw		
585 w	589 s	582 m
560 w	552 m	560 m
430 w	427 s	435 m
		416 m
	320 w	360 m
		266 w

for $Sn(SO_3F)_4$ [33] and $K_2[Sn(SO_3F)_6]$ [32] in Table 8.1

It appears that the Raman spectrum of $CsSn(SO_3F)_5$ contains bands from both the other two compounds' spectra, but some very intense bands have been shifted, indicating the existence of not merely a mixture of the two known compounds. For example, the strong SO_2 symmetric stretch is shifted to 1220 cm^{-1}; similarly, a downward shift of the band at ~1060 cm^{-1} is also evident.

The similarities between the three spectra are not unexpected because $[Sn(SO_3F)_6]^{2-}$ contains only monodentate SO_3F groups, $Sn(SO_3F)_4$ has an equal number of monodentate and bidentate SO_3F groups, and for $CsSn(SO_3F)_5$, there should be one bidentate SO_3F group for every four monodentate SO_3F groups. The presence of the diagnotic band at ~1130 cm^{-1} in both the i.r. and Raman spectra of $CsSn(SO_3F)_6$ confirms the existence of bidentate bridging SO_3F groups.

8.C.2.2 $GeF_2(SO_3F)_2$ AND $(ClO_2)_2[Ge(SO_3F)_6]$

Again because of the fluorescence of the sample when it is irradiated by the laser, only a rather poorly resolved Raman spectrum could be obtained for $GeF_2(SO_3F)_2$. The i.r. spectrum of the compound has a broad absorption from ~1000 to ~1150 cm^{-1}, indicating the presence of bridging SO_3F ligands. The vibrational frequencies of $GeF_2(SO_3F)_2$ are listed in Table 8.2 and compared to the i.r. frequencies of $SnF_2(SO_3F)_2$.

The absence of the strongly Raman active symmetric SO_3

Table 8.2 VIBRATIONAL FREQUENCIES OF $GeF_2(SO_3F)_2$

$GeF_2(SO_3F)_2$		$SnF_2(SO_3F)_2$ [208]	
I.R.	R.	I.R.	Assignment
1390 vs	1426 w	1420 m,sh 1405 vs,b	νSO_3
~1100 vs,sh	1095 w	1115 vs,b 1103 s,sh	νSO_3
~1050 vs,vb	1064 w 1055 w	1070 s,b	νSO_3
880 vs	880 vs	855 vs	νSF
770 vs			νGe-F asym
		691 s	νSn-F
660 s	656 w,sh	628 ms	SO_3 bend
	648 m		νGe-F sym
570 s	576 w	590 s	SO_3 bend
555s	560 w	548 vs	SO_3 bend
495 s	490 w		$\nu Ge\text{-}OSO_2F$
420 m	437 w	430 ms	SO_3 rock
		~350 m	$\nu Sn\text{-}OSO_2F$
	280 w		

stretch at ~1220 cm^{-1} in the spectrum of $GeF_2(SO_3F)_2$ denotes the absence of monodentate, tridentate and ionic SO_3F groups. Therefore, together with the feature noted in the SO_2 stretching region in the i.r. spectrum, it can be concluded that the fluorosulfate is present in a bidentate form. A good comparison can be made with the i.r. spectrum of $SnF_2(SO_3F)_2$ [208], suggesting similarities in the structure and bonding of the two compounds. A strong band at 770 cm^{-1} in the i.r. spectrum of $GeF_2(SO_3F)_2$, not observed in its Raman spectrum, is assigned to the asymmetric stretching of the Ge-F bonds. A relatively strong Raman band at 648 cm^{-1} is most likely the νGe-F sym (this assignment is based on the fact the band at ~650 cm^{-1} is usually not very strongly Raman active relative to the bands at ~450 and ~280 cm^{-1}). For the tin compound, the analogous vibrations are found at 691 and 612 cm^{-1}. The mutual exclusion of the two Ge-F stretching vibrations indicates a linear or nearly linear configuration for the [F-Ge-F] unit; a similar conclusion has been reached for the chlorine [33], fluorine [208] and methyl [96] derivatives of tin(IV), thus indicating that all four compounds are closely related structurally.

Assuming a linearity in the [Hal-M-Hal] bonds, a comparison can be made on the approximate stretching force constants of $GeF_2(SO_3F)_2$, $SnF_2(SO_3F)_2$ and $SnCl_2(SO_3F)_2$ [206] (stretch-bend interactions are ignored):

$$\nu_1(A_{1g}) = \left(\frac{\mu_H(k + k_i)}{5.889\times10^{-7}} \right)^{\frac{1}{2}} \qquad (8.9)$$

$$\nu_2(A_{2u}) = \left(\frac{(\mu_H + 2\mu_m)(k + k_i)}{5.889\times10^{-7}} \right)^{\frac{1}{2}} \qquad (8.10)$$

where ν is the frequency in cm^{-1},

μ is the reciprocal of the atomic masses of the halogen or metal atoms in a.m.u., and

k, k_i are the stretching and stretch-stretch interaction force constants in m dynes/Å, respectively.

By using ν_1(Ge-F) = 648 cm^{-1}, ν_2(Ge-F) = 770 cm^{-1},

ν_1(Sn-F) = 612 cm^{-1}, ν_2(Sn-F) = 691 cm^{-1} [208],

ν_1(Sn-Cl) = 356 cm^{-1}, ν_2(Sn-Cl) = 411 cm^{-1} [33],

the following force constants are obtained:

k(Ge-F) = 4.53	k_i(Ge-F) = 0.17
k(Sn-F) = 4.12	k_i(Sn-F) = 0.07
k(Sn-Cl) = 2.43	k_i(Sn-Cl) = 0.22

Stretch-stretch interaction can also arise from the involvement of π orbitals in the bonding; as one M-Hal bond stretches, lessening the interaction of the d_π orbitals on the metal to the halogen, these π orbitals will become more available to the halogen on the other side, and π bonding to them will become stronger. Consequently, this would result in k_i having a positive sign [206]. The degree of π-bonding in the chlorine-containing compound is large, as can be seen from the relative values of k_i and k. This is consistent with chlorine having d-orbitals of lower energy

than fluorine has. In spite of the increase in π-bonding, the Sn-Cl bond is weaker than the Sn-F bond, presumably due to an increase in covalent character in the latter. For the same reason, the Ge-F bond is shown by these calculation to be much stronger than the Sn-F bond, and supports the contention that this may be an important factor contribution to the preferential formation of $GeF_2(SO_3F)_2$ instead of $Ge(SO_3F)_4$. By extending the force constant calculations to the literature values for the vibrational frequencies of the tetrahedral fluorides of CF_4, SiF_4 and GeF_4 [210], using the formulae given in reference 206, a comparison can be made in Table 8.3.

Table 8.3 STRETCHING FORCE CONSTANTS OF SOME GROUP IV ELEMENT-FLUORINE BONDS (in mdynes/A)

	$\nu(A_{1g})$	$\nu(F_2)$	$\nu(A_{2u})$	k	k_i
CF_4 [210]	908	1281	—	6.73	0.83
SiF_4 [210]	800	1010	—	6.29	0.29
GeF_4 [210]	738	800	—	5.50	0.20
$GeF_2(SO_3F)_2$	648	—	770	4.53	0.17
$SnF_2(SO_3F)_2$ [208]	612	—	691	4.12	0.07

It can be seen that the element-fluorine bond strengthens as the element becomes more electronegative. The substitution of a fluorine atom with two bridging fluorosulfate groups tends to weaken the covalent Ge-F bond by possibly a delocalization of the electron density away from germanium. The increase in the stretch-and-stretch interaction for CF_4 is most likely a result of steric

effects in the small molecule. For example, the stretching of one C-F bond would decrease the crowding for the remaining three fluorine atoms, leading to an increase in the strength of the other C-F bonds.

In the vibrational spectrum of $GeF_2(SO_3F)_2$, νS-F is found at 880 cm^{-1}, an unusually high frequency, suggesting the presence of a strong Ge-O bond [92]. This is not unexpected since the Ge-F bond is strong and the electronegativities of oxygen and fluorine are similarly high.

$(ClO_2)_2[Ge(SO_3F)_6]$ is an excellent Raman scatterer, and a good comparison can be made with the Raman frequencies of $(ClO_2)_2$-$[Sn(SO_3F)_6]$ [32] in Table 8. 3.

The ionic nature of the complex is shown by the presence of the three vibrational modes for ClO_2^+ at ~1300, 1063 and 526 cm^{-1} in the Raman spectrum. The rest of the spectrum is essentially that of a monodentate SO_3F group coordinated in a manner similar to other hexakis(fluorosulfato) complexes. It appears that the coordination of six SO_3F groups reduces the polarizing ability of Ge(IV), as can be shown by a lowering of the stretching frequency of the Ge-OSO_2F vibration to 461 cm^{-1} from 495 cm^{-1} in $GeF_2(SO_3F)_2$. Furthermore, νS-F is lowered to the normal range at ~820 to ~850 cm^{-1} from 880 cm^{-1} in $GeF_2(SO_3F)_2$. These observations are not surprising in view of the increased delocalizing ability of a SO_3F group as compared to a fluorine atom.

Table 8.4 VIBRATIONAL FREQUENCIES OF $(ClO_2)_2[Ge(SO_3F)_6]$

$(ClO_2)_2[Ge(SO_3F)_6]$		$(ClO_2)_2[Sn(SO_3F)_6]$ [32]	
R.	I.R.	R.	Assignment
1414 w 1390 m 1380 m	1385 vs	1412 w 1386 s	νSO_2 asym.
1307 w 1295 vw	1305 s 1295 s	1308 m 1295 w	$\nu_3(ClO_2^+)$
1272 m 1215 s 1205 s	~1200 vs,b	1265 ms 1206 s	νSO_2 sym.
1098 m		1092 m	
1063 vs		1062 vw	$\nu_1(ClO_2^+)$
1001 w 985 vw 965 vw	1020 vs,b	1030 s 990 sh	$\nu O\text{-}SO_2F$
847 w 821 w	820 vs,b	842 m 820 m	$\nu S\text{-}F$
631 m	640 s	624 s	SO_2 bend
591 w 567 w	580 s	582 m	SO_2 bend
554 w	550 s	555 m	SO_2 bend
526 m	520 m	526 m	$\nu_2(ClO_2^+)$
461 w			$\nu Ge\text{-}OSO_2F$
436 m	432 w,sh	429 m	SO_2 rock
274 m 255 m		399 w 348 m 264 m	$\nu Sn\text{-}OSO_2F$

8.C.3 CONDUCTOMETRIC STUDIES IN HSO_3F

Neither $GeF_2(SO_3F)_2$ nor $Sn(SO_3F)_4$ [33] show any appreciable solubility in HSO_3F, and thus solution studies on the systems are limited to the anionic complexes. In the previous chapters, the conductivities of solutions of $[M(SO_3F)_6]^{2-}$, where M=Pd, Pt, Ir, Sn, have been found to be almost identical, suggesting a similar ionization scheme for all the complexes. From solution studies of the platinum(IV)-fluorosulfate system, $[Pt(SO_3F)_6]^{2-}$ has been shown to undergo a basic dissociation in HSO_3F.

A conductometric titration of $KSn(SO_3F)_5$ with KSO_3F was undertaken to investigate the acid-base behavior of the complex in HSO_3F. $KSn(SO_3F)_5$ is potentially a SO_3F acceptor according to:

$$KSn(SO_3F)_5 + KSO_3F \longrightarrow K_2[Sn(SO_3F)_6] \ . \qquad (8.11)$$

But by analogy with $[Pt(SO_3F)_6]^{2-}$, the reverse reaction may be appreciable. The result of such a titration is shown in Fig 8.1 and Table 8.5. The procedure involved in the calculation is described in detail in Appendix A but will be briefly explained here.

Since there is no reason for the polymeric units of $KSn(SO_3F)_5$ to remain intact in the relatively dilute solution in which the titration was performed in, the species most likely present under such a condition is the solvated monomeric species, $H[Sn(SO_3F)_6]^-$. The titration is therefore the neutralization of this 'acid' by SO_3F^- according to:

$$H[Sn(SO_3F)_6]^- + SO_3F^- \underset{}{\overset{K_1}{\rightleftharpoons}} [Sn(SO_3F)_6]^{2-} + HSO_3F \ . \qquad (8.12)$$

FIG 8.1

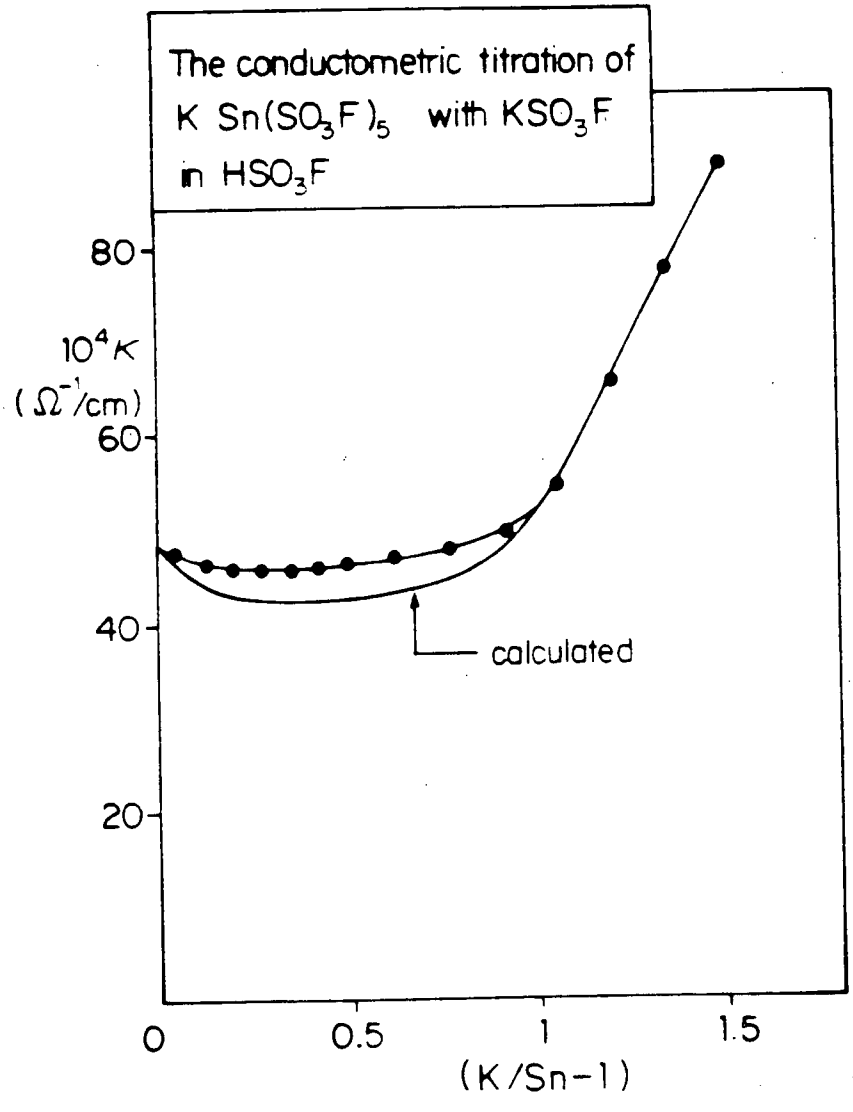
The conductometric titration of
K Sn(SO3F)5 with KSO3F
in HSO3F
80
10⁴K
(Ω⁻¹/cm)
60
40
20
calculated
0
0.5
1
1.5
(K/Sn-1)

Table 8.5 CONDUCTOMETRIC TITRATION OF $KSn(SO_3F)_5$ WITH KSO_3F IN HSO_3F

R	κ(obs)	κ(calc)*	I(calc)
0.0	48.52	48.52	0.090
0.1	46.69	43.90	0.100
0.2	45.99	43.12	0.112
0.3	45.76	42.83	0.123
0.4	45.98	42.73	0.133
0.5	46.35	42.80	0.143
0.6	46.86	43.09	0.152
0.7	47.46	43.72	0.160
0.8	48.13	44.94	0.167
0.9	49.16	47.29	0.173
1.0	51.50	51.50	0.178
	$10^{-4}\Omega^{-1}cm^{-1}$	$10^{-4}\Omega^{-1}cm^{-1}$	$mol \cdot kg^{-1}$ units

* Calculated using the following parameters:

$\lambda_o^*(H_2SO_3F^+) = 320$

$\lambda_o^*(SO_3F^-) = 227$

$\lambda_o^*(K^+) = 29$

$\lambda_o^*(H[Sn(SO_3F)_6]^-) = 28$

$\lambda_o^*([Sn(SO_3F)_6]^{2-}) = 29$

$K_1 = 5.1 \times 10^{-5}$ $mol \cdot kg^{-1}$

By fixing the initial (R=0), and the last points (R=1) in the titration curve, $\lambda_o^*([Sn(SO_3F)_6]^{2-})$ and K_1 can be obtained for each set of the other four variables listed in Table 8.5. In addition, the mobility of $H_2SO_3F^+$ is fixed at 320 [24] and those of SO_3F^- and K^+ are related [21]. Because the system is only weakly acidic, the autoprotolysis of HSO_3F must also be taken into account. A reasonable fit with the experimental curve is obtained with the parameters listed in Table 8.5. The ionic mobilities and the value for K_1 compare quite well with those obtained for the platinum - fluorosulfate system, described in Chapter 5. Again, $[Sn(SO_3F)_6]^{2-}$ has about the same ionic mobility as K^+ and $H[Sn(SO_3F)_6]^-$, and can be attributed to the opposing effects of it being a doubly charged ion and the resulting increased solvation.

The equilibrium constant for the solvolysis of $[Sn(SO_3F)_6]^{2-}$ in HSO_3F according to:

$$[Sn(SO_3F)_6]^{2-} + HSO_3F \rightleftharpoons H[Sn(SO_3F)_6]^- + SO_3F^- \quad , \qquad (8.13)$$

is about 7.5×10^{-4} mol/kg, indicating a weakly basic behavior for the solute.

In general, the two curves in Fig 8.1 deviates from each other by less than 8 %, this can be caused by:

a) the dependence of λ^* on I used in the calculation is not a good approximation, and

b) the average concentration of all ionic species during the titration is about 0.1 mol/kg, which cannot be strictly defined as being dilute. Polymerization according to:

$$2H[Sn(SO_3F)_6]^- \rightleftharpoons [Sn_2(SO_3F)_{10}]^{2-} + 2HSO_3F \qquad (8.14)$$

and

$$2[Sn(SO_3F)_6]^{2-} \rightleftharpoons [Sn_2(SO_3F)_{10}]^{2-} + 2SO_3F^-, \qquad (8.15)$$

etc, would serve to increase the basicity of the solution, and since $H[Sn(SO_3F)_6]^-$ is only a very weak acid, the conductivity for the most part of the titration (from R slightly greater than 0) would be increased.

The validity of the calculated K_1 and λ_o^* values is tested by calculating the conductivity of $CsSn(SO_3F)_5$ and $K_2[Sn(SO_3F)_6]$ [32] solutions in HSO_3F, shown in Fig 8.2. The concentration range covered is quite large, and the approximation in λ^* is not expected to adequately describe the real system, especially when the λ's were extrapolated from concentrated solutions in which solutions do not behave ideally. In any case, the calculated curves fit the experimental curves better at higher concentrations, and no further attempts were made to modify the dependence of λ^* on I.

In summary, the conductometric studies on solutions of $KSn(SO_3F)_5$ in HSO_3F suggest a complicated behavior, involving both polymer-formation and weak proton-accepting properties. N.m.r. results, to be discussed later, also support such a hypothesis. The series of $[M(SO_3F)_6]^{2-}$, where M=Sn, Pd, Pt, Ir, all appear to ionize in a similar manner in HSO_3F, forming weakly basic solutions.

$(ClO_2)_2[Ge(SO_3F)_6]$ dissolves in HSO_3F to give light yellow solutions, suggesting the presence of solvated ClO_2^+ [32]. The

FIG 8.2

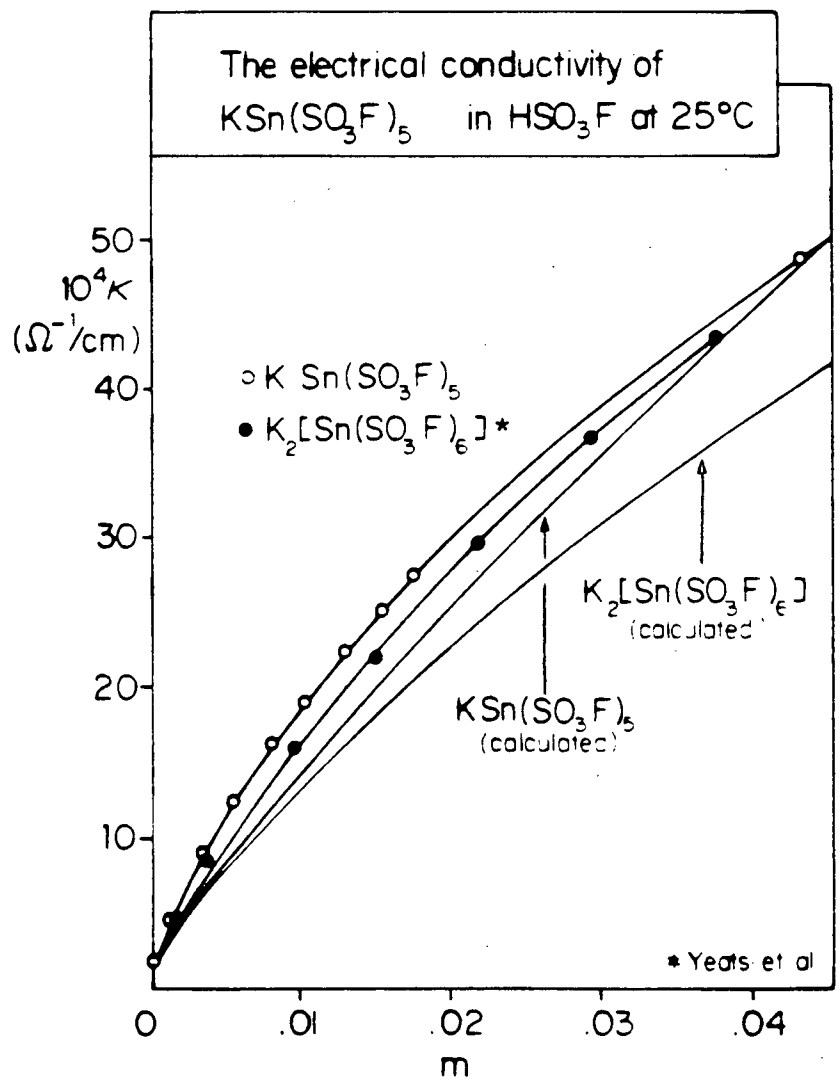
The electrical conductivity of
KSn(SO3F)5 in HSO3F at 25°C
50
10⁴κ
(Ω⁻¹/cm)
40
30
20
10
○ K Sn(SO3F)5
● K2[Sn(SO3F)6]*
K2[Sn(SO3F)6]
(calculated)
KSn(SO3F)5
(calculated)
* Yeats et al
0
.01
.02
.03
.04
m

conductivity of $(ClO_2)_2[Ge(SO_3F)_6]$ in HSO_3F is shown in Fig. 8.3 and Table 8.6. In comparing these results with those of the corresponding platinum species, it is evident that the latter system has a higher conductivity of about 30%. The high conductivity of $[Pt(SO_3F)_6]^{2-}$ and related solutes in HSO_3F has been attributed to solvolysis reactions, giving rise to SO_3F^-, which, like HSO_3F^+, has a high mobility in the solvent. It may also be inferred from this that in the solutions containing $[Ge(SO_3F)_6]^{2-}$, the protonation according to:

$$[Ge(SO_3F)_6]^{2-} + HSO_3F \rightleftharpoons H[Ge(SO_3F)_6]^- + SO_3F^-, \qquad (8.16)$$

occurs to a lesser extent. By assuming $\lambda_o^*([Ge(SO_3F)_6]^{2-}) = 30$, and $\lambda_o^*(ClO_2^+) = 25$, for a 0.01 mol/kg solution of $(ClO_2)_2[Ge(SO_3F)_6]$ that undergoes a dissociation giving rise to only ClO_2^+ and $[Ge(SO_3F_6]^{2-}$, the conductance of the solution should be about 9×10^{-4} $\Omega^{-1}cm^{-1}$, when solvent conductivity is included. With $\lambda_o^*(SO_3F^-) = 230$, it can be calculated that the equilibrium constant for equation (8.16) is about 25% that of the other $[M(SO_3F)_6]^{2-}$ complexes in solutions, or of the order of the solvent dissociation constant.

Therefore, solutions of $[Ge(SO_3F)_6]^{2-}$ are anomalous when compared to those of the other $[M(SO_3F)_6]^{2-}$ complexes investigated in this study, displaying a much less conductivity. It is also not expected that the other $[M(SO_3F)_6]^{2-}$ complexes, where M=Pd, Pt, Ir, Sn, should have identical equilibrium constants in solution but slight variations in them are masked by the autoprotolysis of HSO_3F because the amount of SO_3F^- derived from both

FIG 8.3 CONDUCTIVITY OF $(ClO_2)_2[Ge(SO_3F)_6]$ IN HSO_3F

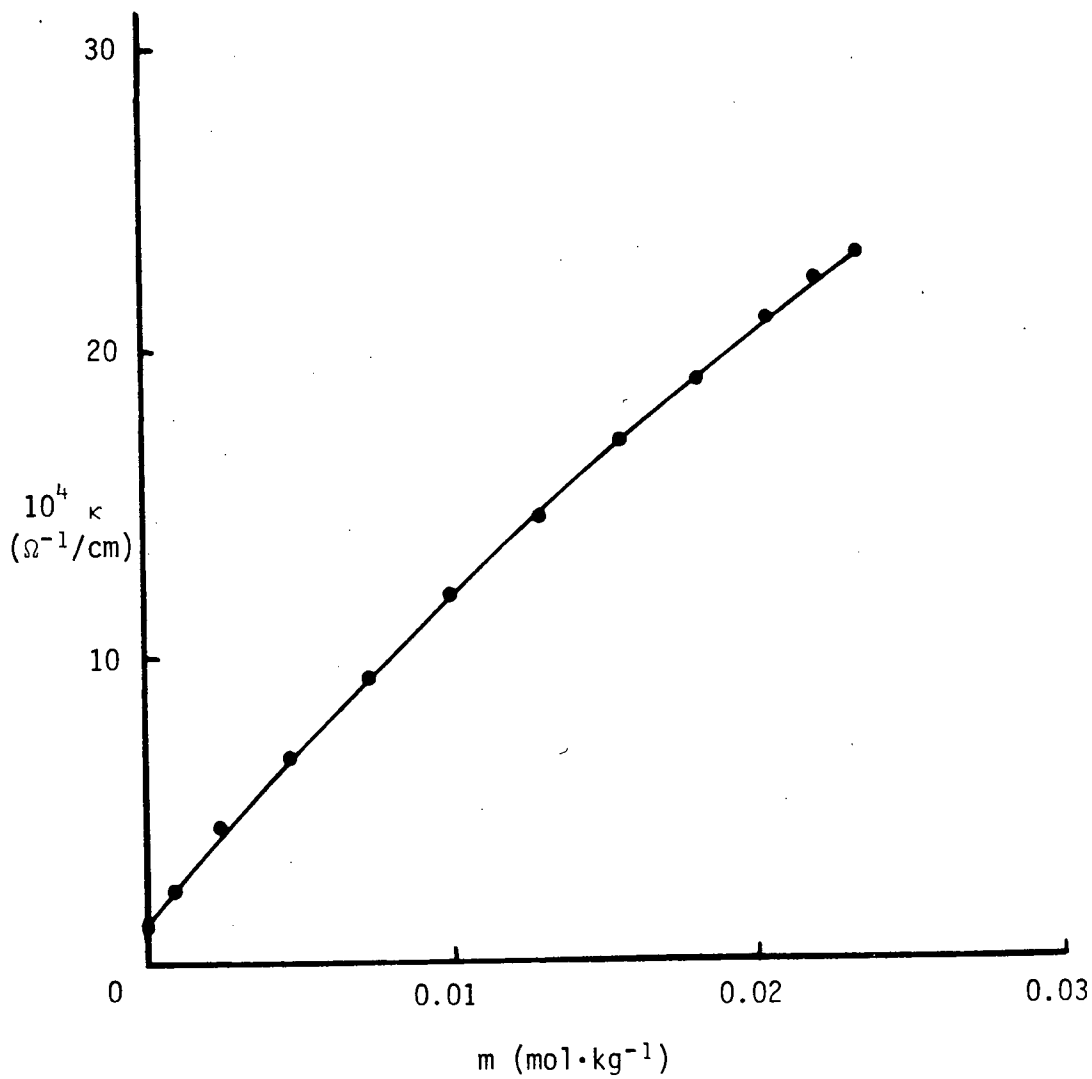

Table 8.6 CONDUCTIVITY OF $(ClO_2)_2[Ge(SO_3F)_6]$ IN HSO_3F *

m	κ
0.0000	1.162
0.0020	3.699
0.0040	5.799
0.0060	7.854
0.0080	9.806
0.0100	11.70
0.0120	13.56
0.0140	15.35
0.0160	17.04
0.0180	18.69
0.0200	20.34
0.0220	21.96
$mol \cdot kg^{-1}$	$10^{-4}\Omega^{-1}cm^{-1}$

* interpolated

equilibria are of about the same order of magnitude.

8.C.4 N.M.R. STUDIES IN HSO_3F

Both ^{119}Sn- and ^{19}F-n.m.r. spectroscopy were applied to the study of the Sn(IV)-fluorosulfate system in HSO_3F solution. The ^{119}Sn-n.m.r. spectra of $CsSn(SO_3F)_5$ and $Cs_2[Sn(SO_3F)_6]$ are shown in Fig 8.4.

Of all the naturally occurring isotopes of tin, two have nuclear spins of ½, they are ^{117}Sn with an abundance of 7.61% and ^{119}Sn with an abundance of 8.58%. ^{119}Sn- n.m.r. has a relative sensitivity of 5.18×10^{-2} compared to ^{1}H-n.m.r., and for a 80 MHz spectrometer, the resonance for ^{119}Sn is at about 29.88 MHz. Both of the ^{119}Sn-n.m.r. spectra consist of a single resonance, with that of $CsSn(SO_3F)_5$ shifted 41 Hz down-field from that of $Cs_2[Sn(SO_3F)_6]$ (the frequency indicated on the spectra is simply for use as a reference). It becomes evident that the resonance for $CsSn(SO_3F)_5$ is broad (~25 Hz at half-height as compared to ~9 Hz for $Cs_2[Sn(SO_3F)_6]$). The same is also found for the ^{19}F-n.m.r. spectra; even at a concentration of 0.12 m, much lower than used for the ^{119}Sn-n.m.r. spectra, a single relatively broad peak occurs at -41.00 ppm. As an excess of KSO_3F was added to the solution, two sharp resonances appeared, a low intensity one at -41.75 ppm assigned to $[Sn\text{-}SO_3F]$ species and a solvent reso-

FIG 8.4 ^{119}Sn-N.M.R. SPECTRA IN HSO_3F

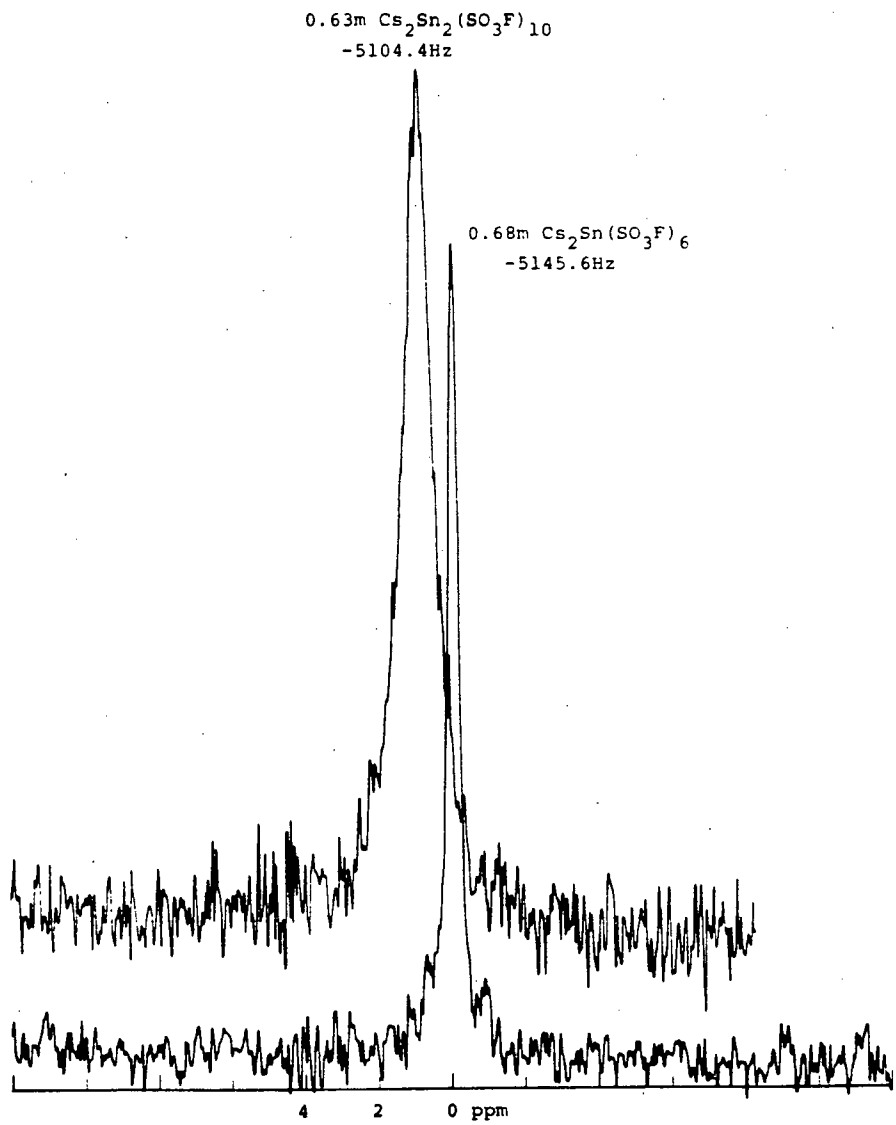

nance at -40.75 ppm. The solvent peak is hardly changed from that of pure HSO_3F, and the solute peak compares well with that reported for $[Sn(SO_3F)_6]^{2-}$ solutions [32]. For more concentrated solutions of $KSn(SO_3F)_5$, such as at 0.88 mol/kg, the single resonance is shifted to -41.42 ppm (close to that for other [Sn-SO_3F] species) and the resonance is noticeably broadened (~24 Hz at half-height). A 'titration' of $KSn(SO_3F)_5$ monitored by ^{19}F-n.m.r. is shown in Fig. 8.5; the sharpening and splitting of the resonance upon the addition of KSO_3F are well illustrated .

It therefore appears that an exchange process, involving SO_3F groups, must be present in $MSn(SO_3F)_5$, where M=K, Cs, as proton exchange in species such as $H[Sn(SO_3F)_6]^-$ is not expected to give rise to the observed broadening in the spectra. The dimerization of $H[Sn(SO_3F)_6]^-$ according to:

$$2H[Sn(SO_3F)_6]^- \rightleftharpoons [Sn_2(SO_3F)_{10}]^{2-} + 2HSO_3F \ , \qquad (8.17)$$

could produce such an effect. The dimerization of $[Sn(SO_3F)_6]^{2-}$ according to:

$$[Sn(SO_3F)_6]^{2-} \rightleftharpoons [Sn_2(SO_3F)_{10}]^{2-} + 2SO_3F^- \ , \qquad (8.18)$$

may not occur as readily because of its strong dependence on the acidity of the solution. This is especially true when an excess of KSO_3F is added, resulting in the reduction of the solvolysis of $[Sn(SO_3F)_6]^{2-}$ to form $H[Sn(SO_3F)_6]$. The small difference in the chemical environments of the fluorine atoms when the SO_3F group is bound as a terminal or a bridging ligand can also lead to the broadening in the ^{19}F-n.m.r. spectrum of $KSn(SO_3F)_5$.

FIG. 8.5

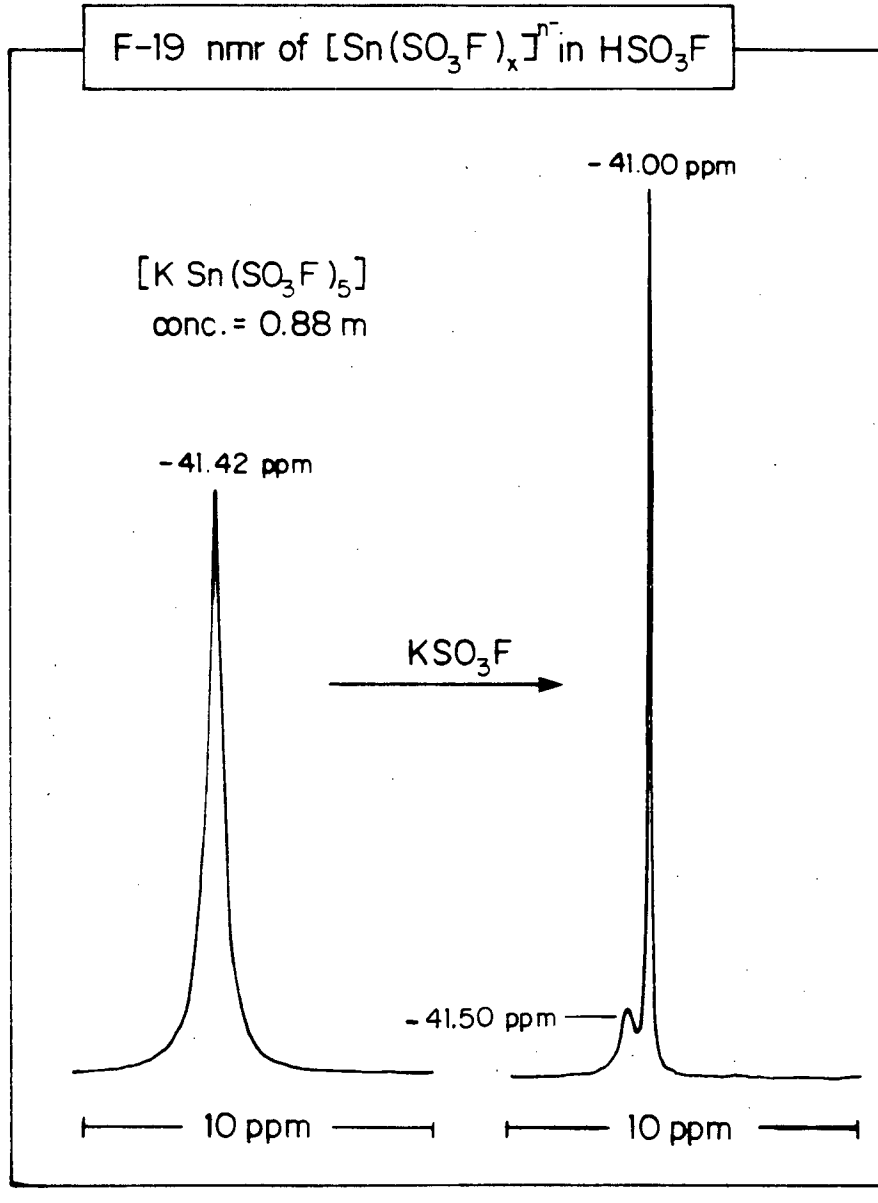
F-19 nmr of [Sn(SO3F)x]n- in HSO3F
-41.00 ppm
[K Sn(SO3F)5]
conc. = 0.88 m
-41.42 ppm
KSO3F
-41.50 ppm
10 ppm
10 ppm

In summary, it appears that the species present in HSO_3F solutions of $M^{I}Sn(SO_3F)_5$ are dynamically exchanging SO_3F-containing moieties with the solvent, leading to a broadening and coalescence of the ^{19}F resonance; this is supported also by the ^{119}Sn-n.m.r. results.

Some differences exist between the n.m.r. studies described here and those involving platinum:

a) There was no Sn-F coupling observed. For the ^{19}F spectra, the low natural abundance of ^{117}Sn and ^{119}Sn may be a factor here. For the ^{119}Sn spectra, in which a septet is expected for $[Sn(SO_3F)_6]^{2-}$, the relatively sharp resonance suggests that either no Sn-F coupling occurs, or J(Sn-F) is very small ($\leq$5 Hz).

b) In the ^{19}F-n.m.r. spectra of the platinum compounds, no shifting or broadening in the resonance was observed. This is most likely due to the large separation between the solvent resonance and the [Pt-SO_3F] resonance, and does not rule out the occurrence of exchange reactions.

8.D CONCLUSION

Complexes of the type of $M^{I}Sn(SO_3F)_5$, where M=Cs, K, have been prepared and characterized by vibrational spectroscopy and solution studies involving conductometry and n.m.r. spectroscopy. These complexes are similar to those containing Pt(IV); the analogy also extends to the hexakis(fluorosulfato)-complexes of Pt(IV), Ir(IV) and Pd(IV) in terms of their structures and solution behaviors. Unlike $K[Au(SO_3F)_4]$, $KSn(SO_3F)_5$ is weakly acidic, and $K_2[Sn(SO_3F)_6]$ is weakly basic, when dissolved in HSO_3F. Using n.m.r. spectroscopy, exchange reactions involving the transfer of SO_3F groups seem to be prevalent in solutions of $KSn(SO_3F)_5$; this has been attributed to a dimerization or polymerization in solution. Unfortunately, no ^{119}Sn Mössbauer studies could be performed on the complexes, as a suitable source was not available.

This study confirms the conclusion arrived in the palladium-fluorosulfate system that $Sn(SO_3F)_4$ is a strong fluorosulfate acceptor, and it would have been a practical superacid in the HSO_3F solvent system if not for its insolubility.

In the germanium-fluorosulfate system, the tetrakis(fluorosulfate) was not obtainable; instead, $GeF_2(SO_3F)_2$ was obtained as the product from the oxidation of germanium metal with $S_2O_6F_2$. From vibrational spectroscopy, the fluoride-fluorosulfate seems to be isostructural with $SnF_2(SO_3F)_2$. Although $Ge(SO_3F)_4$ could not be successfully prepared, an anionic complex containing $[Ge(SO_3F)_6]^{2-}$ could be isolated, but it too displays limited thermal

stability in vacuo. The [Ge-SO_3F] system bridged a gap between the highly unstable fluorosulfates of carbon and silicon, and the easily formed $Sn(SO_3F)_4$.

CHAPTER 9 CONCLUSION

From a synthetic point of view, this study has provided a very versatile preparative reagent for the synthesis of metal fluorosulfates and their anionic complexes. The mixture of $S_2O_6F_2$/HSO_3F combines the strong oxidizing ability of $S_2O_6F_2$ with the ionic solvating property of HSO_3F, and can be used from below room temperature up to almost 200°C. The usefulness of this oxidizing mixture is in its adaptability to most of the synthetic reactions described in this thesis, giving rise to compounds containing the highest oxidation state of the metal in the fluorosulfate system. Fluorosulfonation reactions using $S_2O_6F_2/HSO_3F$ do not result in the formation of a reactive by-product, like the halogen-monofluorosulfates do, and in cases where by-products are formed, they usually come from the decomposition of the metal fluorosulfate.

Of the systems investigated here, $Au(SO_3F)_3$ and $Pt(SO_3F)_4$ have been found to be superacids in HSO_3F, with acidities comparable to that of $SbF_2(SO_3F)_3$, the strongest superacid in the solvent system. Novel polybromine cations, Br_3^+ and Br_5^+ can be stabilized by $[Au(SO_3F)_4]^-$, illustrating the low basicity and low oxidizing ability of the anion. The two ansolvo acids are polymerized in the solid state, and, in the platinum system, also in solution, as illustrated by conductivity results and the synthesis of $CsPt(SO_3F)_5$-type complexes.

Although being a strong acceptor of SO_3F^- is the first requirement for a superacid, too strong an acceptor property also seems to lead to its demise. This can be illustrated in the Sn-SO_3F system, for which evidence from electronic spectra of Pd(II)-fluorosulfato complexes seems to suggest an extremely strong SO_3F-accepting property. It is perhaps because of this reason that $Sn(SO_3F)_4$ is highly polymeric and insoluble in HSO_3F.

The study into the palladium system provided the first interpretation of the ligand field parameters of Pd(II) in an octahedral ligand field. The magnetic susceptibility of Pd(II) in various fluorosulfato complexes was found to have Curie-Weiss Law behavior in magnetically dilute systems. The iridium-fluorosulfate system is essentially a paramagnetic analogue of platinum's.

SUGGESTIONS FOR FURTHER WORK IN THIS AREA

a) A quantitative measure of acidity, the Hammett coefficients, should be applied to $H[Au(SO_3F)_4]$ and $H_2[Pt(SO_3F)_6]$. It may also be useful to investigate the n.m.r. technique of measurement [51,52].

b) The application of the two superacids is a definite possibility, especially in view of their high acidity, high thermal stability and low oxidizing power. The catalytic polymerization of small organic molecules such as CH_4 should serve

as a comparison with the HSO_3F-SbF_5 superacid system.

c) Since $[Au(SO_3F)_4]^-$ can stabilize Br_5^+, other similarly large novel cations may be synthesized, containing the same counter-anion.

d) The application of ^{119}Sn Mössbauer to the study of $[Sn(SO_3F)_5]_x^{x-}$, and ^{195}Pt-n.m.r. to the platinum-fluorosulfate system should provide insights into the polymerization and bonding in these compounds.

e) The group IVB halides such as $TiCl_4$, TiF_4, are also strong Lewis acids; their corresponding fluorosulfates may provide economical alternatives to the noble metal superacids.

f) The group VB and VIB oxyfluorosulfates appear to be complicated, multicomponent systems; some preliminary results from this study seem to indicate exchange reactions resulting in the formation of metal-fluorine bonds and weakly acidic behavior in the tantalum system. These may merit further investigations.

g) The HSO_3CF_3 solvent system is more tolerant to water than HSO_3F is. Although $Au(SO_3CF_3)_3$ is insoluble in HSO_3CF_3 [212], and $Pt(SO_3CF_3)_4$ appears to behave likewise, this may be the next solvent system to expand into, especially since it is also a very strongly acidic medium.

REFERENCES

1) T.E. Thorpe and W. Kirman, J. Chem. Soc. London, 921 (1892).

2) W. Traube, Chem. Ber., 46, 2513 (1913).

3) A.A. Woolf, J. Chem. Soc., 2840 (1954).

4) E. Hayek and A. Czaloun, Monatsh, 87, 790 (1956).

5) R.C. Paul, K.K. Paul, and K.C. Malhotra, Inorg. Nucl. Chem. Lett., 5, 689 (1969).

6) W. Traube and E. Reubke, Chem. Ber., 45B, 1618 (1921).

7) W. Lange, Z. Anorg. Allg. Chem., 215, 321 (1933).

8) R.J. Gillespie and E.A. Robinson, Can. J. Chem., 40, 644 (1962).

9) R.J. Gillespie, J.B. Milne, and J.B. Senior, Inorg. Chem., 5, 1233 (1966).

10) W. Lange, Fluorine Chemistry, 1, 167 (1950).

11) G.J. Gillespie, Acc. Chem. Res.,1, 202 (1968).

12) R.J. Gillespie and T.E. Peel, Adv. Phys. Org. Chem., 9, 1 (1971).

13) R.C. Thompson, Inorg. Sulfur Chem., Edited by G. Nickless, Elsevier, Amsterdam (1968).

14) A.W. Jache, Adv. Inorg. Chem. Radiochem., 16, 177 (1975).

15) S. Natarajan and A.W. Jache, Chem. of Non Aqueous Solvents, VB, 53 (1978).

16) G. Olah and J. Sommer, Récherche, 10, 624 (1979).

17) G.C. Cady, Adv. Inorg. Chem. Radiochem., 2, 123 (1960).

18) S.M. Williamson, Prog. Inorg. Chem., 7, 39 (1968).

19) R.A. De Marco and J.M. Shreeve, Adv. Inorg. Chem. Radiochem., 16, 109 (1974).

20) A. Engelbrecht, Angew Chem. Int., Ed., 4, 641 (1965).

21) J. Barr, R.J. Gillespie, and R.C. Thompson, Inorg. Chem., 3, 1149 (1964).

22) A. Commeyras and G.A. Olah, J. Am. Chem. Soc., 91, 2929 (1969).

23) G.A. Olah, Chem. Eng. News., 45, 76 (March 27, 1967).

24) R.C. Thompson, J. Barr, R.J. Gillespie, J.B. Milne, and R.A. Rothenbury, Inorg. Chem 4, 1641 (1965).

25) R.J. Gillespie and J. Passmore, Adv. Inorg. Chem. Radiochem., 17, 49 (1975).

26) W.W. Wilson and F. Aubke, J. Fluorine Chem., 13, 431 (1979).

27) R.E. Noftle and G.H. Cady, J. Inorg. Nucl. Chem., 29, 969 (1967).

28) R.J. Gillespie and M.J. Morton, Inorg. Chem., 11, 586 (1972).

29) R.J. Gillespie and M.J. Morton, Inorg. Chem., 11, 591 (1972).

30) R.J. Gillespie and E.A. Robinson, Can. J. Chem., 39, 2189 (1961).

31) P.A. Yeats, B. Landa, and F. Aubke, Inorg. Chem., 15, 1452 (1976).

32) P.A. Yeats, J.R. Sams, and F. Aubke, Inorg. Chem., 12, 328 (1973).

33) P.A. Yeats, B.L. Poh, B.F.E. Ford, J.R. Sams, and F. Aubke, J. Chem. Soc. A, 2188 (1970).

34) M. Lustig and G.H. Cady, Inorg. Chem., 1, 714 (1962).

35) H.A. Carter, S.P.L. Jones, and F. Aubke, Inorg. Chem., 9, 2485 (1970).

36) R.J. Gillespie and J.B. Milne, Inorg. Chem., 5, 1236 (1966).

37) F. Aubke and G.H. Cady, Inorg. Chem., 4, 269 (1965).

38) F. Aubke and R.J. Gillespie, Inorg. Chem., 7, 599 (1968).

39) R.J. Gillespie, Inorganic Sulfur Chem., Edited by G. Nickless, Elsevier, Amsterdam (1968).

40) Handbook of Chemistry and Physics, 53rd Edition., Chemical Rubber Company Press, Cleveland (1973).

41) P.A.W. Dean and R.J. Gillespie, J. Am. Chem. Soc., 92, 2362 (1970).

42) R.J. Gillespie and T. Birchall, Can. J. Chem., 41, 148 (1963).

43) R.J. Gillespie and E.A. Robinson, Can. J. Chem., 40, 675 (1962).

44) G.A. Olah, Chem. in Brit., 8, 281 (1972).

45) G.A. Olah and C.W. McFarland, Inorg. Chem., 11, 845 (1972).

46) R.J. Gillespie and E.A. Robinson, Can. J. Chem., 39, 2171 (1961).

47) A. Engelbrecht and E. Tschager, Z. Anorg. Allg. Chem., 433, 19 (1977).

48) R.J. Gillespie and T.E. Peel, J. Am. Chem. Soc., 95, 5173 (1973).

49) R.J. Gillespie, T.E. Peel, and E.A. Robinson, J. Am. Chem. Soc., 93, 5083 (1971).

50) R.J. Gillespie, K. Ouchi, and G. P. Pez, Inorg. Chem., 8, 63 (1969).

51) J. Sommer, P. Rimmelin, and T. Drakenberg, J. Am. Chem. Soc., 98, 2671 (1976).

52) J. Sommer, S. Schwartz, P. Rimmelin, and P. Canivet, J. Am. Chem. Soc., 100, 2576 (1978).

53) G.M. Krammer, J. Org. Chem., 40, 298 (1975).

54) G.M. Krammer, J. Org. Chem., 40, 302 (1975).

55) R.J. Gillespie, 1973 I.U.P.A.C. Symposium on Non Metal Chem.

56) R.J. Gillespie and J.B. Milne, Inorg. Chem., 5, 1577 (1966).

57) R.J. Gillespie and K.C. Malhotra, Inorg. Chem., 8, 1751 (1969).

58) R.J. Gillespie and M.J. Morton, Chem. Comm., 24, 1565 (1968).

59) G.A. Olah and M.B. Comisarow, J. Am. Chem. Soc., 90, 5033 (1968).

60) R.J. Gillespie and M.J. Morton, Inorg. Chem., 9, 811 (1970).

61) D.A.Edwards, M.J. Stiff, and A.A. Woolf, Inorg. Nucl. Chem. Lett., 3, 427 (1967).

62) J. Goubeau and J.B. Milne, Can. J. Chem., 45, 2321 (1967).

63) O. Ruff, Chem. Ber., 47, 656 (1914).

64) J.N. Brazier and A.A. Woolf. J. Chem. Soc. A., 99, (1967).

65) R.J. Gillespie and R.A. Rothenburg, Can. J. Chem., 42, 416 (1964).

66) E. Hayek, A. Czaloun, and B. Krismer, Monatsh, 87, 741 (1956).

67) E.L. Muetterties and D.D. Coffmann, J. Am. Chem. Soc., 80, 5914 (1958).

68) F.B. Dudley, J. Chem. Soc., 3407 (1963).

69) S.D. Brown and G.L. Gard, Inorg. Nucl. Chem. Lett., 11, 19 (1975).

70) F.B. Dudley and G.H. Cady, J. Am. Chem. Soc., 79, 513 (1957).

71) J.M. Shreeve and G.H. Cady, Inorg. Syntheses, 7, 124 (1963).

72) F.B. Dudley and G.H. Cady, J. Am. Chem. Soc., 85, 3375 (1963).

73) E. Castellano, R. Gatti, J.E. Sicre, and H.J. Schumacher, Z. Phys. Chem. (Frankfurt am Main), 42, 174 (1964).

74) H. Imoto and F. Aubke, J. Fluorine Chem., 15, 59 (1980).

75) R. Dev, W.M. Johnson , and G.H. Cady, Inorg. Chem., 11, 2259 (1972).

76) A. Storr, P.A. Yeats, and F. Aubke, Can. J. Chem., 50, 452 (1972).

77) W.P. Gilbreath and G.H. Cady, Inorg. Chem., 2, 496 (1963).

78) J.E. Roberts and G.H. Cady, J. Am. Chem. Soc., 82, 352 (1960).

79) D.D. DesMarteau, Inorg. Chem., 7, 434 (1968).

80) C. Chung and G.H. Cady, Z. Anorg. Allg. Chem., 385, 18 (1971).

81) W.M. Johnson and G.H. Cady, Inorg. Chem., 12, 2481 (1973).

82) W.M. Johnson, R. Dev, and G.H. Cady, Inorg. Chem., 11, 2260 (1972).

83) P.C. Leung and F. Aubke, Inorg. Nucl. Chem. Lett., 13, 263 (1977).

84) P.C. Leung and F. Aubke, Inorg. Chem., 17, 1765 (1978).

85) W.W. Wilson and F. Aubke, Inorg. Chem., 13, 326 (1974).

86) P.A. Yeats, W.W. Wilson, and F. Aubke, Inorg. Nucl. Chem. Lett., 9, 209 (1973).

87) C.S. Alleyne, K. O'Sullivan-Mailer, and R.C. Thompson, Can. J. Chem., 52, 336 (1974).

88) G.C. Kleinkoff and J.M. Shreeve, Inorg. Chem., 3, 607 (1964).

89) J.E. Roberts and G.H. Cady, J. Am. Chem. Soc., 82, 353 (1960).

90) J.M. Shreeve and G. H. Cady, J. Am. Chem. Soc., 83, 4521 (1961).

91) W.W. Wilson, Ph. D. Thesis, U.B.C., 1975.

92) D.W.J. Cruickshank and B.C. Webster, Inorganic Sulfur Chemistry, Ed. by G. Nickless, Elsevier, Amsterdam, 1968.

93) K. O'Sullivan, R.C. Thompson, and J. Trotter, J. Chem. Soc. A, 2024 (1967).

94) A.M. Qureshi, H.A. Carter, and F. Aubke, Can. J. Chem., 49, 35 (1971).

95) A.M. Qureshi, L.E. Levchuk, and F. Aubke, Can. J. Chem., 49, 2544 (1971).

96) P.A. Yeats, B.F.E. Ford, J.R. Sams, and F. Aubke, J. Chem. Soc., Chem. Comm., 791 (1969).

97) F.A. Allen, J. Lerbscher, and J. Trotter, J. Chem. Soc. A., 2507 (1971).

98) K.C. Lee and F. Aubke, Can. J. Chem., 57, 2058 (1979).

99) J.M. Taylor and R.C. Thompson, Can. J. Chem., 49, 511 (1971).

100) J.R. Dalziel, R.D. Klett, P.A. Yeats and F. Aubke, Can. J. Chem., 52, 231 (1974).

101) A. Vogel, Quantitative Inorg. Analysis, 3rd Ed., J. Wiley and sons, New York (1961).

102) J.E. Lind, J.J. Zwolenik, and R.M. Fuoss, J. Am. Chem. Soc., 81, 1557 (1959).

103) R.J. Gillespie, J.B. Milne, and R.C. Thompson, Inorg. Chem., 5, 468 (1966).

104) N. Bartlett and R. Maitland, Acta Crystallogr., 11, 747 (1958).

105) H.C. Clark and R.J. O'Brien, Can. J. Chem., 39, 1030 (1961).

106) B.N. Figgis and R.S. Nyholm, J. Chem. Soc., 4190 (1958).

107) Landolt-Börnstein, Numerical Data and Functional Relationships in Science and Technology, Vol. 2 and Sup. 2, Springer-Verlag, Berlin (1966,1976).

108) N. Bartlett and P.R. Rao, Proc. Chem. Soc., 393 (1964).

109) H.A. Carter, A.M. Qureshi, and F. Aubke, J. Chem. Soc., Chem. Comm., 1461 (1968).

110) F.A. Cotton and G. Wilkinson, Adv. Inorg. Chem., 3rd Ed., p. 924, Interscience, New York (1972).

111) W.E. Falconer, F.J. DiSalvo, A.J. Edwards, J.E. Griffiths, W.A. Sunders, and M.J. Vasile, J. Inorg. Nucl. Chem. Supplement, 59 (1976).

112) L.F. Warren and M.F. Hawthorne, J. Am. Chem. Soc., 92, 1157 (1970).

113) N. Bartlett and M.A. Hepworth, Chem. and Industry, 1425 (1957).

114) E.L. Wagner and D.F. Hornig, J. Chem. Phys., 18, 296 (1950).

115) D. Babel, in Structure and Bonding, 3, Springer-Verlag (1967).

116) D. Paus and R. Hoppe, Z. Anorg. Allg. Chem., 431, 207 (1977).

117) N. Bartlett and J.W. Quail, J. Chem. Soc., 3728 (1961).

118) Brauer, Handbook of Prep. Inorg. Chem., Academic Press, N.Y.,(1963).

119) Ref. 110, p. 1031.

120) M. Wilhelm and R. Hoppe, Z. Anorg. Allg. Chem., 424, 5 (1976).

121) R. Mattes, Z. Anorg. Allg. Chem., 364, 290 (1969).

122) N. Bartlett, Angew. Chem., Int. Ed., 7, 433 (1968).

123) A.G. Sharpe, J. Chem. Soc., 3444 (1950).

124) R.S. Nyholm and A.G. Sharpe, J. Chem. Soc., 3579 (1952).

125) A. Tressaud, M. Wintenberger, N. Bartlett, and P. Hagenmuller, C.R. Herbd. Seances Acad. Sci. Ser. C., 282, 1069 (1976).

126) H. Henkel and R. Hoppe, Z. Anorg. Allg. Chem., 359, 160 (1968).

127) P.R. Rao, A. Tressaud, and N. Bartlett, Inorg. Nucl. Chem. Lett, 23 (1976).

128) A.F. Wright, B.E.F. Fender, N. Bartlett, and K. Leary, Inorg. Chem., 17, 746 (1978).

129) R. Hoppe and W. Klemm, Z. Anorg. Allg. Chem., 268, 364 (1952).

130) A.G. Sharpe, J. Chem. Soc., 197 (1953).

131) L. Graham, Lawrence Berkeley Lab. Report, 1978, LBL-8088.

132) K.C. Lee and F. Aubke, Can. J. Chem., 55, 2473 (1977).

133) A. MacCragh and W.S. Koski, J. Am. Chem. Soc., 87, 2496 (1965).

134) H.A. Carter, Ph. D. Thesis, 1970, U.B.C..

135) D.D. DesMarteau and M. Eisenberg, Inorg. Chem., 11, 2641 (1972).

136) M. Wechberg, P.A. Bulliner, F. O. Sladky, R. Mews and N. Bartlett, Inorg. Chem., 11, 3063 (1972).

137) C.S. Alleyne, M. Sc. Thesis, 1968, U.B.C..

138) K.O. Christe, C. J. Schack, D. Pilipovich, and W. Sawodny, Inorg. Chem., 8, 2489 (1969).

139) A.B.P. Lever, Inorganic Electronic Spectroscopy, Elsevier, Amsterdam, (1968).

140) Ref. 110, p. 998.

141) B.N. Figgis, Introduction to Ligand Fields, Interscience, N.Y. (1967).

142) H.B. Gray and C.J. Ballhausen, J. Am. Chem. Soc., 85, 260 (1963).

143) Ref. 110, p. 561.

144) P. Kohler, W. Massa, D. Reinen, B. Hofmann, and R. Hoppe, Z. Anorg. Allg. Chem., 446, 131 (1978).

145) T.M. Dunn, Trans. Far. Soc., 48, 1441 (1961).

146) V. Halpen, Proc. Roy. Soc., 291A, 113 (1966).

147) F.O. Sladky and N. Bartlett, J. Chem. Soc. A., 2188 (1969).

148) R.C. Thompson, unpublished results.

149) W. Rüdorff, J. Kändler, and D. Babel, Z. Anorg. Allg. Chem., 317, 261 (1962).

150) A. Westland, R. Hoppe, and S. Kaseno, Z. Anorg. Allg. Chem., 338, 319 (1965).

151) R.P. Rao, Ph. D. Thesis, U.B.C. 1965.

152) J.H. Waters and H.B. Gray, J. Am. Chem. Soc., 87, 3534 (1965).

153) K. Leary and N. Bartlett, J. Chem. Soc., Chem. Comm., 903 (1972).

154) K. Leary, A. Zalkin, and N. Bartlett, J. Chem. Soc., Chem. Comm.,131 (1973).

155) M.J. Vasile, T. J. Richardson, F.A. Stevie, and W.E. Falconer, J. Chem. Soc., Dalton 351 (1976).

156) B. Armer and H. Schmidbaur, Angew. Chem. Int., Ed., 9, 101 (1970).

157) B.F.G. Johnson, Gold Bulletin Johannesberg, 4, 9 (1971).

158) H. Schmidbauer, Angew. Chem. Int., Ed., 15, 728 (1976).

159) R.J. Puddephatt, The Chemistry of Gold, Elsevier, Amsterdam, 1978.

160) F.W.B. Einstein, P.R. Rao, J. Trotter, and N. Bartlett, J. Chem. Soc. (A.), 478 (1967).

161) A.J. Edwards and G.R. Jones, J. Chem. Soc. A., 1936 (1969).

162) C.D. Garner and S.C. Wallwork, J. Chem. Soc. A., 3092 (1970).

163) A.M. Qureshi and F. Aubke, Inorg. Chem., 10, 1116 (1971).

164) A.A. Woolf, J. Chem. Soc., 433 (1955).

165) K.C. Lee and F. Aubke, Inorg. Chem., 18, 389 (1979).

166) K.C. Lee and F. Aubke, Inorg. Chem., 19, 119 (1980).

167) R.S. Nyholm and A.G. Sharpe, J. Chem. Soc., 3579 (1952).

168) L.B. Asprey, F.H. Kruse, K.H. Jack, and R. Maitland, Inorg. Chem., 3, 602 (1964).

169) D.W.A. Sharp and J. Thorley, J. Chem. Soc., 3557 (1963) and references therein.

170) O. Glemser and A. Smalc, Angew. Chem. Int., Ed., 8, 517 (1969).

171) A. Smalc, Abstract, 4th European Symposium on Fluorine Chemistry, 1972.

172) W.W. Wilson, J.M. Winfield and F. Aubke, Inorg. Chem., 11, 2260 (1972).

173) D.J. Merryman, P.A. Edwards, J.D. Corbett and R.E. MacCarley, J. Chem. Soc., Chem. Comm., 779 (1972).

174) J.W. Moore, J.W. Baird, and H.B. Miller, J. Am. Chem. Soc., 90, 1359 (1968).

175) C.S. Alleyne and R.C. Thompson, Can. J. Chem., 52, 3218 (1974).

176) W.W. Wilson, B. Landa, and F. Aubke, Inorg. Nucl. Chem. Lett., 11, 529 (1975).

177) C.C. Addison, G.S. Brownlee, and N. Logan, J. Chem. Soc., Dalton, 1440 (1972).

178) P. Gallezot, D. Weigel, and M. Prettre, Acta Crystallogr., 22, 699 (1967).

179) K.O. Christe, and C.J. Schack, Adv. Inorg. Chem. Radiochem., 18, 319 (1976).

161) A.J. Edwards and G.R. Jones, J. Chem. Soc. A., 1936 (1969).

162) C.D. Garner and S.C. Wallwork, J. Chem. Soc. A., 3092 (1970).

163) A.M. Qureshi and F. Aubke, Inorg. Chem., 10, 1116 (1971).

164) A.A. Woolf, J. Chem. Soc., 433 (1955).

165) K.C. Lee and F. Aubke, Inorg. Chem., 18, 389 (1979).

166) K.C. Lee and F. Aubke, Inorg. Chem., 19, 119 (1980).

167) R.S. Nyholm and A.G. Sharpe, J. Chem. Soc., 3579 (1952).

168) L.B. Asprey, F.H. Kruse, K.H. Jack, and R. Maitland, Inorg. Chem., 3, 602 (1964).

169) D.W.A. Sharp and J. Thorley, J. Chem. Soc., 3557 (1963) and references therein.

170) O. Glemser and A. Smalc, Angew. Chem. Int., Ed., 8, 517 (1969).

171) A. Smalc, Abstract, 4th European Symposium on Fluorine Chemistry, 1972.

172) W.W. Wilson, J.M. Winfield and F. Aubke, Inorg. Chem., 11, 2260 (1972).

173) D.J. Merryman, P.A. Edwards, J.D. Corbett and R.E. MacCarley, J. Chem. Soc., Chem. Comm., 779 (1972).

174) J.W. Moore, J.W. Baird, and H.B. Miller, J. Am. Chem. Soc., 90, 1359 (1968).

175) C.S. Alleyne and R.C. Thompson, Can. J. Chem., 52, 3218 (1974).

176) W.W. Wilson, B. Landa, and F. Aubke, Inorg. Nucl. Chem. Lett., 11, 529 (1975).

177) C.C. Addison, G.S. Brownlee, and N. Logan, J. Chem. Soc., Dalton, 1440 (1972).

178) P. Gallezot, D. Weigel, and M. Prettre, Acta Crystallogr., 22, 699 (1967).

179) K.O. Christe, and C.J. Schack, Adv. Inorg. Chem. Radiochem., 18, 319 (1976).

180) P.A. Yeats, J.R. Sams and F. Aubke, Inorg. Chem., 11, 2634 (1972).

181) R.J. Gillespie and E.A. Robinson, Can. J. Chem., 39, 2179 (1961).

182) A.J. Edwards and G.R. Jones, J. Chem. Soc. A., 1467 (1969).

183) W.W. Wilson, J.M. Winfield, and F. Aubke, J. Fluorine Chem., 7, 245 (1976).

184) W,J, Moore, Physical Chemistry, 4th Ed., Prentice-Hall Inc., New Jersey, 1972.

185) R.J. Gillespie and R.F.M. White, Can. J. Chem., 38, 1371 (1960).

186) R. Savoie and P.A. Gignere, Can. J. Chem., 42, 277 (1964).

187) C.D. Desjardins and J. Passmore, J. Fluorine Chem., 6, 379 (1975).

188) E.E. Aynsley, R.D. Peacock, and P.L. Robinson, Chem. Ind., 1117 (1951).

189) L.H. Vogt, J.L. Katz, and S.E. Wiberley, Inorg. Chem., 4, 1157 (1965).

190) Ref. 110, p. 998.

191) A. Tressaud, F. Pintchovski, L. Lozano, A. Wold, and P. Hagenmuller, Mat. Res. Bull., 11, 689 (1976).

192) N. Bartlett and D.H. Lohmann, J. Chem. Soc., 619 (1964).

193) N. Bartlett and D.H. Lohmann, J. Chem. Soc., 5253 (1962).

194) K.O. Christe, Inorg. Chem., 12, 1580 (1973).

195) D.F. Evans and G.K. Turner, J. Chem. Soc., Dalton, 1238 (1975).

196) W.P Griffith, The Chemistry of the Rarer Platinum Metals, Interscience-Wiley, New York (1968).

197) V. Norman and J.C. Morrow III, J. Chem. Phys., 31, 455 (1959).

198) Ref. 110, p. 772.

199) Ref. 110, p.1018.

200) I.R. Beattie, K.M.S. Livingston, D.J. Reynolds and G.A. Ozin, J. Chem. Soc. A., 1210 (1970).

201) E.I. Stiefel, Prog. Inorg. Chem., 22, 1 (1977).

202) O. Jarchow, F. Schroder, and H. Schulz, Z. Anorg. Allg. Chem., 363, 58 (1968).

203) D.M. Adams and R.G. Churchill, J. Chem. Soc. (A.), 2310 (1968).

204) D.L. Kepert, The Early Transition Metals, Academic Press, 1972.

205) C.G. Barraclough, J. Lewis, and R.S. Nyholm, J. Chem. Soc., 3552 (1959).

206) E.O. Fisher, N.Q. Dao, and W.R. Wagner, Angew. Chem. Int., Ed. 17, 50 (1978).

207) H.A. Carter, C.A. Milne, and F. Aubke, J. Inorg. Nucl. Chem., 37, 282 (1975).

208) L.E. Levchuk, J.R. Sams, and F. Aubke, Inorg. Chem., 11, 43 (1972).

209) P.C. Leung, Ph. D. Thesis, U.B.C., 1979.

210) K. Nakamoto, I.R. Spectra of Inorg. and Coord. Compounds, J. Wiley and Sons, New York (1963).

211) F.B. Dudley and G.H. Cady, J. Am. Chem. Soc., 85, 3375 (1963).

212) P.C. Leung, K.C. Lee, and F. Aubke, Can. J. Chem., 57, 326 (1979).

213) R.E. Noftle and G.H. Cady, Inorg. Chem., 4, 1010 (1965).

214) D.D. DesMarteau, J. Am. Chem. Soc., 100, 340 (1968).

Appendix A CONDUCTIVITY CALCULATIONS

INTRODUCTION

In this study, a theoretical treatment of the conductivity results is applied to three systems in HSO_3F — $Au(SO_3F)_3$, $Pt(SO_3F)_4$ and $KSn(SO_3F)_5$. The purpose of these calculations is to attempt to describe the solution behavior of these species in a semi-quantitative manner, to have a comparison of their acidities with other systems, and to obtain ionic mobility values for ions hitherto unknown. As with any treatment of this type, a few assumptions have been made.

a) The equilibrium constants are set to be invariant throughout the range of a particular experiment. This is not entirely valid as they do have a dependence on the ionic strength of the solution.

b) The autoprotolysis constant for HSO_3F, i.e., $[H_2SO_3F^+]\cdot[SO_3F^-]$ is 3.8×10^{-8} $mol\cdot kg^{-1}$, although this has only been approximately determined[103]. This is not expected to have a large contribution to the conductivity of solutions in HSO_3F except at or near neutrality conditions.

c) The molal conductivity of $H_2SO_3F^+$ at infinite dilution, $\lambda_o^*(H_2SO_3F^+)$, is set at 320. Also the sum of $\lambda_o^*(SO_3F^-)$ and $\lambda_o^*(K^+)$ is set at 256, using the value of KSO_3F [21].

d) A dependence of λ^* on the ionic strength, I, is approximated as follows:

$$\lambda^* = \lambda_o^* \times \exp(-1.567 \times I). \qquad (A.1)$$

The Limiting Law predicts a decrease of λ^* with respect to $I^{\frac{1}{2}}$, but this is seldom obeyed in solutions with concentrations greater than ~10^{-3} mol·kg^{-1}. An empirical fit was attempted on the published data on solutions of $M^{I}SO_3F$ and $M^{II}(SO_3F)_2$, where M^{I}=Li, Na, K, NH_4, Rb, and M^{II}=Sr, Ba [21]. Although polynomials, usually of less than the 3rd degree, were found to provide the best least-square fit within the range of the data, as is usually found for curve fitting of this type, extrapolations outside the limits are extremely unreliable. Furthermore, the coefficients of the polynomials obtained for different solutions vary from solution to solution. The best compromise between the ability to extrapolate (required for the concentrated solutions in the $KSn(SO_3F)_5$ system), and the degree of fit with the experimental data was obtained for an exponential relationship of the form of equation (A.1). The coefficient of -1.567 was obtained by taking an average of all the different solutions' values (these range from -1.4 to -1.7). In general, a difference of less than 2% was encountered for solutions of concentrations higher than ~0.01 mol·kg^{-1}, when equation (A.1) was applied to the solutions in reference 21. While it may be an over-simplification to expect other ions to behave as the alkali and alkali earth cations, and SO_3F^-, equation(A.1) does provide a crude means of adjustment, and it improves the fit of the calculation performed here. It must also be stated that the equation has no theoretical impli-

cations, and is simply the result of a quantitative fit. To illustrate the degree of variation in the ionic strength during a titration, it is included in the appropriate tables.

A.1 HSO_3F-$Au(SO_3F)_3$

$H[Au(SO_3F)_4]$ is a strong acid in HSO_3F, as can be illustrated by its titration with KSO_3F. The autoprotolysis of HSO_3F can be ignored for the most part of the calculation except at the end of the titration, at which point the solution is essentially neutral. In order to adjust for the solvent conductance without involving the autoprotolysis equilibrium constant into the calculation, a quantity of $1.0\times10^{-4}\ \Omega^{-1}cm^{-1}$ is subtracted from the conductance at the end point.

For the titration, the calculation for a strong acid-strong base is applied. The titration can be represented by:

$$\underset{m-x-z}{H[Au(SO_3F)_4]} + HSO_3F \xrightleftharpoons{K_1} \underset{x}{H_2SO_3F^+} + \underset{x+z}{[Au(SO_3F)_4]^-} \qquad (A.2)$$

$$K_1 = \frac{(x)\times(x+z)}{(m-x-z)} \qquad (A.3)$$

and

$$\kappa = \lambda^*_H \times(x) + \lambda^*_{Au}\times(x+z) + \lambda^*_K\times(z) \qquad (A.4)$$

where m=total concentration of all Au-species

x=dissociation of $H[Au(SO_3F)_4]$

z=amount of KSO_3F added, $z=r\times m$

r=K/Au

$\lambda^*_H=\lambda^*(H_2SO_3F^+)$

$\lambda^*_{Au}=\lambda^*([Au(SO_3F)_4]^-)$

$\lambda^*_K=\lambda^*(K^+)$

a) For each value of λ^*_K, λ^* Au is obtained from κ at r=1 and converted into λ^*_o Au.

b) λ^*'s are found at r=0 by letting I=m.

x is obtained from κ at r=0, z=0.

I is obtained from x.

λ^*'s are recalculated using the new I.

This procedure is repeated a total of 3 times to get a good approximation for I.

K_1 is calculated from equation (A.3).

c) For each value of r, m, and z are calculated (m changes because of dilution).

d) By solving equation (A.3) for x, the following can be obtained — I, λ^*, κ.

e) Likewise, the conductivity of solutions of pure $Au(SO_3F)_3$ can be found by doing procedure d at r=z=0 for the required concentration, m.

A.2 HSO_3F- $KSn(SO_3F)_5$

The titration of $KSn(SO_3F)_5$ with KSO_3F indicates the former's weak acicity in HSO_3F, and therefore the autoprotolysis of HSO_3F has to be taken into account. For reasons discussed in Chapter 8, polymerization in solution is ignored in a first approximation. The titration can be represented by the following two equilibria and equations:

$$\underset{m-x-z}{H[Sn(SO_3F)_6]^-} + HSO_3F \xrightleftarrows{K_1} \underset{x+y}{H_2SO_3F^+} + \underset{x+z}{[Sn(SO_3F)_6]^{2-}} \qquad (A.5)$$

$$2HSO_3F \xrightleftarrows{K_2} \underset{x+y}{H_2SO_3F^+} + \underset{y}{SO_3F^-} \qquad (A.6)$$

$$K_1 = \frac{(x+y)\times(x+z)}{(m-x-z)} \qquad (A.7)$$

$$K_2 = (x+y)\times(y) \text{ , and} \qquad (A.8)$$

$$\kappa = \lambda^*H\times(x+y) + \lambda^*S\times(y) + \lambda^*HSn\times(m-x-z) + \lambda^*Sn\times(x+z) \qquad (A.9)$$

where, most of the terms have similar definitions as in Appendix (A.1)

and y = dissociation of HSO_3F

$\lambda^*S = \lambda^*(SO_3F^-)$

$\lambda^*HSn = \lambda^*(H[Sn(SO_3F)_6]^-)$

$\lambda^*Sn = \lambda^*([Sn(SO_3F)_6]^{2-})$

$r = KSO_3F/KSn(SO_3F)_5$

a) For each set of λ^*K and λ^*HSn,

K_1 is found at r=0 and r=1, using κ at r=0 and κ at r=1, respectively, and a test value for λ^*Sn. Using the Secant method, the two K_1 values (which should be identical), are

made to converge by solving for:

$$K_1|_{r=0} \div K_1|_{r=1} - 1 = 0 \qquad (A.10)$$

As I is unknown at the begining of this procedure, it is found by successive approximation by resubstitution similar to procedure b) in Appendix (A.1), λ^*Sn and K_1 are obtained.

b) In equation (A.7), x is substituted by y using equation (A.8). A polynomial of 3rd order in y, for which the roots can be found, is obtained. The titration is calculated for increasing values of r, therefore x should become progressively smaller. The value of x which is closest to, but less than, the last x is chosen.

c) I can then be obtained, and subsequently, κ.

d) For the conductivity of $KSn(SO_3F)_5$ solutions at the above set of λ^* values, for increasing concentrations, using procedures b) and c), the results of x,I and κ are calculated by letting z=0.

e) Similarly, procedures b) and c) can be used to calculate the conductivity of $K_2[Sn(SO_3F)_6]$ solutions by letting z=m. Because of the choose-x procedure in b), the calculation begins at the highest concentration.

A.3 HSO_3F-$Pt(SO_3F)_4$

This system is a combination of the two previous ones, and the titration consists of both a strong and a weak acid with a strong base. Two assumptions are made: the conductivity ar r=0 is essentially that of the strong acid, and at r=0, the conductivity is due solely to the dissociations of $[Pt(SO_3F)_6]^{2-}$ and HSO_3F. Again, no polymerization is taken into account. The titration can be represented by the following three equilibria and equations.

$$\underset{m-w}{H_2[Pt(SO_3F)_6]} + HSO_3F \xrightleftharpoons{K_1} \underset{w-x}{H[Pt(SO_3F)_6]^-} + \underset{w+x+y-z}{H_2SO_3F^+} \qquad (A.11)$$

$$\underset{w-x}{H[Pt(SO_3F)_6]^-} + HSO_3F \xrightleftharpoons{K_2} \underset{x}{[Pt(SO_3F)_6]^{2-}} + \underset{w+x+y-z}{H_2SO_3F^+} \qquad (A.12)$$

$$HSO_3F \xrightleftharpoons{K_3} \underset{w+x+y-z}{H_2SO_3F^+} + \underset{y}{SO_3F^-} \qquad (A.13)$$

$$K_1 = \frac{(w-x) \times (w+x+y-z)}{(m-w)} \qquad (A.14)$$

$$K_2 = \frac{(x) \times (w+x+y-z)}{(w-x)} \qquad (A.15)$$

$$K_3 = (w+x+y-z) \times (y) \qquad (A.16)$$

and

$$= \lambda^*H\times(w+x+y-z) + \lambda^*S\times(y) + \lambda^*K\times(z) + \lambda^*HPt\times(w-x) + \lambda^*Pt\times(x) \qquad (A.17)$$

where w = dissociation of $H_2[Pt(SO_3F)_6]$

x = dissociation of $H[Pt(SO_3F)_6]$

y = dissociation of HSO_3F

z = amount of KSO_3F, $z = r \times m$

$r = K/Pt$

$\lambda^*HPt = \lambda^*(H[Pt(SO_3F)_6]^-)$

$\lambda^*Pt = \lambda^*([Pt(SO_3F)_6]^{2-})$

a) For each value of r, m, and z are calculated.

b) For each set of λ^*K, λ^*HPt and λ^*Pt,

K_1 is obtained from κ at r=0 and by letting x=y=z=0,

K_2 is obtained from κ at r=2 and by letting w=m.

A check at the end of the calculation shows that both approximations are valid.

c) Equations (A.14) and (A.15) are combined into one containing only x and w as the variables.

$$K_1(m-w) \times (w-x) - K_2x \times (w-x) = 0 \qquad (A.18)$$

w can be calculated given x.

d) By solving equation (A.16), y can be calculated given x and w.

e) By solving equation (A.14), K_1 can be calculated given x, w, and y.

f) For each value of r, x is found by applying the Secant Method to solve for:

$$K_1^* \div K_1 - 1 = 0 \qquad (A.19)$$

where K_1^* is the value of K_1 calculated for each test value of x using procedures c), d), and e). Although K_1 can be substituted by K_2 in equation (A.19), a higher degree of accuracy is obtained in calculating K_1 because $K_1 > K_2$. When

K_2 was used, the function described by equation (A.19) also became quite ill-conditioned and was found not to converge in certain cases.

g) After finding the value of x (therefore w and y) that satisfies equation (A.18). κ can be calculated.

h) For all the calculations involving λ^* and an unknown quantity of I, the latter is found by the successive approximation method similar to that described in procedure b) in Appendix (A.1).

i) The conductivity of pure HSO_3F-$Pt(SO_3F)_4$ is found by using equation (A.14), letting x=y=z=0.

APPENDIX B GOLD-TRIFLUOROMETHYLSULFATE

B.1 INTRODUCTION

The gold-trifluoromethylsulfate system was investigated as a possible ansolvo-acid in the HSO_3CF_3 solvent system. While the acidity of HSO_3CF_3 is only slightly lower than that of HSO_3F [47], the former has the advantage of being stable in the presence of water. If $Au(SO_3CF_3)_3$ is found to be a strong acid in HSO_3CF_3 and if it is also compatible with the aqueous system, then the scope of application of this superacid system could conceivably be wider than that of the corresponding fluorosulfate system. $Ag(SO_3CF_3)_2$ was also studied in this laboratory [209], and the results of both investigations have been published in reference 212; the gold-SO_3CF_3 system will be discussed briefly here as it is related to a degree to the topic of this thesis. For a more detailed discussion, the reader is asked to refer to reference 212.

B.2 DISCUSSION

The number of known synthetic routes to trifluoromethylsulfates is very limited, mainly due to the instabilities of oxidizing agents such as $(CF_3SO_3)_2$ [213] and CF_3SO_3Cl [214], the analogues of $S_2O_6F_2$ and $ClSO_3F$ in the fluorosulfate system. Most

known syntheses involve the solvolysis of salts of other acids in HSO_3CF_3. $Au(SO_3CF_3)_3$ and $Cs[Au(SO_3CF_3)_4]$ are prepared by the following reactions:

$$Au(SO_3F)_3 + HSO_3CF_3 \longrightarrow Au(SO_3CF_3)_3 + HSO_3F \qquad (B.1)$$

$$Cs[Au(SO_3F)_4] + HSO_3CF_3 \longrightarrow Cs[Au(SO_3CF_3)_4] + HSO_3F \quad , \qquad (B.2)$$

the HSO_3F formed presumably decomposed by reactions with HSO_3CF_3. These are most likely mass-action type reactions, since the reversal of both reactions was found to occur when HSO_3F was added to the trifluoromethylsulfates.

Neither compounds were found to be very soluble in HSO_3CF_3, thus limiting the possiblity of $Au(SO_3CF_3)_3$ being a useful ansolvo-acid in the solvent system. The formation of $Cs[Au(SO_3CF_3)_4]$, however, does indicate that $Au(SO_3CF_3)_3$ may act as a trifluoromethylsulfate ion acceptor.

The vibrational spectra of these two diamagnetic compounds suggest structural similarities to the fluorosulfates——square planar coordination for Au(III), the presence of monodentate SO_3CF_3 groups in $Cs[Au(SO_3CF_3)_4]$ and the presence of both monodentate and bidentate SO_3CF_3 groups in $Au(SO_3CF_3)_3$.

B.3 CONCLUSION

$Au(SO_3CF_3)_3$ was found to exhibit a lower sensitivity to moisture than $Au(SO_3F)_3$, but it is still very hygroscopic.

Furthermore, the former's low solubility in the parent acid limited its use as an ansolvo-acid in the system. Lewis acidity towards $SO_3CF_3^-$, however, was established for the compound by the synthesis of the complex $Cs[Au(SO_3CF_3)_4]$. The solvolysis of a fluorosulfate in HSO_3CF_3 should find use as a synthetic route to trifluoromethylsulfates containing transition metals in relatively high oxidation states.

APPENDIX C LIST OF ABBREVIATIONS

Magnetochemistry and Electronic Spectroscopy

B	interelectronic repulsion parameter, unit=cm^{-1}
B°	B of free ion
β	B/B°
D_q	ligand field splitting parameter, unit=cm^{-1}
Δ_o	octahedral ligand field splitting energy, $\Delta_o=10\ D_q$
k	electronic delocalization factor
$\Sigma\chi_{dia}$	sum of all diamagnetic susceptibilities in c.g.s. units
χ_m	molar magnetic susceptibility
χ_m^c	χ_m corrected for $\Sigma\chi_{dia}$
θ	Weiss constant
TIP	Temperature Independent Paramagnetism
μ_B	Bohr Magneton
μ_{eff}	effective magnetic moment, unit=μ_B
μ_{eff}^T	μ_{eff} corrected for TIP
λ	spin orbital coupling constant, unit=cm^{-1}

Vibrational Spectroscopy

s	strong	υ_s	symmetric stretch
m	medium	υ_{as}	asymmetric stretch
w	weak	ρ	bending mode
v	very	δ	deformation mode
b	broad		

Conductometry

H_o	Hammett acidity function
K_{ap}	autoprotolysis equilibrium constant
mmol	10^{-3} mole
κ	specific conductance, unit=$\Omega^{-1}cm^{-1}$
R	base/acid ratio in a titration
Λ^+	molar conductivity of the cation
Λ^-	molar conductivity of the anion